PACLITAXEL LOADED POLY(L-LACTIC ACID) MICROSPHERES: CHARACTERISATION AND INTRAPERITONEAL ADMINISTRATION

by

RICHARD LIGGINS

B.Sc. (Pharm), University of British Columbia, 1993

A THESIS SUBMITTED IN PARTIAL FULFILMENT OF
THE REQUIREMENTS FOR THE DEGREE OF

DOCTOR OF PHILOSOPHY

in

THE FACULTY OF GRADUATE STUDIES

Faculty of Pharmaceutical Sciences
Division of Pharmaceutics and Biopharmaceutics

We accept this thesis as conforming
to the required standard

THE UNIVERSITY OF BRITISH COLUMBIA

October 1998

© Richard Liggins, 1998

In presenting this thesis in partial fulfilment of the requirements for an advanced degree at the University of British Columbia, I agree that the Library shall make it freely available for reference and study. I further agree that permission for extensive copying of this thesis for scholarly purposes may be granted by the head of my department or by his or her representatives. It is understood that copying or publication of this thesis for financial gain shall not be allowed without my written permission.

Faculty of Pharmaceutical Sciences

The University of British Columbia
Vancouver, Canada

Date: October 13, 1998

DE-6 (2/88)

ABSTRACT

Paclitaxel is a drug of choice for the treatment of ovarian cancer but despite its widespread usage, the solid state properties of paclitaxel are not clearly understood. There is speculation that several solid forms may exist because of the wide range of reported values for the water solubility of paclitaxel. In this work, two distinct anhydrous crystalline forms, a dihydrate and an amorphous solid form were identified. Dissolution profiles of the as received anhydrous form showed a maximum apparent solubility of 3.5 µg/ml after 2 hours that decreased to 1 µg/ml after 20 hours due to conversion of the anhydrous form to the dihydrate.

Microsphere delivery systems for paclitaxel were developed using poly(L-lactic acid) (PLLA) polymers in order to provide controlled release of the drug. The ability to resuspend microspheres, the total content of paclitaxel in microspheres, and polymer thermal properties all varied with polymer molecular weight. The greatest changes in these properties occurred in the molecular weight range of 1k to 4k g/mol. For microspheres manufactured from 100k g/mol PLLA, surface morphology, thermal properties and paclitaxel release profiles were dependent on the microsphere size range and on the paclitaxel loading level. Microspheres were manufactured in the size ranges of 1-10, 10-35, and 35-105 µm and had theoretical loading levels between 10 and 30%. Addition of paclitaxel to the microspheres resulted in a dimpled surface morphology which was believed to be due to paclitaxel's effect on the formation of the outer surface of the microspheres. Depression of the glass and melting transition temperatures of the polymer by up to 6°C indicated that paclitaxel was dissolved in the amorphous phase of the semicrystalline polymer matrix. *In vitro* release profiles of paclitaxel from

100k g/mol PLLA microspheres showed an initial rapid phase of release for 3 days, followed by a slower phase of apparently zero-order release. The rate and extent of release increased with increasing paclitaxel loading levels and decreasing particle size.

In order to alter the release profiles for paclitaxel from PLLA microspheres the polymer matrix was modified by blending low and high molecular weight PLLA polymers. Blends of 2k and 50 g/mol PLLA and 1k and 100k g/mol PLLA were prepared with blend compositions between 0 and 100% of the low molecular weight component and their thermal properties were characterised. Both blend systems exhibited a single glass transition over the entire range of compositions, indicating that the polymers were miscible. As the amount of low molecular PLLA increased, the melting temperature of the polymer blend decreased from 175°C to 145°C and from 175°C to 110°C for the 2k/50k g/mol and 1k/100k g/mol PLLA blends, respectively. Microspheres made from all blends of 2k/50k g/mol PLLA were spherical and easily resuspended from the dry state. However, for 1k/100k g/mol PLLA blends, 60% was the highest proportion of 1k g/mol PLLA that could be used to form spherical microspheres that were resuspendable. The blend containing 60% 1k g/mol PLLA (PB60) was therefore selected for the formulation of paclitaxel loaded polymer blend microspheres.

Thermal properties and paclitaxel release profiles from PB60 microspheres were dependent on the microsphere size range and on the paclitaxel loading level. The incorporation of paclitaxel into PB60 microspheres did not result in the dimpled appearance observed for 100k g/mol PLLA microspheres. Depression of the melting transition temperature of the polymer by up to 6°C indicated that paclitaxel was dissolved in the PB60 polymer matrix. However, the glass transition temperature of the blend was

increased by the addition of paclitaxel, indicating that the amorphous phase was stiffened by the addition of the drug. *In vitro* release profiles for paclitaxel released from PB60 microspheres showed an initial rapid phase of release for 3 days, followed by a constant rate of diffusion controlled release until day 21 of the release study. Around day 21, PB60 microspheres in all size ranges and paclitaxel loadings exhibited a sudden increase in the release rate due to the onset of erosion of the matrix.

Microspheres made from 100k g/mol PLLA were used in two sets of *in vivo* studies in rats. The first study determined the size of microspheres that would be retained in the peritoneal cavity. The second study determined the efficacy of intraperitoneal paclitaxel loaded microspheres in preventing 9L glioblastoma tumour growth following a tumour cell spill. To simulate the spill two million tumour cells were injected into the peritoneal cavity through an incision in the abdomen of rats.

Microspheres with diameters of less than 24 μm were observed in the lymphatic system of rats. It is believed that these microspheres passed from the peritoneal cavity to the lymphatic system through fenestrations in the diaphragm. Microspheres in the size range of 35-105 μm were selected for the efficacy study to ensure that they would be retained in the peritoneum. A dose of 100 mg of 30% loaded microspheres, administered at the time of the simulated tumour cell spill, was efficacious in preventing tumour cell implantation and growth for up to six weeks.

TABLE OF CONTENTS

vii

LIST OF TABLES

LIST OF FIGURES

LIST OF ABBREVIATIONS

%w/v	percent weight in volume
%w/w	percent by weight
°2θ	X-ray diffraction angle
°C	degrees Celsius
μl	microlitre
μg	microgram
μmol	micromole
ϕ_n	fractional proportion of component n in a mixture
[η]	intrinsic viscosity
a	a constant in the Mark-Houwink equation
C	concentration
C_{18}	octadecylsilane
C_{max}	peak plasma concentration
Cp	heat capacity
CPPSA	poly(carboxyphenoxy propane-co-sebacic acid)
Cs	aqueous drug solubility
D	diffusion coefficient
DSC	differential scanning calorimetry
EVA	poly(ethylene-co-vinyl acetate)
eV	electron volt
g	gram
GPC	gel permeation chromatography
h	hour
HPLC	high performance liquid chromatography
J	joule
k	kilo
K	a constant in the Mark-Houwink equation
Kd	binding constant
kV	kilovolts
L	litre

l	polymer chain folding length
$l*$	ideal polymer chain folding length
l_S	thickness of a slab
LCMS	liquid chromatography-mass spectrometry
LLA	L-lactic acid
M_0	theoretical drug loading
MePEG	methoxy poly(ethylene glycol)
mg	milligrams
m	meter
min	minute
ml	millilitre
M_{GPC}	molecular weight determined by GPC
mm^3	cubic millimeters
M_n	number average molecular weight
mol	mole
M_t	amount of drug released at time t
M_v	viscosity average molecular weight
MW	molecular weight
M_w	weight average molecular weight
nmol	nanomole
NS	normal saline
PBS	phosphate buffered saline
PBS-A	phosphate buffered saline with albumin
PCL	poly(ε-caprolactone)
PDLLA	poly(D,L-lactic acid)
PEG	poly(ethylene glycol)
PGA	poly(glycolic acid)
PLA	poly(lactic acid)
PLGA	poly(lactic-co-glycolic acid)
PLLA	poly(L-lactic acid)
PLLA-LA	poly(L-lactic acid) initiated with L-lactic acid oligomers
PLLA-PS	poly(L-lactic acid) obtained from Polysciences Inc.

PLLA-SA	poly(L-lactic acid) initiated with stearyl alcohol
PMMA	poly(methyl methacrylate)
PVA	poly(vinyl alcohol)
ε	porosity
R	chromatographic resolution, gas constant
r	radius of a sphere
R_η	hydrodynamic radius
R^2	coefficient of determination
rpm	revolutions per minute
RSD	relative standard deviation
SEM	scanning electron microscopy
t	time
t_{50}	time for evaporation of 50% of solvent
Tc	recrystallisation temperature
Td	degradation temperature
Tg	glass transition temperature
Tg^∞	theoretical glass transition temperature for infinite molecular weight
TGA	thermogravimetric analysis
Tm	melting transition temperature
Tm^0	equilibrium melting transition temperature
τ	tortuosity
Tr	retention time
V	volume
V_0	initial rate of paclitaxel release
W	watt
η	viscosity
W/g	watts per gram
X_C	degree of crystallinity
XRPD	X-ray powder diffraction
ΔCp	change in heat capacity
Δh	enthalpy of fusion of a polymer repeat unit
ΔH_c	enthalpy of recrystallisation

ΔH_f enthalpy of fusion

ΔH_r enthalpy of glass relaxation

$\Delta H_{r\infty}$ enthalpy of glass relaxation after infinite relaxation

σ_e surface free energy of a polymer crystallite

ACKNOWLEDGEMENT

1. INTRODUCTION

Paclitaxel has become a drug of choice in the treatment of ovarian cancer and is undergoing clinical trials for use in the treatment of several other cancers (Rowinsky, 1994). Despite its widespread usage, the solid state properties of paclitaxel are not clearly understood. There is speculation in the literature of the existence of a hydrate form and an amorphous form of paclitaxel (Dordunoo and Burt, 1996; Adams *et al.*, 1993). Solvates of paclitaxel have also been identified (Mastropaolo *et al.*, 1995). Elucidation of the solid state properties of paclitaxel and the identification of different solid forms of the drug could explain the wide range of solubility data that have been reported in the literature. Values of aqueous solubility of paclitaxel between 0.3 and 30 µg/ml have been reported (Sharma *et al.*, 1995).

The delivery of chemotherapeutic agents using polymeric microspheres has become a popular area of research because of the possibilities of achieving controlled release and of localising the delivery of cytotoxic agents. This strategy has been applied to the intraperitoneal injection of cisplatin for the treatment of ovarian cancer (Kumagai *et al.*, 1996). Paclitaxel has also been identified as a good candidate for intraperitoneal injection because of its slow clearance from the peritoneum (Eisman *et al.*, 1994), and effectiveness in treating ovarian cancer. The efficacy of paclitaxel is dependent on both drug concentration and on exposure time (Rowinsky *et al.*, 1988). Thus microspheres that remain in the peritoneal cavity and release paclitaxel for a prolonged period while limiting systemic exposure would represent an improvement over the current systemic

1

formulation. Despite this potential advantage, paclitaxel loaded microspheres have never been evaluated for this purpose.

Another application of intraperitoneal chemotherapy is the prevention of intraperitoneal carcinomatosis. In tumour resection surgeries there is the potential for a tumour cell spill that can cause intraperitoneal carcinomatosis due to handling of tumours or cutting through tumour margins (Jacquet *et al.*, 1995). The freed tumour cells can circulate within the peritoneum resulting in proximal metastases to the abdominal wall and the organs within the peritoneum. It is hypothesised that paclitaxel loaded microspheres of sufficient size, administered at the time of surgery, could remain entrapped in the peritoneum due to their large size and release paclitaxel over several weeks in order to prevent growth of tumours after a tumour spill.

The drug release properties of microsphere formulations are dependent on several factors. These include the nature of the polymer and the drug, the polymer molecular weight, and the manufacturing conditions which, in turn, affect properties such as microsphere size, surface morphology and the physical state of the polymer and drug within the matrix. Blending technology, which allows the production of new biomaterials without the need to resort to chemical synthesis of new compounds (Gesner, 1969) may also be used to alter the properties of the matrix of polymer microspheres. Polymer blending has been used to alter drug release profiles, mechanical strength, swelling characteristics, and biodegradation profiles of microspheres (Bodmeier *et al.*, 1989, Heya *et al.*, 1991). Therefore, paclitaxel microsphere formulations with different release characteristics can be made by altering the polymer composition and manufacturing parameters.

2

In this work, paclitaxel loaded microspheres were made using blends of poly(L-lactic acid) (PLLA) polymers. PLLA has well-established biocompatibility (Kulkarni *et al.*, 1971) and biodegradability (Holland *et al.*, 1986) and has been used for other microsphere formulations (Kishida *et al.*, 1990; Pavanetto *et al.*, 1993). PLLA was selected for this work because it has been shown to be semicrystalline over a wide range of molecular weights (Celli and Scandola, 1991). Therefore low molecular weight PLLA would be expected to be harder and able to form paclitaxel loaded microspheres with good handling characteristics, whereas low molecular weight, completely amorphous polymers, such as poly(lactic-co-glycolic acid) (PLGA), have been shown to form paclitaxel microspheres that are soft and cannot be resuspended (Guan, 1996). There are no reports in the literature in which PLLA polymers of different molecular weight have been blended to alter drug release from a drug delivery system.

In this project it was hypothesised that by blending different molecular weights of PLLA, drug release and matrix erosion profiles of paclitaxel loaded microsphere could be modulated. It is essential to characterise the thermal properties and polymer crystallinity in microspheres with different polymer compositions, since these would affect release properties by controlling drug transport out of the matrix and the rate of erosion of the matrix.

The specific aims of this project were to:

1) Characterise the solid state properties of paclitaxel and confirm the existence of hydrate or amorphous forms of paclitaxel.

2) Characterise the effects of polymer molecular weight on the physical properties and drug release profiles of paclitaxel loaded PLLA microspheres.

3) Characterise the effects of blending low and high molecular weight PLLA on the physical properties and drug release profiles of paclitaxel loaded microspheres.

4) Determine the particle size of PLLA microspheres that could be retained in the peritoneal cavity of rats.

5) Evaluate the efficacy of paclitaxel loaded microspheres in an *in vivo* model of intraperitoneal carcinomatosis caused by a tumour cell spill.

2.   BACKGROUND

2.1.   Solid state properties of drugs

2.1.1.   Models of crystallinity and degree of crystallinity

A crystalline solid is one in which the constituent molecules are regularly

arranged within a crystal lattice with long range order. Crystals are generally regarded as

"imperfect" since every crystal lattice possesses regions that deviate from the regular

geometry, called crystal defects. The most common defects include dislocations,

vacancies and impurities.

The term "degree of crystallinity" has been used to describe the degree of order

within a crystalline lattice where degrees of crystallinity vary over a continuous scale

from 100% for a perfect crystal to 0% for an amorphous material (Suryanarayanan and

Mitchell, 1985). According to this concept of crystallinity, called the "one-state model",

the degree of crystallinity decreases as the level of disorder caused by defects increases.

Degree of crystallinity has also been defined as the fraction "of crystalline drug in a

sample containing both amorphous and crystalline states" (Black and Lovering, 1977).

This is called the "two-state model".

The degree of crystallinity has been calculated using X-ray powder diffraction

(XRPD) peak intensities (Black and Lovering, 1977; Nakai *et al.*, 1982) and heats of

recrystallisation and fusion (Yoshioka *et al.*, 1994; Saleki-Gerhardt *et al.*, 1994).

Solution calorimetry (Pikal *et al.*, 1978), density measurements (Duncan-Hewitt and

Grant, 1986) and infrared absorption measurements (Black and Lovering, 1977) have

also been used. The general principle in all of these methods is the comparison of the

5

value of the property in question with values for 100% crystalline and amorphous materials. The general equation for the calculation of the degree of crystallinity is:

$$X_C = \frac{P_S - P_A}{P_C - P_A} \times 100\%$$ Equation 1

where X_C is the degree of crystallinity. P_S, P_C and P_A are the values of a property that depends on crystallinity, such as density, enthalpy of solution or enthalpy of fusion for the sample being measured, 100% crystalline and amorphous materials, respectively. Values of P_A and P_C are obtained from standards selected to approximate 100% amorphous and crystalline material, respectively.

2.1.2. Amorphous solids

Amorphous solids possess no long-range order within the solid matrix. Amorphous solids have been formed by lyophilization and spray drying of solutions, grinding of crystalline solids (Otsuka and Kaneniwa, 1988) and by rapid cooling from a melt, called quench cooling (Yoshioka et al., 1994; Hancock and Zografi, 1997).

Quench cooling of a liquid has the effect of producing a highly viscous material with random orientation of the molecules in the solid form. Thus amorphous solids may be regarded as metastable, supercooled liquids possessing liquid properties such as the ability to flow when stress is applied (Martin, 1993a). Other properties of amorphous materials include a diffuse XRPD pattern (Suryanarayanan and Mitchell, 1985) and a dissolution rate and apparent solubility greater than those observed for crystalline forms of the same compound (Florence and Salole, 1975; Hancock and Zografi, 1997).

6

The thermal properties of amorphous materials have been widely investigated for both small molecules (Yonemochi *et al.*, 1997; Hancock and Zografi, 1997) and polymers (Gee, 1970; Rosen, 1993c). Amorphous materials exhibit a transition between the glassy and rubbery states at the glass transition temperature (Tg). Below the Tg, in the glassy state, amorphous solids are brittle because molecular motion is highly restricted and flow is observed only over very long periods of time. Above the Tg, molecular motion is increased and amorphous solids become rubbery. The transition from a glassy to a rubbery state results in a decrease in heat capacity (Cp) and an increase in the coefficient of thermal expansion (Rosen, 1993c; Hancock and Zografi, 1997).

Above the Tg, molecules in an amorphous solid may attain sufficient mobility to recrystallise in a more stable form. Saleki-Gerhardt and Zografi (1994) have investigated the factors inducing crystallisation from the amorphous state. The degree of supercooling below the melting point (Tm) of the crystalline form provides the driving force for nucleation of crystals, while heating above Tg results in an increased mobility of the molecules diffusing to the growing crystal surface. Thus, increasing the temperature decreases the nucleation rate but increases the rate of crystal growth. Jolley (1970) has addressed the mechanism of crystallisation from amorphous solids and the effects of these two opposing factors in his studies of amorphous gelatin. Generally, a range of temperatures exists near the halfway point between Tg and Tm where crystallisation is observed. However, recrystallisation of indomethacin has been shown to occur at temperatures below Tg (Otsuka and Kaneniwa, 1988; Yoshioka *et al.*, 1994), indicating that sufficient molecular motion for crystallisation can exist even in some glasses.

Glassy materials have been categorised as being either fragile or strong (Angell *et al.*, 1991, 1994). Strong glasses exhibit only small changes in heat capacity (Cp) at the glass transition and the ratio of Tm to Tg (in degrees K) is greater than 1.5. Conversely, fragile glasses exhibit larger changes in Cp, and a Tm to Tg ratio less than 1.5. Glass fragility describes the way in which an amorphous solid responds to changes in temperature. An ideal strong glass has an Arrhenius-type linear dependence of the logarithm of viscosity on the inverse of temperature. Fragile glasses deviate negatively from this behaviour. This relationship is described by the Volgel-Fulchen-Tamman equation:

$$\ln \eta = A + \frac{B}{T - C} \qquad \qquad \text{Equation 2}$$

where A, B, and C are constants and η and T are the viscosity and temperature, respectively. For strong glasses, C is close to zero and B represents the apparent activation energy of molecular motion. For increasingly fragile glasses, C becomes larger and the apparent activation energy of molecular motion becomes temperature dependent. In these cases, temperature has a greater effect on molecular mobility near Tg than would be expected for stronger glasses.

The extent of molecular motion will also determine the rate of relaxation that occurs in an amorphous solid below Tg. Volume and enthalpy relaxation occur as metastable glasses rearrange their structure through limited molecular motion to achieve a more favourable conformation. Due to their high viscosity, recrystallisation is generally not possible in the matrix. Enthalpy relaxation is observed for drugs such as

8

indomethacin which readily forms a glass (Yoshioka *et al.*, 1994) and is very common among polymers (Hancock *et al.*, 1995; Brunacci *et al.*, 1997).

2.1.3. Polymorphism

A polymorphic compound is one that can exhibit more than one crystalline form in the solid state. Polymorphs have different solid state properties, but are identical in the liquid and vapour states (McCrone, 1965; Haleblian, 1975). Several classes of drugs such as steroids (Mesley and Johnson, 1965) barbiturates (Mesley and Clements, 1968; Mesley *et al.*, 1968) and nonsteroidal anti-inflammatories (Summers *et al.*, 1970; Vercer *et al.*, 1991) have been extensively characterised with respect to polymorphism.

Altering the conditions under which the solid recrystallises may produce polymorphic forms. Changes in recrystallisation temperature (Behme *et al.*, 1985) solvent (Griesser *et al.*, 1997; Tros de Ilarduya *et al.*, 1997) and cooling and evaporation rates of solutions (Griesser *et al.*, 1997) have been used to produce polymorphs. Different thermal conditions used to recrystallise a solid from the melt may also result in the formation of different polymorphs (McCrone, 1962).

Polymorphism and its effects on the physical properties of solids have been reviewed by several authors (Hartshorne and Stuart, 1960; Haleblian and McCrone, 1969; Haleblian, 1975). Polymorphs of a drug can exhibit differences in solubility (Behme *et al.*, 1985), chemical stability and bioavailability (Haleblian, 1975). Crystal structure information obtained by XRPD and infra-red (IR) spectral studies are used to provide evidence for the existence of polymorphic forms (Wu *et al.*, 1993; Tros de Ilarduya *et al.*, 1997; Griesser *et al.*, 1997).

Except at an equilibrium transition point between two forms, only a single polymorphic form is stable at a given temperature and pressure; all others are metastable. The stability of different solid forms relative to one another is described in terms of monotropic and enantiotropic systems (McCrone, 1965; Haleblian and McCrone, 1969; Yu, 1995). In a monotropic system, one polymorphic form is less stable than another at all temperatures and pressures. In an enantiotropic system, ranges of temperature and pressure exist in which each of the two forms are the most stable. A change of phase between polymorphs is irreversible in monotropic systems but reversible in enantiotropic systems.

2.1.4. Solvates

A solvate is a compound that contains solvent molecules incorporated into the crystalline lattice. A stoichiometric relationship exists between the number of parent and solvent molecules in the lattice. Several solvates of a parent compound may exist with different stoichiometric amounts of solvent molecules within the lattice. When the solvent molecules are water, the solvate is referred to as a hydrate. There are numerous reports of solvates of drugs (Pfeiffer et al., 1970; Kitaoka et al., 1995) and pharmaceutical excipients (Saleki-Gerhardt et al., 1995). Each solvate is a compound distinct from the non-solvated form, and may exhibit different properties such as X-ray diffraction pattern (Suryanarayanan, 1989), solubility, dissolution rate and enthalpy of solution (Ledwidge et al., 1996). Generally, the solubility of a solvate is lower and the dissolution rate slower compared to the non-solvated form.

Solvates may be formed by recrystallisation from the solvent to be incorporated in the lattice (Shefter and Higuchi, 1963). Pfeiffer et al. (1970) observed that by altering

10

the composition of a ternary solvent system of water, methanol and acetic acid, five

distinct solvates and one non-solvated form of cephaloglycin were produced. By varying

the vapour pressure of water in contact with raffinose, hydrates with varying

stoichiometries were produced (Saleki-Gerhardt *et al.*, 1995).

Complete dehydration was achieved in raffinose hydrates by decreasing the

vapour pressure below a critical level or by heating. Dehydration has also been observed

to occur as a result of milling or direct compression of cyclophosphamide monohydrate

(Ketolainen *et al.*, 1995). However, the crystal lattice structure may not change with

desolvation (Garner, 1955). Rather, the lattice points formerly occupied by solvent

molecules become vacancies. Thus X-ray diffraction peak positions may be unchanged

while their intensities are reduced due to a decrease in the degree of crystallinity.

2.2.   Paclitaxel

2.2.1.   Sources

Paclitaxel (shown in Figure 1) was first obtained by extraction from the bark of

the Western Yew (*Taxus brevifolia*) (Wani *et al.*, 1971) with a yield of 0.01%w/w.

Other methods of extraction have achieved yields as high as 0.04%w/w (Rao *et al.*,

1995). The limited supplies of slow growing yew trees and low yields of paclitaxel after

extraction have made alternative sources of paclitaxel necessary. Paclitaxel has been

extracted from harvested needles of another species of yew trees, *Taxus x media*

Hicksii, (Witherup *et al.*, 1990). A semisynthetic method for the production of paclitaxel

from 10-deacetyl baccatin III obtained from needles of *Taxus baccata* has been

developed, which has gained commercial application (Denis *et al.*, 1991; Holton *et al.*, 1992). Total synthesis of paclitaxel has also been accomplished by Holton *et al.* (1994) and Nicholaou *et al.* (1994).

Figure 1. The chemical structure of paclitaxel. Numbers in italics are the numbers assigned to carbons in the structure in IUPAC nomenclature.
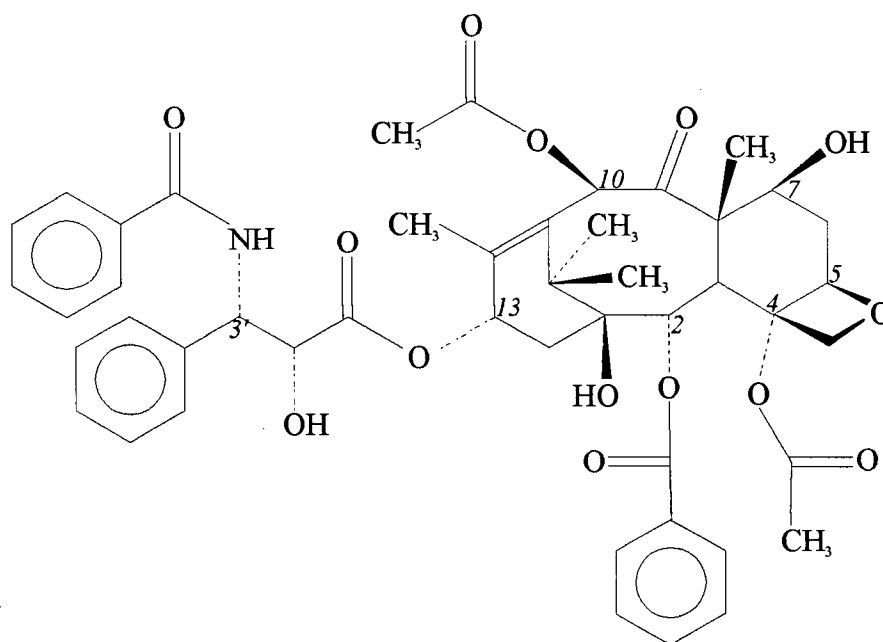
2.2.2. Chemistry

2.2.2.1. Structure

Paclitaxel is a member of a group of compounds called taxanes (Lythgoe *et al.*, 1964) which are characterised by the presence of a tricyclic ring system in the structure. The chemical structure (Figure 1) shows the taxane core composed of a C-20 skeleton, a complex side chain at C-13, two acetoxy groups at C-4 and C-10 and a phenoxy group at C-2. The numbering scheme conforms to the IUPAC nomenclature. The structure of

12

paclitaxel has been elucidated by NMR and X-ray crystallographic techniques. Several authors have reported spectra using ^{1}H-NMR (Miller *et al.*, 1981; Kingston *et al.*, 1982) and ^{13}C-NMR (Magri, 1985). Proton and carbon assignments have been reported with the spectra and these have been summarised by Kingston (1991).

Single crystal X-ray crystallographic data have been reported for paclitaxel crystals precipitated from a cosolvent system of dioxane, water and xylene (Mastropaolo *et al.*, 1995). The analysis showed that the solid form was a solvate containing several dioxane and water molecules, but the stoichiometry was not reported.

The conformation of pure paclitaxel in organic solvents has been studied for chloroform, acetonitrile, methanol and benzene at concentrations of paclitaxel up to 0.9 mg/ml (Chmurny *et al.*, 1992; Vander Velde *et al.*, 1993; Balasubramanian *et al.*, 1994). NMR data in chloroform were used to propose a three dimensional structure for paclitaxel with the cup-shaped taxane ring structure and an extended side chain similar to that of the crystalline molecular conformation. However, in more hydrophilic solutions a conformational change is observed in which the C-13 side chain is less extended (Vander Velde *et al.*, 1993).

2.2.2.2. Solubility

Values for the aqueous solubility of paclitaxel at 37°C of 0.7 μg/ml (Mathew *et al.*, 1992), 6 μg/ml (Tarr and Yalkowsky, 1987), 11 μg/ml (Lundberg, 1997) and 30 μg/ml (Swindell and Krauss, 1991) have been reported. Dissolution studies at 25°C have shown an initial apparent solubility of 6 μg/ml with a decrease to 0.34 μg/ml after a 24 hour period (Sharma *et al.*, 1995). Adams *et al.* (1993) suggested that the higher initial apparent solubility could be due to an amorphous form of paclitaxel. The solubility of

paclitaxel in organic solvents has not been studied. However, a solubility at 37°C for paclitaxel in 50:50 ethanol:water of 14 μg/ml has been reported (Dordunoo and Burt, 1996).

2.2.2.3. Stability

Dordunoo and Burt (1996) determined the chemical degradation of paclitaxel in aqueous buffers. Hydrolytic degradation followed pseudo-first order kinetics and the major degradation products were baccatin III, 10-deacetylbaccatin III and baccatin V. Degradation of paclitaxel was pH dependent, being catalysed by both acids and bases, with the greatest drug stability in the pH range of 3 to 5. Paclitaxel also underwent pseudo first-order degradation in methanol to produce baccatin III and 10-deacetylbaccatin III (Wani *et al.*, 1971; MacEachern-Keith *et al.*, 1997). More vigorous methanol treatment at pH 9 gave baccatin III as the major degradation product with small amounts of 10-deacetyltaxol, baccatin V, 10-deacetylbaccatin III and 10-deacetylbaccatin V also being produced (Ringel and Horwitz, 1987; Lataste *et al.*, 1984). MacEachern-Keith *et al.* (1997) showed that paclitaxel had excellent stability in DMSO and isobutyl alcohol, having a half-life in both solvents of 28 years.

2.2.3. Pharmacology

2.2.3.1. Mechanism of action

Paclitaxel binds to the beta-tubulin sub-unit and promotes the assembly of microtubules (Parness and Horwitz, 1981; Collins and Vallee, 1987; Rao *et al.*, 1994). Collins and Vallee (1987) and Parness and Horwitz (1981) both reported a binding constant of approximately 0.9 μmol/L for paclitaxel and polymerised tubulin but a value

14

of 10 nmol/L has also been published (Caplow *et al.*, 1994). Concentrations as low as 0.05 µmol/L have been shown to be effective in promoting the polymerisation of tubulin sub-units *in vitro* (Schiff and Horwitz, 1980). Microtubules formed in the presence of paclitaxel are dysfunctional (Mole-Bajer and Bajer, 1983; Rowinsky *et al.*, 1988), causing the interruption of normal cell functions including mitosis (Jordan *et al.*, 1993), intracellular transport, secretion of vesicles (Stearns and Wang, 1992) and cell motility (Schiff and Horwitz, 1980) as well as cytotoxicity (Wood, 1995). *In vitro*, paclitaxel is cytotoxic at concentrations between 0.1 and 1 µmol/L for several tumour cell lines including glioblastoma (Cahan *et al.*, 1994) and leukaemia (Rowinsky *et al.*, 1988).

Structure-activity relationships have been studied extensively and are reviewed by Kingston (1991). The most important feature of paclitaxel's structure with respect to activity is the C-13 side chain. Deletion of the side chain yields baccatin III, which showed a 1700-fold decrease in anti-mitotic activity in KB (human nasopharyngeal carcinoma) cells (Wani *et al.*, 1971; Miller *et al.*, 1981). Modification of the side chain substituents resulted a 10 to 300-fold reduction in activity in both microtubule and cell culture assays (Wani *et al.*, 1971; Lataste *et al.*, 1984). Modifications of the taxane ring structure and of its side groups resulted in a decrease in activity for all derivatives studied (Guéritte-Voegelein *et al.*, 1991). Acylation or epimerization of the C-7 hydroxyl group was responsible for only a slight decrease in activity whereas acetylation and oxidation of this group caused a greater than 400 and 1000-fold decrease in activity against KB cells, respectively (Lataste *et al.*, 1984). Opening of the oxetane ring incorporating carbons 4 and 5 resulted in a 1000 to 10000-fold decrease in activity (Kingston *et al.*, 1990).

2.2.3.2. Anticancer activity

Although paclitaxel has been demonstrated to be clinically effective against a variety of cancers (Rowinsky, 1994), it is only approved for ovarian and breast cancers. Phase II trials of single agent paclitaxel against recurrent ovarian cancer have produced response rates in the range of 20 to 37%, with complete responses in 3 to 12% of cases (Enzig et al., 1992; McGuire et al., 1989; Thigpen et al., 1990). Breast cancer treatment has also shown positive results in phase II trials. Holmes et al. (1991) and Seidman et al. (1992) both reported total response rates of approximately 60%. The patients all had advanced breast cancer and had received no prior treatment. In a trial with patients who had failed conventional therapy, response rates were between 22 and 29% (Gelmon et al., 1994).

2.2.3.3. Toxicity

Because of paclitaxel's poor water solubility, it is currently administered as a solution in equal parts of polyethoxylated castor oil (Cremophor EL®) and absolute ethanol (Taxol®) which is diluted prior to infusion in 5% Dextrose Injection. The Cremophor EL® vehicle caused life-threatening anaphylaxis in early human trials (Weiss et al., 1990) so patients must be premedicated with corticosteroids, antihistamines and H_2 receptor antagonists (Arbuck et al., 1993). However, even with premedication, anaphylaxis-type reactions were still observed in under 5% of patients (Weiss et al., 1990; Arbuck et al., 1993).

Forty phase I and II clinical trials of paclitaxel at doses between 5 and 390 mg/m^2 administered by intravenous infusion over 1 to 96 hours were reviewed by Spencer and Faulds (1994). The dose limiting toxicity was neutropenia or leukopenia in the majority

16

of cases. Peripheral neuropathy occurred in greater than 60% of patients receiving doses of 200 mg/m² and higher. Other toxicities, ranked in order of greatest frequency, were anaemia, alopecia, gastrointestinal effects, myalgia/arthralgia, hypersensitivity reactions, thrombocytopaenia, and cardiac and hepatic effects.

2.2.4. Pharmacokinetics

In pharmacokinetic studies, paclitaxel has been administered by intravenous infusion over 1 to 24 hours. After a 6 hour infusion of a 275 mg/m² dose of paclitaxel, the maximum concentration in plasma (C_{max}) was 10 µmol/L (Wiernik *et al.*, 1987a). After a 24 hour infusion of the same dose, the C_{max} was 5 µmol/L (Wiernik *et al.*, 1987b). At a dose of 135 mg/m² given as a 24 hour infusion the C_{max} was 0.2 µmol/L (Huizing *et al.*, 1993). Values of the apparent steady-state volume of distribution for paclitaxel are high, ranging from 59 – 657 L/m² with a mean of 166 L/m² (Rowinsky and Donehower, 1995; Kuhn 1994).

Paclitaxel is 95 to 98% plasma protein bound (Rowinsky *et al.*, 1992), with a mean clearance from plasma of 19 L/h/m² and a range between 8 and 26 L/h/m² (Rowinsky and Donehower, 1995; Kuhn, 1994). Renal elimination of paclitaxel accounts for between 4 and 8% of the total dose (Wiernik *et al.*, 1987a; Longnecker *et al.*, 1987) and biliary excretion accounts for approximately 20% of the drug (Monsarrat, 1990). The major route of elimination of paclitaxel is metabolism in the liver and excretion in faeces. After seven days, 75% of a radiolabeled dose of paclitaxel was recovered from human faeces (Monsarrat, 1990). The major metabolite of paclitaxel in humans is 6α-hydroxypaclitaxel (Kumar *et al.*, 1994a). Cytochrome P450 isozymes 2C and 3A have

17

been shown to convert paclitaxel into 6α-hydroxypaclitaxel (Cresteil *et al.,* 1994; Kumar *et al.,* 1994b).

2.3.   Polymeric drug delivery

Polymeric drug delivery systems have been used to achieve both targeted and controlled delivery of drugs. The goal of targeted delivery is to deliver a drug to a specific site in the body, minimising the systemic drug exposure and side effects. Targeting of a drug can be achieved by administering it at its site of action using polymeric implants or microspheres. Poly(methyl methacrylate) (PMMA) implants containing mitomycin, adriamycin and 5-fluorouracil have been implanted in the treatment of glioblastoma and astrocytoma (Domb *et al.,* 1991). Microspheres containing cisplatin (Spenlehauer *et al.,* 1986; Li *et al.,* 1994) and 5-fluorouracil (Çiftçi *et al.,* 1994) have been used in chemoembolic therapies to localise anticancer drugs in the liver.

The goal of controlled release technology is to produce formulations that can deliver a therapeutic concentration of drug over a prolonged period and at a controlled rate with minimal toxicity (Langer, 1990). Research interest in polymeric drug delivery has moved increasingly towards the use of biodegradable polymers that can be eliminated from the body without the need for invasive retrieval processes required for nondegradable polymers such as poly(ethylene-co-vinyl acetate).

Biodegradation has been most broadly defined by Gilding (1981) as breakdown of a polymer by any mechanism *in vivo.* A more precise definition has been described using the terms direct, indirect, and macrobiological biodegradation, meaning degradation accomplished by enzymatic, oxidative, and mechanical pathways respectively (Griffin, 1980). Biodegradable polymers of interest include polyesters such

as poly(ε-caprolactone) (PCL) (Pitt, 1990), and poly(DL-lactic acid) (PDLLA) (Kwong *et al.*, 1986) and poly(glycolic acid) (PGA) (Holland *et al.*, 1986). These have been used to produce implant devices (Pitt, 1990; Chasin *et al.*, 1990) as well as microparticulate systems (Bogdansky, 1990; Pitt, 1990). New polymers are constantly being developed for use in controlled delivery devices (Holland *et al.*, 1986; Pulapura and Kohn, 1992).

In order to provide prolonged drug delivery and to find an alternative to the Cremophor vehicle, polymeric formulations containing paclitaxel have been developed. Walter *et al* (1994) prepared paclitaxel loaded disks of poly[bis-(*p*-carboxyphenoxy)-propane-co-sebacic acid] (CPPSA). From an 11 mg disk containing 20%w/w paclitaxel, approximately 80% of the total paclitaxel was released *in vitro* over six weeks. The implants were evaluated *in vivo* in a model of malignant glioma in the brains of rats. The survival times of the rats, in which were implanted 1 mm^3 9L-glioblastoma tumours, were extended 1.5 to 3.2 fold by treatment with 20%w/w paclitaxel loaded disks and the implants appeared to be well tolerated by the animals. Winternitz *et al.* (1996a) have produced a paste from blends of PCL and methoxy(polyethylene glycol) (MePEG). The paste was loaded with paclitaxel at levels up to 30%w/w and *in vitro* release studies showed that less than 10% of the total loaded amount was released after three weeks. *In vivo* evaluation of the paste showed that a delay in tumour regrowth of five days could be achieved by implantation of the paste in mice after partial resection of an established RIF-1 tumour (Winternitz, 1996b).

Burt *et al* (1995) were the first to develop paclitaxel loaded microspheres made from a blend of poly(ethylene vinyl-co-acetate) (EVA) and PDLLA. Paclitaxel loaded microspheres have also been formed from PCL (Dordunoo *et al.*, 1995) and PLGA

(Wang *et al.*, 1996, 1997). For all formulations, between 2 and 15% of the paclitaxel

incorporated into the microspheres was released *in vitro* over a three week period. The

extent of release was increased to 60% from PLGA microspheres over the same time

period by the addition of a hydrophobic additive, isopropyl myristate (Wang *et al.*, 1997).

Two nanosphere formulations incorporating paclitaxel into PDLLA (Bartoli *et al.*, 1990)

and poly(vinyl pyrrolidone) (Sharma *et al.*, 1996) have also been reported.

2.4.   Drug release mechanisms

2.4.1.   Mathematical models and factors affecting release

Diffusion of a dissolved drug through a polymer matrix is described by Fick's first law,

$$\text{Flux} = -D\frac{dC}{dx} \qquad \text{Equation 3}$$

where D is the diffusion coefficient and dC/dx is the concentration gradient. The

negative sign in Equation 3 accounts for diffusion proceeding from the point of highest

concentration to the lowest. In the case of a monolithic drug delivery system in which a

drug is dissolved and uniformly dispersed within the matrix, no concentration gradient

exists in the matrix prior to the onset of drug release. As the drug begins to be released

from the surface of the matrix, a concentration gradient is established. Drug begins to

diffuse down the concentration gradient from the interior of the matrix towards the

surface and is gradually released at the surface.

The kinetics of this process for a slab have been described by Crank (1956),

$$\frac{M_t}{M_0} = 1 - \sum_{n=0}^{\infty} \frac{8e^{(-D(2n+1)^2\pi^2 t/l_s^2)}}{(2n+1)^2\pi^2} \qquad \text{Equation 4}$$

where M_t and M_0 are the total amount released and total amount of drug loaded into the matrix, respectively, l_S is the slab thickness and t is time. For release from a spherical matrix, the release kinetics have also been described (Crank, 1956) and reduced to two approximation equations which deviate by less than 1% from the equation of Crank (Baker, 1987),

$$\frac{M_t}{M_0} = 6\left(\frac{Dt}{r^2\pi}\right)^{1/2} - \frac{3Dt}{r^2} \qquad \text{for } 0 \leq M_t/M_0 \leq 0.4 \qquad \text{Equation 5}$$

and,

$$\frac{M_t}{M_0} = 1 - \frac{6}{\pi^2}e^{\left(\frac{-\pi^2 Dt}{r^2}\right)} \qquad \text{for } 0.6 \leq M_t/M_0 \leq 1 \qquad \text{Equation 6}$$

where r is the radius of the sphere and is analogous to l_S, the slab thickness.

If the amount of drug incorporated into a polymer matrix exceeds the solubility of the drug in the matrix material, a solid dispersion termed a "granular matrix" results (Higuchi, 1963). A granular matrix has pores that contain the phase-separated drug. Porosity (ε) is a dimensionless number equal to the product of the amount of drug per unit volume of the matrix and the specific volume of the drug. As the porosity increases, pores begin to interconnect to form channels. The geometry of these channels is described by a term called tortuosity (τ). Higuchi derived an equation for diffusion of drugs through granular matrices, incorporating both ε and τ. The equation is a "pseudo-steady state" equation for Fickian release for dispersions where the amount of drug dissolved in the matrix remains constant due to the presence of excess undissolved drug. The equation describing release from a spherical granular matrix is (Higuchi, 1963):

$$\frac{3}{2}\left[1-\left(\frac{M_t}{M_0}\right)^{\frac{2}{3}}\right]-\frac{M_t}{M_0}=\frac{3D\varepsilon}{\tau}\frac{C_s}{r^2 C_0}\cdot t \qquad\qquad \text{Equation 7}$$

where C_s and C_0 are the solubility of the drug in the matrix and the initial total drug concentration, respectively.

When a biodegradable or soluble polymer is used to form the matrix from which drug is released, the kinetic equations become difficult to solve because values of A, D, ε, τ and r (for spheres) change with degradation and erosion of the matrix. Generally release rates increase with degradation or erosion of the matrix.

The effects of polymer and drug properties on release kinetics have been investigated and modelled by several authors. Heya et al. (1991) observed a greater initial burst phase release of thyrotropin releasing hormone from PLGA microspheres as the loading level increased. The effects of drug loading have been the subject of mathematical modelling using compounds with a wide range of solubilities (El-Arini and Leuenberger, 1995) and monolithic matrices that allowed release from a single surface with controlled area. For water soluble compounds, release obeyed Fickian release kinetics, but for less soluble compounds, a non-Fickian mechanism resulted in near zero-order release. In both cases, the rate increased as the loading level increased.

Polymer molecular weight affects drug release rates in a number of ways. As the molecular weight of a polymer decreases, the matrix generally becomes more permeable to drugs. This has been attributed to increased hydrophilicity of the matrix (Heya et al., 1991), decreased density and a lowered glass transition temperature (Omelczuk and McGinity, 1992) which allows swelling of the matrix and greater molecular mobility of

22

the drug and polymer chains. The molecular weight is also related to degradation and erosion rates of the matrix (Sanders *et al.*, 1986; Heya *et al.*, 1991).

Polymer crystallinity can affect drug release rates by impeding the diffusion of drugs through the matrix as well as lowering the degradation and erosion rates of the matrix (Pitt, 1990). Crystalline regions within the matrix are less accessible to water and drug molecules than are amorphous regions. Therefore, swelling is decreased and the diffusion pathway for drugs becomes longer with increased tortuosity as drug molecules must diffuse around crystallites.

Figure 2 shows a schematic diagram illustrating the drug release profiles from microspheres that can result from various release mechanisms. Curves A and B in Figure 2 show the release kinetics of Baker (1987) and Higuchi (1963) for drugs from monolithic solutions and granular matrices, respectively. In both cases an initial rapid phase of release is observed which slows with time. Curve C illustrates the same diffusion mechanism as in Curve A, with the onset of a second rapid phase of release after some time. This type of profile is observed for diffusion from a matrix that begins to degrade and erode resulting in a sudden increase in the release rate. Curve C represents three separate phases of release that have been observed for microspheres made from biodegradable polymers (Ghaderi *et al.*, 1996); a "burst phase" of diffusion controlled release that gives way to a slower phase of diffusion controlled release and finally the onset of more rapid degradation controlled release.

2.4.2. The burst phase of drug release

For most microsphere formulations, drug release begins with a "burst phase", or a period of rapid release of drug which is located in the superficial layers of the matrix

called "surface associated" drug (refer to Curves A to C in Figure 2). The burst effect has

been shown to be dependent on microsphere size (Cowsar *et al.*, 1985; Ghaderi *et al.*,

Figure 2. Schematic diagram of drug releases profiles showing the effects of different
drug release mechanisms.
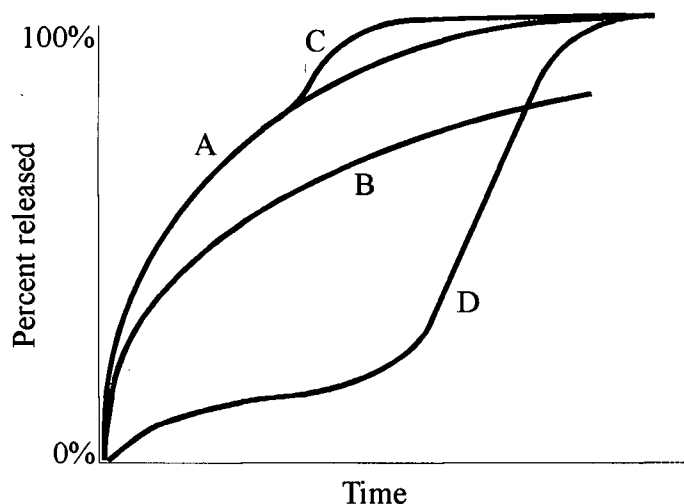
A) Diffusion controlled release from a sphere containing
   dissolved drug (Baker, 1987)
B) Diffusion controlled release from a granular matrix with
   spherical geometry (Higuchi, 1963)
C) Triphasic release: initially diffusion controlled release
   (Baker, 1987) followed by the onset of degradation
   controlled release
D) Sigmoidal release: initially diffusion controlled release
   (Baker, 1987) with a reduced initial "burst phase" an
   delayed onset of degradation controlled release

1996). Microspheres of smaller sizes possess a larger surface area/volume ratio, thus a

higher proportion of surface associated drug will be present and a more extensive burst

effect will be observed. The method of manufacturing microspheres has been shown to

affect the burst phase of drug release (Izumikawa *et al.*, 1991). Reducing the pressure

under which solvent was removed from microspheres during their formation resulted in

24

the elimination of the burst phase, illustrated by Curve D in Figure 2. The later increase

in the drug release rate (Curve D, Figure 2) illustrates the onset of degradation and

erosion controlled release for degradable matrices. Elimination of the burst phase by

altering the solvent removal technique coincided with a change in the surface

morphology of the microspheres (Izumikawa et al.,1991). To eliminate the burst phase

effect, microspheres have been coated with a polymer matrix which contains no drug

(Göpferich et al., 1994; Pekarek et al., 1994) and washed after manufacture to remove

surface associated drug (Kwong et al., 1986).

2.4.3. Diffusion and degradation controlled release

Following the burst phase is a period of slower release generally ascribed to

diffusion of the drug out of the matrix. Release of hydrocortisone from PDLLA

microspheres showed an initial rapid phase of release that slowed over time. The drug

release profile fit the Higuchi equation for release from a spherical granular matrix

(Leelarasamee et al., 1986). However, attempts to match release profiles to kinetic

equations are usually not possible because too many variables exist. PDLLA

microspheres which released oxytetracycline (Vidmar et al., 1984) followed apparent

zero-order release kinetics which are inconsistent with the equations for diffusion of drug

in solution, (Equations 5 and 6) or from a granular matrix (Equation 7). However,

PDLLA microspheres containing mitomycin C did not exhibit zero-order drug release

(Tsai et al., 1986). The observed deviations from diffusion controlled kinetics are due to

the influence of other processes that affect the kinetic parameters D and ε, such as

swelling of the matrix with water, and degradation of polymer chains in the matrix. Tsai

et al. (1986) hypothesised that the aqueous solubility of the drug was too high for the drug release kinetics to fit the equation for diffusion.

A sigmoidal release profile (Curve D, Figure 2) was obtained for PLGA microspheres containing albumin as a model drug (Crotts and Park, 1995). The burst phase was very small, followed by a slow phase of release prior to the onset of erosion of the polymer matrix. When an early burst phase and later a degradation controlled phase are observed in the release profile, a triphasic release pattern results (Curve C, Figure 2) . Ghaderi *et al.* (1996) and Wakiyama *et al.* (1981) reported this behaviour for mannitol loaded PLGA and tetracaine loaded PDLLA microspheres, respectively.

2.5. Polymer Chemistry

2.5.1. Structure

2.5.1.1. Constitution and conformation

The term polymer constitution has been used by several authors (Miller, 1962; Billmeyer, 1984) to describe the atomic structure that makes up the repeating unit of a polymer. Changing the constitution of a polymer requires the breaking and reforming of interatomic bonds. Elements of structure that are important in determining the properties of a polymer such as chirality, isomerism, the presence of side groups, rigidity and planarity are defined by its constitution. Another element of polymer structure is that of conformation. Individual polymer chains can adopt many possible conformations by rotating each bond in the polymer backbone.

2.5.1.2. Morphology and models of crystallinity

Polymer morphology describes the arrangement in three dimensions of polymer chains with respect to long range order and the topic is well reviewed by several authors (Wünderlich, 1973; Eisenburg, 1993; Rosen, 1993b). Polymers do not achieve an equilibrium state in the solid form. Rather, polymer chains are disordered or only partly ordered with respect to adjacent chains, giving rise to amorphous or semicrystalline materials, respectively.

Two models of crystallinity have been used to describe the nature of semicrystalline polymers (Rosen, 1993b). The "Fringed Micelle Model" describes crystalline regions called crystallites interspersed in an amorphous matrix, as shown in Figure 3A. Several polymer chains are involved in each crystallite and each chain contributes to both amorphous and crystalline regions of the matrix. The model proposes the coexistence of crystalline and amorphous regions which are not separated by distinct boundaries, but it describes only a two-dimensional plane rather than a three dimensional matrix and does not account for chain folded crystallisation, observed in many polymer systems. Figure 3B shows a schematic of the "Chain Folded Model" of polymer crystallinity in which a single polymer chain folds upon itself to form lamellar crystallites interspersed in an amorphous phase. Several chains are involved in each crystallite, and extend into the amorphous regions of the matrix.

2.5.2. Polymer crystallinity

Polymers may adopt chain folded or extended chain (e.g polyethylene crystals) or helical (e.g. polypeptides) conformations (Wünderlich, 1973; Hearle, 1982).

Figure 3. Schematic drawings illustrating A) the Fringed Micelle Model and B) the Chain Folded Model of crystallinity. (Grey areas indicate crystallites.)
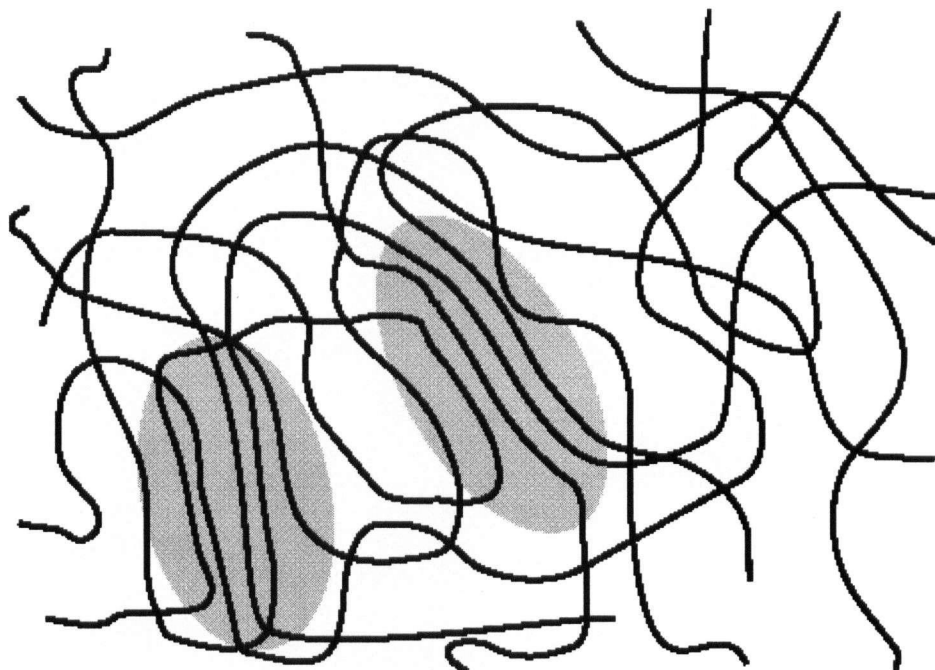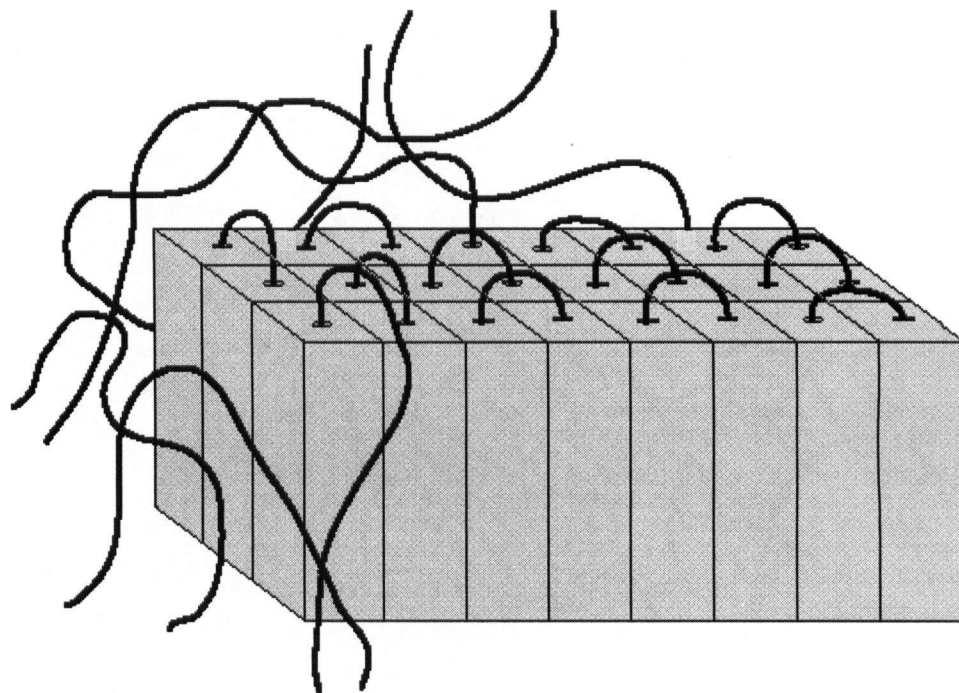
Irrespective of conformation, the crystalline regions of polymers are regularly ordered with polymer backbones aligned parallel to one another and side groups oriented in a regular fashion (Mandelkern, 1993). Several factors which contribute to crystallisation have been identified: a lack of side groups or branching, rigidity of the backbone, regular monomer configuration and the ability to form hydrogen bonds or dipole interactions (Rosen, 1993b).

Crystallisation can be achieved from a melt (bulk crystallisation) or by precipitation from solution. In dilute solutions, polymer chains experience minimal interactions with other chains and a maximal degree of mobility. As a result, single crystals with high degrees of perfection can be produced. Bulk crystallisation usually results in chain folded crystals (Wünderlich, 1973). Crystallisation from concentrated solutions is similar to bulk crystallisation except that solvent molecules may act as diluents or plasticizers (Mandelkern, 1964b).

Chain folding occurs as a result of competing driving forces during crystallisation. Interactions between and within polymer chains are required for crystalline structure and an increased number of interactions results in improved crystallite stability. In order for long chain molecules to maximise the number of interactions as it attaches to a growing crystallite face (whose length is several orders of magnitude smaller than the chain length), the chain must fold back on itself. Thus, as the crystallite grows, the faces that are not growing are formed of chain folds. These surfaces represent strain in the polymer chains and thus have increased surface energy relative to unfolded surfaces, resulting in decreased crystal stability. An optimal folding length that provides a balance between increased chain folding frequency giving a greater

number of intermolecular interactions and decreased frequency that minimises surface free energy has been described by Lindenmeyer (1967).

2.5.3. Molecular weight

Polymers consist of molecules that have a distribution of molecular weights. The best characterisation of a polymer's molecular weight therefore requires direct quantitative measurement of the entire distribution. However, it is more convenient to describe the distribution in terms of average polymer molecular weights. The number average molecular weight (M_n) is the arithmetic average of the molecular weight distribution. M_n is equal to total polymer weight divided by the number of molecules in the polymer. This average is sensitive to the presence of very small chains since all molecules contribute equally to the average value (Rosen, 1993a). A small fraction, by weight, may exist as small polymer chains or low molecular weight impurities, yet this fraction may represent a large proportion of the total number of molecules present in the polymer, skewing M_n to a lower value. The weight average molecular weight (M_w) is less sensitive to the presence of short chains in a polymer. M_w is weighted so that the contribution of each chain length fraction depends on its contribution by weight to the total sample (Rosen, 1993a). Thus ten small chains would have the same weighted importance as one chain ten times their length. The lower sensitivity of M_w to low molecular weight chains means that M_w values are always greater than M_n values. Example calculations of M_n and M_w values for a molecular weight distribution are shown in Appendix I.

The shape of a molecular weight distribution is reflected by the ratio of M_w to M_n, called the polydispersity index, or simply the polydispersity; wider distributions have

larger polydispersity indexes. However, despite the use of several averages, and a measure of polydispersity, the molecular weight distribution is not completely described. M_n, M_w and the polydispersity index cannot be used to describe the modality of a polymer molecular weight distribution, or the shape of a skewed unimodal distribution. In the case of bi- or trimodal distributions, the average values become misleading since each peak of the distribution has its own average values and polydispersity. These properties may be determined by gel permeation chromatography (GPC) which separates polymer chains based on their molecular weight and thus provides information on the entire molecular weight distribution.

2.5.3.1. Direct measurement of molecular weight

Direct measurement of M_n requires the quantification of the number of molecules in a polymer sample. End-group titration and osmotic pressure measurements have both been used for this purpose (Rosen, 1993a). If a polymer possesses a reactive end group, the concentration of the functional group in a solution can be determined. For this information to be related to the M_n, the stoichiometric relationship of the functional group concentration to the number of polymer chains must be known. Thus the presence of reactive side groups on a polymer chain would prohibit the use of this technique. Another limitation to this method is that as the molecular weight of a polymer increases, the concentration of the end groups per unit volume of total material decreases, and the sensitivity of the titration drops off rapidly. Thus this technique is useful only for polymers with M_n below 10k g/mol (Rosen, 1993a).

2.5.3.2. Indirect measurement of molecular weight

Two methods of indirect measurement of polymer molecular weight averages are based on the relationship of the molecular weight to the intrinsic viscosity ([η]) and the molecular size, described by the hydrodynamic radius (R_η), of a polymer chain, given by Einstein's equation of intrinsic viscosity:

$$[\eta] = \frac{CR_\eta^3}{MW}$$

Equation 8

where MW is the molecular weight and C is a proportionality constant. An intrinsic viscosity value of a polymer can be calculated using viscosity data obtained for dilute solutions of the polymer. Intrinsic viscosity can be used to calculate a molecular weight average using the Mark-Houwink equation:

$$[\eta] = KM_v^a$$

Equation 9

where K and a are constants and M_v is the viscosity average molecular weight. The value of M_v lies between the values of M_n and M_w, but will be closer to that of M_w.

Molecular size is measured by GPC (Kwei, 1979). Using this method, the rate of permeation of polymer chains in solution through a gel with fixed pore sizes, expressed as retention time, is related to the hydrodynamic volume of each chain. Passing a polymer through the gel results in fractionation of the polymer chains based on molecular size and thus the shape of the distribution is observed. The retention times of the polymer fractions are related to molecular weight by comparing them to standard curves constructed from the retention times of polymer standards with known molecular weights. The molecular weight at the peak of a GPC chromatogram (M_{GPC}) has been compared to various molecular weight averages. Hamielec and Ouano (1978) proposed

32

that M_{GPC} most closely approximates M_n. However, others have shown that M_{GPC} is closer to, but less than, M_w (Berger and Schultz, 1965; Hester and Mitchell, 1980). Kolínský and Janca (1974) have shown for poly(vinyl chloride) that calibration curves relating retention time to the root mean square average molecular weight (M_{RMS} = $(M_n*M_w)^{0.5}$) have higher coefficients of determination than curves of either M_n or M_w. In all cases, M_{GPC} lies between M_n and M_w.

2.5.4. Thermal properties of semicrystalline polymers

2.5.4.1. The glass transition temperature

The amorphous phase is best described by the properties that change at the glass transition temperature (Tg). Below Tg, the amorphous component of a polymer is a hard and brittle glass and above Tg, it becomes a softer, more flexible, rubbery material. Below Tg, polymers lack sufficient energy for the translational movement of chains required for flow, and for the mobility of chain segments required for flexibility and elasticity.

The glass transition of a polymer is affected by the polymer molecular weight. Flory and Fox described this relationship by the equation:

$$Tg = Tg^\infty - \frac{k}{M_n}$$

Equation 10

where Tg and Tg^∞ are the glass transition temperatures of the polymer with molecular weight M_n and infinity, respectively (Eisenburg, 1993). The constant k is a value directly proportional to the free volume per chain end (Kelley and Bueche, 1961) and reflects the magnitude of free volume change with a change in molecular weight. The relationship is

expected to be linear over the entire range for a given polymer with unchanging end group characteristics.

2.5.4.2. The melting transition

The degree of crystallinity and properties of polymer crystallites can be obtained by DSC. Changes in the peak temperature and enthalpy of fusion (ΔH_f) of a polymer have been used to measure the effects of annealing and different methods of solidification on the crystallinity of polymers (Lemstra *et al.*, 1972; Oswald *et al.*, 1977). Melting of polymers is not observed at the equilibrium melting temperature (Tm°) and near-perfect crystals cannot be obtained except under very specific conditions with certain polymers such as polyethylene (Wünderlich, 1973). The deviation of polymer crystallites from equilibrium is characterised by the observed Tm. The surface energy and thickness of lamellar crystallites make them less stable than they would be at equilibrium, according to the Thomas-Gibbs equation (Wünderlich, 1980):

$$Tm = Tm^\circ(1 - \frac{2\sigma_e}{\Delta h \cdot l})$$

Equation 11

where Tm is the observed melting point, Tm° is the equilibrium melting point, Δh is the enthalpy of fusion per repeat unit and σ_e and l are the crystallite surface free energy and lamellar thickness, respectively, which are both related to the chain folding frequency.

Polymer melting temperature is also dependent on molecular weight (Mandelkern, 1993), as described by the equation:

$$\frac{1}{Tm} - \frac{1}{Tm^\infty} = \frac{2R}{\Delta h} \times \frac{1}{M_n}$$

Equation 12

where Tm^{∞} is the melting temperature of a polymer with infiinite molecular weight and R is the gas constant. As the molecular weight increases, its influence on melting point depression is decreased. In practice, polymers melt over a range of temperatures, reflecting both a range in the nature of crystallites within the matrix and in the molecular weights of polymer chains in polydisperse materials (Mandelkern, 1993).

Double melting endotherms have also been observed for many polymers including polystyrene (Lemstra *et al.*, 1972), poly(ethylene terephthalate) (Sweet and Bell, 1972) and poly(β-hydroxybutyrate) (Pearce and Marchessault, 1994). A theory that explains this behaviour is as follows. Crystallites within the polymer melt at a Tm lower than Tm° because they are not at equilibrium. The metastable melt subsequently recrystallises below Tm° to form more stable crystallites with a melting point closer to the equilibrium value. Finally the more stable crystallites melt resulting in a second melting endotherm (Sweet and Bell, 1972). An alternate theory that two forms of polymer crystals exist in the polymer with different values of Tm fails to explain the disappearance of double melting peaks observed by DSC at rapid scanning rates (Sweet and Bell, 1972; Lemstra *et al.*, 1972).

2.6.   Poly(L-lactic acid)

2.6.1.   Structure and synthesis

The structure of poly(lactic acid) (PLA) is shown in Figure 4. PLA has a chiral carbon in the lactic acid repeat unit of the polymer chain. Thus two stereoregular forms, poly(D(-)-lactic acid) and poly(L(+)-lactic acid) (PDLA and PLLA, respectively) and the racemic form, poly(D,L(-,+)-lactic acid) (PDLLA) of PLA exist. Of the two stereoregular forms, PLLA has almost exclusively been used in biomaterials research

because the monomer, L-lactic acid, is endogenous in humans. Some investigators

favour the racemic form because it is amorphous and therefore has uniform properties

Figure 4. The chemical structure of poly(L-lactic acid). The asterisk (*) denotes a chiral
carbon in the polymer backbone.

$$\left[\begin{array}{c} \quad\;\; CH_3 \\ \quad\;\;\; | \\ -O-C^{*}-C- \\ \quad\; | \quad\; \| \\ \quad\; H \quad O \end{array} \right]_n$$
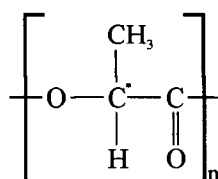
(Holland *et al.*, 1986). However, PLLA possesses higher strength and is therefore

suitable for orthopaedic applications (Matsusue *et al.*, 1992), as a fibre-forming material

(Hoogsteen *et al.*, 1990).

In the polymeric drug delivery literature, two names for PLLA are used,

depending on the method of polymer synthesis. Polymers synthesised by condensation of

L(+)-lactic acid are named poly(L(+)-lactic acid). The L designation describes the

configuration of the chiral centre and (+) specifies the optical rotation of light by the

monomer. However, when L(+)-lactic acid is converted to a cyclic diester, the rotation of

light is reversed, giving L(-)-lactide. Polymers made by ring-opening polymerisation of

L(-)-lactide are called poly(L(-)-lactide), even though they are structurally equivalent to

poly(L(+)-lactic acid) polymers. Often for simplicity, the (+) or (-) is removed in the

naming of PLLA polymers and these symbols will not be used any further in this thesis.

Several authors have reported the synthesis of PLLA with a molecular weight up

to 8500 g/mol by polycondensation of L-lactic acid. The syntheses were carried out by

heating a solution of L-lactic acid in water (Jamshidi *et al.*, 1988; Fukuzaki *et al.*, 1989)

or in xylene (Celli and Scandola, 1992) to approximately 180°C for several hours. To synthesise PLLA with higher molecular weights, ring opening polymerisation methods have used L-lactide and a catalyst at temperatures between 130-200°C for several hours. Kulkarni et al. (1971) have reported that 0.02% tetraphenyl tin used as a catalyst produces high yields. Leenslag and Pennings (1987) and Hoogsteen et al., (1990) have both reported a method using stannous 2-ethyl hexanoate as a catalyst at levels as low as 0.007%. Stannous 2-ethyl hexanoate has been identified as an effective catalyst for the synthesis of polyesters and it also has the advantage of acceptance by the FDA (Gilding and Reed, 1979).

Synthesis using an alcoholic initiator and a catalyst allows for stoichiometric control of the polymer molecular weight. Schindler et al. (1982) have reported alcohol initiated synthesis of poly(ϵ-caprolactone) in which predicted M_n and observed M_n values did not differ by more than 6 and 8% when using 1,6-hexanediol and dodecanol, respectively. Stoichiometric control is achieved because the number of growing chains is equal to the number of initiator molecules present and remains constant throughout the reaction (Saotone and Kodaira, 1965). PLLA has been synthesised by this method using lauryl alcohol (Asano et al., 1991) and polyethylene glycol (PEG) (Nijenhuis et al., 1996) as the initiator. However, in the case of PEG, the aim was not to control molecular weight, but rather to synthesise a block copolymer of ethylene glycol and L-lactic acid.

2.6.2. Thermal properties

The enantiomeric purity of PLLA imparts a semicrystalline morphology to the polymer (Holland et al., 1986). Reports of the degree of crystallinity of PLLA have varied from 20 to 75% (Celli and Scandola, 1992; Engelberg and Kohn, 1991). The Tg

and Tm for PLLA have been observed to be dependent on polymer molecular weight, and previous processing conditions (Izumikawa *et al.*, 1991).

Engelberg and Kohn (1991) and Celli and Scandola (1992) have studied the effects of thermal history and ageing on the glass and melting transitions. Annealing of PLLA below Tg resulted in enthalpy relaxation of the amorphous polymer phase. The rate and extent of relaxation was dependent on the annealing temperature and polymer molecular weight. Annealing of PLLA above Tg resulted in an increase in the degree of crystallinity of the polymer (O'Reilly and Karasz, 1966).

Both single and double endotherms at the melting transition of PLLA have been observed (Izumikawa *et al.*, 1991; Celli and Scandola, 1992). This phenomenon is believed to be evidence of melting of a single form of non-equilibrium PLLA crystallites, immediately followed by recrystallisation and a second melting event. However, two distinct forms of PLLA crystals have been identified by Hoogsteen *et al.* (1990), α and β forms, which melt around 175 and 185 °C, respectively.

2.6.3. Biocompatibility

Non-degraded PLLA was first demonstrated to be biocompatible by Kulkarni *et al.* (1971). The biocompatibility of PLLA was classified as "excellent" by authors who studied PLLA *in vivo* over several months (Gourlay *et al.*, 1978; Bos *et al.*, 1991). Only minimal localised inflammation was visible by histological examination in the very early and late phases of *in vivo* evaluation of PLLA bone fixation plates that were examined over a two year period. A similar study of PLLA plates and screws examined three years after implantation showed a foreign body reaction at the site of the implant although the presence of inflammation was considered minimal (Bergsma *et al.*, 1993).

2.6.4. Biodegradation

2.6.4.1. Indirect (oxidative) biodegradation

Biodegradation of PLLA is generally agreed to be accomplished by simple hydrolysis, with only minor involvement of enzymatic pathways (Reed and Gilding, 1981; Leenslag et al., 1987). Hydrolysis of ester bonds in PLLA is catalysed by both H_3O^+ and OH^- ions at low and high pH, respectively. At pH 7.4, base catalysis is believed to predominate (Makino et al., 1986). As ester bonds are hydrolysed, carboxylic acid groups are evolved which are capable of catalysing further hydrolysis (Lam et al., 1994; Pitt and Gu, 1987). Homogeneous degradation is the pattern most often observed for PLLA and other similar polyesters (Holland et al., 1986). In order for homogeneous degradation to occur, water must diffuse into the polymer matrix, thus hydrophobicity and crystallinity both contribute to a slowing of PLLA degradation (Holland et al., 1986).

As hydrolysis proceeds and the molecular weight of the polymer decreases, several effects on the physical properties of the polymer are observed. Pistner et al. (1993), Lam et al. (1994) and Migliaresi et al. (1994) have all reported an increase in the degree of crystallinity in the polymer as degradation proceeds. Lam et al.(1994) proposed that both preferential degradation of amorphous regions of the polymer and "degradation induced recrystallisation" explain this phenomenon. Despite the increase in crystallinity of the matrix, the mechanical strength of PLLA was decreased as degradation proceeded (Reed and Gilding, 1981; Li et al., 1990; Lam et al., 1994). A reduction in both molecular weight and mechanical strength resulted in loss of mass in the polymer matrix as the matrix fragments and oligomers and monomers dissolved (Makino et al., 1985; Li et al., 1990; Rozema et al., 1994).

2.6.4.2. Direct (enzymatic) biodegradation and bioresorption

The final elimination phase in which dissolved monomers and oligomers and microparticles of polymers are absorbed is called bioresorption (Vert *et al.*, 1992). Small particles of PLLA and dissolved oligomers are taken up into macrophages for digestion by lysozomal enzymes (Woodward *et al.*, 1985; Bos *et al.*, 1991; Rozema *et al.*, 1994). Lactic acid produced through enzymatic degradation is believed to be metabolised to carbon dioxide and eliminated through the lungs to complete the bioresorption process (Kulkarni *et al.*, 1966).

Several enzymes have been tested *in vitro* for activity in degrading PLLA (Williams, 1981; Makino *et al.*, 1985). Of the enzymes studied, the greatest activity was observed with carboxylic esterase, pronase, proteinase-K and bromelain, which when incubated with PLLA caused mass loss in the polymer matrix with the evolution of L-lactic acid. However, because of the high molecular weight of the enzymes, they could not penetrate into the polymer matrix, and enzymatic degradation occurred only at the surface.

2.6.5. Poly(L-lactic acid) in medical devices and polymeric drug delivery systems

There are many applications for PLLA in medical devices, including bone fixation pins (Matsusue *et al.*, 1992), plates and screws (Bergsma *et al.*, 1993), fibres for surgical sutures (Hoogsteen *et al.*, 1990) and polymeric stents for use in urological (Kempainen *et al.*, 1993) and vascular applications (Agrawal *et al.*, 1992).

The drug delivery applications for which PLLA microspheres have been developed are listed in Table 1. PLLA microspheres have been manufactured in size ranges between 1 and 300 µm by spray drying (Pavanetto *et al.*, 1993) but most

40

commonly by the solvent evaporation technique in an oil/water dispersion (Jalil and Nixon, 1989; Mumper and Jay, 1992; Kofler *et al.*, 1996). PLLA microspheres have been administered by intra-articular (Mumper *et al.*, 1992) and subcutaneous injections (Kwong *et al.*, 1986) and by implantation into bone lesions (Anselme *et al.*, 1993).

Table 1.   Therapeutic applications of PLLA microspheres.

Therapeutic application	Incorporated drug	Reference
Antimalarial therapy	Pyrimethamine	Tsakala *et al.*, 1990
Cancer chemotherapy	Etoposide	Kishida *et al.*, 1990
	Vitamin D3	Pavanetto *et al.*, 1993
	Adriamycin	Ike *et al.*, 1990
Cancer radiation therapy	^{90}Yittrium	Häfeli *et al.*, 1994
	^{165}Holium	Mumper and Jay, 1992
Diabetes management	Insulin	Kwong *et al.*, 1986
Radionuclide synovectomy	^{165}Holium	Mumper *et al.*, 1992
Vaccination	Bacterial antigen	Kofler *et al.*, 1996
	Tetanus toxoid	Göpferich *et al.*, 1994

2.7.   Polymer blending

2.7.1.   Blend compatibility

The miscibility of polymers has been identified as a very important factor in determining the thermal and mechanical properties of a blend (Chu and Berner, 1993; Hseih and Peiffer, 1993). The enthalpy and entropy of mixing for two polymers, predict that without specific interactions between polymers, mixing results in a phase separated morphology (Liu and Donovan, 1995). Hydrogen bonding (Aubin and Prud'homme, 1980), acid-base interactions (Zhou and Eisenberg, 1983) and complex formation (Cruz *et al.*, 1979) have all been shown to contribute to exothermic mixing, and polymer miscibility.

2.7.2. Effects of blending on polymer properties

2.7.2.1. Glass transition

Miscible polymer blends form a single amorphous phase which exhibits a single glass transition. The Tg is composition-dependent and its relationship to blend ratio has been described by the Fox equation (Fox, 1956):

$$\frac{1}{Tg} = \frac{\phi_1}{Tg_1} + \frac{\phi_2}{Tg_2}$$

Equation 13

where ϕ_1 and ϕ_2 are the fractional proportions and Tg_1 and Tg_2 are the glass transition temperatures of each polymer, respectively. This relationship has been used to fit experimental data for miscible polymer systems (Grandfils *et al.*, 1996; Liu and Donovan, 1995). In the case of immiscible blends, two amorphous phases exist, and each of the individual polymer glass transitions are observed, although the Tgs may become broadened and shift closer to one another (Gesner, 1969).

2.7.2.2. Crystallinity and melting

Melting point depression is observed in blending semicrystalline polymers. This was first described mathematically by Nishi and Wang (1975) and has been modified to account for non-equilibrium polymer systems by Martinez-Salazar *et al.* (1996). The equation relates the melting point depression to the blend composition, the interaction parameter (χ) and the molar volumes and molecular weights of each polymer component. A reduced form was also presented for blends of high and low molecular weight polymers with identical chemical structure:

$$\frac{1}{Tm_2} - \frac{1}{Tm_2^o} = \frac{R}{\Delta h} \frac{1}{m_1} (1-\phi_2)$$

Equation 14

42

where ϕ_2, Δh, Tm_2 and $Tm°_2$ are the weight fraction, heat of fusion of the polymer repeating unit, and depressed and equilibrium melting points of a semicrystalline component in a polymer blend respectively, and m_1 is the molar volume of the other component of the blend.

Changes in the Tg and Tm of polymers in a blend alter the temperature range over which recrystallisation may occur. The rate and extent of crystallisation of one polymer can be affected by addition of a second. Both increases and decreases in the degree of crystallinity of a polymer after blending have been demonstrated. The degree of crystallinity of nylon 6 was reduced from 25% for the pure polymer to 5% in a 1:1 blend with poly(hexamethylene isophthalamide) (Liu and Donovan, 1995). However, upon annealing of the blend, the degree of crystallinity of nylon 6 increased to 35% while annealing pure nylon 6 did not result in an increase above 25% crystallinity.

2.7.2.3. Permeability and biodegradation of polymer blends

Polymer blending can be used to produce matrices with specific permeability and biodegradation profiles. In the manufacture of microspheres, phase separation has been shown to increase the porosity and therefore the permeability of the polymer blend matrix. In a blend of PCL and poly(hydroxybutyrate-co-hydroxyvalerate), the highest observed porosity was seen at a blend ratio of 1:1 (Embleton and Tighe, 1993). The permeability of PDLLA to water has been enhanced by incorporating PDLLA oligomers into the matrix (Bodmeier et al., 1989; Grandfils et al., 1996) to increase swelling of the matrix, decrease Tg of PDLLA, increase the hydrophilicity of the matrix, and increase rates of hydrolytic degradation and erosion. Asano et al. (1991) also incorporated lower

43

molecular weight PDLLA into a PDLLA matrix and observed a decrease in the lag phase observed prior to onset of erosion of the matrix. Preferential hydrolytic degradation of the low molecular weight fraction was also observed.

2.7.2.4. Drug release from polymer blends

The effects of blending on the release of drugs from a polymer matrix have been explained largely by the observed effects of blending on polymer biodegradation and on the permeability of drugs in the matrix. Microspheres composed of a blend of PLLA with PLGA and L-methadone released drug at rates intermediate between those observed from the single polymer matrices due to changes in the permeability of the polymer matrices (Cha and Pitt, 1988). Yeh *et al.* (1995) reported that the addition of PEG to PLGA microspheres resulted in increased hydration and pore formation after the PEG leached out of the matrix, resulting in an increased *in vitro* drug release rate. The release rate of caffeine from PDLLA microspheres was increased by the addition of a PDLLA oligomer (Bodmeier *et al.*, 1989).

2.7.3. Polymer blends incorporating poly(L-lactic acid)

PLLA has been blended with other biodegradable and non-biodegradable polymers to modulate both the biodegradation rate of PLLA and drug release rates from the delivery systems. Cha and Pitt (1990) blended PLLA with PLGA and measured an increased degradation rate of PLLA chains relative to the rate observed for a PLLA matrix. Thermal analysis of the blends indicated that PLLA and PLGA were immiscible. Blending of PLLA with another polyester, poly(hydroxybutyrate) (PHB), yielded blends with miscibility dependent on the blend composition and on the molecular weight of PLLA (Blümm and Owen, 1995). Polymer molecular weight is an important factor

44

because it affects its molar volume, a parameter which contributes to the Flory-Huggins interaction parameter, χ (Martin, 1993b) which determines the enthalpy of mixing of polymers. The miscibility of PLLA with other polymers has been demonstrated to be dependent on the hydrophilicity of the second polymer (Park *et al.*, 1992).

PLLA has been blended with its optical isomer, PDLA, by casting from a common solution in various solvents (Tsuji *et al.*, 1991a, 1991b). The formation of racemic crystals was observed in the miscible blend of PLLA and PDLA, which melted at 225 °C.

2.8.   Intraperitoneal chemotherapy

2.8.1.   Rationale

"The basic goal of intraperitoneal delivery of cytotoxic agents is to expose tumour in the compartment to higher drug concentrations for longer time periods than would be possible with systemic drug administration" (Markman, 1996). Both pharmacokinetic and pharmacodynamic advantages have been demonstrated with intraperitoneal administration of chemotherapeutic drugs. Litterst *et al.* (1980) examined seventeen chemotherapy drugs and determined that drugs with a molecular weight greater than 500 g/mol are poorly absorbed from the peritoneum and that a hypertonic administration vehicle could improve retention.

Given their slow clearance, drugs whose chemotherapeutic activity is related to concentration and duration of exposure, such as *cis*-diamminedichloroplatinum (cisplatin) (Markman, 1996) and paclitaxel (Rowinsky *et al.*, 1988) may show enhanced effectiveness with intraperitoneal administration. Slow drug clearance from the peritoneum into the systemic circulation can lead to decreased systemic toxicity as shown

45

for intraperitoneal cisplatin administered in combination with cyclophosphamide (Alberts *et al.*, 1995). Intraperitoneal administration also reduces first pass hepatic metabolism of drugs, which may result in increased bioavailability for drugs which are primarily metabolised in the liver, such as paclitaxel (Monsarrat *et al.*, 1990).

2.8.2. Limitations

While patients who are sensitive to a chemotherapeutic agent may benefit from a second intraperitoneal course after intravascular administration of the drug, the opposite is also true. In patients previously shown to be resistant to cisplatin, higher drug concentrations and prolonged exposure to drug with intraperitoneal administration was not effective at reversing drug resistance in ovarian cancer (Markman *et al.*, 1991). Intraperitoneal administration of cisplatin was also not effective in patients with tumour masses larger than 1 cm in diameter due to poor drug penetration. Measurement of intracellular platinum levels in tumour masses after intraperitoneal drug administration showed that cisplatin penetrated only 3 mm into solid tumour masses (McVie *et al.*, 1985) while doxorubicin penetrated less than 0.5 mm into tumour masses (Ozols *et al.*, 1979).

2.8.3. Applications

2.8.3.1. Ovarian cancer

The disease most often treated with intraperitoneal chemotherapy is ovarian cancer and numerous clinical trials have evaluated cisplatin, 5-fluorouracil and methotrexate for this purpose. The early trials have been reviewed by Brenner (1986).

More recently, trials of α-interferons (Berek *et al.*, 1985; Moore *et al.*, 1995) and paclitaxel (Markman *et al.*, 1992) have been reported.

A report of a trial comparing intravenous and intraperitoneal cisplatin in treating stage III ovarian cancer which was begun in 1985 showed that intraperitoneal therapy resulted in a 20% increase in survival times and significantly less neutropenia and ototoxicity, compared to intravenous therapy (Alberts *et al.*, 1995). Clinical investigation of intraperitoneal paclitaxel therapy has only reached Phase I trials (Markman *et al.*, 1992) and Phase II protocols have been published (Markman, 1995). Markman *et al.* (1992) compared AUCs for plasma and peritoneal fluid and found almost a thousand-fold higher drug exposure in the peritoneum than in the general circulation. An extremely low clearance of 0.0175 $L/h/m^2$ was reported compared to 8 to 26 $L/h/m^2$ after intravenous administration (refer to section 2.2.4). The toxicity was described as acceptable, with dose limiting abdominal pain reported at a dose of 175 mg/m^2.

2.8.3.2. Peritoneal carcinomatosis and gastrointestinal cancers

Surgery for cancers of the colon and rectum has traditionally involved exploratory surgery. Recently, laparoscopic surgery has gained popularity in the treatment of these cases because it is well tolerated with respect to morbidity and mortality during surgery (Bleday *et al.*, 1993). Patients receiving laparoscopic gastrointestinal surgery have shorter hospital stays, lower complication and post-operative mortality rates and more rapid recovery times compared to patients receiving an open surgery (Phillips *et al.*, 1992). However, the problem of incomplete resection or contamination with tumour cells of previously unaffected tissues by laparoscopic techniques has become evident. Several occurrences of peritoneal carcinomatosis, or

wide-spread dissemination of tumours in the peritoneal cavity, due to seeding of the peritoneum with tumour cells during laparoscopic surgery have been reported. Jacquet *et al.* (1995) summarised twenty-five case reports of peritoneal seeding after laparoscopic colectomy and other reports have involved gallbladder (Sailer *et al.*, 1995) and pancreatic (Charnley *et al.*, 1995) cancers.

Intraperitoneal chemotherapy has been employed to combat this problem. Jacquet *et al.* (1995) reported two cases of patients with recurrent cases of colorectal cancer who were successfully treated with laparoscopic surgery and with intra-operative mitomycin C and post-operative 5-fluorouracil, both administered intraperitoneally. Cancers of the gastrointestinal system in the peritoneum often lead to peritoneal carcinomatosis even without prior intervention. The outcome for these patients is very poor and treatment has involved palliative cytoreductive surgery and intraperitoneal and intravascular chemotherapy. An intraperitoneal administration of mitomycin C after cytoreductive surgery in patients with recurrent metastatic colon cancer was demonstrated to be a safe palliative treatment which prevented regrowth of tumours for a median of six months (Schneebaum *et al.*, 1996). Another trial using cisplatin had negative results (Sautner *et al.*, 1994). In this trial, no measurable improvement in patient survival times was found with post-operative chemotherapy compared to a group of patients who received surgical treatment alone.

2.8.4. Intraperitoneal administration of chemotherapy using microparticulate delivery systems.

There are a limited number of studies of intraperitoneal delivery of chemotherapeutic agents from microspheres. Ike *et al.* (1990) encapsulated adriamycin

48

in PLLA microspheres with average diameter of 50 μm and injected them into the peritoneal cavity of mice concurrently with two million P815 mastocytoma tumour cells. Compared to mice receiving a solution of adriamycin intraperitoneally, those mice receiving microsphere encapsulated drug had up to a 100% increase in survival time, which was ascribed to decreased systemic drug toxicity. However, in this study, drug toxicity was responsible for the early death of all animals and no therapeutic benefit was observed, compared to mice receiving control microspheres. Edman and Sjöholm (1979) encapsulated L-asparaginase in poly(acrylamide) microspheres. The microspheres were administered intraperitoneally to healthy rats and the systemic activity of the enzyme was demonstrated to be prolonged by several days compared to an intraperitoneally administered L-asparaginase solution. Cisplatin loaded PLGA microspheres were administered intraperitoneally to rats in a model of ovarian cancer (Kumagai *et al.*, 1996). Improved tolerability, higher intraperitoneal drug concentration and increased survival times were obtained in rats that received cisplatin microspheres compared to an aqueous solution of the drug. A similar study in mice using P815 tumour cells also showed increased survival times and decreased toxicity (Itoi *et al.*, 1996).

Other particulates with diameters in the nanometer size range have been investigated for the intraperitoneal administration of chemotherapeutic drugs. In these applications, the drugs are targeted to the lymphatic system, which absorbs particles less than 1 μm in diameter from the peritoneum. Activated carbon particles have been coated with mitomycin C (Takahashi *et al.*, 1995) and methotrexate (Hagiwara *et al.*, 1996) for the treatment of peritoneal carcinomatosis and lymph node metastases.

2.8.4.1. Clearance of microspheres from the peritoneum of rats

Particulate materials are cleared from the peritoneal cavity through the diaphragm into lymphatic capillaries. Florey and Witts (1928) developed the idea of a sieve-like structure in the diaphragm through which particles can penetrate. The anatomy of the diaphragm in mice was more accurately defined by Allen (1936) who observed openings with diameter 5 µm, called stomata, at the junctions of mesothelial cells in the peritoneal lining. The stomata lead to fenestrations in the basement membrane and a network of lymphatic lacunae that drain via ducts to the parathymic and mediastinal lymph nodes (Flessner et al., 1983; Abernethy et al., 1991; Abu-Hijleh et al., 1994). Clearances and the mechanism of clearance for particles with diameters less than 2 µm from the peritoneum of rodents and dogs were studied by several authors during the first half of this century and these have been reviewed (Allen, 1956). However, clearance of larger particles was not studied until 1956 by Allen. Table 2 summarises studies published after 1956 that have examined clearance of particulates from the peritoneum of rats. Particles with diameter up to 25 µm are cleared through stomata within several hours. Larger particles can be cleared after several days (Ludwig, 1971; Edman and Sjöholm, 1979). Investigations using particles of different materials (Allen, 1956) and several animal models including mouse, rat and cat models (Allen and Weatheford, 1959) indicates that variation exists between different materials and between different species.

2.8.4.2. Animal models for intraperitoneal administration of paclitaxel

The pharmacokinetics of paclitaxel administered in solution into the peritoneum of mice has been reported (Eiseman et al., 1994; Innocenti et al., 1995). Innocenti et al. (1995) observed that after administering either 18 or 36 mg/kg paclitaxel in a 1:1

Cremophor EL®:ethanol solution, the drug accumulated primarily in the organs located in the peritoneum. The peak plasma concentration of paclitaxel, observed after 2 hours, was lower than the peak concentrations observed in liver, colon, pancreas and kidney tissues. However, the plasma concentration at both dose levels was sufficient to induce cytotoxic effects *in vitro*, indicating that systemic exposure is not prevented by intraperitoneal administration. In contrast, Eiseman *et al.* (1994) did not detect any paclitaxel in plasma after intraperitoneal administration of 22.5 mg/kg paclitaxel in mice. In their study, injected volumes between 10 and 150 ml/kg were used and no effect of the volume of the paclitaxel solution on the absorption of paclitaxel from the peritoneum was observed.

The toxicity of paclitaxel has been investigated in animals after intraperitoneal injection. Cavaletti *et al.* (1995) were able to induce peripheral neuropathy in rats after five weekly intraperitoneal injections of 16 mg/kg paclitaxel in 1:1 Cremophor® EL:ethanol. The effect of paclitaxel and Cremophor® EL on histamine release in the peritoneum has also been examined (Decorti *et al.*, 1996). Only a moderate histamine response was observed in an *in vitro* assay of mast cells harvested from the peritoneal cavity of rats using a paclitaxel dose of 100 $\mu g/10^5$ cells in 1 ml of isotonic salt solution. Similar histamine release was observed in controls that received 8 μl Cremophor® EL. The effect of paclitaxel on wound healing after a surgical procedure in rats has also been recently reported (Hopkins *et al.*, 1997). The rat model showed that post-operative administration of paclitaxel in 1:1 Cremophor® EL:ethanol at a dose of 3 mg/kg was sufficient to decrease the strength and scar thickness of an incision site in the peritoneal lining compared to control animals after two weeks of healing time.

Table 2.   The effect of microsphere size on clearance from the peritoneum of rats.

Particulate material	Particulate material size range (μm)	Max. size recovered in lymph nodes (μm)	Time	Reference
Poly(methyl methacrylate) nanospheres	0.5	0.5	6 hours	Maincent *et al.*, 1992
Liposomes	<1	<1	5 hours	Hirano and Hunt, 1985
Glass beads	3-18	12	8 min	Allen, 1956
Polystyrene microspheres	1-30	17	2 days	Allen and Weatherford, 1959
Paraffin/asphalt microspheres	Not reported	22	8 min	Allen, 1956
Ceramic microspheres	5-50	25	7 days	Ludwing, 1971
Polyacrylamide microspheres	0.3-36	36	15 days	Edman and Sjöholm, 1979

Despite the promising pharmacokinetic data for intraperitoneal paclitaxel and the initiation of clinical trials of intraperitoneal paclitaxel in ovarian cancer, very little animal data have been published concerning the effectiveness of paclitaxel against peritoneal tumours. The efficacy of intravenous paclitaxel against intraperitoneally implanted human ovarian tumour xenografts in mice has been studied (Nicoletti *et al.*, 1993, 1994). Paclitaxel and its analogue, docetaxol, were both determined to be more effective at doses of 16 to 34 mg/kg than equitoxic doses of cisplatin, with prolonged survival times and complete responses in 50% of the mice receiving 34 mg/kg paclitaxel.

3. EXPERIMENTAL

3.1. Materials and supplies

3.1.1. Drugs

Paclitaxel and 7-epitaxol were obtained from Hauser (Boulder, CO). Baccatin III was obtained from Inflazyme Pharmaceuticals (Vancouver, BC).

3.1.2. Polymers and reagents used for polymerisation reactions

Poly(L-lactic acid) polymers: 2k and 50k g/mol polymers (Polysciences Inc., Warrington, PA) and 100k g/mol polymer (Birmingham Polymers Inc., Birmingham, AB)

Stannous 2-ethyl hexanoate (Sigma, St. Louis, MO)

L-lactic acid 60%w/w in water (Aldrich Chemical Company, Milwaukee, WI)

L(-)lactide (Polysciences Inc., Warrington, PA)

Stearyl alcohol (Stanley Pharmaceuticals, North Vancouver, BC)

Poly(vinyl alcohol) (PVA) 13-20k g/mol (Aldrich Chemical Company)

Polystyrene molecular weight standards ranging from 300 g/mol to 233k g/mol (Pressure Chemical Company and Polysciences Inc.)

3.1.3. Naming of the poly(L-lactic acid) polymers used in this work

PLLA polymers obtained from Polysciences Inc. are abbreviated as "PLLA-PS" Two molecular weights of PLLA-PS were studied. These will be designated by the molecular weights given by the manufacturer, e.g. "2k g/mol PLLA-PS". PLLA obtained from Birmingham Polymers Inc. will be referred to as 100k g/mol PLLA, designating the

molecular weight given by the manufacturer. The term "LLA oligomer" will be used to designate the product of a polycondensation reaction of L-lactic acid. PLLA polymers synthesised by a ring-opening polymerisation reaction using stearyl alcohol as the initiator will be called "PLLA-SA" polymers. Different molecular weights will be identified using the value of molecular weight predicted by the synthesis (Mn*), e.g. "10k g/mol PLLA-SA". PLLA polymers synthesised using the PLLA oligomer by the ring-opening polymerisation method will be called "PLLA-LA" polymers. The molecular weight of these polymers will be identified using the molecular weight determined for each by GPC, e.g. "3.5k g/mol PLLA-LA" for the polymer with a predicted molecular weight of 10k g/mol but a measured value of 3.5k g/mol.

3.1.4. Buffers, stock solutions and solvents

Phosphate buffered saline with 0.4% albumin (pH=7.4) (PBS-A) was prepared containing sodium chloride, 8.22 g, sodium phosphate monobasic dihydrate, 0.315 g, sodium phosphate dibasic heptahydrate, 2.15 g, bovine serum albumin (Fraktion V), 1.6 g, and distilled water, 4.0 L. All PBS-A ingredients were from Fisher Scientific (Fairlawn, NJ) except the albumin, which was from Boehringer Mannheim (Germany). All ingredients were combined in a 4 L Erlenmeyer flask and stirred at room temperature to dissolve the solids. The pH of the buffer was in the range of 7.2 – 7.4. PBS-A was stored at 4°C and any unused PBS-A discarded after 48 hours.

A 10% poly(vinyl alcohol) (PVA) solution in distilled water was prepared by combining 35 g PVA with 350 ml distilled water in a covered beaker, and heated to boiling with stirring to dissolve the PVA. The 10% PVA solution was then cooled, stored at 4°C and discarded if the solution became hazy.

Distilled water was used throughout. Sodium dried toluene was prepared by Mr.

P. Franchini in the Faculty of Pharmaceutical Sciences at U.B.C. The sodium was

obtained from BDH (Poole, England) and the toluene was from Aldrich Chemical

Company. All other solvents were HPLC grade and were obtained from Fisher

Scientific.

3.1.5. Materials used for *in vivo* studies

The Brain Tumour Research Center (San Francisco, CA) supplied 9L

glioblastoma cells. Phosphate buffered saline (PBS) was prepared as described in section

3.1.4 except that no albumin was included. Chemicals for the preparation of histology

slides: proteinase K, Immunomount®, Coverbond®, haematoxylin and eosin stain, and

formalin, anaesthetic and post-surgery narcotic drugs: Innovar®, atropine, fluothane and

buprenorphine HCl and 0.9% Sodium Chloride Injection (NS) were obtained from the

Pathology Department of Vancouver Hospital and Health Sciences Centre, U.B.C.

Pavilions. Media for the culturing of 9L glioblastoma cells and 5% trypsin-EDTA

solution were kindly donated by Dr. U. Steinbrecher of the Faculty of Medicine at U.B.C.

3.1.6. Other reagents

Potassium hydroxide (Fisher Scientific, Fairlawn, NJ)

Benzyl alcohol (Aldrich Chemical Company, Milwaukee, WI)

Phenolphthalein (Sigma Chemical Company, St. Louis, MO)

Polysorbate 80 (Aldrich Chemical Company, Milwaukee, WI)

3.1.7. Glassware

Test tubes for *in vitro* release studies were 15 ml and 50 ml Kimax® brand test tubes with Teflon® lined screw capped lids. Beakers, Erlenmeyer flasks and graduated cylinders were Pyrex® brand. Microsphere and paclitaxel samples were stored in 20 ml glass vials with polypropylene lined screw capped lids. All glassware was obtained from Fisher Scientific (Toronto, ON).

3.2. Equipment

3.2.1. HPLC

Chromatographic analyses of paclitaxel were performed using a Waters HPLC system (Millipore Corporation, Bedford, MA). The components were a model 717+ autosampler, a model 600 controller and pump module, a model 486 tunable absorbance detector and a model 746 data collection module. The analytical column was a Novo-Pak C_{18} column with dimensions 3.9 x 150 mm (Millipore Corporation).

3.2.2. Gel permeation chromatography instrumentation

Gel permeation chromatographic analyses of polymers were performed using a Shimadzu HPLC system (Shimadzu Corporation, Tokyo, Japan). The components were a 20 µl loop injector (Rheodyne Inc., Cotati, CA), a model LC-10AD HPLC pump, a model RID-6A refractive index detector and a model CR601 Chromatopac data recorder. Three PLgel GPC columns were used with pore sizes of 50, 10^3 and 10^4 Å. The bead size of the gel was 5 µm and the column dimensions were 7.5 x 300 mm (Hewlett Packard, Richmond, BC).

3.2.3. Karl Fischer titration

A model DL18 Karl Fischer titrator (Mettler Instruments, Hightstown, NJ) was used for the Karl Fischer titration of water content in paclitaxel samples. A titration apparatus composed of 20 ml capacity glass burette, a glass beaker with a screw-cap Teflon lid, a magnetic stirrer and a Karl Fischer electrode (Labindustries Inc., Berkeley, CA) was used for the analysis of water content in polymer samples.

3.2.4. Microsphere manufacture

The apparatus for the manufacture of microspheres consisted of a Dyna-Mix overhead stirrer model 143 (Fisher Scientific Inc., Fairlawn, NJ) which allowed variable speed control of an impeller that was immersed in a glass beaker containing the dispersion. The dimensions of the impeller and of the beakers used in the manufacture are provided in Figure 5.

3.2.5. Scanning electron microscopy

Samples were prepared using a Hummer sputter coater (Technics Inc., Alexandra, VA) and analysed using a model S-2300 scanning electron microscope (Hitachi, Tokyo, Japan).

3.2.6. Particle size analysis

Microsphere size distributions were measured with a model LS130 Coulter laser diffraction particle size analyser (Coulter Scientific, Amherst, MA) controlled with Coulter LS100/LS130 version 1.53 software.

Figure 5. A schematic diagram of the apparatus used for the manufacture of microspheres.

bottom view of impeller:

22 mm

250 ml beaker: 63 mm

750 ml beaker: 85 mm

beaker (250 ml capacity beaker used for microspheres with diameter greater than 10 mm, 750 ml capacity beaker used for smaller microspheres.

stirring impeller

15° (both beaker sizes)

10 mm (both beaker sizes)
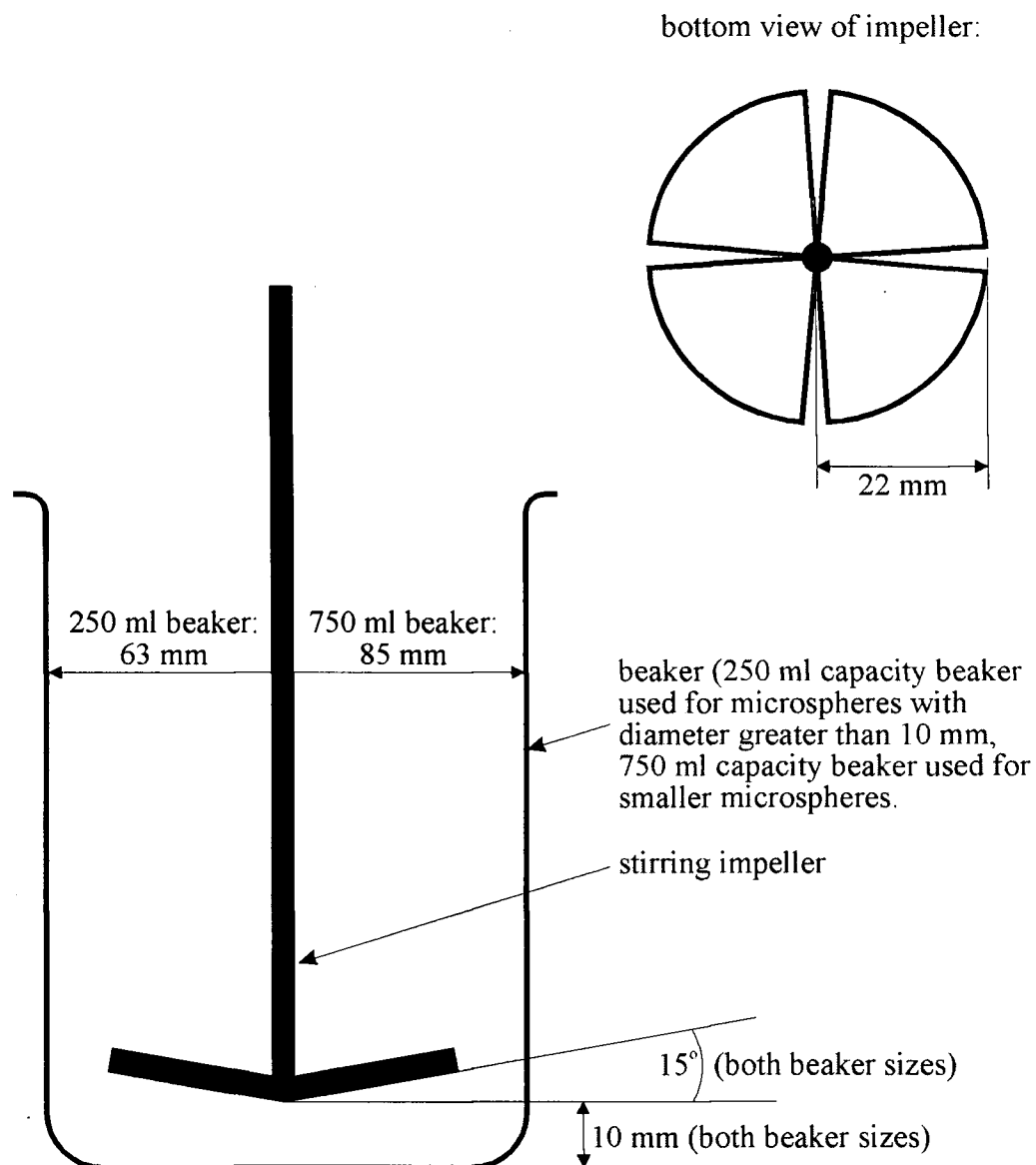
3.2.7. Thermal analysis

Thermal analysis was conducted using a differential scanning calorimeter model 910S, and a thermogravimetric analyser model TGA51 from Dupont Instruments Inc. (New Castle, DL). The thermal analysis system was controlled using TA thermal analyst 2000 software on an IBM computer. Aluminum sample pans were crimped using a Perkin Elmer (Norwalk, CT) model GC14767 crimper for non-hermetically sealed pans and a Dupont Instruments Inc. (New Castle, DL) model 900878-901crimper for hermetically sealed pans.

3.2.8. X-ray powder diffraction

A model XDS 2000 X-ray powder diffractometer (Scintag) equipped with a High-Tran heat and temperature controller model 828D (Micrista) and a Geigerflex X-ray powder diffractometer (Rigaku Inc., Tokyo, Japan) without temperature control were used to determine paclitaxel X-ray powder patterns.

3.2.9. Liquid chromatography-mass spectrometry

The HPLC system used for liquid chromatography-mass spectrometry (LCMS) was a model 1090 series II system (Hewlett Packard, Palo Alto, CA). Detection was accomplished using a mass spectrometry-mass spectrometry (MS-MS) VG Quattro system (Fisons Instruments, Altrincham, England). A C_{18} Hypersil column with dimensions of 5 μm x 2.1 mm x 100 mm was used for chromatographic separation.

3.2.10. Ovens and incubators

A Shel-Lab oven (Sheldon Manufacturing Inc., Portland, OR) was used for *in vitro* release studies. Paclitaxel samples were maintained at constant temperature in an Isotemp incubator (Fisher Scientific Inc., Fairlawn, NJ) during moisture uptake studies. A Napco vacuum oven model 5831 (Precision Scientific Inc., Chicago, IL) equipped with an Emerson vacuum pump model SA55NXGTE4870 (Emerson Motor Division, St Louis, MO) was used to dry paclitaxel samples to constant weight and a Thelco model 16 oven (Precision Scientific Inc., Chicago, IL) to heat reaction vessels for polymer synthesis.

3.2.11. Centrifuges

Two centrifuges, models GPR and GS-6 (Beckman Instruments Inc., Palo Alto, CA) where used for centrifugation in the manufacture of microspheres and in the assay for *in vitro* drug release.

3.2.12. Other equipment

Accumet pH meter model 610A (Fisher Scientific Inc., Fairlawn, NJ)

Hygroskop-BT relative humidity meter (Rotroni, Zurich, Switzerland)

Mettler balances models PJ300, AJ100, and AE163 (Mettler Instruments, Zurich, Switzerland)

Corning hot plate stirrer model PC-351 (Corning Glass Works, Corning, NY)

VWR Vortexer-2 (Scientific Industries Inc., Bohemia, NY)

Maxi-Mix II vortexer, model M37615 (Thermolyne Inc., Dubuque, IA)

Corning AG Mega-Pure water still (Corning, NY)

Freezer (Caltec Scientific, Richmond, BC)

Branson 2200 ultrasonic cleaner (Branson Ultrasonics Corporation, Danbury, CT)

Olympus BH-2 microscope (Olympus Optical Company Limited, Japan)

Contax 35 mm camera, model 167MT (Kyocera Corporation, Tokyo, Japan)

Reacti-Vap III gas drying module (Pierce Inc., Rockford, IL)

Reactiv-Therm III heating/stirring module (Pierce Inc., Rockford, IL)

Butane torch, model RK-2020 (Rekrow Inc., Taiwan)

3.3. Methods for the solid state characterisation of paclitaxel

3.3.1. Preparation of paclitaxel I

Paclitaxel was dried to constant weight at ambient temperature and reduced pressure (200 mmHg) in a vacuum oven equipped with an external pump. Commercial paclitaxel dried to constant weight will be referred to as "paclitaxel I".

3.3.2. Preparation of paclitaxel•2H$_2$O

A hydrate form of paclitaxel was prepared as follows. In an Erlenmeyer flask 4 L of distilled water and 8 mg of paclitaxel I were stirred at ambient temperature for 24 hours. Solid paclitaxel was collected by filtration. The material collected was dried to constant weight as described above. This form of paclitaxel will be referred to as "paclitaxel•2H$_2$O".

3.3.3. Determination of the water content of paclitaxel

Water content determinations were accomplished by Karl Fischer titration. Sample sizes were 40 mg for paclitaxel I and 10 mg for paclitaxel•2H$_2$O. The titrant was standardised by titrating 5 µl of distilled water (n=5). Immediately prior to analysis,

61

paclitaxel samples were dissolved in anhydrous methanol. The end-point of each titration

was determined by an electrochemical detector. Values of water content were based on

three separate measurements and are reported as average ± standard deviation.

3.3.4. Scanning electron microscopy

Paclitaxel samples were mounted on aluminum disks with a double sided

adhesive impregnated with carbon (Marivac Ltd., Halifax, ON). The mounted samples

were coated with 100 Å of gold-palladium and analysed using an electron voltage of 10-

20 kV.

3.3.5. Thermogravimetric analysis

TGA of paclitaxel I and paclitaxel•$2H_2O$ was carried out using samples weighing

20 ± 2 mg scanned at a rate of $10°C/min$. The purge gas was nitrogen flowing at a rate of

40 ml/min. Weight losses reported for TGA were based on three runs for paclitaxel I and

five runs for paclitaxel•$2H_2O$.

3.3.6. Differential scanning calorimetry

DSC of paclitaxel was carried out using samples weighing 3.00 ± 0.20 mg in

open (crimped non-hermetically), and hermetically sealed aluminum pans in which a

pinhole was made in the top, referred to as "pinhole" pans. The cell was purged with N_2

flowing at 40 ml/min. All measurements were made with a scan rate of $10°C/min$ unless

otherwise stated. Isothermal studies were carried out by heating to $45°C$ at $20°C/min$,

holding the sample isothermally for 150 minutes followed by heating at $10°C/min$.

The reversibility of transitions was tested by cooling and reheating the samples,

called a "heat-cool-heat" cycle. Paclitaxel I was heated to $195°C$ and cooled by placing

the sample directly into a chamber at ambient conditions (a relative humidity of $43 \pm 3\%$ at $23^{\circ}C$); after 24 hours, the sample was re-analysed by TGA and DSC. Paclitaxel I was also heated to $220^{\circ}C$ by DSC, quench cooled under a nitrogen atmosphere with dry ice to $25^{\circ}C$ and re-analysed by DSC.

Samples of paclitaxel•$2H_2O$ were heated to $100^{\circ}C$ and to $195^{\circ}C$ and cooled from each temperature in two different ways: by placing the sample directly into a $23^{\circ}C$ chamber at $43 \pm 3\%$ relative humidity (RH) for 24 hours or by cooling the sample under nitrogen atmosphere at $10^{\circ}C/min$ in the DSC. Samples were re-analysed by TGA and DSC.

All reported peak transition temperatures and enthalpies of transition for DSC were based on three separate measurements and are expressed as average $\pm$ one standard deviation.

3.3.7. X-ray powder diffraction

For both instruments the X-ray source was CuKα radiation (45 kV, 40 mA). The sample sizes were approximately 60 mg for the Scintag instrument and 500 mg for the Geigerflex instrument. Two samples of paclitaxel I were heated at $10^{\circ}C/min$ to $25^{\circ}C$ and $195^{\circ}C$ in the temperature controlled X-ray diffractometer and held isothermally for 10 minutes prior to XRPD analysis at each temperature. Similarly, paclitaxel•$2H_2O$ was analysed by XRPD at temperatures of $25^{\circ}C$, $100^{\circ}C$ and $195^{\circ}C$. The $^{\circ}2\theta$ range scanned was 5 to 40° at a rate of $5^{\circ}2\theta/min$ at increments of $0.03^{\circ}2\theta$. Paclitaxel•$2H_2O$ was heated to $100^{\circ}C$ and $195^{\circ}C$ by DSC and allowed to cool to room temperature at approximately 40% RH prior to X-ray diffraction analysis. The range scanned was 5 to $40^{\circ}2\theta$ at a rate

of 0.5°2θ/min at increments of 0.02°2θ. All temperature controlled XRPD analysis was completed in the lab of Dr. R. Suryanarayanan at the University of Minnesota.

3.3.8. Relative humidity studies

Samples of paclitaxel I (n=3) were stored at 25.0 ± 0.5°C in an incubator, in desiccator jars over saturated solutions of $CaCl_2 \cdot 2H_2O$, $NaNO_2$ and KNO_3. The solutions maintained relative humidities of 32%, 66% and 93.7%, respectively at 25°C (Nyquist, 1983). Silica gel was used to maintain a relative humidity of 0.3%. Weight changes as a percent were recorded for 96 days.

3.3.9. Preparation of a standard curve for paclitaxel by LCMS-MS

Three sets of standards of paclitaxel were prepared in the concentration range of 0.5 to 10 µg/ml in 50:50 acetonitrile:water. The sets of standards were prepared independently by serial dilution of 10 µg/ml solutions, immediately prior to analysis. Two sets of standards were analysed at the beginning and end of the LCMS-MS assay of paclitaxel samples, respectively, and the third was analysed at the mid-point of the sample run.

3.3.10. Dissolution studies

Approximately 1 mg of paclitaxel I or paclitaxel•$2H_2O$ was placed in a 50 ml Erlenmeyer flask (n = 4) and 5 ml of water at 37°C added with vortexing for 15 seconds. Additional water at 37°C was added to 50 ml. The flasks were sealed and placed in a 37°C water bath equipped with an orbital shaker. At various sampling intervals, 1 ml of solution was removed and passed through a 0.22 µm Millipore filter and diluted 50% with 1 ml of acetonitrile. Twenty µl of each sample were assayed by LCMS-MS with a

mobile phase of 2 mmol/L ammonium acetate in acetonitrile:water 60:40 flowing at a rate of 150 μl/min. The sample was introduced into the detector and ionised by electrospray using a cone voltage of 3000 V. The parent ion for detection was 852 amu and the monitored negative daughter ion was 521.1 amu. A dwell time of 1 sec and a collision energy of 40 eV were used.

3.4. Methods for the synthesis of poly(L-lactic acid) polymers

3.4.1. Synthesis by a polycondensation reaction

The synthesis of oligomers was based on the method of Fukuzaki *et al* (1988). To synthesise a LLA oligomer with molecular weight in the range of 250 – 350 g/mol, L-lactic acid monomers were reacted as follows. A volume of 250 ml of an aqueous L-lactic acid solution (60 %w/w) was placed in a 500 ml round-bottom flask. A thermometer, stirring paddle attached to an overhead mechanical stirrer, and a glass tube through which nitrogen gas was delivered were placed in the liquid. The round bottom flask was submerged below the level of the L-lactic acid into a mineral oil bath previously equilibrated at 170°C. The polymerising L-lactic acid was stirred for seven hours and nitrogen gas was bubbled through to prevent oxidation. The reaction was terminated when the molecular weight was estimated to be in the desired range. The estimation was accomplished by comparing the viscosity of the LLA oligomer with the viscosity of batches of LLA oligomer which had M_n values above and below the range of 250 – 350 g/mol. The LLA oligomer was stored in a beaker sealed with Parafilm at -20°C.

3.4.2. Synthesis by a ring opening polymerisation reaction

PLLA was synthesised by ring-opening polymerisation (Schindler *et al.*, 1982) from L(-)lactide using an initiator and stannous 2-ethyl hexanoate (approximately 0.5%w/w) as the catalyst (Leenslag and Pennings, 1987). Two types of PLLA were synthesised. One was initiated using stearyl alcohol (PLLA-SA) and the other using LLA oligomer (PLLA-LA). L(-)lactide and initiator (either stearyl alcohol or oligomer) were combined in glass ampoules in varying weight ratios to achieve different final molecular weights of polymer. Two grams of L(-)lactide were used for each synthesis and the mass of initiator used was calculated using equation 15.

$$\left(\frac{Mn^*}{MW_{INI}} \right) - 1 = \frac{M_{LA}}{M_{INI}} \qquad \text{Equation 15}$$

where Mn^* is the predicted molecular weight of PLLA, MW_{INI} is the molecular weight of the initiator (stearyl alcohol: 273 g/mol, oligomer: 337 g/mol), and M_{LA} and M_{INI} are the amounts of L(-)lactide and initiator, respectively, added to the mixture. To the mixture were added 100 μl of a 10% solution of stannous 2-ethyl hexanoate in dichloromethane. The ampoules were evacuated using a vacuum pump to remove the dichloromethane and the neck sealed using a butane torch. After fifteen minutes, the evacuated ampoules were sealed and heated to 150°C in an oven and allowed to react for 3-4 hours. Several batches of both PLLA-SA and PLLA-LA were synthesised with predicted molecular weights between 500 g/mol and 10k g/mol.

3.5. Methods for the characterisation of polymers

3.5.1. Water content determination of oligomers

Water content was determined by Karl Fischer titration. The Karl Fischer reagent was standardised by titrating 25 µl of distilled water (n=5). Samples of the oligomers weighing between 0.5 and 0.8 g were dissolved in sodium-dried toluene immediately prior to analysis. The water content of LLA oligomer was based on three separate measurements and reported as the average ± standard deviation.

3.5.2. Validation of the intrinsic viscosity determination method

Values of intrinsic viscosity of polystyrene (233k g/mol) and PLLA (100k g/mol) calculated from Huggins and Kraemer plots and from the equation of Solomon and Ciuta (1962) were compared by a single factor ANOVA test. The viscosity determinations were done in triplicate for both polystyrene and PLLA. Huggins and Kraemer plots were constructed for a polystyrene molecular weight standard (233k g/mol) and for PLLA (100k g/mol) by plotting the following relationships (Martin, 1993c):

$$\frac{\dfrac{t_x}{t_0} - 1}{c_x} = mc_x + b \qquad\qquad \text{Equation 16}$$

$$\frac{\ln\left(\dfrac{t_x}{t_0}\right)}{c_x} = mc_x + b \qquad\qquad \text{Equation 17}$$

where t_x is the time required for a solution of polymer in chloroform with concentration c_x to flow through a viscometer and t_0 is the time for chloroform alone. Polymer concentrations were in the range of 0.1 to 1.0 %w/v. The linear regressions for each set

67

of data were used to calculate intrinsic viscosity from the intercept value according to the

Huggins (1942) and Kraemer (1938) equations:

$$\frac{\eta_{sp}}{c} = [\eta] + k_1[\eta]^2 c \qquad \text{Equation 18}$$

$$\frac{\ln(\eta_{rel})}{c} = [\eta] + k_2[\eta]^2 c \qquad \text{Equation 19}$$

where η_{sp} is specific viscosity, η_{rel} is relative viscosity, and $[\eta]$ is intrinsic viscosity.

Relative viscosity data for polymer solutions with concentrations between $0.20 - 0.35$

%w/v were used to calculate $[\eta]$ using the equation of Solomon and Ciuta (1962):

$$[\eta] \cong \frac{\sqrt{2}}{c_x} \cdot \sqrt{\frac{t_x}{t_0} - 1 - \ln\left(\frac{t_x}{t_0}\right)} \qquad \text{Equation 20}$$

The p value obtained from the ANOVA test of the data was used to describe the

differences in values of $[\eta]$ obtained by the three methods. A lack of significant

difference in values was defined as a p value greater than 0.025. The precision of $[\eta]$

values was described by the relative standard deviation (RSD) of the average of three

replicate values. A RSD value of less than 5% was defined as sufficient precision for the

method.

3.5.3. Intrinsic viscosity determination

Values of intrinsic viscosity of commercial PLLA polymers were measured in

chloroform at $25 \pm 1°C$ using a Canon-Fenske type viscometer (size 25). Values of $[\eta]$

were calculated using the method of Solomon and Ciuta (1962) and are reported as the

average $\pm$ standard deviation of three replicate determinations for each polymer.

3.5.4. Calibration of gel permeation chromatography columns

Three GPC columns (pore sizes 50, 10^3 and 10^4 Å) were calibrated using polystyrene molecular weight standards. Assay conditions for the analysis of 0.2%w/v polystyrene solutions were an injection volume of 20 µl, a mobile phase of chloroform flowing at 1 ml/min, and a refractive index detection cell temperature of 40°C. A calibration curve for the 50 Å column was generated by plotting the log of the molecular weights of polystyrene standards against the retention times of the standards. Universal calibration curves were generated for the 10^3 and 10^4 Å columns by plotting the log of the product of molecular weight and inherent viscosity of each standard against the retention time. Values of inherent viscosity of polystyrene used in the universal calibration curve were determined experimentally for polystyrene with molecular weights of 17.5k g/mol and greater. Values of inherent viscosity for 4k and 9k g/mol polystyrene were calculated using the Mark-Houwink equation. Values of K and a constants were calculated by plotting the [η] versus molecular weight of the 17.5k – 233k g/mol standards according to the rearranged Mark-Houwink equation:

$$\log K + a \cdot \log(MW) = \log[\eta] \qquad\qquad \text{Equation 21}$$

3.5.5. Molecular weight determinations

3.5.5.1. Determination of M_n by end group titration

End-group titration methods were adapted from the method of Fukuzaki *et al.*, (1988). LLA oligomers were titrated in a benzyl alcohol solution as follows. The titrant was potassium hydroxide dissolved in benzyl alcohol standardised with benzoic acid dissolved in benzyl alcohol. The end point of the titration was determined

colourimetrically using three drops of a 1% solution of phenolphthalein in benzyl alcohol as an indicator. The indicator and oligomer solution was placed in a 250 ml Erlenmeyer flask and stirred with a magnetic stir bar. The titrant solution was added drop-wise from a 40 ml capacity glass burette. The molecular weight of the oligomer was calculated using the equation:

$$\frac{M_{Oligomer} \times C_{KOH}}{V_{KOH}} = Mn_{Oligomer} \qquad \text{Equation 22}$$

where $M_{Oligomer}$ and $Mn_{Oligomer}$ are the mass titrated and number average molecular weight of the LLA oligomer, respectively, and C_{KOH} and V_{KOH} are the concentration and volume used of the titrant, respectively. Values of $Mn_{Oligomer}$ were calculated based on three separate titrations of each oligomer and are reported as the average ± standard deviation.

3.5.5.2. Calculation of M_v

Values of M_v for polymers were calculated from values of [η] using the Mark-Houwink equation (Equation 9) using the values of K and a constants reported by Schindler and Harper (1979) equal to 5.45 x 10^{-4} and 0.73, respectively, for PLLA. Values of [η] were determined as described in section 3.5.3.

3.5.5.3. Determination of M_{GPC} by gel permeation chromatography

The molecular weights of PLLA polymers and LLA oligomer were calculated from GPC data. Oligomers were analysed on the 50 Å column and PLLA polymers synthesised by ring-opening polymerisation were analysed on the 10^3 Å column. M_{GPC} values for PLLA synthesised by ring opening polymerisation were calculated using the

70

slope (m) and intercept (b) of the universal calibration equation for the 10^3 Å column in the equation:

$$M_{GPC} = \sqrt[a+1]{\frac{10^{(m \times Tr + b)}}{K}}$$

Equation 23

where $K = 5.45 \times 10^{-4}$ and $a = 0.73$ (Schindler and Harper, 1979) and Tr is the retention time of the polymer on the GPC column. Commercially obtained PLLA polymers were analysed on both the 10^3 and 10^4 Å columns and values of intrinsic viscosity used in the calculation of M_{GPC} were determined experimentally. M_{GPC} was calculated using the values of slope and intercept of the appropriate universal calibration curve in the equation:

$$M_{GPC} = \frac{10^{(m \times Tr + b)}}{[\eta]}$$

Equation 24

3.6. Preparation and characterisation poly(L-lactic acid)-paclitaxel dispersions.

Mixtures of 100k g/mol PLLA and paclitaxel with drug compositions of 0, 20, 40 and 60% and a total weight of 100 mg were dissolved in 1 ml of dichloromethane. The solvent was allowed to evaporate over 24 hours after pouring the mixture onto a glass slide in a fume hood at ambient temperature. The dried material was stored sealed in glass vials at ambient temperature. Samples of the mixtures were analysed by SEM, DSC and XRPD as described for paclitaxel samples in sections 3.3.3 through 3.3.6 with the following modifications. DSC analysis was carried out in unsealed aluminum pans with a heating rate of 10 °C/min. XRPD patterns were obtained at ambient conditions using the Rigaku diffractometer. A sample of PLLA solidified from a melt was prepared for XRPD analysis by heating approximately 300 mg of 100k g/mol PLLA to 200°C for

15 minutes in a X-ray diffraction sample holder and allowing the melt to solidify at ambient conditions.

3.7. Manufacture of microspheres

Microspheres were prepared using the oil in water solvent evaporation method (Jalil and Nixon, 1989). PLLA and paclitaxel, total weight 0.5 g, were dissolved in 10 ml dichloromethane. The organic phase was added to 100 ml of an aqueous solution of PVA in a beaker and stirred at 24 ± 2 °C. A schematic diagram of the apparatus is shown in Figure 5. Paclitaxel loadings of 0, 10, 20, and 30%w/w were obtained by varying the paclitaxel/polymer ratio. Microspheres ranging between 1 and 105 μm in diameter were obtained by varying the PVA concentration in the range of 1 and 10%w/v and the stirring speed in the range of 900 ± 20 and 2100 ± 20 rpm.

The progress of evaporation of dichloromethane from the stirring dispersion was measured gravimetrically for several batches of microspheres. The beakers in which the microspheres were manufactured were placed on a digital balance and at 5 minute intervals, the stirring was stopped and the weight of the dispersion was measured. Stirring rates of 900 and 2100 rpm and PVA concentrations of 1 and 2.5% were used to manufacture microspheres in large and small size ranges, respectively. To minimise variability due to changes in geometry, the same two beakers were used to manufacture microspheres in two size ranges, and the position of the beaker relative to the stirring impeller (refer to Figure 5) and volumes of both aqueous and organic phases were all held constant. The ambient temperature during the manufacturing process of these microsphere batches ranged from 22.0 – 25.5°C. The contribution of evaporation of water to the weight loss of the dispersion was estimated as the weight loss from 105 ml of

aqueous solutions of PVA with no organic phase stirred under the same conditions used to make microspheres.

3.8. Methods for the *in vitro* characterisation of microspheres

3.8.1. Particle size analysis

Particle size distributions of microspheres were determined using a Coulter LS-130 laser diffraction particle size analyser. Microsphere samples were suspended in water with 0.01% polysorbate 80 and sonicated for 5 minutes to prevent aggregation of microspheres in the measurement cell

3.8.2. Resuspension index

The extent to which microspheres could be resuspended in water after drying was determined and expressed as a "resuspension index":

$$R.I. = \frac{(Mass\ Resuspended)}{(Mass\ Resuspended + Mass\ Aggregated)} \times 100\% \qquad \text{Equation 25}$$

R.I. is the resuspension index and the masses of resuspended and aggregated materials were measured as described below. Approximately 50 mg (accurately weighed) of microspheres were placed in a 1.5 ml Eppendorf tube and 1 ml of distilled water added. The mixture was vortexed for one minute and allowed to stand for one minute to allow any aggregates to settle to the bottom. The supernatant was transferred to a tared 20 ml glass vial. The process was repeated twice, each time adding the supernatant to the same vial. The remaining aggregates in the Eppendorf tube were transferred to another tared 20 ml glass vial. Both vials were centrifuged at 1500 rpm for ten minutes and the water

removed. After drying the samples for 24 hours, the vials were weighed. Values of R.I. are based on three replicates and are reported as the average ± standard deviation.

3.8.3. Scanning electron microscopy

Microspheres were analysed in the same way as paclitaxel samples, as described in section 3.3.4 except that the electron voltage was between 5-10 kV.

3.8.4. Thermal analysis

DSC of PLLA microspheres was done in a manner similar to that of paclitaxel samples, described in section 3.3.5 with the following exceptions. All microsphere samples were analysed in open aluminum pans. Sample weights varied between 3 and 5 mg. The degree of crystallinity (X_C) of PLLA was calculated using the equation:

$$X_C = \frac{\Delta H_f - \Delta H_c}{93.7 \text{ J/g}} \cdot 100\%$$

Equation 26

where ΔH_f and ΔH_c are the enthalpies of fusion and recrystallisation, respectively calculated from the area under the curve for both recrystallisation and melting peaks. The enthalpy of fusion for 100% crystalline polymer has been reported as 93.7 J/g (Celli and Scandola, 1992).

3.8.5. X-ray powder diffraction

XRPD patterns of microspheres were obtained as described earlier in sections 3.3.7 and 3.6. Samples of microspheres with weights between 150 and 250 mg were top-loaded into sample holders and analysed using the Rigaku X-ray diffractometer.

3.8.6. Validation of the paclitaxel standard curves used for HPLC analysis

All procedures for the validation of analytical techniques for the quantification of paclitaxel were based on the recommendations of Shah *et al.* (1992b). Standard curves were prepared for paclitaxel dissolved in acetonitrile and in 60:40 acetonitrile:water over a concentration range of 0.1 – 20 μg/ml. The injection volume was 20 μl and the mobile phase used was 58:37:5 acetonitrile:water:methanol flowing at 1 ml/min through a NovoPak C_{18} column. The detection wavelength was 232 nm. Standard curves were validated by measuring four sets of standards on three separate days. Inter- and intra-day precision, accuracy and linearity of the standard curves were measured.

Intra-day precision was expressed in terms of relative standard deviation (RSD) of the average of the four replicate data points on each day. Inter-day precision determinations was expressed in terms of RSD of the average of the twelve replicate data points collected over three days. Values of RSD of less than 10% indicated an acceptable level of precision at each concentration. Inter-day precision was also expressed as the significance level of ANOVA tests between each of the three days' sets of four replicate data points for each concentration. A value of p less than 0.05 indicated a significant difference between days (lack of acceptable intra-day precision) in the averages obtained for a given concentration of paclitaxel.

Accuracy was expressed in terms of average percent bias (bias) based on three replicate spiked paclitaxel solutions. Bias is the average deviation from the expected value of paclitaxel concentrations measured from spiked samples for each of the eight concentration data points in the standard curve. Sufficient accuracy of each standard curve concentration was defined as a bias of less than 10%. For all reported observed

peak areas (precision data) and predicted concentrations of spiked samples (accuracy data), values are presented as the average ± standard deviation. Linearity was expressed as the coefficient of determination (R^2).

3.8.7. Determination of the total content of paclitaxel in microspheres

Approximately 5 mg of microspheres, accurately weighed, were dissolved in 1 ml of dichloromethane. To the solution were added 20 ml of 60:40 acetonitrile:water, and two clear phases allowed to separate, with PLLA precipitating at the interface. The paclitaxel content of the organic (top) phase was determined by HPLC. The HPLC sample was prepared by diluting 100 μl of the organic phase with 900 μl of acetonitrile. Values of total content of paclitaxel are based on four replicates for each formulation and are reported as the average ± standard deviation.

3.8.8. Validation of the assay for total content of paclitaxel in microspheres

One ml of a solution containing 3.5 mg 100k g/mol PLLA and 1.5 mg paclitaxel in dichloromethane was combined with 20 ml 60:40 acetonitrile:water. The volumes of the organic and aqueous phases were measured and the paclitaxel content was determined in both phases by HPLC. The organic phase was diluted ten-fold with acetonitrile prior to injection onto the column and the aqueous phase was injected directly. Percent recoveries in each phase and the total percent recovery were determined. Inter-sample variability was calculated and expressed as the RSD. The selectivity of the assay for paclitaxel was determined by injecting a blank and by measuring the resolution of the paclitaxel and dichloromethane peaks observed on the chromatograms of samples of the organic phase.

3.8.9. Determination of *in vitro* paclitaxel release profiles

The assay for measuring *in vitro* paclitaxel release from microspheres was based on the method given by Burt *et al.* (1995) but with some modifications. Into 50 ml glass, screw capped tubes were placed 50 ml of 10 mM PBS-A and 3 mg (accurately weighed) paclitaxel loaded microspheres. The tubes were tumbled end-over-end at 30 rpm at 37 °C in a thermostatically controlled oven and at given time intervals, centrifuged at 1500 rpm for 10 minutes and the 5 ml of the supernatant saved for analysis. The remainder of the supernatant was removed and the microsphere pellets were resuspended in fresh PBS-A (50 ml). The buffer was replaced at each sampling interval in order to maintain sink conditions, which were taken to be a paclitaxel concentration in the PBS-A not exceeding 15% of its solubility (Carstensen, 1977). The amount of paclitaxel in 5 ml of the supernatant was determined by extraction of paclitaxel into 1 ml dichloromethane followed by evaporation to dryness at 45 °C under a stream of N_2, reconstitution in 1 ml of 60:40 acetonitrile in water and analysis by HPLC.

3.8.10. Validation of the procedure for paclitaxel extraction from PBS-A

Paclitaxel was dissolved in acetonitrile at a concentration of 10 µg/ml and aliquots of the solution were added to 15 ml glass test tubes. The amounts of paclitaxel were 0.2, 0.5, 1, 2 and 5 µg in each tube. The acetonitrile was allowed to evaporate and to each tube was added 1 ml of dichloromethane to dissolve the paclitaxel, followed by 5 ml PBS-A. The tubes were vortexed for 15 seconds and after phase separation had occurred the aqueous phase was discarded. The organic phase was dried and reconstituted in the same manner as the extract in the release study assay. The extraction efficiency assay was repeated four times for each amount of paclitaxel on each of three

days. Inter-and intra-day precision (expressed as RSD) and percentage efficiency of the extraction (expressed as average ± standard deviation) at each concentration were measured.

During analysis of paclitaxel in PBS-A samples from release studies, an additional chromatographic peak was occasionally observed and was attributed to 7-epitaxol. The selectivity of the HPLC assay for paclitaxel over 7-epitaxol was determined by injecting a blank and by measuring the resolution (R) of the paclitaxel and 7-epitaxol peaks when a mixture of paclitaxel and 7-epitaxol standards were injected.

3.8.11. Determination of the chemical stability of paclitaxel in PBS-A

Four test tubes containing 30% paclitaxel loaded 35-105 μm microspheres and PBS-A were prepared in the same manner as for *in vitro* release studies as described in section 3.8.9. The tubes were tumbled end-over-end at 30 rpm at 37°C. After six hours, the tubes were centrifuged at 2000 rpm for 15 minutes. From each tube, 5 ml of the supernatant were saved for analysis by HPLC. Forty ml of the supernatant were transferred to a new 50 ml tube and stored at 37°C (without tumbling). After an additional 18 and 42 hours, 5 ml of the supernatant were removed from each tube for analysis.

The amount of paclitaxel in the 5 ml of supernatant was determined as described in section 3.8.9, but with the following modifications. A mobile phase containing 45:55 acetonitrile:water, flowing at 1 ml/min was used. The chromatographic separation was accomplished using two Nova-Pak C_{18} columns connected in series. Standard curves for paclitaxel, baccatin III, and 7-epitaxol in 50:50 acetonitrile:water were constructed from

the HPLC analysis of standard solutions of each compound in the concentration range of 1 to 20 µg/ml.

3.9. Methods for the *in vivo* studies using microspheres

3.9.1. The effect of microsphere size on their clearance from the peritoneum

Control (no paclitaxel) microspheres manufactured from 100k g/mol PLLA were used for this experiment. The particle size distributions were determined by optical microscopy using a stage micrometer. One hundred microspheres were observed in the field of view of the microscope and at least three fields of view were observed for each sample.

For all *in vivo* studies, rats were housed in the Animal Care Facility of the Vancouver Hospital and Health Sciences Centre and cared for by Mr. Michael Boyd. Prior to any animal experiments, ethical approval of procedures by the Animal Care Committee at U.B.C. was obtained. Healthy male Wistar rats weighing between 300 and 500 g were anaesthetised with 0.4 ml/kg atropine and 0.33 ml/kg Innovar® and were maintained on 2-3% fluothane. The rats received a midline laparotomy incision (approximately 0.5 cm) and through it were delivered 100 mg of microspheres in 2 ml NS through a 3 ml syringe without a needle attached. Prior to closing the incision, five rats were insufflated through the incision with 11 mmHg carbon dioxide for 45 minutes (insufflated rats). Five rats received no treatment after the microspheres were instilled. After 3-5 hours, the rats were humanely killed with carbon dioxide and the anterior and posterior mediastinal lymph nodes were removed. The lymphatic tissue from each rat was treated with proteinase K for 3 hours at 52 °C. The digested material was then centrifuged (2000 rpm for 15 minutes) and the sediment transferred to a microscope slide

for permanent fixation with Immunomount® followed by Coverbond®. Microspheres alone were incubated in proteinase K for several hours at 52°C and mounted onto a microscope slide in the same manner. The particle size distributions of microspheres observed in the samples were determined in the same manner as for the microspheres after manufacture. All surgical procedures, euthanasia of rats and the preparation of histology slides were the primary responsibility of Dr. J. Demetrick.

3.9.2. Intraperitoneal carcinomatosis rat model

3.9.2.1. Culturing of 9L glioblastoma cells

9L glioblastoma cells were thawed and cultured in minimum essential media with 10% fetal calf serum and 1% gentamicin at 37°C. Prior to injections, the cells were washed with PBS followed by 5% trypsin-EDTA solution. Cells were centrifuged at 2000 rpm for 5 minutes, and then resuspended in PBS. The cell concentration was determined using a haemocytometer. The cell suspension was diluted in PBS at a concentration of two million cells/ml. Cells were cultured by Drs. J. Demetrick and S. D'Amours at the Jack Bell Research Center (Vancouver, BC).

3.9.2.2. Surgical procedures

Male Wistar rats weighing 350-500 grams were anaesthetised as described in section 3.9.1. Each rat received a 0.5 cm midline incision and 1 ml of PBS containing two million 9L glioblastoma cells was injected into the peritoneal cavity. The incisions were closed and the rat allowed to recover from the anaesthetic. The animals were housed and checked daily for signs of distress according to the U.B.C. animal care guidelines. Two weeks following the introduction of the 9L glioblastoma cells the

animals were humanely sacrificed using carbon dioxide euthanasia. Representative samples of the incision site, omentum, and visceral peritoneum were fixed in formalin, stained with haematoxylin and eosin, and analysed by a pathologist.

3.9.2.3. Dose escalation study

To determine the effect of different doses of paclitaxel loaded microspheres on rats in the intraperitoneal carcinomatosis model, a dose escalation study was completed using four groups of five Wistar rats. Each rat underwent the procedure described in section 3.9.2.2 to establish intraperitoneal carcinomatosis. However, prior to closing the incision each rat received an additional treatment. Groups I to IV received 30% paclitaxel loaded microspheres in the amounts of 50, 100, 150 and 350 mg, respectively. Group V received 100 mg of control microspheres and group VI received 1 ml of NS. The microspheres were suspended in 1 ml of NS immediately prior to injection. All surgical procedures except the administration of microspheres and tumour cells were carried out by Dr. J. Demetrick. Post-mortem dissections were completed with the assistance of Dr. J. Demetrick.

3.9.2.4. Cecotomy repair model

Intraperitoneal carcinomatosis was established as described in section 3.9.2.2 with the following modifications. The weight of each rat was between 300 and 400 g. Each rat received a 2 cm midline incision into the peritoneal cavity and two million 9L glioblastoma cells were injected in 1 ml PBS. Immediately following the injection of tumour cells a 1.5 cm anti-mesenteric incision was made into the cecum. The cecotomy was repaired with a 6-0 proline running suture. Immediately following the cecotomy repair, each rat received intraperitoneally either 100 mg of 30% paclitaxel loaded 35-

81

105 μm microspheres in 2 ml NS (treatment group), 100 mg control microspheres in the same size range in 2 ml of NS (control group), or no treatment (sham group). The fascia was closed with 3-0 proline buried interrupted sutures. The skin was closed with a 4-0 Vicryl subcutaneous running stitch. After recovery from anaesthesia each rat received 0.032 mg buprenorphine as an analgesic.

Two or six weeks following the surgery, the rats were sacrificed using carbon dioxide euthanasia. The peritoneum of each rat was observed for gross signs of carcinomatosis. If no tumours or obvious cancerous nodules were observed, representative samples of the cecotomy repair, omentum, and any suspicious nodules were removed, fixed in formalin, stained with haematoxylin and eosin, and analysed by a pathologist. The surgical repair of the colon, euthanasia of the rats, and preparation of histology samples were completed by Dr. S. D'Amours. Samples of microsphere aggregates were removed from the surface of the small bowel, omentum and liver of two rats that had received paclitaxel. The microspheres were observed by SEM and the total content of remaining paclitaxel was analysed as described in sections 3.8.3 and 3.8.7, respectively.

3.10. Statistical treatment of data

Data collected by measurement of several samples from different batches of material are presented as the average $\pm$ standard deviation. For ANOVA tests and t-tests the level of significance was a p value of 0.05 and the hypothesised difference between populations was zero.

Particle size distribution data was summarised as the average, mode and standard deviation of the particle size distribution. When several batches were measured, the

average and standard deviation of each of these parameters was calculated and presented as "average ± standard deviation".

For *in vitro* release studies, measurements were made on four samples of microspheres taken from each batch. Values of the average and standard deviation were calculated from the cumulative amount of paclitaxel release from each of the four samples. In figures representing these data, the average values are plotted and the error bars represent one standard deviation of the average.

For all other data collected by repeated measurement of samples from a single batch of material, the average was calculated. The relative standard deviation of this type of average was used to calculate the precision in the measurements.

4. RESULTS

4.1. Solid state characterisation of paclitaxel

4.1.1. Water content

Karl Fischer analysis showed that paclitaxel I contained $0.53 \pm 0.03\%$w/w water. Paclitaxel which had been stirred in water for 24 hours recrystallised as a hydrate. The hydrate form of paclitaxel contained 4.47 ± 0.72 %w/w water, equivalent to 2.22 ± 0.36 moles water per mole of paclitaxel. Therefore the hydrated form was likely to be paclitaxel dihydrate (paclitaxel•$2H_2O$), containing a small amount of non-structural water retained in the solid.

4.1.2. Morphology of crystals

Scanning electron micrographs for paclitaxel I and paclitaxel•$2H_2O$ revealed that both forms of paclitaxel exhibited a needle shaped (acicular) crystal habit. Micrographs of both forms of paclitaxel are shown in Figure 6.

4.1.3. Thermal properties and water uptake studies

Thermogravimetric analysis of paclitaxel I revealed a $0.20 \pm 0.06\%$ weight loss in the temperature range 30 - 100°C. The degradation temperature (T_d) was taken as the onset of a weight loss of over 50% that accompanied a visible charring of the sample. T_d of paclitaxel I was 248.5 ± 1.0°C. Figure 7A shows a representative thermogravimetric profile of paclitaxel I. Thermogravimetric analysis of five batches of paclitaxel•$2H_2O$ was carried out to determine the between-batch reproducibility with which paclitaxel I

was completely converted to paclitaxel•$2H_2O$ after 24 hours. All batches showed similar

weight losses of 4.69 ± 0.29% equivalent to a loss of 2.33 ± 0.15 mole of water per mole

of paclitaxel. Figure 7B is representative of thermograms observed for all five batches.

The derivative of the weight loss profile showed two maxima at 50 and 72°C, indicating

that each mole of water was lost separately. All batches of paclitaxel•$2H_2O$ were

subsequently pooled and mixed to create one final batch used for all further

characterisation. The T_d of paclitaxel•$2H_2O$ measured by TGA was 228 ± 1.2°C.

DSC thermograms for both forms of paclitaxel were obtained between 25 and

250°C (Figure 8) and the observed thermal events are summarised in Table 3. Figure 8A

shows a representative thermogram of paclitaxel I obtained in an open pan. Paclitaxel I

exhibited a small change in baseline around 60°C due to the removal of residual,

probably adsorbed or non-structural water. A single melting endotherm at 223.0°C, just

prior to degradation was also observed (Figure 8A). Both pan types (open and pinhole

pans) yielded thermograms with similar peak melting temperatures and enthalpies of

fusion. The thermogram for amorphous paclitaxel (paclitaxel I heated to melting and

quench-cooled to 25°C) (Figure 8B) showed a glass transition temperature of 152.4 ±

0.9°C (Table 3). The melting point of crystalline paclitaxel and the glass transition

temperature and ΔCp of amorphous or glassy paclitaxel are also shown in Table 4. The

data were compared with literature data for the Tg and ΔCp of the glass forming

materials indomethacin and sucrose. The thermogram for paclitaxel•$2H_2O$ (Figure 8C)

showed two endothermic dehydration and vaporisation peaks at approximately 85 and

119°C, resulting in the phase referred to as "dehydrated paclitaxel•$2H_2O$". An

endothermic solid-solid transition occurred at 168°C (Figure 8C) as dehydrated

paclitaxel•2H$_2$O was converted to a semicrystalline material called "paclitaxel I/am" which melted at 221°C, just prior to degradation. Paclitaxel I/am showed an X-ray diffraction pattern similar to that of paclitaxel I (refer to section 4.1.4). Both the open and pinhole pans for paclitaxel•2H$_2$O yielded similar peak melting temperatures and enthalpies of fusion. At slower heating rates (6 and 2°C/min), the peak temperatures for dehydration, solid-solid transition and melting were all shifted to lower temperatures and at 2°C/min were lowered by 30°C, 10°C, and 10°C, respectively. Samples of all forms of paclitaxel showed discoloration at temperatures above 210°C after heating at 1°C/min by DSC. No discoloration or charring was observed in any samples when scan rates greater than 1°C/min were used.

Isothermal treatment of paclitaxel•2H$_2$O at 45°C resulted in the disappearance of the endothermic dehydration peaks (by DSC) and a total weight loss (by TGA) equivalent to 2.12 moles of water per mole of paclitaxel, yielding dehydrated paclitaxel•2H$_2$O. The isothermal thermogravimetric profile of paclitaxel•2H$_2$O is shown in Figure 9. The profile shows a biphasic weight loss pattern. A 2.57% weight loss, equivalent to 1.30 moles of water per mole of paclitaxel, was observed in the first 6.5 minutes (which included one minute of heating to 45°C). Over the next 60 minutes a slower phase of dehydration resulted in a weight loss of 1.62%, equivalent to 0.82 moles of water/mole of paclitaxel. Following cooling under ambient atmospheric conditions for 30 minutes, the sample showed a TGA weight loss profile identical to that of paclitaxel•2H$_2$O. A representative DSC thermogram of paclitaxel•2H$_2$O held at 45°C for 2.5 hours followed by heating through degradation is shown in Figure 8E. A very broad and small

endothermic event was observed between 50 and 120°C with a solid-solid and melting transitions occurring at 167 and 219 °C, respectively.

Paclitaxel•2H₂O samples that underwent a heat-cool-heat cycle by DSC with cooling accomplished in a nitrogen atmosphere prior to reheating, showed no thermal events upon cooling from either 100 or 195°C. Further, no endotherms associated with dehydration were seen upon reheating either sample. Paclitaxel•2H₂O heated to 195°C and cooled in a nitrogen atmosphere did not exhibit a solid-solid transition on reheating.

Paclitaxel•2H₂O samples were subjected to a heat-cool-heat cycle by DSC with cooling accomplished in ambient atmospheric conditions prior to reheating. The TGA and DSC thermograms of the samples cooled from 100°C were identical to those of paclitaxel•2H₂O (Figures 7B and 8C, respectively). However, samples cooled from 195°C (paclitaxel I/am) showed a broad endotherm around 80°C, a glass transition at 151°C and a melting endotherm at 217.7 ± 1.0°C (see Figure 8D and Table 3). During the cooling phase of the heat-cool-heat cycle, gravimetric analysis of paclitaxel•2H₂O previously heated to 100°C showed a weight gain of 5.42 ± 0.56% equivalent to 2.57 ± 0.31 mole of water per mole of paclitaxel. Samples of paclitaxel I and paclitaxel•2H₂O heated to 195°C showed a weight gain of less than 1% for each sample during cooling under ambient conditions. Subsequent TGA of these samples showed weight loss of 0.08 ± 0.05% and 0.68 ± 0.03% between 30 and 65°C for paclitaxel I and paclitaxel I/am (produced from paclitaxel•2H₂O), respectively.

No statistically different change in weight due to moisture uptake was observed in paclitaxel I after exposure to relative humidities ranging from 0 to 93.7%. T-tests had value of p greater than 0.05 at all relative humidities.

4.1.4. X-ray powder diffraction patterns

X-ray powder diffraction patterns for paclitaxel I and paclitaxel•$2H_2O$ at temperatures from 25°C to 195°C are shown in Figure 10 with d-spacings given in Table 5. Paclitaxel I at 25 (Figure 10A) and 195°C showed similar patterns. However, paclitaxel I at 195°C showed several additional weak peaks between 14 and 25 °2θ, and increased intensity relative to paclitaxel I at 25°C. Paclitaxel•$2H_2O$ (Figure 10B) showed peaks which were different to paclitaxel I at 25°C (e.g. 6.1, 9.5, 13.2, 13.8 °2θ). Dehydrated paclitaxel•$2H_2O$ at 100°C (Figure 10C) showed a pattern different from both paclitaxel•$2H_2O$ and paclitaxel I at 25°C (e.g. 6.4, 11.4, 14.1 16.3, and 18.7 °2θ). The X-ray pattern for paclitaxel I/am at 195°C (Figure 10D) (obtained from paclitaxel•$2H_2O$ heated to 195°C) is similar to that of paclitaxel I, having all the major peaks in common but with lower peak intensities. Two peaks observed in the paclitaxel I pattern were not observed in the pattern of paclitaxel I/am (14.1 and 25.9 °2θ).

4.1.5. Dissolution of paclitaxel in water

Three LCMS-MS standard curves and corresponding regression analyses for paclitaxel in 50:50 acetonitrile are shown in Figure 11. Coefficients of determination exceeded 0.986 for all three curves. The three standard curves were obtained at different times in the chromatographic analysis of paclitaxel dissolution study samples in order to account for changes in sensitivity of the LCMS-MS assay over time. Each standard curve was obtained by injection of the same set of standard solutions. The first standard curve was obtained immediately prior to analysis of the first sample. The second was obtained after half the samples were assayed, and the last immediately after analysis of the final sample.

The dissolution profiles of both paclitaxel I and paclitaxel•$2H_2O$ are shown in Figure 12. The maximum apparent solubility of paclitaxel I in water was 3.59 ± 0.41 µg/ml after 3 hours of dissolution at 37°C. The maximum apparent solubility of paclitaxel•$2H_2O$ was 0.93 ± 0.14 µg/ml after 20 hours of dissolution. By 20 hours the apparent solubilities of paclitaxel I and paclitaxel•$2H_2O$ approached a single value near 1 µg/ml. The solubilities at this point were not statistically different (two-tailed t-test, $p=0.095$).

Table 3. A summary of thermal events observed by DSC for paclitaxel I, amorphous paclitaxel, paclitaxel•2H₂O and paclitaxel I/am.

Form of paclitaxel	Dehydration endotherms		Glass transition	Solid-solid transition	Melting transition
	I	II			
	Peak (°C) (ΔH J/g)	Peak (°C) (ΔH J/g)	Inflection point (°C) (ΔCp J/g·K)	Peak (°C) (ΔH_f J/g)	Peak (°C) (ΔH_f J/g)
Paclitaxel I	--	--	--	--	223 (63)
Amorphous paclitaxel	--	--	153 (0.307)	--	--
Paclitaxel•2H₂O	85 (110)	119 (81)	--	168 (8.5)	221 (36)
Paclitaxel I/am	81 (13)[a]		151 (0.157)	--	217 (31)

[a] A single broad endotherm due to removal of non-structural water.

Table 4. Melting point and glass transition data for indomethacin, sucrose, and paclitaxel.

	Indomethacin[a]	Sucrose[a]	Paclitaxel
Tg (deg K)	320	350	493 [b]
Tm (deg K)	438	453	426 [c]
Tm/Tg	1.37	1.29	1.16
ΔCp (J/mol·K)	167	186	266 [b]

[a] Data from Hancock *et al.*, (1995). Heating rates were 20 K/min compared with 10 K/min for paclitaxel in this study.
[b] Tg and ΔCp values observed by DSC for amorphous paclitaxel.
[c] Tm value observed by DSC for paclitaxel I.

Table 5. Paclitaxel crystal d-spacing values from X-ray diffraction peak locations (°2θ) for paclitaxel I at 25 and 195°C, paclitaxel I/am at 195°C, paclitaxel•2H$_2$O at 25°C, and dehydrated paclitaxel•2H$_2$O at 100°C. Peak strengths are described as strong, medium or weak.[a]

| X-ray peaks: | | Peak Strength | | | | |
°2θ	d-spacings (Å)	Paclitaxel I[b]	Paclitaxel I[c]	Paclitaxel I/am[c]	Paclitaxel •2H$_2$O[b]	Dehydrated paclitaxel •2H$_2$O[d]
6.1	14.5				Strong	
6.4	13.8					Strong
8.8	10.0	Strong	Strong	Strong	Strong	Strong
9.5	9.30		Weak		Medium	Weak
10.9	8.11				Medium	Medium
11.1	7.96	Medium	Medium	Weak		
11.4	7.75					Medium
12.1	7.31	Medium	Strong	Strong	Strong	Strong
12.3	7.19	Medium	Strong	Strong	Strong	Strong
13.3	6.65				Medium	Strong
13.8	6.41				Medium	
14.1	6.27	Weak	Weak			Medium
16.3	5.43		Weak			Medium
18.7	4.74					Strong
19.3	4.59	Weak	Weak	Weak		
25.9	3.44	Medium	Weak			

[a] Strong peaks: relative intensity greater than 50, medium peaks: relative intensity between 20 and 50, weak peaks: relative intensity less than 20.
[b] Scan obtained at 25°C.
[c] Scan obtained at 195°C.
[d] Scan obtained at 100°C.

Figure 6. Scanning electron micrographs of A) paclitaxel I and B) paclitaxel•2H$_2$O. (Magnification of both micrographs is 10000x.)
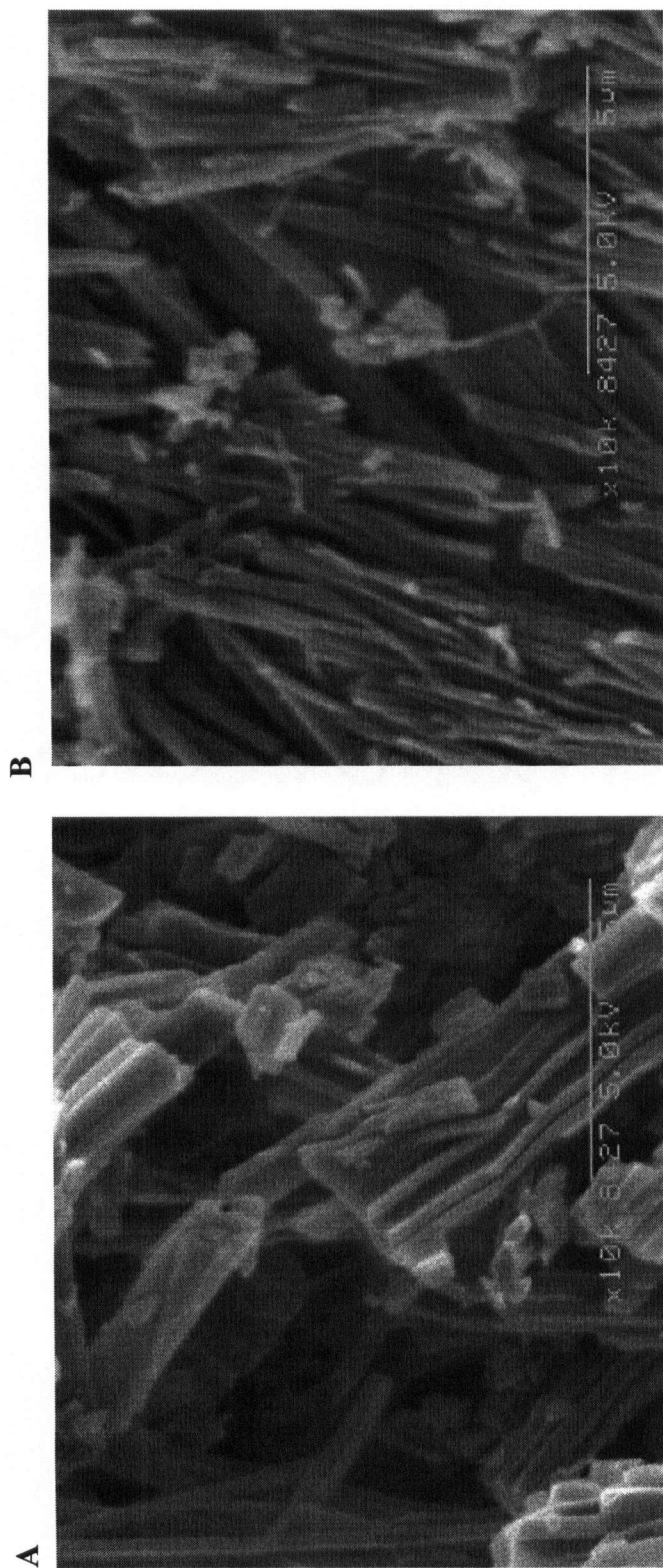
Figure 7. Thermogravimetric profiles of A) paclitaxel I and B) paclitaxel•2H₂O, Curves labelled a) and b) correspond to the percentage of initial weight remaining and the derivative of percentage weight loss with respect to temperature (dW/dT), respectively.
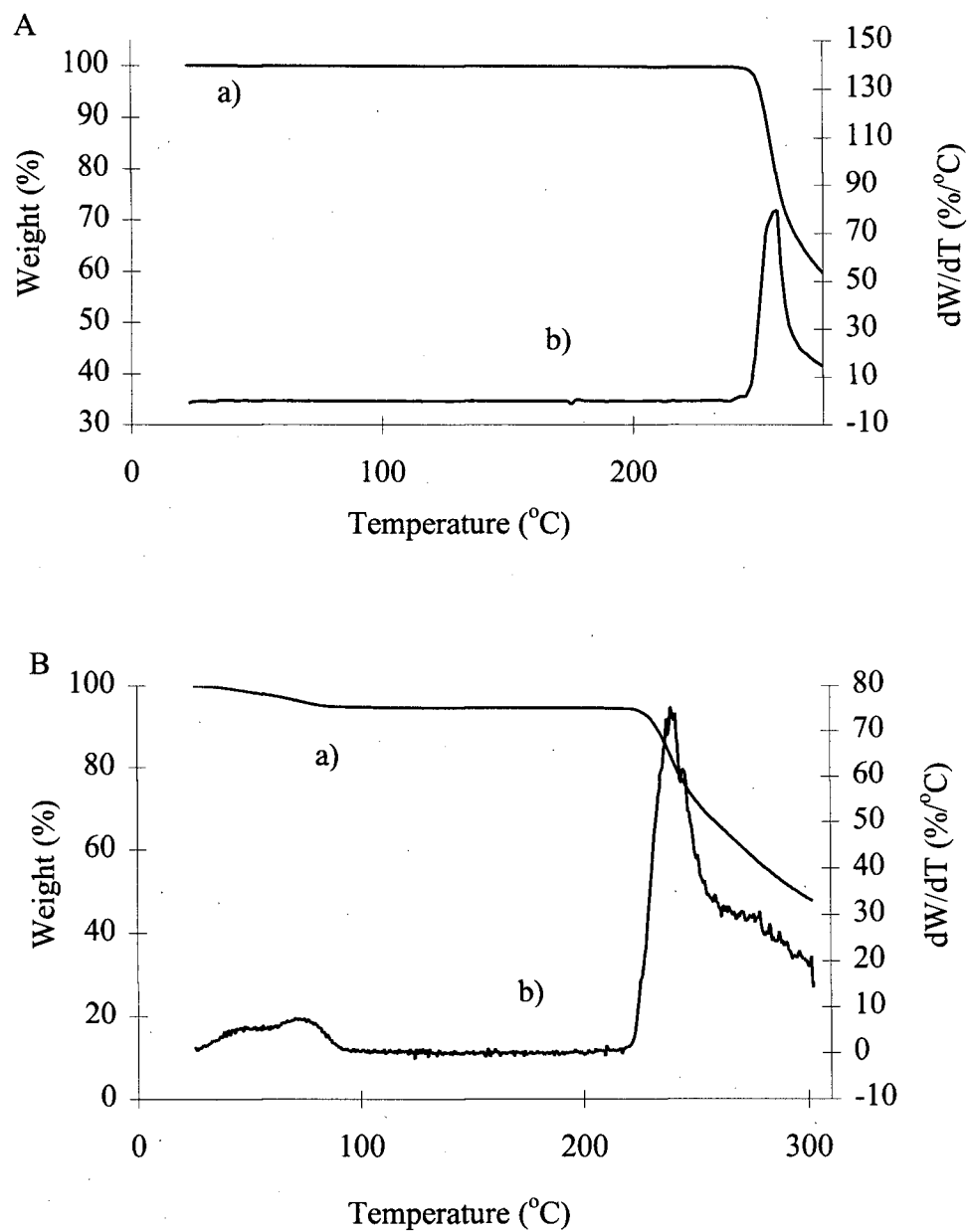
Figure 8. Representative DSC thermograms of A) paclitaxel I, B) quench cooled paclitaxel I, C) paclitaxel•2H$_2$O, D) paclitaxel I/am, E) paclitaxel•2H$_2$O held isothermally at 45°C for 150 minutes followed by heating to 250°C.
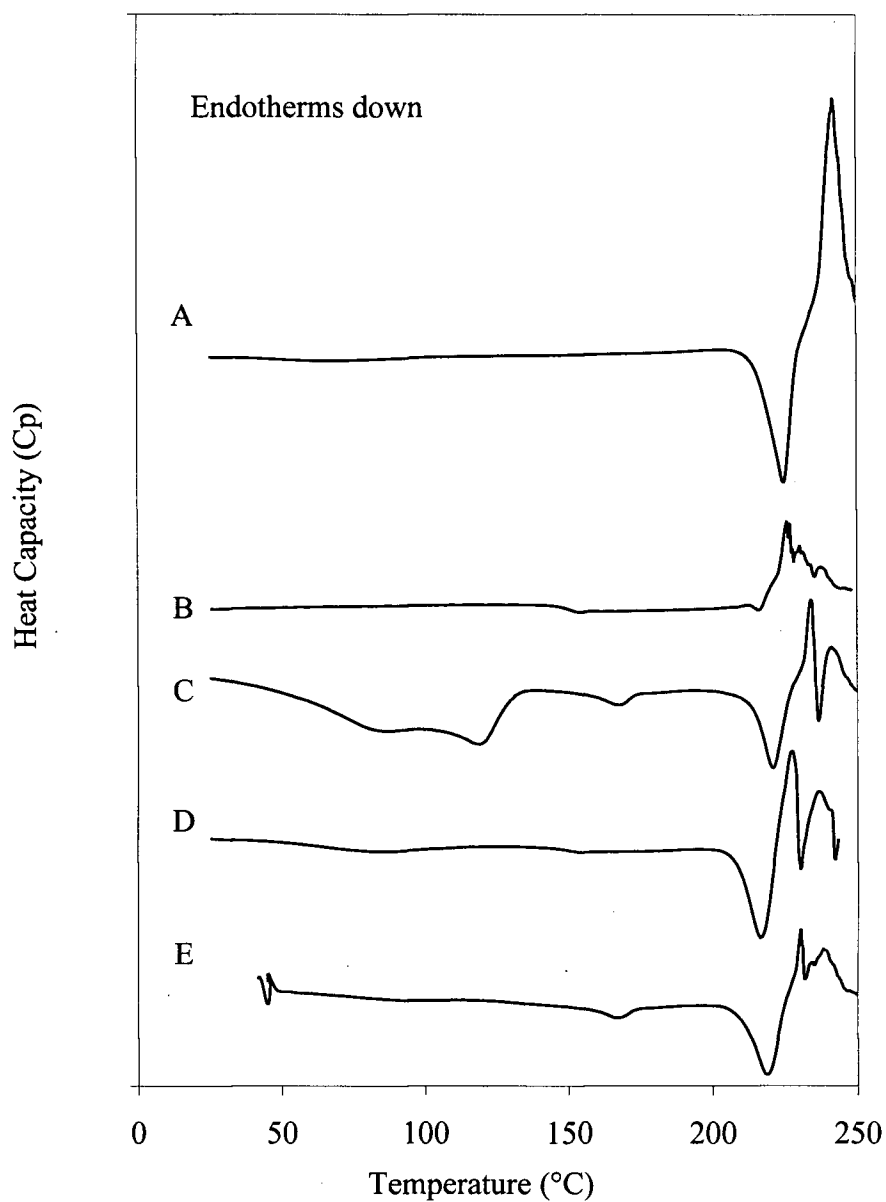
Figure 9. Thermogravimetric analysis of paclitaxel•2H$_2$O held isothermally at 45°C for 150 minutes.
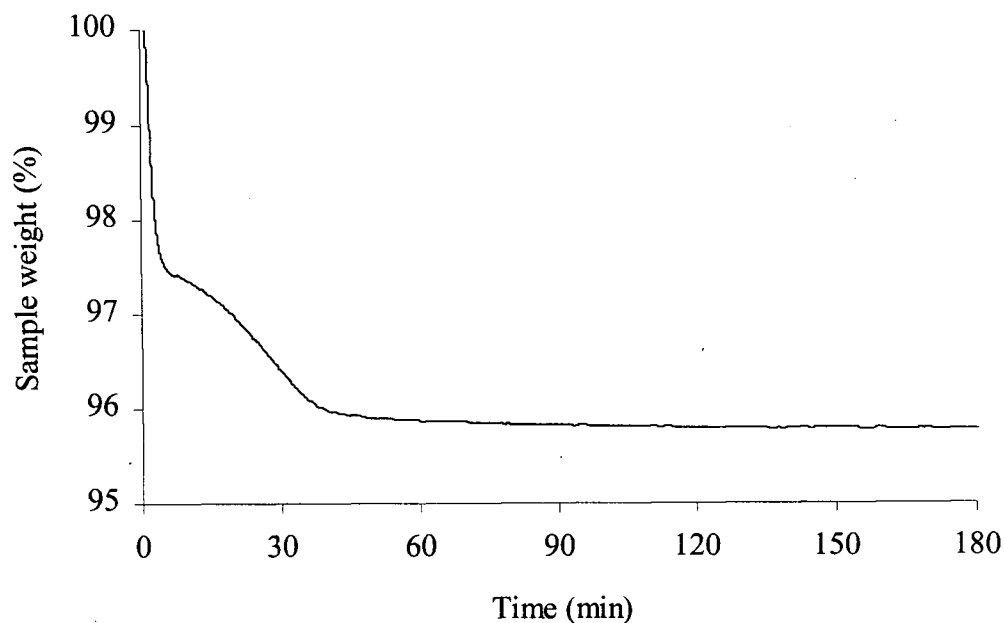
Figure 10. X-ray powder diffraction patterns of A) paclitaxel I at 25°C, B) paclitaxel•2H$_2$O at 25°C, C) dehydrated paclitaxel•2H$_2$O at 100°C and D) paclitaxel I/am at 195°C.
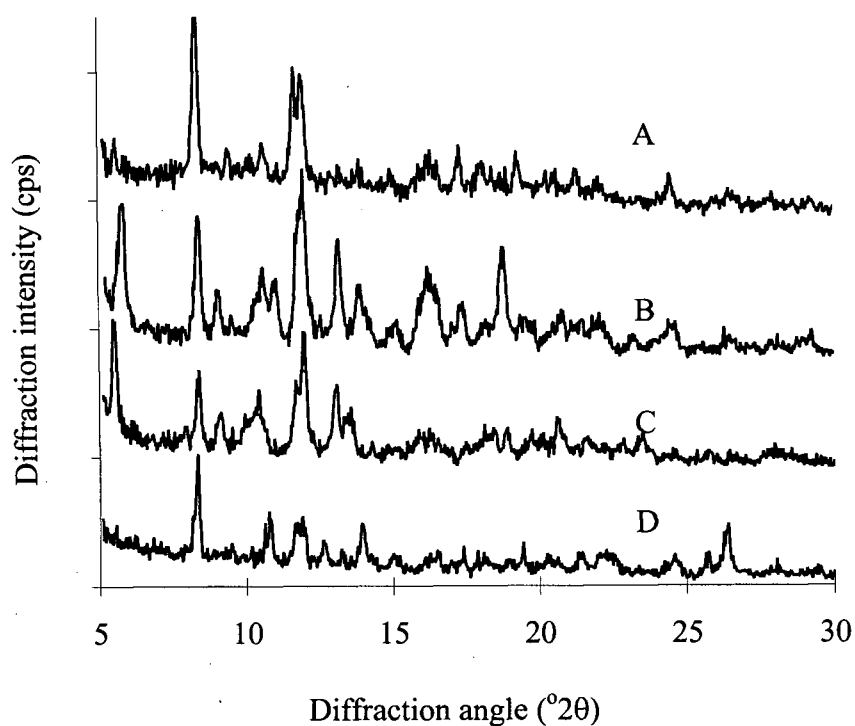
Figure 11. Standard curves of paclitaxel in 50:50 acetonitrile:water. LCMS-MS analysis parameters: 20 μL injection on a C_{18} Hypersil column with a mobile phase of 2 mmol/L ammonium acetate in 60:50 acetonitrile:water flowing at 150 μL/min with MSMS detection..
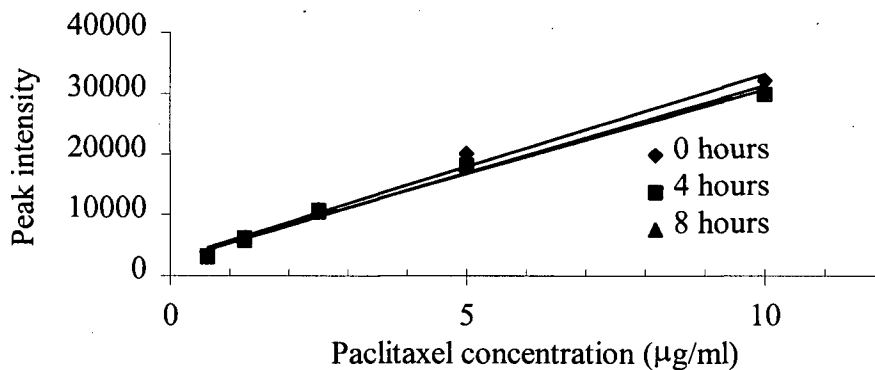
Regression analysis parameters: $y = mx + b$, R^2

0 hours: $y = 3072x + 2660$, $R^2 = 0.986$

4 hours: $y = 2800x + 2827$, $R^2 = 0.989$

8 hours: $y = 2901x + 2495$, $R^2 = 0.990$

Figure 12. Dissolution profiles of paclitaxel I and paclitaxel•$2H_2O$ in distilled water at 37°C.
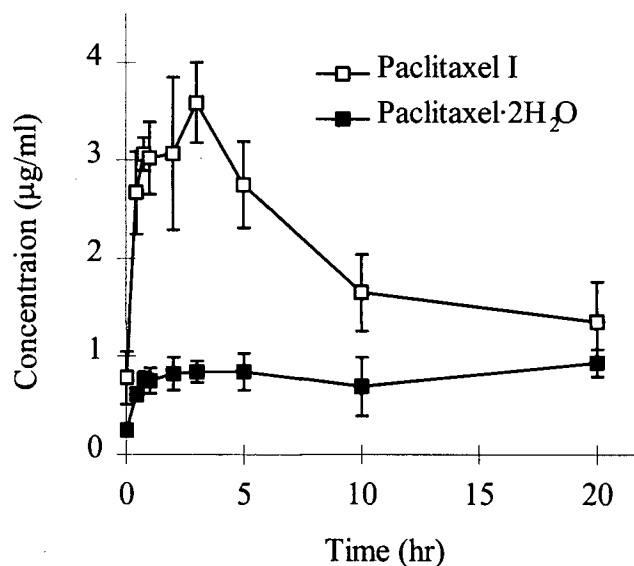
4.2. Polymer synthesis and molecular weight determination

4.2.1. Characterisation of the LLA oligomer

Karl Fischer analysis showed that the water content of the oligomer was 3 %w/w. End group titration was used to determine M_n of the LLA oligomer. The M_n of the LLA oligomer, after seven hours of reaction time, was 337 g/mol, equivalent to an average of 4.7 repeating units per chain.

4.2.2. Molecular weight determination for PLLA polymers

4.2.2.1. Intrinsic viscosity determinations

Preliminary determinations of intrinsic viscosity of a PLLA polymer at ambient temperatures of 23 and 26°C gave values of 1.94 and 1.92, respectively. These values differed by 1.3% and all further determinations were conducted within this range of ambient temperatures. Representative Huggins and Kraemer plots of viscosity data obtained for 100k g/mol PLLA-PS are shown in Figure 13. Coefficients of determination (R^2) for all Huggins and Kraemer plots were greater than 0.95. Table 6 summarises the intrinsic viscosity data calculated using the Huggins (1942), Kraemer (1938) and Solomon and Ciuta (1962) equations (Equations 18, 19 and 20, respectively). For both PLLA and polystyrene, no significant difference was observed in values calculated using the three equations, determined by a single factor ANOVA. The relative standard deviations (standard deviation expressed as a percentage of the average) for intrinsic viscosities calculated using the Solomon and Ciuta equation for 100k g/mol PLLA and 233k g/mol polystyrene were 0.3 and 1.9% respectively. The approximation method of

Solomon and Ciuta was used for all further intrinsic viscosity calculations for PLLA and polystyrene.

Values of the intrinsic viscosity for the 17.5k, 30k, 50k, 100k, and 233k g/mol polystyrene standards required to generate the universal calibration curve were 0.147, 0.326, 0.356, 0.500, and 1.128 dl/g, respectively. The values were an average of three measurements and the percent RSD for all measurements was less than 8%. Values of intrinsic viscosity for 4k and 9k g/mol polystyrene were calculated using the Mark-Houwink equation (Equation 9) with values of $K = 1.77 \times 10^{-4}$ and $a = 0.701$ determined from the intercept and slope respectively, of the plot shown in Figure 14.

Intrinsic viscosity measurements of commercially obtained PLLA and values of M_v are given in Table 7.

4.2.2.2. Gel permeation chromatography

Universal calibration curves (Coll and Gilding, 1970) for the 10^3 and 10^4 Å columns are shown in Figure 15. Elution profiles of mixtures of polystyrene molecular weight standards injected onto the 10^3 Å and 10^4 Å columns illustrate the effect of a polymer's molecular weight on its retention time on the columns used (Figure 16 and 17). The linear ranges for the 10^3 and 10^4 Å columns were 2k – 50k and 9k - 100k g/mol, respectively. R^2 values for both calibration curves exceeded 0.99.

The molecular weights of PLLA polymers synthesised by ring opening polymerisation were calculated from GPC data and the universal calibration curve for the 10^3 Å column. Figure 18A and B show representative GPC elution profiles of PLLA-SA and PLLA-LA polymers, respectively. Figure 19 relates the predicted values of M_n^* of PLLA polymers based on Equation 15 to corresponding values of M_{GPC} for both PLLA-

SA and PLLA-LA. The molecular weight of PLLA-SA was controlled by the stoichiometric ratio of stearyl alcohol to L-lactide addition over the entire predicted molecular weight range. However, as the intercept of the regression curve indicates, the experimentally determined or observed molecular weight was overestimated by Equation 15 by approximately 1.2k g/mol for all molecular weights.

For PLLA-LA polymers, the regression analysis of the relationship between predicted and observed molecular weight was linear up to 2k g/mol and the predicted and observed molecular weight values were similar. However, above 2k g/mol, observed molecular weights were much less than those predicted. At a predicted M_n^* of 10k g/mol, M_{GPC} was 3.5k g/mol, which represented the maximum molecular weight achievable by this method of synthesis. M_{GPC} values for commercial polymers are given in Table 7 and their GPC elution profiles are shown in Figure 18C.

Table 6. Intrinsic viscosity data for 100k g/mol poly(L-lactic acid) and 233k g/mol polystyrene. Values are an average calculated from three measurements ± standard deviation.

	Huggins equation	Kraemer equation	Solomon and Ciuta equation
Poly(L-lactic acid) (molecular weight: 100k g/mol)			
Intrinsic viscosity (dl/g)	1.194 ± 0.016	1.196 ± 0.011	1.199 ± 0.004
Polystyrene (molecular weight 233k g/mol)			
Intrinsic viscosity (dl/g)	1.145 ± 0.016	1.123 ± 0.017	1.105 ± 0.021

Table 7. Molecular weights of PLLA polymers obtained commercially determined from intrinsic viscosity determination and gel permeation chromatography data.

PLLA Source	Manufacturer's claimed molecular weight (g/mol)	Intrinsic viscosity[a] (dl/g)	M_v[b] (g/mol)	M_{GPC} (g/mol)
Birmingham Polymers Inc.	100k	1.067 ± 0.016	32k	107k
Polysciences Inc.	2k	0.153 ± 0.011	2k	3k
	50k	0.855 ± 0.003	28k	41k

[a] Average ± standard deviation of three measurements.
[b] M_v calculated using K and a constants from Schindler and Harper (1979).

Figure 13. Huggins and Kraemer plots of viscosity data for 100k g/mol PLLA-PS in chloroform at 25°C. Y-intercept values of each line are the intrinsic viscosity of the polymer.
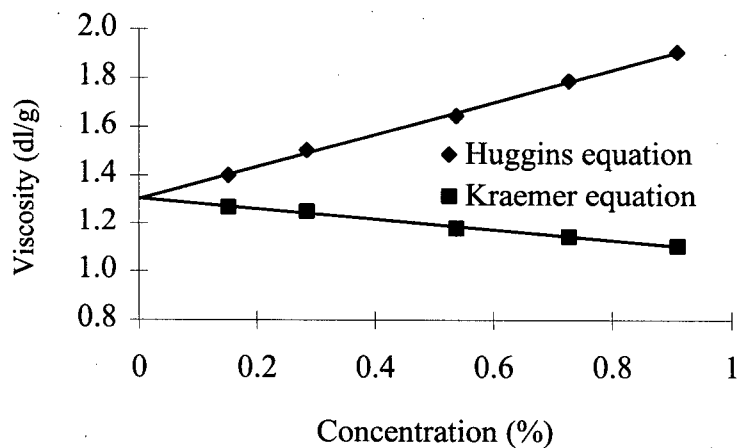
Regression analysis parameters ($y = mx + b$, R^2)

Huggins plot: $m = 0.663$, $b = 1.30$, $R^2 = 0.998$

Kraemer plot: $m = -0.222$, $b = 1.31$. $R^2 = 0.993$

Figure 14. A plot of the Mark-Houwink equation for polystyrene standards. (Equation 9)
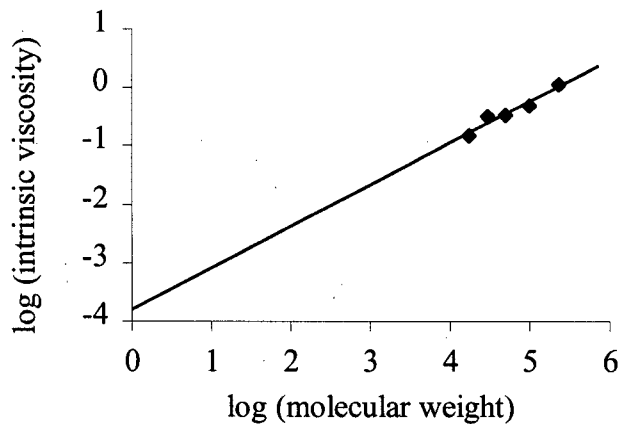
Regression analysis parameters ($y = mx + b$, R^2)

$m = 0.71$, $b = -3.89$, $R^2 = 0.95$

101

Figure 15. Universal calibration curves of polystyrene molecular weight standards injected on A) 10^4 Å and B) 10^3 Å GPC columns.
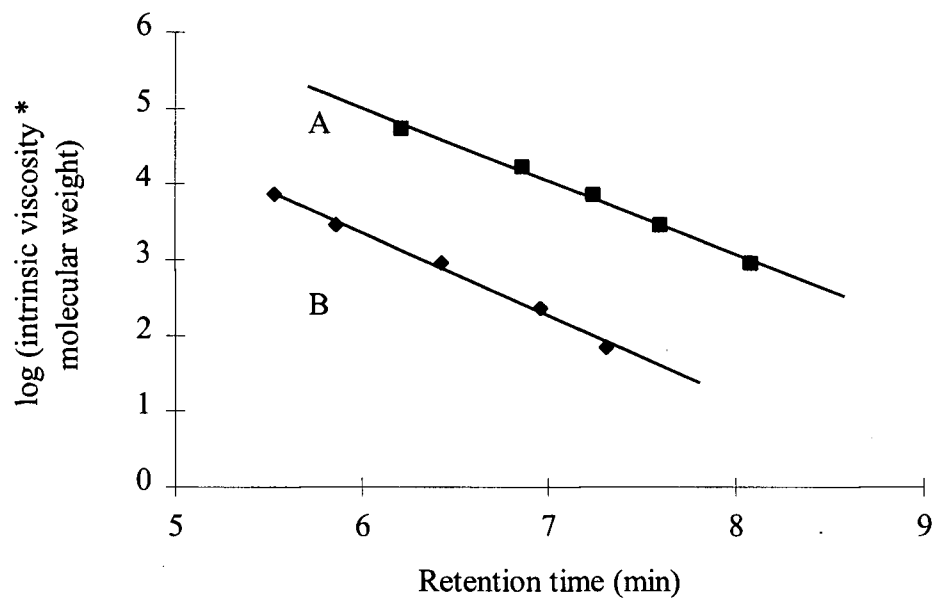
Regression analysis parameters ($y = mx + b$, R^2)

A: 10^4 A column: $m = -0.966$, $b = 10.8$, $R^2 = 0.994$

B: 10^3 A column: $m = -1.09$, $b = 9.91$, $R^2 = 0.994$

Figure 16. Elution profiles of polystyrene molecular weight standards on the 10^3 Å GPC column. Chromatographic conditions: 20 μl injections with mobile phase of chloroform flowing at 1 ml/min and refractive index detection. A: 17.5k g/mol (1), 4k g/mol (2), 1k g/mol (3) B: 30k g/mol (4), 9k g/mol (5), 2k g/mol (6).
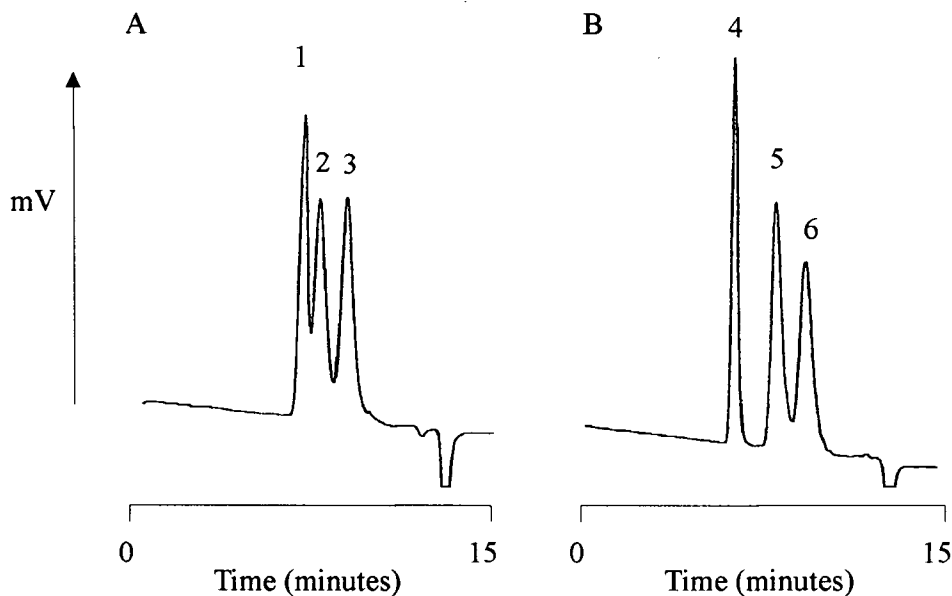
Figure 17. Elution profiles of polystyrene molecular weight standards on the 10^4 Å GPC column. Chromatographic conditions: 20 μl injections with mobile phase of chloroform flowing at 1 ml/min and refractive index detection. A) 233k g/mol (1), 50k g/mol (2), 17.5k g/mol (3), 4k g/mol (4) B) 300k g/mol (5), 100k g/mol (6), 30k g/mol (7), 9k g/mol (8). Peaks labelled "S" are due to solvent elution.
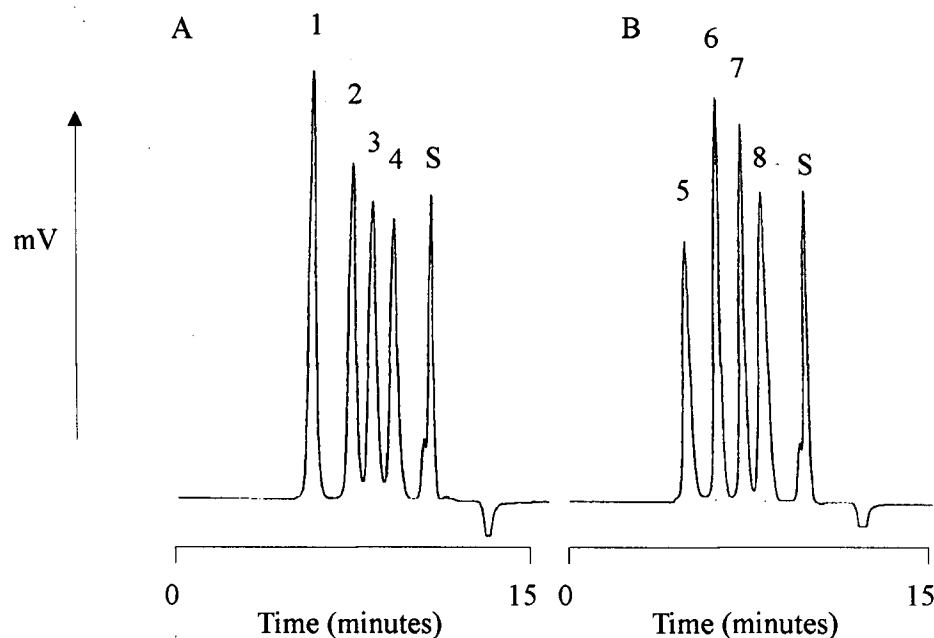
Figure 18. GPC elution profiles of polymerisation products for A) PLLA-SA polymers: a) 1.5k, b) 2k, c) 10k g/mol predicted molecular weight, B) PLLA-LA polymers: a) 1k, b) 2k, c) 7k g/mol predicted molecular weight on the 10^3 Å column, and C) PLLA-PS polymers: a) 2k, b) 50k and c) 100k g/mol molecular weight claimed by the manufacture, on the 10^4 Å column. Chromatographic conditions: 20 μl injection volume with mobile phase of chloroform flowing at 1 ml/min and refractive index detection.

104
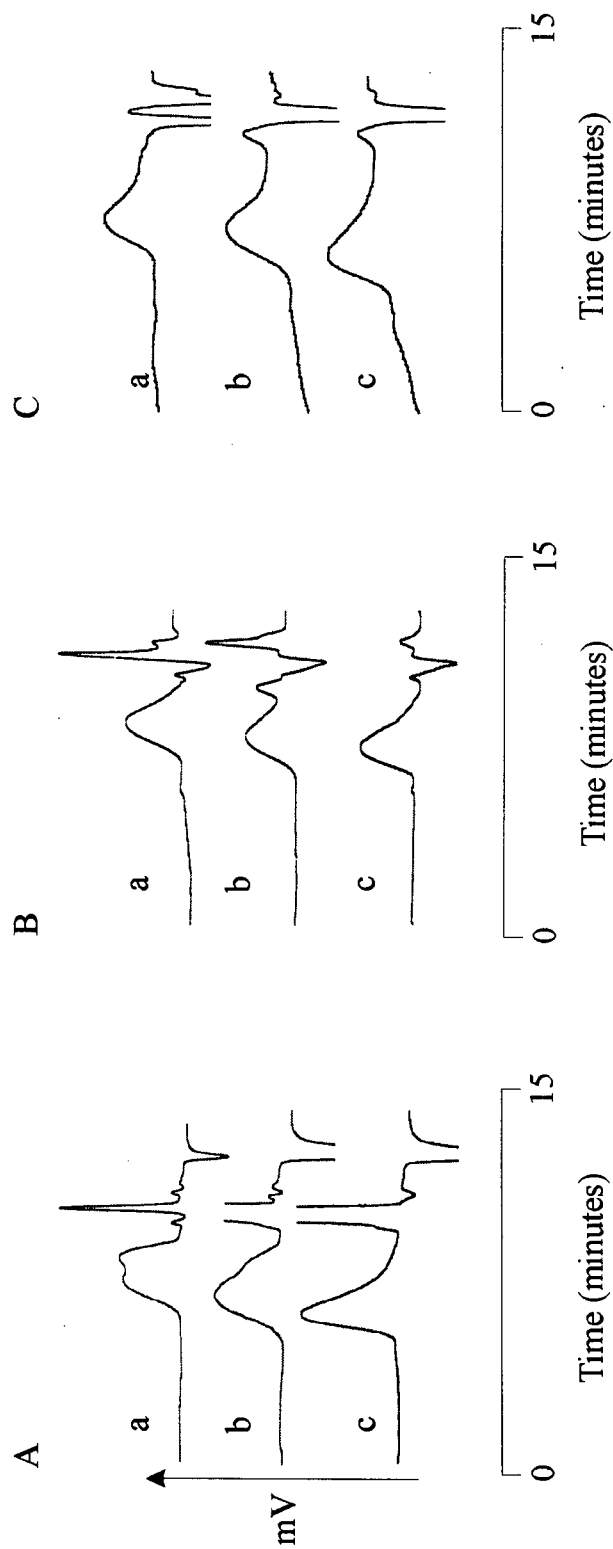
Figure 19. The relationship between predicted molecular weights and experimentally determined values of M_{GPC} for PLLA-SA and PLLA-LA.
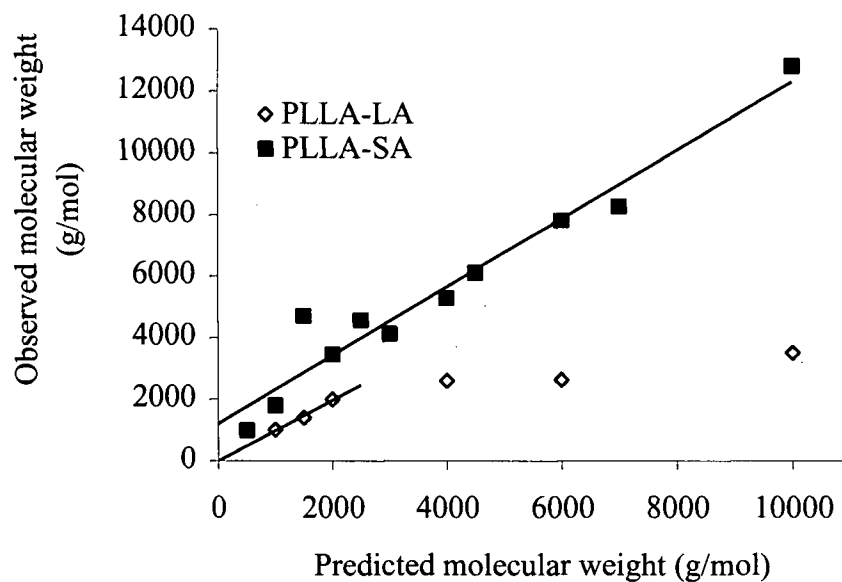
Regression analysis parameters ($y = mx + b$, R^2)

PLLA-LA: $m = 0.98$, $b = 6.7$, $R^2 = 0.99$ (first 3 data points only)

PLLA-SA: $m = 1.1$, $b = 1200$, $R^2 = 0.95$

4.3. Properties of paclitaxel loaded 100k g/mol PLLA microspheres

It was necessary to establish the conditions for preparation of paclitaxel loaded microspheres such that the properties of the microspheres could be adequately controlled and reproduced from batch to batch. For this work, commercial 100k g/mol PLLA was used.

4.3.1. Particle size

Microspheres were manufactured in two size ranges termed "large" and "small" from 100k g/mol PLLA, containing 0 to 30% paclitaxel. Inter-batch variability in microsphere size distributions was described by the standard deviation of the means, modes and standard deviations of the distributions, which are summarised in Table 8. ANOVA tests showed no statistical differences (Table 8) in the parameters describing the size distributions between microspheres with different paclitaxel loadings when comparing either small or large sized microspheres.

4.3.2. Weight loss of the dispersion during microsphere manufacture

Weight loss of the dispersion of the organic phase (paclitaxel and PLLA in dichloromethane) in aqueous PVA during the manufacture of microspheres was measured to calculate the evaporation rate and time for weight loss equal to half of the weight of the organic solvent (t_{50}). Average values (n=3) of t_{50} for control, 10 and 30% loaded microspheres in the small and large size ranges are listed in Table 9. Evaporation rates were linear after five minutes of stirring until weight loss equivalent to evaporation of approximately 90% of the dichloromethane was observed. Coefficients of determination for these data were greater than 0.97. The rate of weight loss decreased from 0.32 ±

106

0.02 g/min for small microspheres at both loadings to 0.10 g/min for 30% loaded large

microspheres. As a control, the rate of evaporation of dichloromethane from a dispersion

of solvent in 2% PVA stirred at 2100 rpm was measured. The rate was constant at 0.32

g/min. The evaporation of water from a solution of 2% PVA (with no organic phase)

stirred at 900 rpm occurred at a rate of 0.02 g/min.

4.3.3. Surface morphology

Scanning electron micrographs of small and large, control and 30% loaded

microspheres are shown in Figure 20. Microspheres appeared spherical and no paclitaxel

crystals were observed in the sample or embedded on the surface of the microspheres.

Paclitaxel loading had a profound effect on the surface morphology of microspheres.

While control microspheres have smooth surfaces, 30% loaded microspheres had a

"dimpled" appearance over the entire surface. The "dimpling" phenomenon was present

but less pronounced in 10% loaded microspheres. A small amount of material which was

not incorporated into the microspheres was observed in micrographs of paclitaxel loaded

large microspheres.

4.3.4. Paclitaxel standard curves

The validation of the standard curve of paclitaxel in acetonitrile and 60:40

acetonitrile:water included measurements of precision, accuracy and linearity and these

data are given in Appendix II. Figures 21A and B show representative chromatograms of

paclitaxel in acetonitrile and in 60:40 acetonitrile:water, respectively. The retention time

of paclitaxel was 2.5 minutes in both chromatograms. Representative standard curves are

shown in Figure 22A.

107

4.3.5. Total paclitaxel content

Table 10 summarises data for the recovery of paclitaxel from spiked solutions of 100k g/mol PLLA in dichloromethane. Phase separation occurred with the addition of 60:40 acetonitrile:water, with precipitation of the polymer at the interface. The volume of each phase did not vary significantly between samples, with a RSD less than 4%. The percent total recovery of paclitaxel was calculated from the sum of HPLC peak areas from the chromatograms of a direct injection of the aqueous phase and a ten-fold dilution in acetonitrile of the organic phase. Total percent recovery had a RSD less than 5%. Almost 100% of the paclitaxel recovered was found in the organic phase. Injection of blank extraction samples showed no peak at 2.5 minutes, the retention time of paclitaxel. The HPLC chromatograms of paclitaxel extracted from spiked samples had two peaks (1.8 minutes and 2.5 minutes) corresponding to dichloromethane and paclitaxel respectively (Figure 21C). The separation factor (α) of the two peaks was 2.05 and the resolution (R) was 3.35.

Average values of total content of paclitaxel in the microspheres are shown in Table 11. No significant difference was measured by ANOVA testing between batches of microspheres, except for 30% loaded small microspheres.

4.3.6. Thermal properties

In order to assess the effect of paclitaxel on melting of 100k g/mol PLLA without manufacturing microspheres, dispersions containing 0 to 60% paclitaxel were prepared by casting both paclitaxel and PLLA from dichloromethane onto a glass surface and allowing the solvent to evaporate. DSC of the dispersions showed that the Tm of 100k g/mol PLLA was depressed from 175 to 163°C for dispersions containing 0 and

60% paclitaxel, respectively. Figure 23 shows the relationship of 1/Tm to paclitaxel content. The relationship was linear over the entire range of paclitaxel concentrations (R^2 = 98). Average values of thermal properties of the microspheres are summarised in Table 12. All small microspheres exhibited small enthalpy relaxation peaks at the glass transition temperature. The enthalpy relaxation phenomenon was also observed in large microspheres, although the peak areas decreased with increasing paclitaxel content and no definite peak could be quantified for 30% paclitaxel microspheres.

Transition temperatures (Tg, Tc and Tm) had RSDs of less than 2% for all sizes and loadings of microspheres. Recrystallisation upon heating of small microspheres above Tg resulted in exothermic peaks with areas between 2 - 5 J/g of PLLA. Recrystallisation could not be quantified in large paclitaxel loaded microspheres, although a small, broad exothermic event was present around 95°C. No effect of paclitaxel loading on polymer crystallinity was observed for either small or large microspheres, based on ANOVA test results shown in Table 12. RSDs for average values of polymer crystallinity were not more than 12% for all types of microspheres. The addition of paclitaxel to the large microspheres resulted in a statistically significant lowering of the Tg and Tm at both 10 and 30% loading levels. Tg and Tm values were depressed by 6 and 7°C, respectively, when comparing control and 30% loaded microspheres. Small microspheres also exhibited a 3°C melting point depression when comparing control and 30% paclitaxel loaded microspheres.

Table 8. Parameters describing the particle size distributions of small and large 100k g/mol PLLA microspheres with p values for ANOVA tests of the data. Data are average values based on measurements of three batches of each formulation ± standard deviation.

Microspheres	Average (μm)	Mode (μm)	Standard deviation of the average (μm)
Small microspheres			
0% paclitaxel	10 ± 0.5	15 ± 1	6 ± 0.5
10% paclitaxel	14 ± 2	15 ± 2	14 ± 4
30% paclitaxel	6 ± 0.5	11 ± 1	5 ± 2
p value	0.46	0.12	0.63
Large microspheres			
0% paclitaxel	75 ± 7	85 ± 8	19 ± 2
10% paclitaxel	78 ± 3	83 ± 5	21 ± 2
30% paclitaxel	74 ± 6	82 ± 3	22 ± 3
p value	0.53	0.41	0.20

Table 9. Time for weight loss due to evaporation of half of the dichloromethane used during microsphere manufacture (t_{50}). Small and large microspheres were manufactured from 100k g/mol PLLA. Values are the average ± standard deviation of three measurements from three batches.

Theoretical paclitaxel loading level	t_{50} (min)	
	Small microspheres	Large microspheres
Control	25 ± 3	34 ± 2
10%	25 ± 3	49 ± 2
30%	26 ± 3	64 ± 2

Table 10. Precision and efficiency of extraction of paclitaxel from microspheres and precision of organic-aqueous phase separation in the total content and residual paclitaxel assays.

	Average ± Standard Deviation (n = 5)	RSD (%)[a]
Volume of top (organic) phase	11.25 ± 0.40 ml	3.51
Volume of bottom (aqueous) phase	10.55 ± 0.33 ml	3.09
Percent total recovery of paclitaxel	105 ± 4%	4.09
Percent of total paclitaxel in top phase	98.9 ± 0.1%	0.15

[a] RSD (Relative standard deviation) is the ratio of the standard deviation to the average, expressed as a percentage.

Table 11. Total content of paclitaxel in small and large 100k PLLA microspheres with initial loads of 10 and 30%.

Microspheres	Paclitaxel content (%)[a]	ANOVA p value
small 10% loaded	88 ± 5	0.74
large 10% loaded	99 ± 4	0.31
small 30% loaded	87 ± 12	0.03[b]
large 30% loaded	96 ± 6	0.32

[a] The total content of each batch was an average of three measurements made per batch ± standard deviation.
[b] The level of significance in the differences observed between batch, $p < 0.05$ indicates significant inter-batch variability.

Table 12. Thermal properties of small and large 100k g/mol PLLA microspheres containing 0, 10, 30% paclitaxel. Values are averages of measurements from each of three batches ± standard deviation.

Microsphere loading	Tg (°C)	Tc (°C)	Tm (°C)	Xc (%)
Small microspheres				
Control	62 ± 2	93 ± 1	174 ± 1	41 ± 4
10%	62 ± 3	94 ± 1	173 [a]	41 ± 2
30%	64 ± 1	94 ± 1	171 [a]	40 ± 5
ANOVA p value	0.97	0.56	<0.001	0.87
Large microspheres				
Control	66 ± 1	95 ± 1	176 [b]	36 ± 6
10%	63 ± 1	---	173 ± 1	38 ± 2
30%	60 ± 1	---	169 ± 1	44 ± 9
ANOVA p value	<0.001	---	<0.001	0.10

[a] The standard deviation of the average melting temperatures was less than 1°C.

Figure 20. Surface morphology of A) small and B) large control and C) small and D) large 30% paclitaxel loaded 100k g/mol PLLA microspheres. (Magnification of all micrographs is 1000x.)
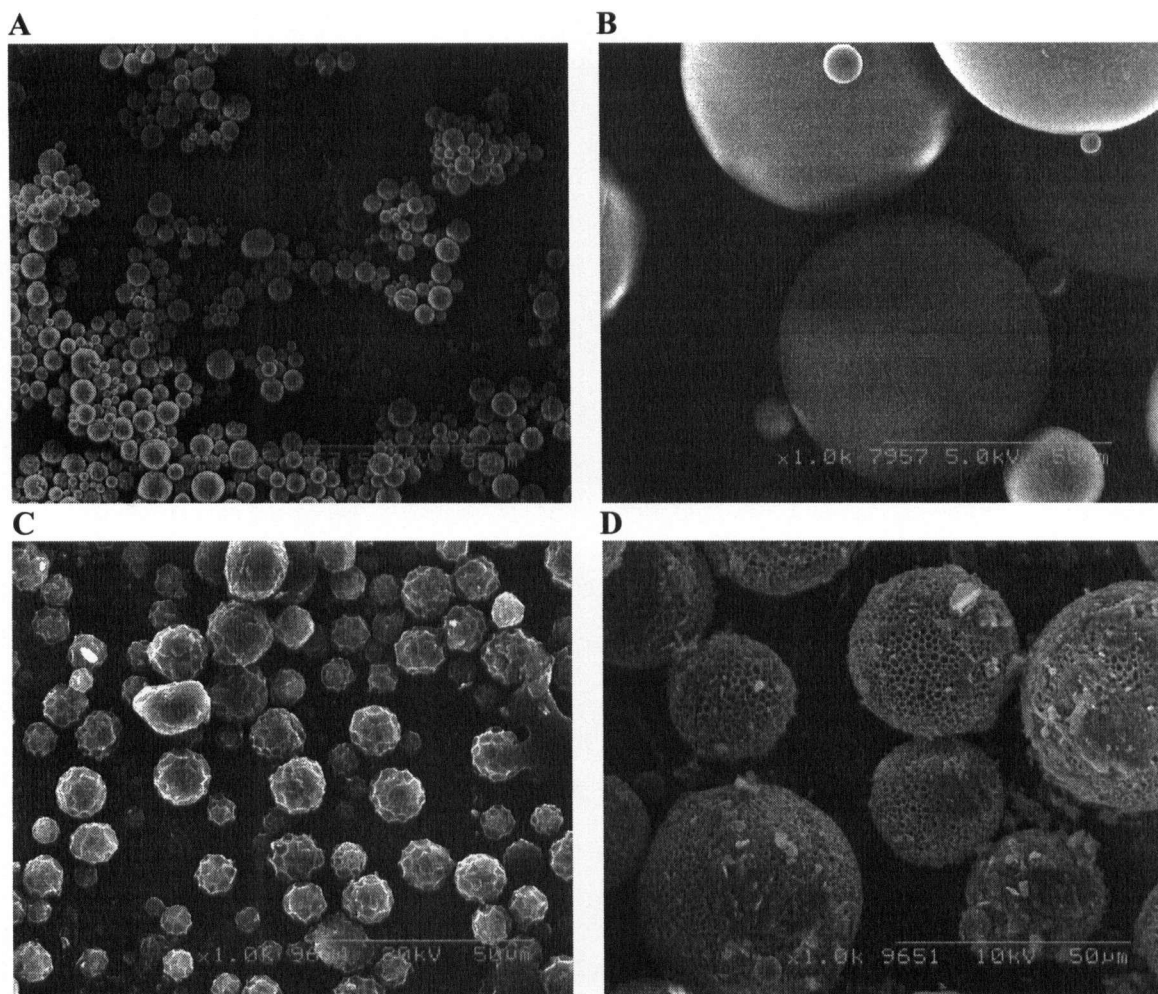
Figure 21. HPLC chromatograms of a 2 μg/ml paclitaxel standard in A) acetonitrile and B) 60:40 acetonitrile:water used for standard curves, and a chromatogram of C) paclitaxel extracted from dichloromethane by the addition of 60:40 acetonitrile:water in an assay for total content of paclitaxel. Chromatographic conditions: 20 μl injection onto a C_{18} column with a mobile phase of 58:37:5 acetonitrile:water:methanol flowing at 1 ml/min and UV detection at 232 nm.

114
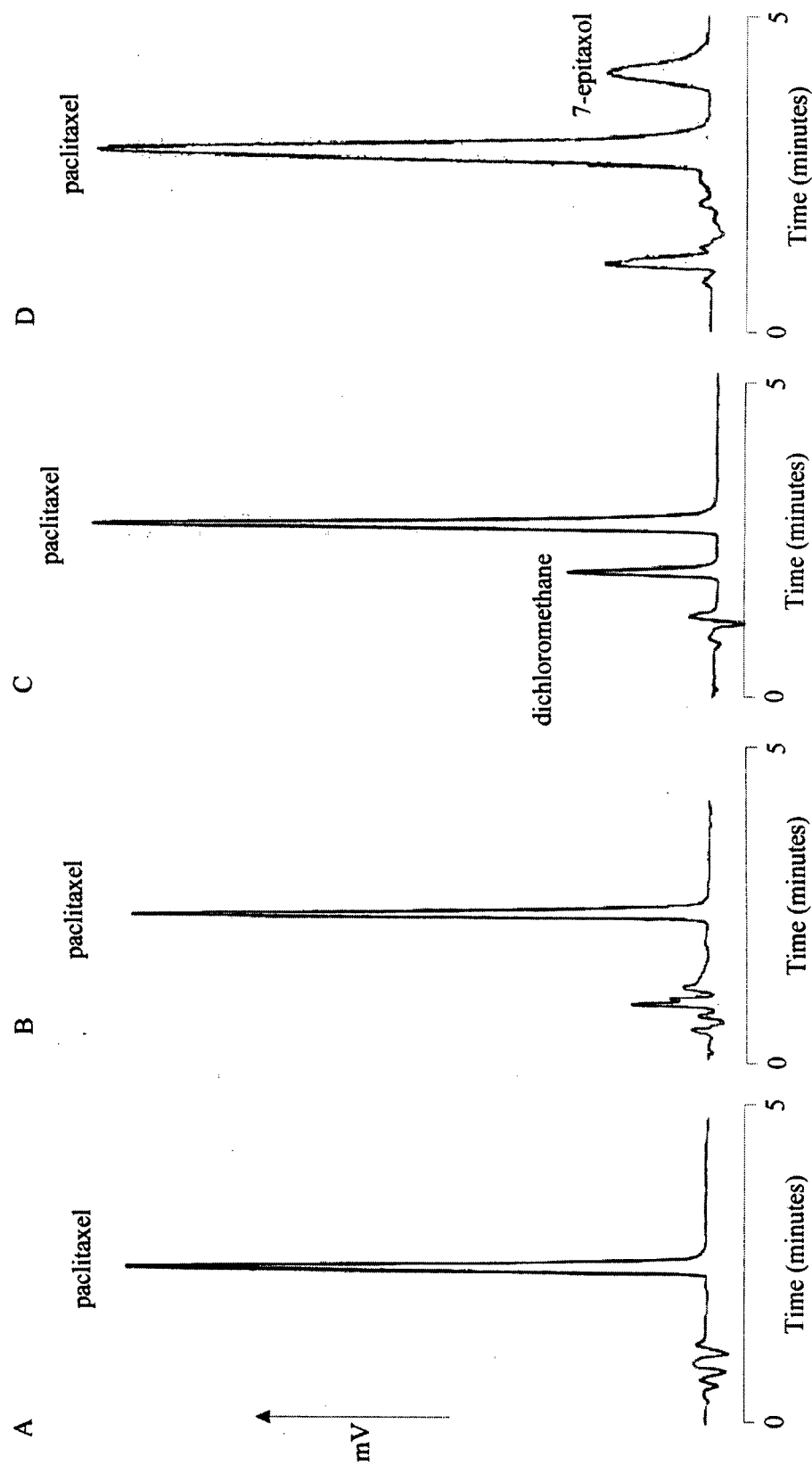
Figure 22. Representative standard curves of paclitaxel in A) acetonitrile and B) 60:40 acetonitrile:water. Chromatographic conditions: 20 μl injection volume onto a C_{18} column, mobile phase: 58:37:5 acetonitrile:water:methanol flowing at 1 ml/min and UV detection at 232 nm.
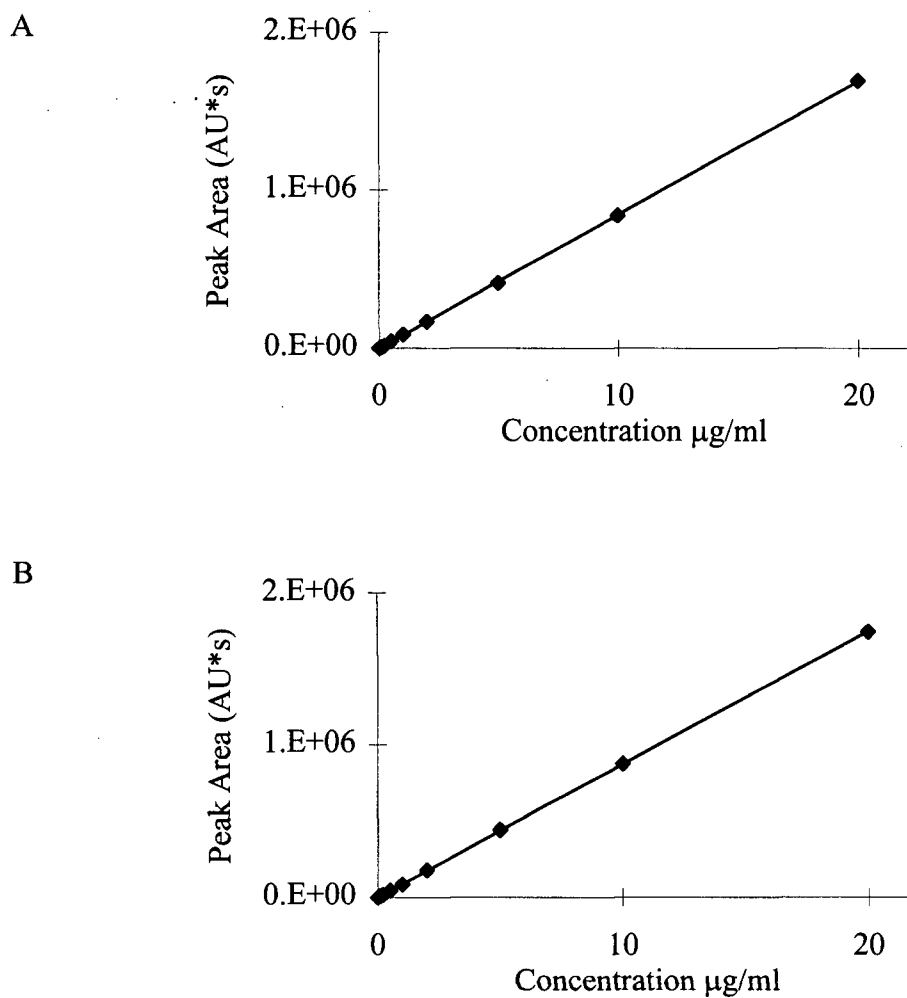
Figure 23. The effect of paclitaxel content on the melting point of paclitaxel-poly(L-lactic acid) dispersions. The data are plotted using Equation 14.
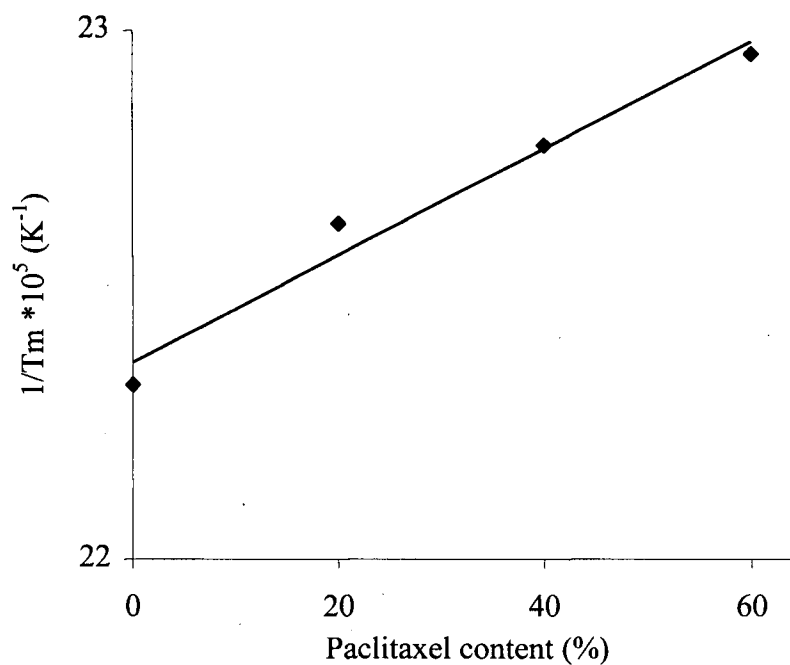
Regression analysis parameters (y = mx + b), R^2

$y = 1.08 * 10^{-6} x + 4.82 * 10^{-5}$, $R^2 = 0.98$

4.4. The effect of polymer molecular weight on microsphere properties

Prior to the blending studies in which microspheres of blends of high and low molecular weight PLLA were evaluated, it was necessary to determine the properties of paclitaxel loaded PLLA microspheres prepared from a wide range of molecular weights of PLLA (1k to 100k g/mol).

4.4.1. Microsphere size range

Various combinations of stirring rate and aqueous phase composition were used in manufacturing microspheres from 50k g/mol PLLA-PS or 100k g/mol PLLA. Using 50k g/mol PLLA-PS, a trend of increasing average microsphere diameter with decreasing PVA concentration and decreasing stirring speed was observed. Aqueous phase compositions of 2% and 5% PVA and a stirring rate of 900 rpm were used for manufacturing microspheres with approximate size ranges of 35-105 μm and 10-35 μm, respectively. A stirring rate of 2100 rpm and 5% PVA were used to make microspheres with an approximate size range of 1-10 μm.

Particle size distributions of control and 20% paclitaxel loaded microspheres prepared from 100k g/mol PLLA in all three size ranges are shown in Figure 24A and B, respectively. Similar data were obtained for 10 and 30% loadings. The particle size ranges of the microspheres were defined as 1-10, 10-35, and 35-105 μm with reference to these and all further batches of microspheres. These ranges were chosen based on extrapolation to the particle size axis of the tangent from the half-height position on several particle size distributions made in each size range. The area under the distribution curve between these limits was greater than 80% of the total.

Incorporation of paclitaxel into microspheres resulted in aggregation during particle size measurement of microspheres in the size ranges of 1-10 and 10-35μm. Aggregation resulted in multimodal distributions with a second peak at a diameter greater than that of the major distribution peak. The area under the second peak accounted for between 5-10% of the total area.

To ensure that changes in the microsphere size distributions due to changes in the polymer molecular weight used would not affect microsphere properties only the 50-90 μm size range was retained. This size range was separated by sieving the microspheres immediately after their manufacture.

4.4.2. Incorporation of PLLA into the microspheres

To examine the incorporation of PLLA into microspheres, samples of the 1k g/mol PLLA-LA were incubated in distilled water at room temperature for several hours to leach out water soluble components. The leaching process was continued over 12 hours until the material reached a constant weight. The final weight was $67.7 \pm 4.8\%$ of the original indicating that approximately one third of the original material was water soluble. It is possible that more water soluble material was present but was not leached out. The physical appearance of the 1k g/mol PLLA changed from a soft, translucent tacky material to a brittle white solid after leaching out the low molecular weight components. It is anticipated that the water soluble component would be at least partly leached out of the material during the microsphere manufacturing process and therefore not all of the polymer would be incorporated into the microsphere matrix.

4.4.3. Total content of paclitaxel

Microspheres with a theoretical loading of 30% paclitaxel made from 2k g/mol PLLA-LA, 4k and 10k g/mol PLLA-SA and 50k g/mol PLLA-PS were manufactured using 2.5% PVA in the aqueous phase and a stirring rate of 600 rpm. Values of total paclitaxel content in the microspheres are listed in Table 13. A higher than expected content was observed in microspheres made with polymers with molecular weights below 50k g/mol. To encapsulate greater than 100% of the expected total content of paclitaxel, the extent of incorporation of the polymer must have been less than that of paclitaxel as reported in section 4.4.2. Assuming that 32.3% of the polymer was not encapsulated due to its dissolution into the aqueous medium used in microsphere manufacture giving a polymer content of 67.7%, and a paclitaxel content equal to the initial paclitaxel loading of 30% a maximal theoretical loading efficiency of 129% would be expected based on the following relationship:

$$\text{Loading efficiency} = \frac{\text{Paclitaxel content}}{\text{Polymer content} + \text{Paclitaxel content}} \times \frac{1}{\text{Initial Paclitaxel Loading}}$$

Generally, the loading efficiencies decreased from 120 to approximately 100% as the molecular weight of the polymers increased (Table 13). Total content data of paclitaxel in microspheres made from 100k g/mol PLLA are summarised in Table 14.

4.4.4. Thermal properties

Representative DSC thermograms of microspheres prepared from PLLA-SA polymers showed trends of increasing T_g and T_m with molecular weight (refer to Figure 25). The glass transition increased from -13°C to 54°C as the molecular weight of

PLLA-SA increased (Figure 25, inset A). The Tg for 10k g/mol PLLA-SA (Figure 25D) was taken as the peak temperature of enthalpy relaxation and the Tg of the other PLLA-SA polymers (Figures 25A-C) were taken as the mid-point in the change in Cp. The endothermic peaks observed around 30°C (Figure 25A and B) were attributed to the melting of polymer crystallites rich in hydrocarbon chains from stearyl alcohol, while the peaks above 100°C (Figure 25A-D) were attributed to the melting of polymer crystallites rich in L-lactic acid chains. A recrystallisation exotherm was observed around 80°C for 10k g/mol PLLA-SA. Figure 26A and B show the relationship of Tg and Tm to molecular weight, according to Equations 10 and 12, respectively. Tg varied in a linear fashion with $1/Mn^*$ for PLLA-SA with a molecular weight greater than 3k g/mol. The relationship between $1/Tm$ and $1/Mn^*$ deviated from the expected linear relationship as the molecular weight decreased.

DSC thermograms of 1k g/mol PLLA-LA as synthesised and the water insoluble fraction of the 1k g/mol PLLA-LA (after incubation in water) are shown in Figure 27A and B. Thermograms for microspheres made from PLLA-LA polymers are shown in Figure 27C to E. As synthesised, 1k g/mol PLLA-LA did not show a clear glass transition and during the melting transition discontinuities were observed in the thermogram indicating degradation of the material (Figure 27A). Enthalpy relaxation accompanied the glass transition for PLLA-LA in microspheres, partial recrystallisation of the amorphous phase in microspheres was observed around 80°C and melting occurred between 115 and 150°C (Figure 27C-E).

4.4.5. Resuspension index

The resuspension index of microspheres manufactured from PLLA-SA polymers increased with the Tg of PLLA-SA (Figure 25, inset B). Greater than 95%w/w of microspheres prepared from polymers with Tgs above ambient temperature (25°C) at which they were stored could be readily resuspended in water.

The resuspension index of microspheres manufactured from PLLA-LA polymers could not be quantified because the material adhered to the walls of the tubes and pipettes used in the assay owing to the increased hydrophilicity of PLLA-LA compared to PLLA-SA. In the absence of a resuspension index for these microspheres, samples were vortexed in water in an Eppendorf tube and the suspension observed visually and by optical microscopy for the presence of aggregates. PLLA-LA microspheres with molecular weights equal to or greater than 1.5k g/mol could be readily resuspended in water.

Microspheres manufactured from PLLA-PS polymers and from 100k g/mol PLLA were all completely resuspended. Paclitaxel loading had no effect on the resuspension of microspheres.

4.4.6. Surface morphology

The surface morphology of microspheres observed by scanning electron microscopy are given in Figure 28A to C for 1-10k g/mol PLLA-SA and 28D to F for 1–3.5k g/mol PLLA-LA. Below 2k g/mol, PLLA polymers did not form spherical microspheres. The 1k g/mol PLLA-SA resulted in a single aggregated mass while 1k g/mol PLLA-LA gave irregularly shaped particles. Microspheres made from 50k and 100k g/mol PLLA polymers were all spherical with a smooth surface.

4.4.7. X-ray powder diffraction patterns of microspheres

Representative XRPD patterns of stearyl alcohol and microspheres made from PLLA-SA and PLLA-LA are shown in Figure 29A-C, respectively. Two peaks at 21.3 and 24.4 °2θ were observed in the pattern of stearyl alcohol, which were absent in the patterns for microspheres. All PLLA-SA and PLLA-LA microspheres had similar XRPD patterns, with the most intense peak located between 16.2 and 16.5 °2θ and a less intense diffraction peak at 18.8 °2θ. A representative XRPD pattern for 30% paclitaxel loaded microspheres made from 100k g/mol PLLA is shown in Figure 29D. Similar data were also obtained for control, 10 and 20% loaded microspheres in all size ranges. Peak positions for 100k g/mol PLLA (Figure 29D) were the same as for PLLA-PS and PLLA-LA polymers (Figure 29A and C) and no peaks could be attributed to crystalline paclitaxel in the microsphere matrix.

4.4.8. *In vitro* release profiles of paclitaxel

4.4.8.1. Preparation of samples for the assay of *in vitro* release of paclitaxel

Table 15 summarises the efficiency in recovering paclitaxel from a mixture of 1 ml dichloromethane and 5 ml PBS-A. Greater than 87% of spiked paclitaxel was recovered for all samples with total paclitaxel content of 0.2 μg and 99% was recovered from all samples with more than 0.2 μg total paclitaxel. A RSD of less than 20% was observed for all samples on all days. Injection of a blank extraction sample showed no peak at 2.5 minutes, the retention time of paclitaxel.

4.4.8.2. The conversion of paclitaxel to 7-epitaxol in *in vitro* release studies

Over the time course of a release study, a second peak at 3.7 minutes was observed in the HPLC assay when quantifying paclitaxel. The peak was due to the presence of 7-epitaxol. The elution profile of a mixture of 7-epitaxol (~0.4 µg/ml) and paclitaxel (2 µg/ml) is shown in Figure 21D. The separation factor "α" for paclitaxel and 7-epitaxol was 1.65 and peak resolution "R" was 2.32, indicating baseline separation. Absence of the 7-epitaxol peak in HPLC analysis of standards of paclitaxel in 60:40 acetonitrile and water over several days confirmed that epimerization did not proceed in standards to levels which could be quantified. Thus epimerization of paclitaxel is believed to occur in the release buffer and the amount of paclitaxel quantified by HPLC does not represent the total amount of drug released from the microspheres.

In several release studies, the 7-epitaxol peak was quantified and the cumulative amount of 7-epitaxol was 8-10% of the amount of paclitaxel quantified in the same study. In the first day of the study, in which the sampling interval was shortest, the amount of 7-epitaxol quantified in the assay was less than 7% of the total amount of paclitaxel quantified over the same interval.

The stability of paclitaxel was assessed in PBS-A over the time period between sampling in the *in vitro* study. Four 15 ml volumes of PBS-A were spiked with 0.1 µg/ml of paclitaxel and incubated at 37 °C. On days one through three of the incubation, 5 ml of each of the paclitaxel solutions was analysed by extraction and quantitation by HPLC. No significant change in the HPLC peak area for paclitaxel was observed over the three days and other than for 7-epitaxol, no other peaks were observed.

4.4.8.3. The effect of polymer molecular weight on release

In vitro release profiles of paclitaxel from microspheres prepared PLLA polymers with molecular weights between 2k and 50k g/mol are shown in Figure 30. Paclitaxel release was greatest during the first two days. A slower phase was observed between days 2 and 14. Based on a solubility value for paclitaxel in the release medium of 3 μg/ml at 37 °C (Winternitz, 1997; Zhang, 1997), it was evident that concentrations near saturation were encountered in the first three days of the study. Using ANOVA and Tukey tests, microspheres prepared from 2k g/mol PLLA-LA, 4k and 10k g/mol PLLA-SA release paclitaxel to a significantly greater extent after fourteen days compared to microspheres made from 50k g/mol PLLA-PS.

Based on the total content data from Table 13, between 10 and 80% of the total paclitaxel was released over the fourteen days of the release study. After the release study was completed, the remaining material was assayed to quantify the amount of residual paclitaxel in the polymer matrix. Based on the total paclitaxel contents (refer to Table 13) values of total amount of paclitaxel recovered for each formulation, called percent mass balance, were 78, 98, 112 and 102% for 2k, 4k, 10k and 50k g/mol PLLA polymers, respectively.

The microspheres were observed in the release medium on a daily basis and it was observed that by the end of the first week, the 2k and 4k g/mol PLLA microspheres were no longer freely suspended in the medium within the tumbling tube. Rather the microspheres had begun to aggregate and adhere to the bottom of the tube.

4.4.8.4. The effect of paclitaxel loading and microsphere size on release

In vitro release profiles of paclitaxel from 1-10, 10-35 and 35-105 μm

100k g/mol PLLA microspheres with paclitaxel loadings of 10, 20 and 30% are shown in

Figure 31. The results of Tukey tests describing a difference in the initial rate over

24 hours (V_0) and total extent (M_{30}) of paclitaxel release are also shown. Sink conditions

were maintained after day 2 of the study for all types of microspheres except for 30%

paclitaxel loaded 1-10 μm microspheres that released paclitaxel the most rapidly. For

these microspheres, paclitaxel concentrations did not exceed 50% of its solubility after

day 3 and sink conditions were achieved by day 7. Following the initial phase of release

characterised by V_0, a slower, apparently linear phase was observed between days 3 and

14. Linear regression analysis of the data between days 3 and 14 gave R^2 values between

0.97 and 1.00 for all but the 20% 1-10 μm microspheres which had a R^2 of 0.93. The

rates of paclitaxel release for the apparently zero-order phase of release between days 3

and 14 from the various microsphere formulations are shown in Table 16. Release rates

decreased with decreasing loading and for a given loading, with increasing microsphere

size. Between days 14 and 30, the rate decreased gradually and the profiles tended to

plateau having rates of release between 1 and 5 μg/day for all formulations.

At loadings of 20 and 30%, microspheres in the 1-10 μm size range had

significantly greater values of V_0 compared to microspheres in larger size ranges,

indicating that microsphere size plays a role in the initial phase of release from the

microspheres. As the loading level increased from 10 to 30%, V_0 increased from 1-9 to

7-29 μg/hr for microspheres in all three size ranges.

125

When values of M_{30} for microspheres with the same initial loading were compared, 1-10 μm microspheres containing 10, 20 and 30% released significantly more paclitaxel than microspheres in the 35-105 μm size range with the same loadings. When comparing microspheres in the same size range, increasing loading level from 10 to 30% resulted in a significantly higher value of M_{30}. For all microspheres, between 24 and 93% of the total amount of paclitaxel present in the microsphere was released over the course of the release study. Microspheres in the 1-10 μm size range released greater than 60% and 35-105 μm released less than 30% of their total paclitaxel loads.

A similar release study of microspheres in the size ranges of 1-10 and 35-105 μm and at 10% and 30% loading was conducted over 63 days. The shape of the release profiles and the effects of size and loading were similar to those shown in Figure 31. After day 30 the plateau phase of slow release continued up unitl day 63.

4.4.8.5. Surface morphology of microspheres after the *in vitro* release study

Erosion of the microspheres made from PLLA with molecular weights between 2k and 50k g/mol was observed by SEM, following removal of samples from the release medium on various days during the *in vitro* release experiment. Representative micrographs of 2k g/mol PLLA-LA microspheres are shown in Figure 32A to C. Initially, the microspheres were smooth and spherical. By day five (Figure 32B), the microspheres showed loss of their spherical shape and by day nine (Figure 32C), small particles (<10 μm in diameter) along with larger debris were visible. Similar results were observed for all microspheres made from PLLA with molecular weight below 10k g/mol while microspheres made with 50k g/mol PLLA-PS remained intact over fourteen days.

Figure 32D to F shows scanning electron micrographs of 20% loaded 100k g/mol PLLA microspheres in the size range of 35-105 µm at day 0, 15 and 70 of an *in vitro* release study. The spherical shape and dimpled appearance of the microspheres was retained throughout the course of the study. However, by day 70 (Figure 32F), the surface of the microspheres showed signs of erosion. Microspheres used in the release study shown in Figure 31 were observed after thirty days in buffer. At all sizes and loadings, the microspheres remained spherical and intact over the course of the release study.

Table 13. Total content of paclitaxel in 50-90 μm PLLA microspheres with theoretical loading of 30%. Values are averages of three measurements made from each batch of microspheres. The precision of the measurements is greater than 94%.

Microsphere composition (molecular weight (g/mol) of PLLA)	Total content of paclitaxel (%w/w)	Efficiency of loading (%)
2k	36	120
4k	34	112
10k	30	99
50k	29	96

Table 14. Total content of paclitaxel in 1-10, 10-35, 35-105 μm microspheres made with 100k g/mol PLLA. Values are averages of three measurements from a single batch. The precision of the measurements is greater than 95%.

Microspheres	Paclitaxel content (% of initial paclitaxel loading)		
	10% loading	20% loading	30% loading
1-10 μm	56	74	97
10-35 μm	51	60	89
35-105 μm	87	89	97

Table 15. Inter- and intra-day precision and percent recovery of paclitaxel from a 5:1 mixture of PBS-A and dichloromethane.

Paclitaxel Amount[a] (μg)	Day 1			Day 2			Day 3			All Days		
	Amount Recovered[b]	RSD[c] (%)	Recovery[d] (%)	Amount Recovered	RSD (%)	Recovery (%)	Amount Recovered	RSD (%)	Recovery (%)	Amount Recovered	RSD (%)	Recovery (%)
0.2	0.16	7.37	81	0.19	8.21	95	0.17	18.61	85	0.17	10.97	87
0.5	0.49	13.96	98	0.46	15.89	92	0.39	16.81	79	0.45	15.47	89
1	1.10	10.24	110	0.91	8.73	91	0.92	11.03	92	0.98	12.43	98
2	2.16	3.14	108	1.91	7.81	96	1.87	8.04	93	1.98	8.80	99
5	4.68	11.98	94	4.80	8.01	96	4.70	8.58	94	4.73	8.74	95

[a] The amount of paclitaxel with which the samples were spiked.

[b] The average (n=3 for each day) amount of paclitaxel recovered and measured by HPLC, using a standard curve of paclitaxel in 60:40 acetonitrile:water.

[c] RSD (Relative standard deviation) is the ratio of the standard deviation to the average, expressed as a percentage. A value less than 20% indicates sufficient precision at each concentration.

[d] Recovery is the ratio of the amount recovered over the amount of paclitaxel spiked into the samples, expressed as a percentage.

129

Table 16. Paclitaxel release rates from 100k g/mol PLLA microspheres ± 95% confidence intervals for the apparently zero-order phase of release between days 3 and 14 of an *in vitro* study.

Paclitaxel loading (%)	Release rates from microspheres with various size ranges (µg/day)		
	1-10 µm microspheres	10-35 µm microspheres	35-105 µm microspheres
10	10[a]	7[a]	6[a]
20	14 ± 1	10 ± 1	9 ± 1
30	26 ± 1	18[a]	16[a]

[a] The 95% confidence interval for the release rate is less than 0.5 µg/day.

Figure 24. Particle size distributions of A) control and B) 20% paclitaxel loaded
100k g/mol PLLA microspheres in size ranges of a) 1-10, b) 10-35 and c) 35-
105 µm.
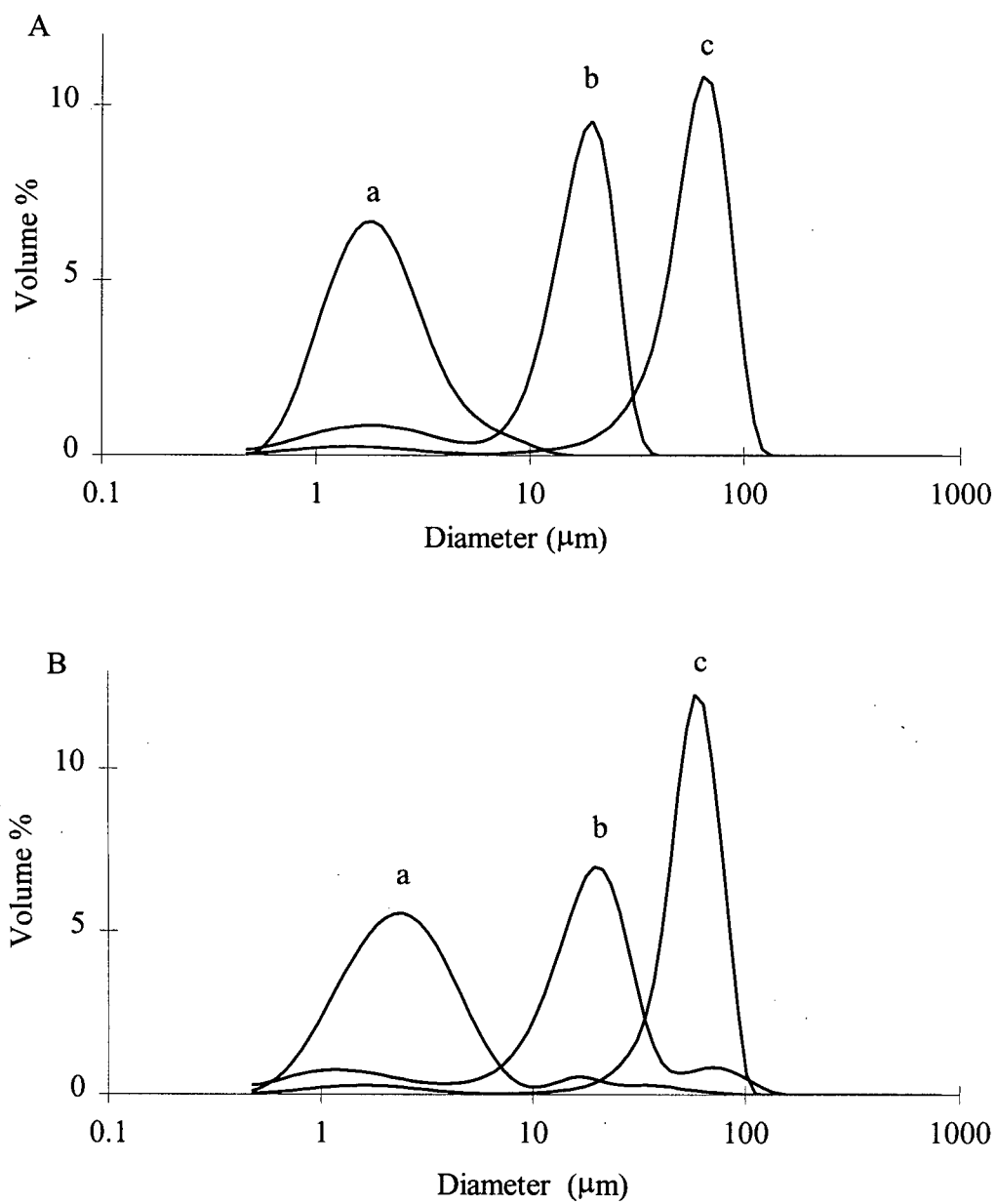
Figure 25. DSC thermograms of microspheres made from A) 1k, B) 1.5k, C) 4k and D) 10k g/mol PLLA-SA. Inset A: the effect of molecular weight on the Tg. Inset B: the effect of the Tg on the resuspension index of microspheres.

INSET A

INSET B
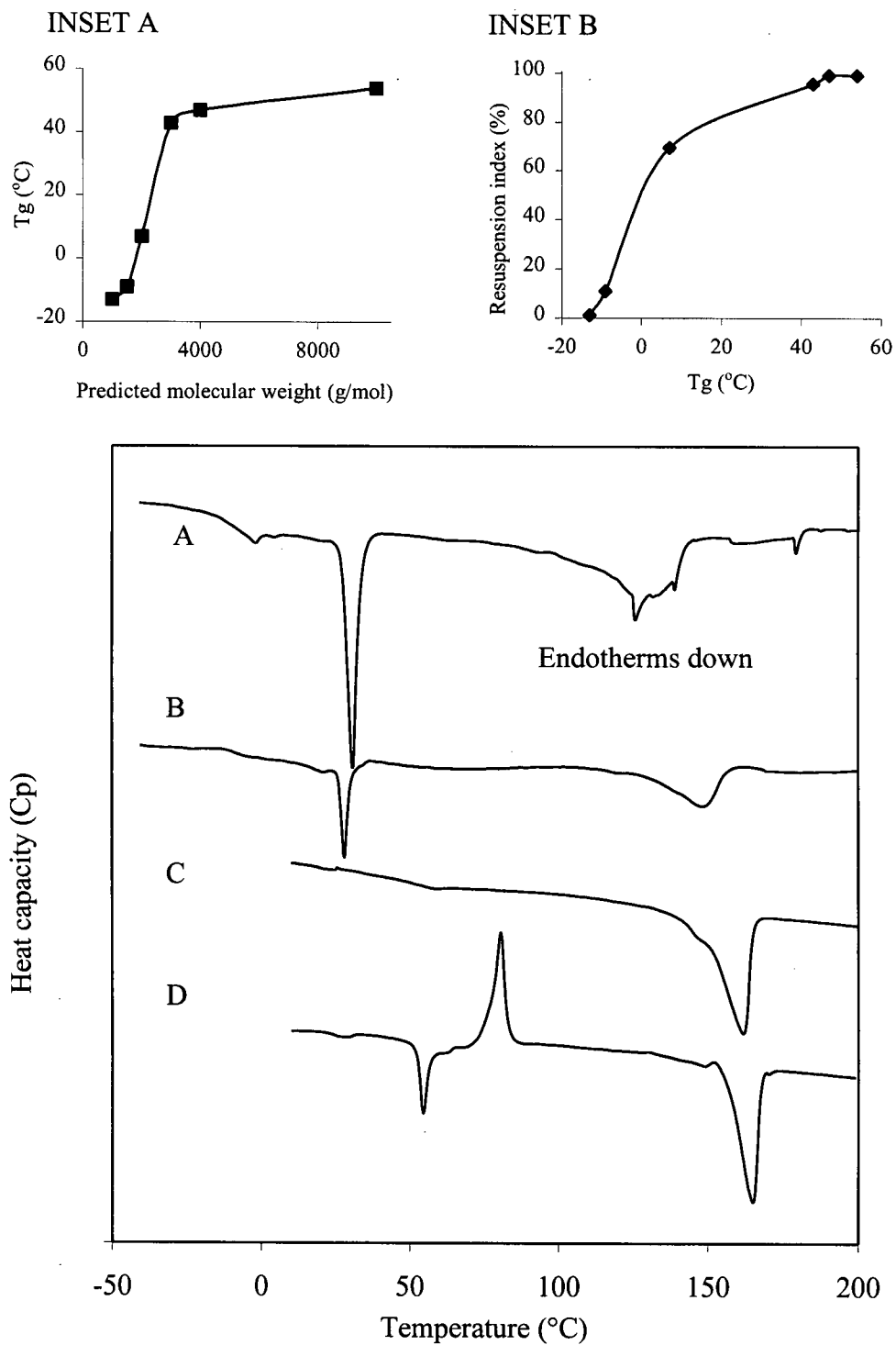
Figure 26. The effect of number average molecular weight on A) Tg and B) Tm of PLLA-SA and PLLA-LA polymers, plotted using Equations 10 and 12, respectively.
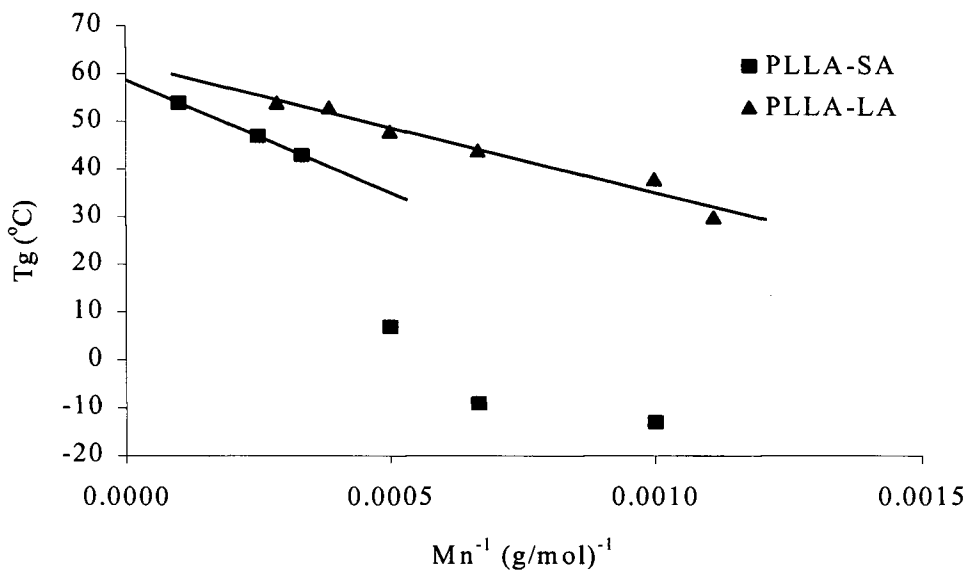
Regression analysis parameters (y=mx + b). R^2

PLLA-SA: y = -27000 x + 62, R^2=0.97 (data plotted using Mn^*)
PLLA-LA: y = -47000 x + 59, R^2=1.00 (data plotted using Mn)
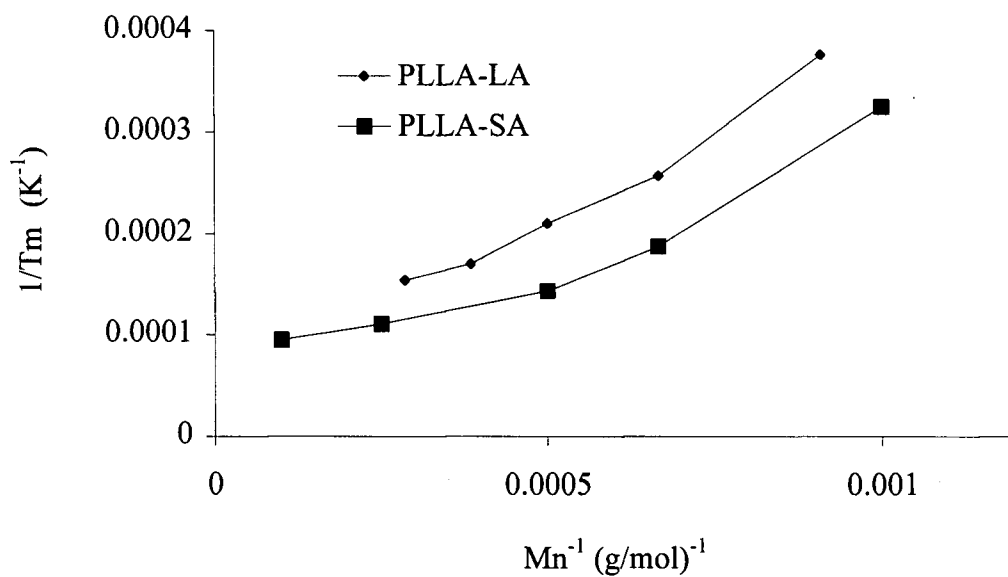
Data are plotted using Mn^* for PLLA-SA and Mn for PLLA-LA

133

Figure 27. DSC thermograms A) 1k g/mol PLLA-LA as synthesised and B) 1k g/mol PLLA-LA after incubation in water to remove water soluble material, and of microspheres manufactured from PLLA-LA polymers with molecular weights of C) 1k, D) 2k and E) 3.5k g/mol.
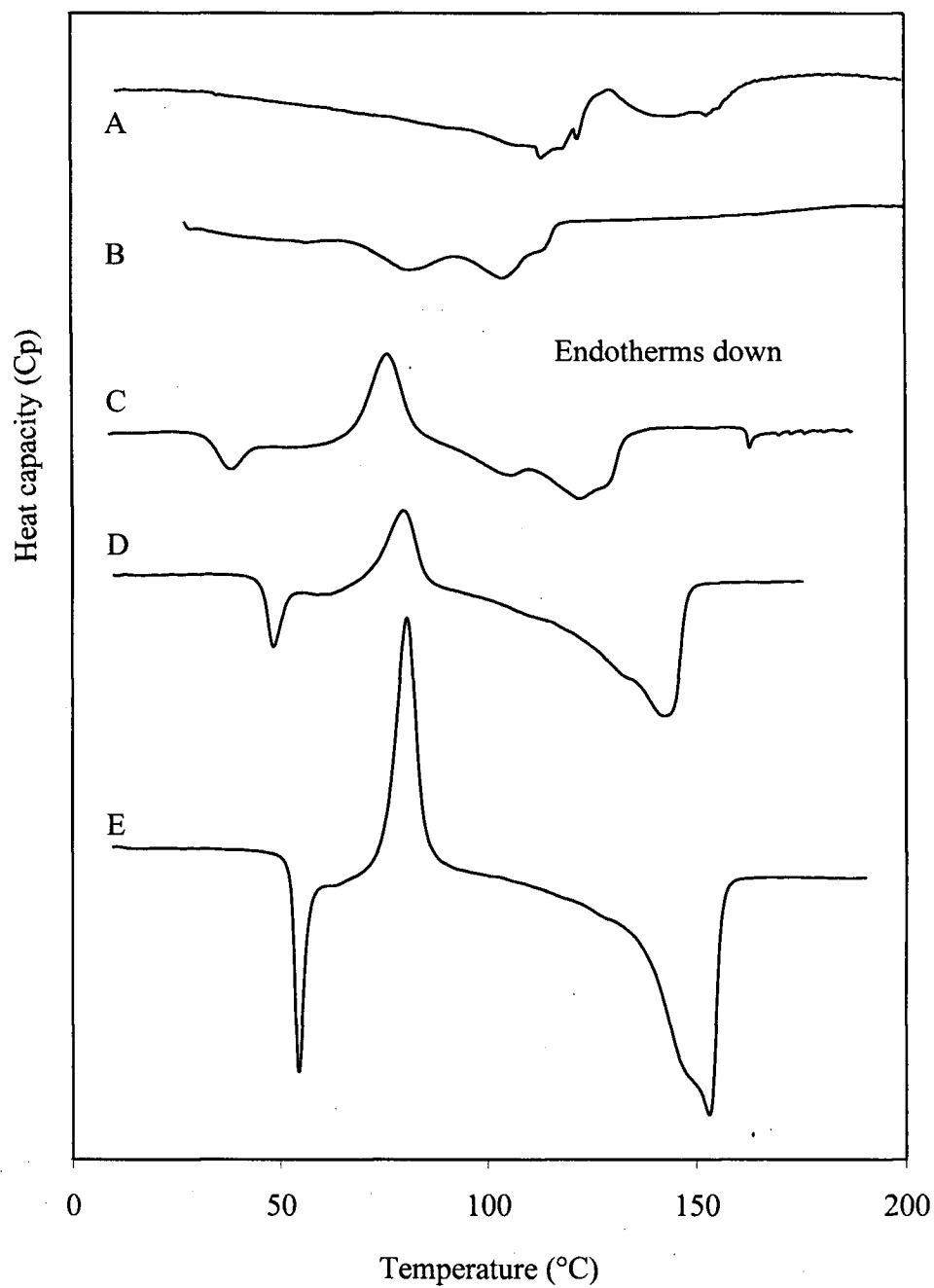
Figure 28. The effect of molecular weight on the surface morphologies of microspheres manufactured from PLLA-SA with molecular weights of A) 1k, B) 2k, and C) 10k g/mol and from PLLA-LA with molecular weights of D) 1k, E) 2k and F) 3.5k g/mol. (Magnification of all micrographs is 1000x.)

135
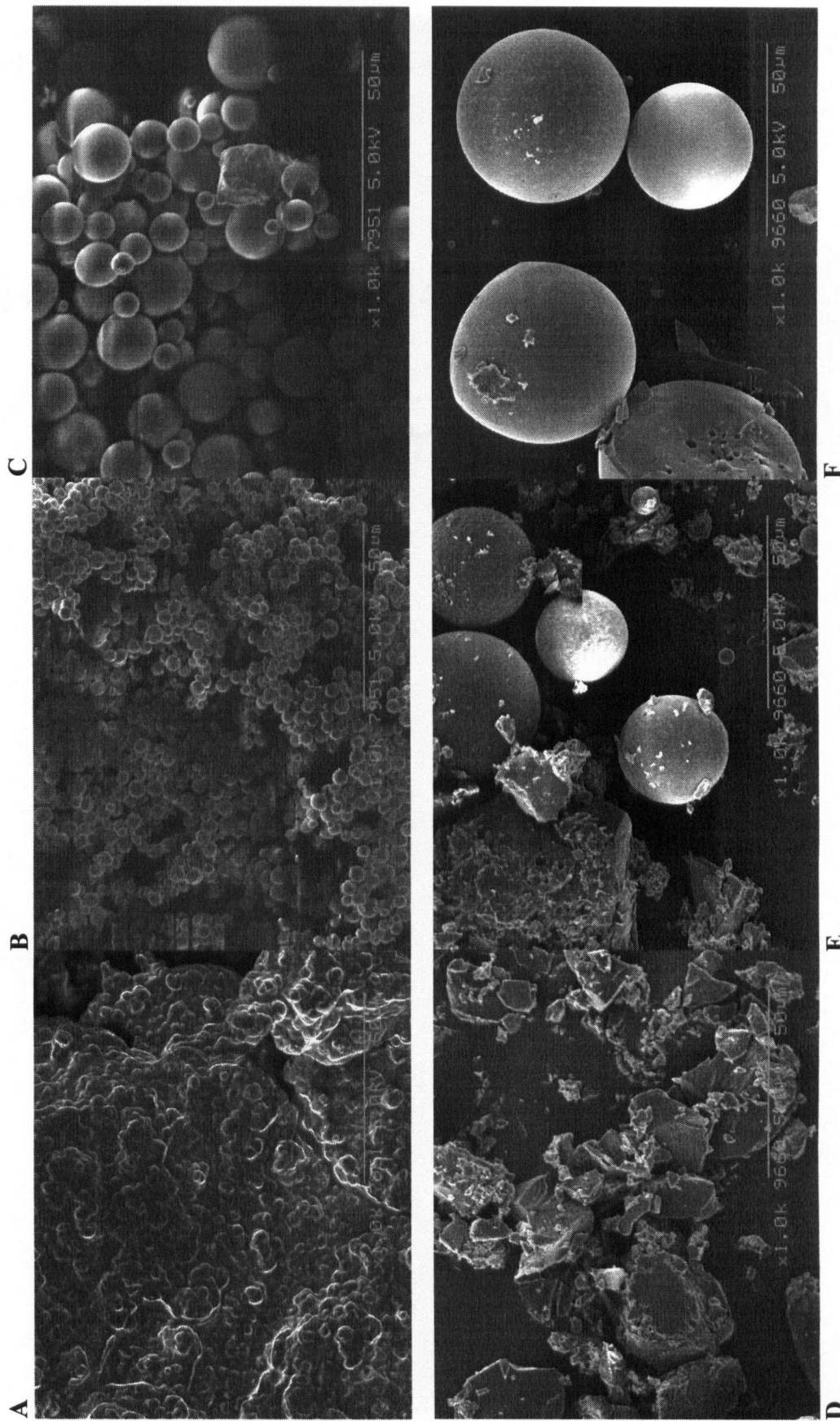
Figure 29. X-ray powder diffraction patterns of A) microspheres made from 1k PLLA-SA, B) stearyl alcohol, microspheres made from C) 1k g/mol PLLA-LA and D) 100k g/mol PLLA with 30% paclitaxel.
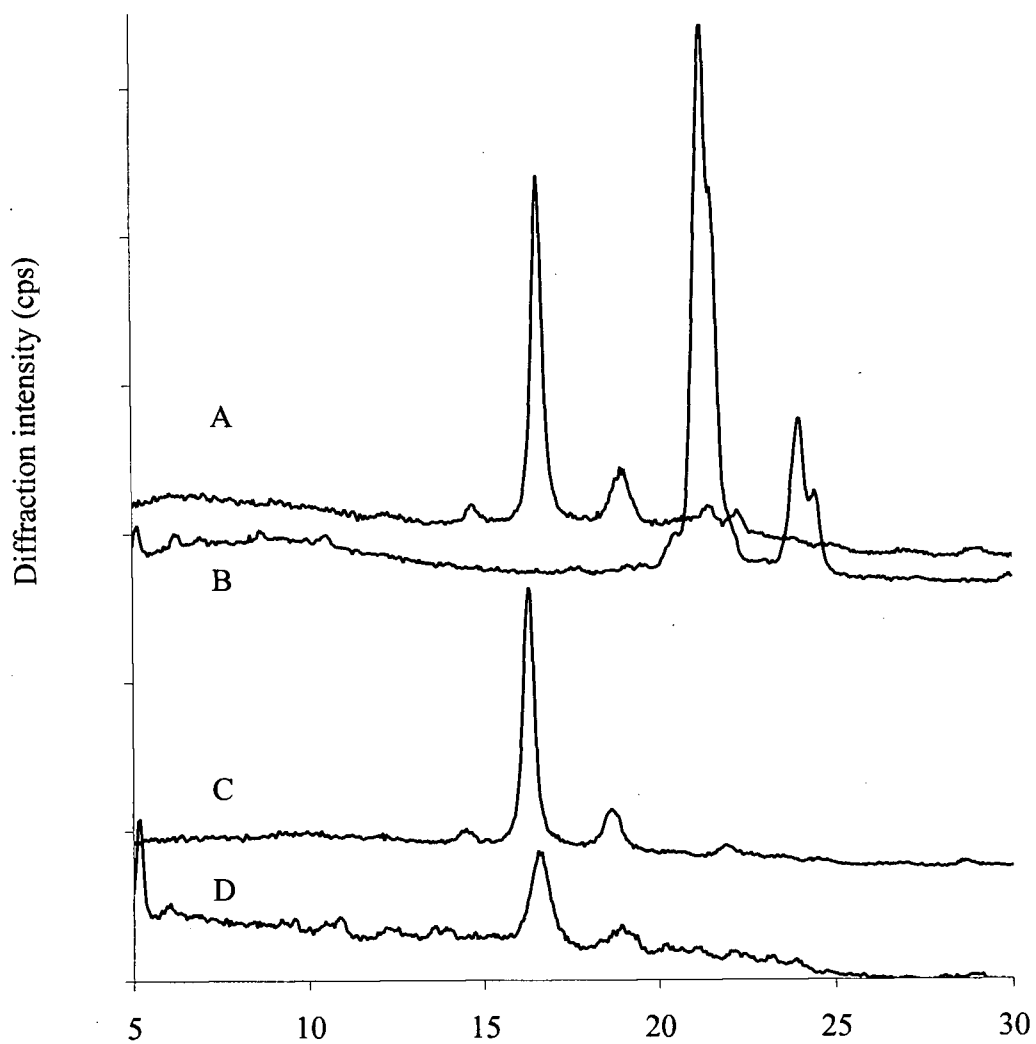
Figure 30. *In vitro* release profiles of paclitaxel from 30% paclitaxel loaded microspheres made from PLLA polymers with molecular weights ranging from 2k to 50k g/mol.
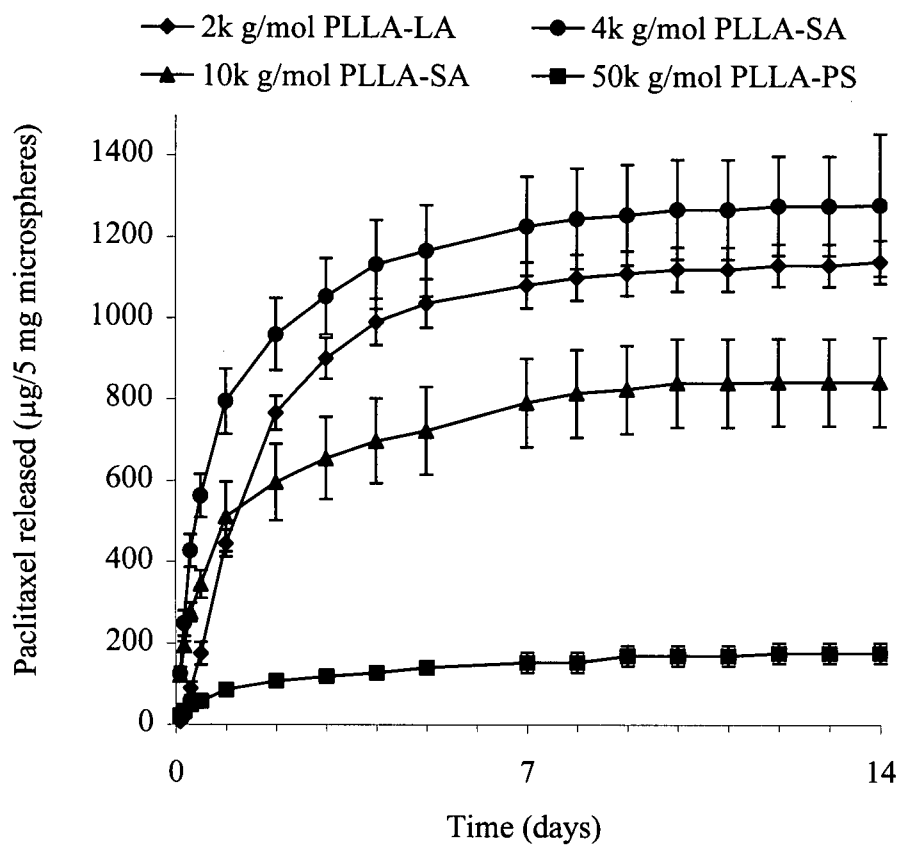
Figure 31. *In vitro* release profiles of paclitaxel from A) 10%, B) 20% and C) 30% paclitaxel loaded 100k g/mol PLLA microspheres. (Note the difference in y-axis scale in Figures A and B compared to C.) Below is a schematic representation of the results of Tukey tests of significant differences in parameters describing the rate over the initial 24 hours (V_0) and total extent (M_{30}) of release. Dark lines identify microspheres between which no significant difference ($p > 0.05$) was observed.

Initial rates (V_0) (μg/hr):

| 30%, 1-10μm | 20%, 1-10μm | 20%, 10-35μm | 30%, 10-35μm | 10%, 1-10μm | 30%, 35-100μm | 20%, 35-100μm | 10%, 10-35μm | 10%, 35-100μm |

Total extent of release (M_{30}) (μg):

| 30%, 1-10μm | 30%, 10-35μm | 20%, 1-10μm | 30%, 35-105μm | 20%, 10-35μm | 10%, 1-10μm | 20%, 35-100μm | 10%, 10-35μm | 10%, 35-105μm |

138
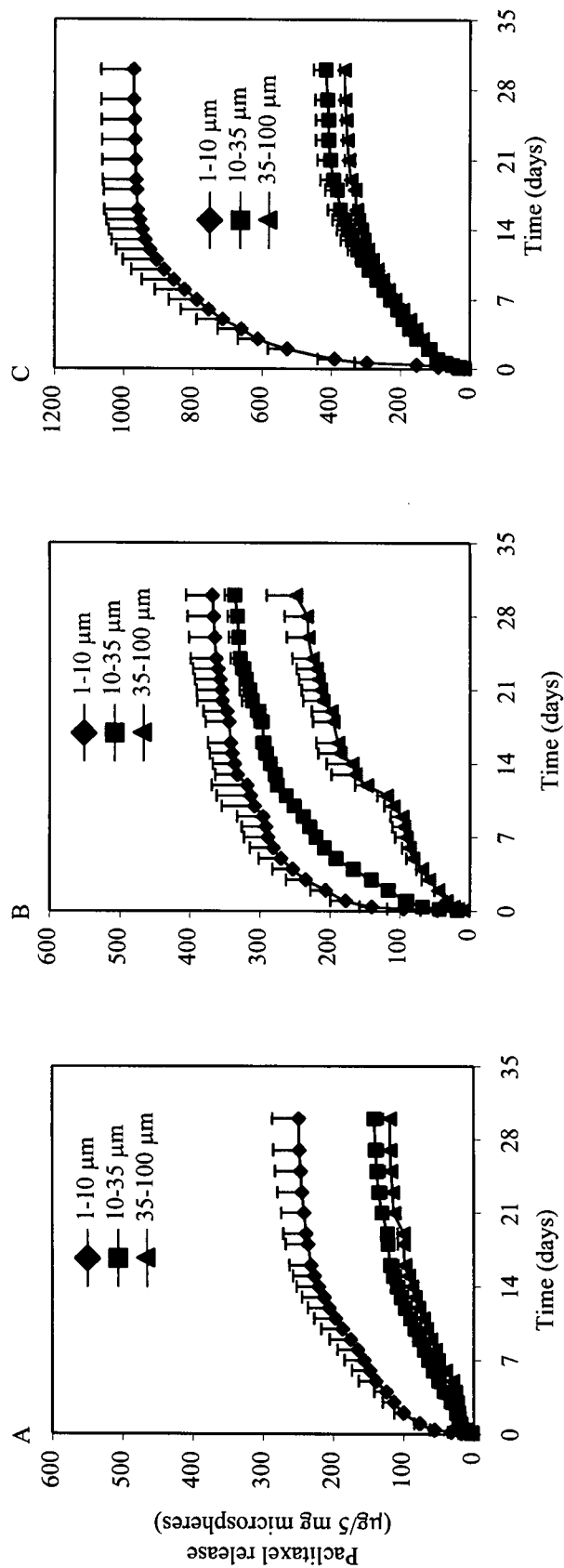
Figure 32. The surface morphology of 2k g/mol PLLA-LA microspheres used in an *in vitro* release study. A) day 0, B) day 5 and C) day 9 of the release study and of 20% paclitaxel loaded microspheres in the size range of 35-105 μm made from 100k g/mol PLLA after A) day 0, B) day 15 and C) day 70 of an *in vitro* release study. (Magnification of micrographs is 1000x.)
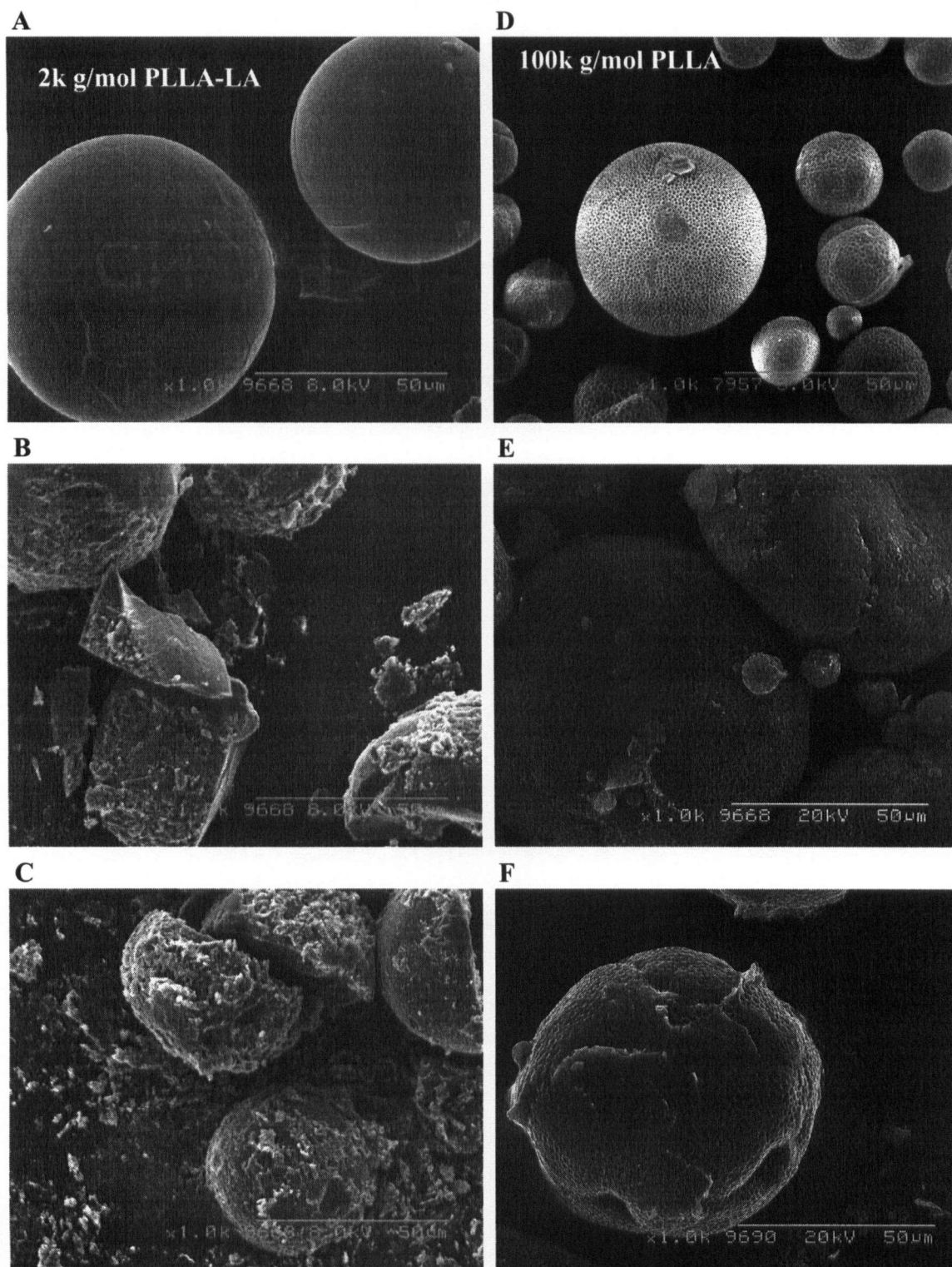
4.5. The effect of polymer blending on microsphere morphology

Two series of blends were selected for study, one series being a combination of commercially obtained 50k and 2k g/mol PLLA-PS and the other series being commercially obtained 100k g/mol PLLA and synthesised 1k g/mol PLLA-LA.

4.5.1. Blending 50k and 2k g/mol PLLA

4.5.1.1. Morphology of microspheres

Microspheres were manufactured from various blend ratios of 2k and 50k g/mol PLLA-PS. An aqueous phase composition of 10% PVA and a stirring rate of 900 rpm were used to maintain a microsphere size range of 1-30 μm at all polymer compositions. Blend compositions were 100:0, 80:20, 60:40, 40:60, 20:80 and 0:100 (2k:50k g/mol PLLA-PS). Five batches of microspheres were made from each of the 2k and 50k g/mol PLLA-PS alone and three batches were made from each blend composition. The yield of microspheres was 66 ± 5% and 84 ± 3% for pure 2k and 50k g/mol PLLA microspheres, respectively. The yields were statistically different ($p<0.005$). The polymer blends had yields intermediate between these two values. Optical and scanning electron microscopy confirmed that the microspheres were spherical with smooth surfaces. All of the microspheres were readily resuspended in water from a dry powder.

4.5.1.2. The effect of heating rate on thermal properties

The effect of the DSC scanning rate on thermograms of microspheres was determined using 50k g/mol microspheres. Scan rates ranged from 1 to 30°C/min. Representative DSC thermograms scanned at 5 and 30°C/min are shown in Figure 33A

140

and B. As the heating rate was increased, transition peaks became broader and the glass transition and recrystallisation events were shifted to higher temperatures. Tg and Tc ranged from 57 - 66°C and 77-97°C, respectively, over the heating rate range of 1-30°C/min. However, the peak area of the recrystallisation exotherm (ΔH_c), Tm and ΔH_f were unaffected, having values of approximately 28 J/g, 173°C and 56 J/g, respectively, at all heating rates. The change in Tg with increasing heating rate followed the relationship described by Barton (1969) over the heating rate range of 10 to 30 °C (Figure 33 inset):

$$\ln (\phi) = C - \frac{Ea}{RTg}$$

Equation 27

where ϕ is the heating rate (°C/min), Tg is in degrees K, C is a constant, R is the gas constant and Ea is the apparent activation energy of the glass transition (kJ/mol).

The relationship also holds for 2k g/mol PLLA in microspheres at heating rates between 10 and 30 °C/min. At slower heating rates, Tg deviates from the relationship and the equation is not recommended for application to rates less than 8°C/min (Barton, 1969). The values of Ea calculated from plots of Equation 27 were 213 and 183 kJ/mol for 2k and 50k g/mol PLLA-PS, respectively. Coefficients of determination (R^2) of the relationships exceeded 0.999 for both polymers.

4.5.1.3. Thermal properties of blends of 2k and 50k g/mol PLLA

Representative DSC thermograms of microspheres made with blends of 2k and 50k g/mol PLLA-PS are shown in Figure 33C-G and the effects of blend composition on thermal properties of the polymers are illustrated in Figure 34. The dashed line in Figure

141

34 shows the T_g calculated for miscible blends of 2k and 50k g/mol PLLA-PS using

Equation 13. A single glass transition was observed for all blends, indicating that the two

polymers are miscible. However, the shape and area of the endothermic peak observed at

the glass transition, evidence of enthalpy relaxation, was dependent on the blend

composition. Measurements of enthalpy relaxation (H_r) were repeated for the 50k and 2k

g/mol PLLA-PS microspheres after several months and these values were taken as the

infinite relaxation ($\Delta H_{r\infty}$). Values of $\Delta H_{r\infty}$ were not greater than values of ΔH_r by more

than 10-20% for both polymers.

Microspheres prepared from all blend ratios showed recrystallisation around

90°C upon heating above the glass transition (Figure 33). For PLLA-PS blends, the

degree of crystallinity decreased as the proportion of 2k g/mol PLLA-PS increased. T_m

was lower for 2k g/mol PLLA-PS (145°C) than 50k g/mol PLLA-PS (173°C)

microspheres and T_m values for blends were between the two extremes (Figure 34B).

Microspheres made from 2k g/mol PLLA-PS microspheres had two peaks at the melting

transition (Figure 33C), indicating the presence of crystallites with a lower degree of

perfection. In contrast, 50k g/mol PLLA-PS microspheres showed a sharper transition

with only a very small endothermic peak prior to the main melting transition. The

addition of 50k g/mol PLLA-PS to the 2k g/mol polymer resulted in an increasingly

sharper melting peak (Figure 33D to G).

4.5.2. Blending 100k and 1k g/mol PLLA

4.5.2.1. Effect of blend composition on microspheres properties

PLLA-LA with molecular weight 1k g/mol was blended in several ratios with

100k g/mol PLLA and used to manufacture microspheres. A PVA concentration of 1%

and stirring rate of 900 rpm were used to make all the microspheres studied in this

section. Microspheres with a blend composition of up to 60% 1k g/mol PLLA-LA were

spherical and could be freely resuspended in water following the drying step in the

manufacturing process. Microspheres with greater than 60% of the low molecular weight

component were irregularly shaped and tended to aggregate. The surface morphologies

of microspheres made from varying blend compositions are shown in Figure 35.

The thermal properties of the polymer blends are shown in Figure 36. The trends

were very similar to those for the 2k and 50k g/mol PLLA-PS blends (Figure 33). The

glass transition and melting temperatures and the degree of polymer crystallinity were all

lowered by the addition of 1k g/mol PLLA to the 100k g/mol PLLA. A double melting

endotherm was observed for blends containing 70% or greater of the 1k g/mol polymer.

The double endotherm was observed as a shoulder on the low-temperature side of the

melting transition at temperatures between 100 and 130°C.

Figure 37 shows the dependence of Tg on blend composition according to the

Fox equation (Equation 13). The dependence of melting point depression on the blend

composition according to Equation 14 is shown in Figure 38. For both Figures 37 and

38, blend composition data were adjusted assuming incomplete incorporation of the

1k g/mol polymer. Blend compositions were calculated based on the starting proportions

of 1k and 100k g/mol polymers and the assumption that 34% of the 1k g/mol polymer

was not incorporated which was the weight of the water soluble fraction of the material determined in section 4.4.2.

The blend ratio of 60% 1k g/mol PLLA to 40% 100k g/mol PLLA was selected for further study because it was the highest ratio of low/high molecular weight polymer which could form spherical microspheres and be resuspended in water. Microspheres made from this blend composition were called polyblend-60 or "PB60" microspheres.

4.5.2.2. Particle size and surface morphology of PB60 microspheres

PB60 microspheres were made using the same manufacturing parameters as for 100k g/mol PLLA microspheres to achieve size ranges of 1-10, 10-35 and 35-105 μm. Particle size distributions were similar to those obtained for 100k g/mol PLLA microspheres (refer to Figure 27). However, the mean and mode of the distribution were decreased by 15-20 μm to approximately 45-55 μm for the microspheres in the 35-105 μm size range. Scanning electron micrographs of 1-10 and 35-105 μm, control and 30% loaded microspheres are shown in Figure 39. In contrast to microspheres made from 100k g/mol PLLA no dimpling was observed on the surface of PB60 microspheres.

4.5.2.3. Total paclitaxel content

PB60 microspheres generally showed higher total content of paclitaxel than did 100k g/mol PLLA microspheres (Table 17). Greater than 100% encapsulation efficiency was observed in five of nine formulations due to incomplete incorporation of polymer into the matrix. Microspheres in the size range of 1-10 μm with theoretical loading of 30% had only 79% of the theoretical amount of paclitaxel in the microspheres.

4.5.2.4. Thermal properties

Thermograms of control and 20% paclitaxel loaded PB60 microspheres in the

35-105 μm size range are shown in Figure 40 and the transitions are summarised in Table

18 with those for 20% loaded microspheres in the 1-10 and 10-35 and 35-105 μm size

ranges. All control microspheres possessed degrees of crystallinity of less than 20% and

less than 5% for control and paclitaxel loaded microspheres, respectively. Similar data

were obtained for 10 and 30% paclitaxel loaded PB60 microspheres. A melting point

depression of 2-4 °C was observed in the 20% loaded microspheres compared to control.

Similar observations were made for 10 and 30% loaded microspheres although the

melting point depression was greatest for microspheres in the larger size range, with 30%

paclitaxel loaded 35-105 μm microspheres having a 6°C depression in Tm. The addition

of paclitaxel to PB60 microspheres was accompanied by a 7-10°C increase in Tg (see

Figure 40 and Table 18). The elevation of Tg was observed in all size ranges and at all

loadings. The recrystallisation temperature (Tc) of the polymer was also higher in

microspheres that contained paclitaxel. Control and paclitaxel loaded microspheres had

values of Tc around 90 and 115°C, respectively.

The addition of paclitaxel also resulted in a change in the shape of the melting

endotherm. A small shoulder peak preceded the major polymer melting peak in

paclitaxel loaded microspheres when thermograms were obtained with a 10°C/min

heating rate (Figure 40B). The peak temperature was 10°C less than the major Tm for

microspheres containing 20-30% paclitaxel and 15°C lower for 10% loaded

microspheres. The ΔH of the shoulder peak varied from approximately 5 to 30% of the

total ΔH_f of the polymer as the paclitaxel loading level increased from 10 to 30%. However, at a scanning rate of 30°C/min, the shoulder peak was not observed.

4.5.2.5. *In vitro* release profiles of paclitaxel

In vitro paclitaxel release profiles for 10, 20 and 30% loaded microspheres in the size ranges of 1-10, 10-35 and 35-105 μm are shown in Figure 41. The features that were common to all of the release profiles were an initial rapid phase (V_0) over 24 hours, a slower phase that lasted until around day 21 at which point the rate then increased, followed by a gradual slowing of the release rate around day 63 of the study. Statistical differences between values of V_0 for different sizes and loading levels are illustrated by a schematic diagram showing results of Tukey tests (Figure 41). V_0 increased from 2-4 μg/hr to 3-19 μg/hr for all sizes of 10 and 30% loaded microspheres. At all loadings V_0 was greater for smaller microspheres (Figure 41). The total extent of release (M_{63}) increased with loading and decreased with increasing microsphere size (207-386, 421-577 and 448-706 μg for 35-105 and 1-10 μm 10, 20 and 30% loaded microspheres, respectively). Based on total content data shown in Table 16, M_{63} accounted for between 30 and 60% of the total paclitaxel loaded into microspheres.

The morphologies of PB60 microspheres at days 0, 15 and 70 of an *in vitro* release study are shown in Figure 42. By day 15 (Figure 42B) the microspheres had begun to show signs of surface erosion. By day 70, PB60 microspheres had disintegrated leaving irregularly shaped particles with diameters up to 75 μm.

Table 17. Total content of paclitaxel in 1-10, 10-35, 35-105 μm microspheres made with a blend of 60:40 1k g/mol PLLA-LA:100k g/mol PLLA. Values are averages of three measurements from a single batch of microspheres. The precision in measurement was greater than 91% for all samples.

Microspheres	Paclitaxel content (% of theoretical paclitaxel loading)		
	10% loading	20% loading	30% loading
1-10 μm	128	106	79
10-35 μm	115	114	109
35-105 μm	112	109	109

Table 18. Thermal properties of control and 20% loaded paclitaxel 60:40 1k g/mol PLLA-LA:100k g/mol PLLA microspheres with size ranges of 1-10, 10-35 and 35-105 μm.

Theoretical loading	Tg^a $(\Delta H_r)^b$ °C (J/g)	Tc^a $(\Delta H_c)^b$ °C (J/g)	Tm^a $(\Delta H_f)^b$ °C (J/g)	Xc (%)
1-10 μm microspheres				
Control	55 (5.5)	83 (13)	166 (46)	18
20%	62 (7.4)	111 (18)	164 (41)	2
10-35 μm microspheres				
Control	52 (4.3)	89 (19)	166 (43)	19
20%	62 (7.3)	120 (26)	164 (40)	1
35-105 μm microspheres				
Control	53 (6.8)	92 (17)	167 (46)	8
20%	61 (7.6)	116 (22)	163 (41)	5

[a] Peak transition temperature data are averages of three measurements made from a single batch of microspheres for each size and loading. Peak temperature values varied by <2 °C for all transitions.

[b] Peak area data varied <1 J/g for ΔH_r and <5 J/g for ΔH_c and ΔH_f

Figure 33. Representative DSC thermograms of 50k g/mol PLLA-PS microspheres obtained using heating rates of A) 5 and B) 30°C/min and of microspheres with size range 1-20 μm prepared from blends of 2k and 50k g/mol PLLA-PS with compositions of C) 100:0, D) 80:20, E) 60:40, F) 20:80, and G) 0:100 2k:50k g/mol PLLA-PS obtained using a heating rate of 10°C/min. Inset: The effect of DSC scanning rate on the Tg of 2k and 50k g/mol PLLA following the relationship of Barton (1969).
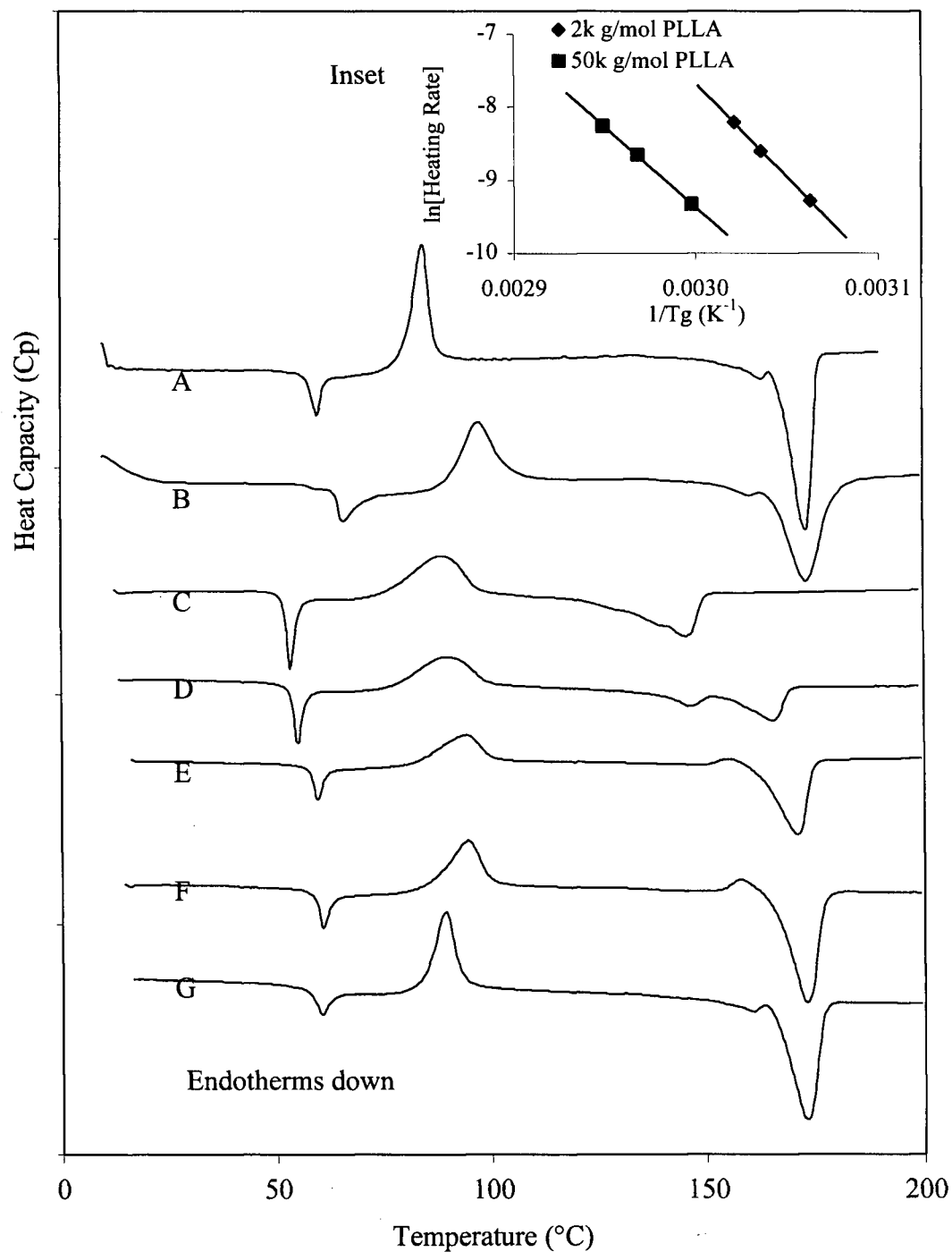
Figure 34. The effects of polymer blend composition in microspheres made from 2k and 50k g/mol PLLA-PS on A) the glass transition and B) the melting transition and degree of crystallinity.
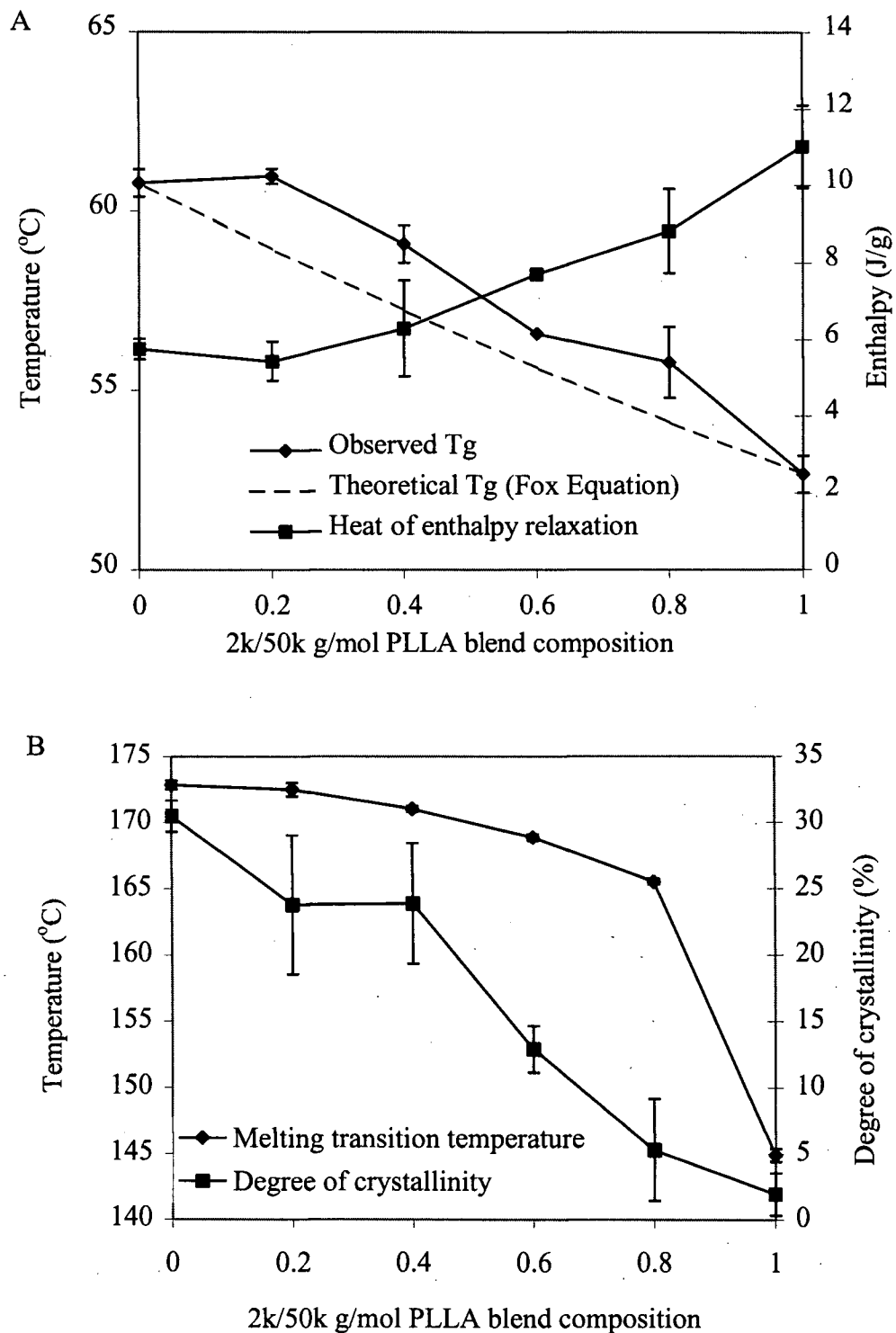
Figure 35. Scanning electron micrographs showing the surface morphology of microspheres made from a blend of 1k g/mol PLLA-LA and 100k g/mol PLLA in ratios of A) 0:100, B) 60:40, C) 80:20 and D) 100:0. (The magnification of all micrographs is 1000x.)
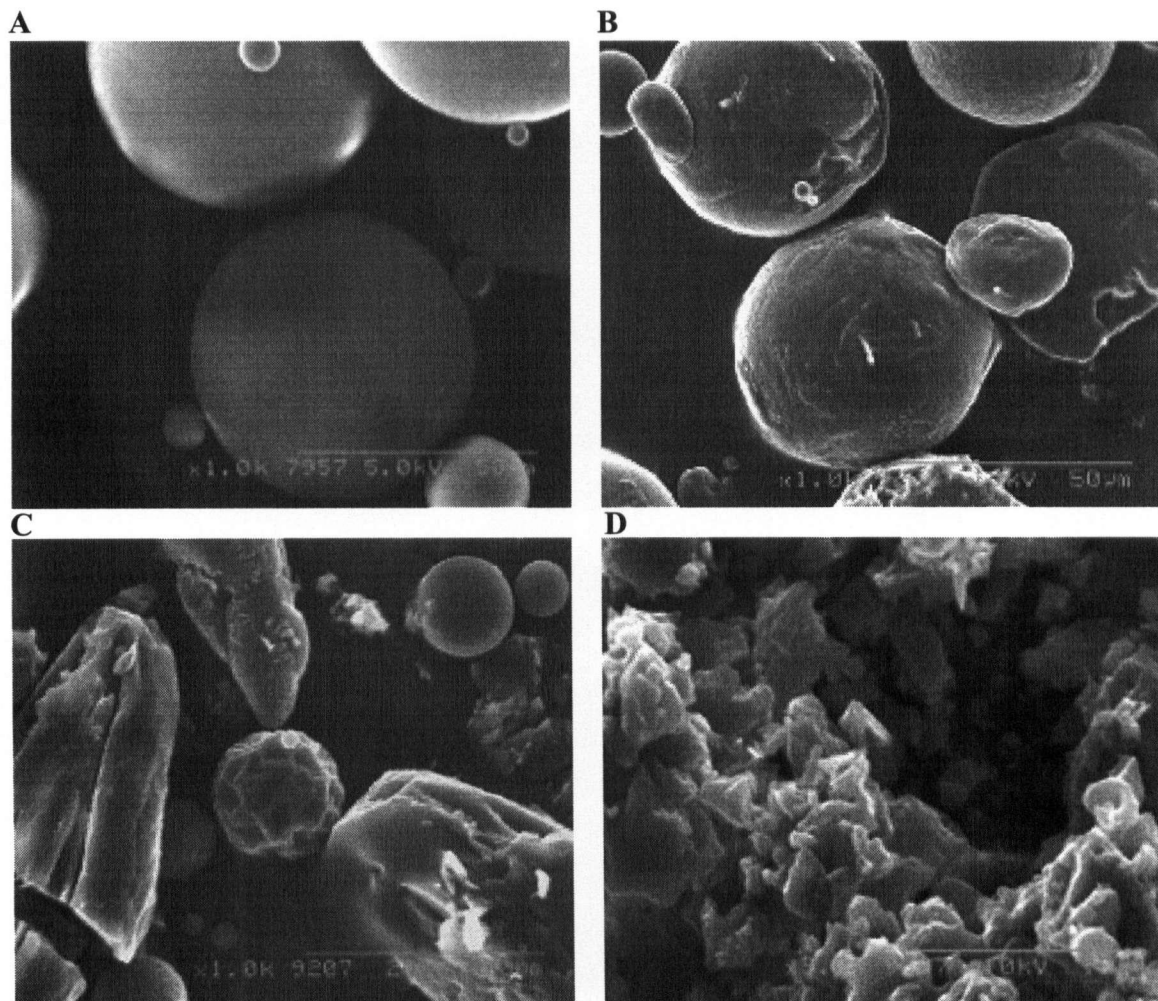
Figure 36. The effects of polymer blend composition in microspheres made from
1k g/mol PLLA-LA and 100k g/mol PLLA on A) the glass transition and B)
the melting transition and degree of crystallinity.

A

1k/100k g/mol PLLA blend composition

B

1k/100k g/mol PLLA blend compositoin

151
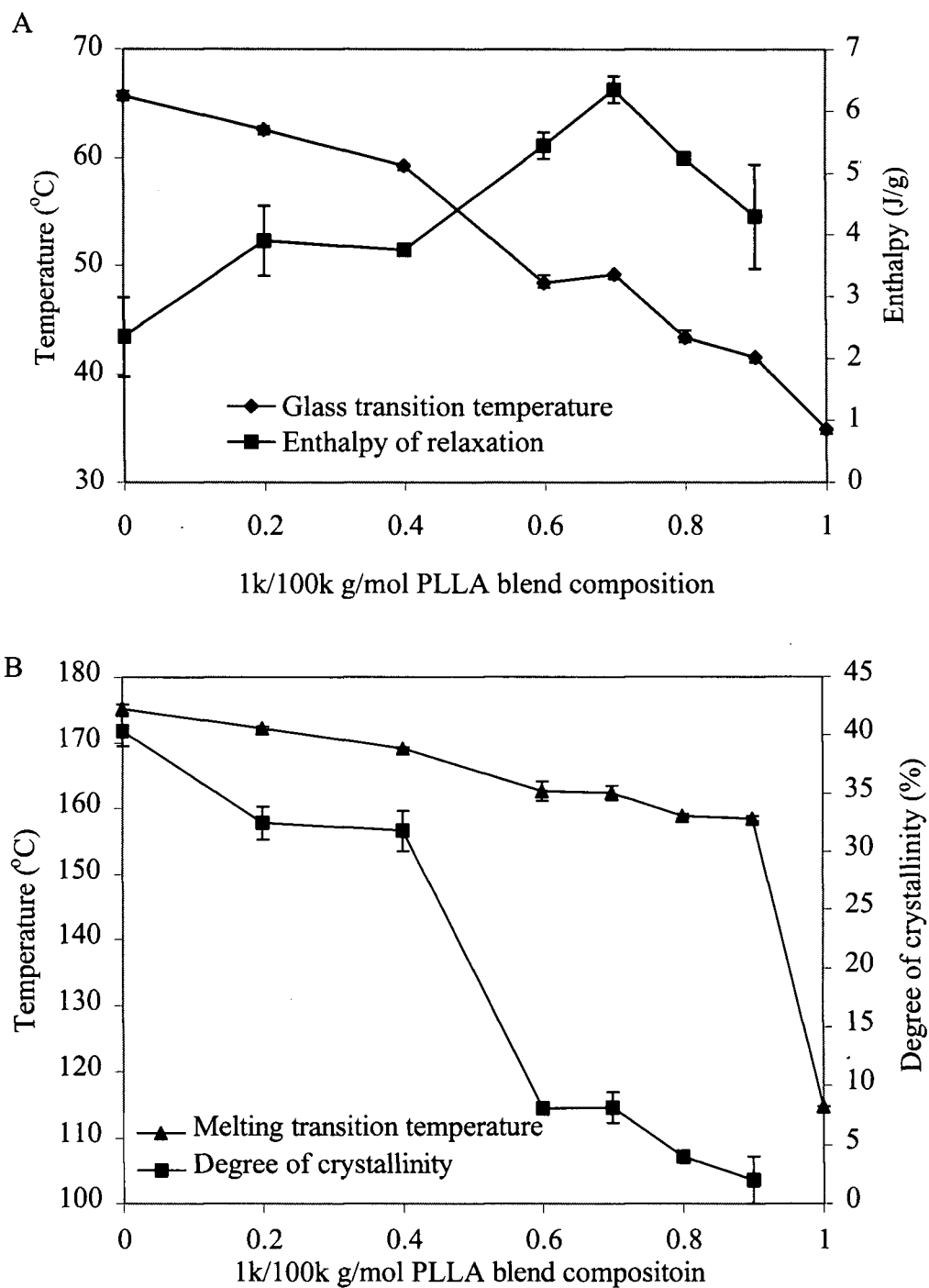
Figure 37. Change in the Tg with the addition of 1k g/mol to 100k g/mol PLLA compared to the Tg calculated from Equation 13 (solid line). (Composition data adjusted for loss of the water soluble fraction of 1k g/mol PLLA.).

1k/100k g/mol PLLA blend composition
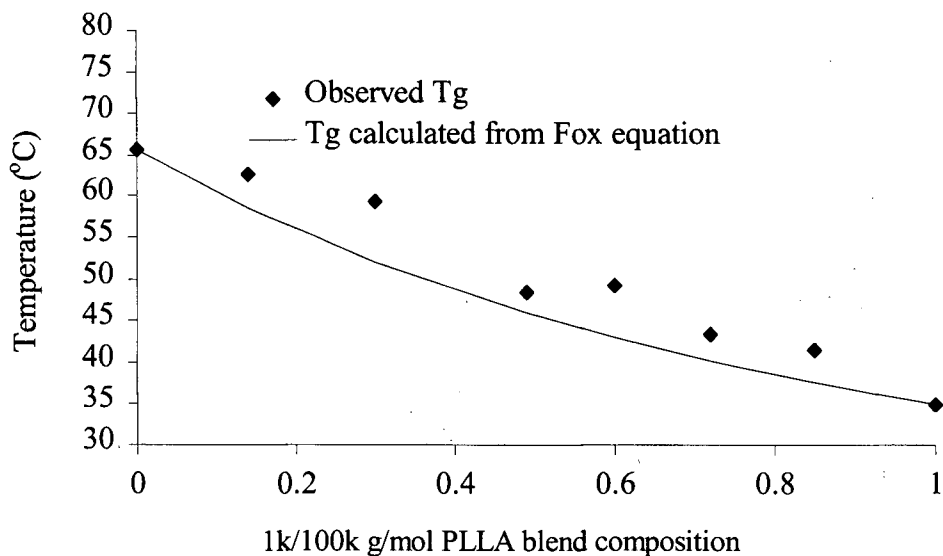
Figure 38. Change in the observed melting temperature (Tm) with the addition of low molecular weight PLLA to higher molecular weight PLLA for 2k/50k g/mol PLLA-PS and 1k/100k g/mol PLLA blends calculated from Equation 14. (Composition data adjusted for loss of the water soluble fraction of 1k g/mol PLLA.)

Low/High MW PLLA Blend composition
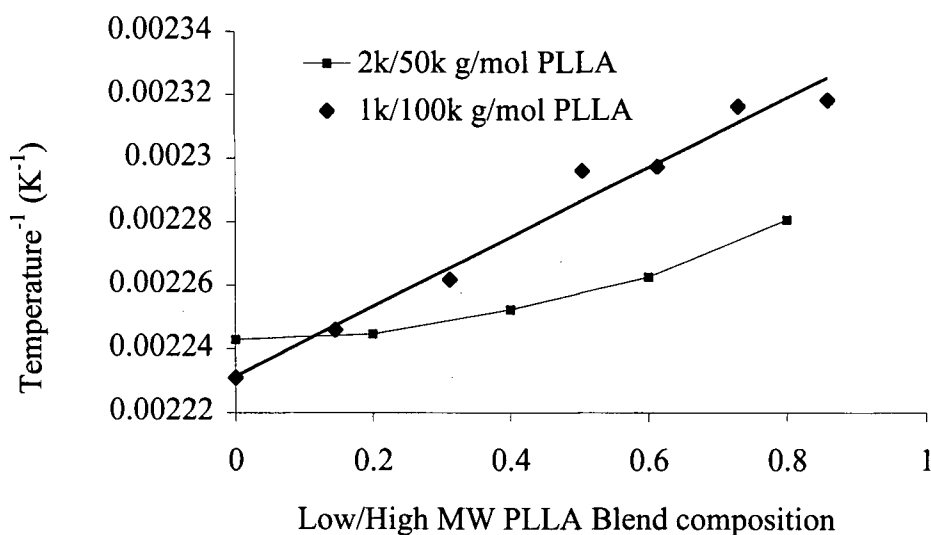
Regression analysis for the 1k/100k g/mol PLLA blend:(y = mx + b, R^2)
y = 0.000109x + 0.0223, R^2 = 0.97

152

Figure 39. Surface morphology of A) 1-10 μm and B) 35-105 μm control and C) 1-10 μm and D) 35-105 μm 30% paclitaxel loaded microspheres made from a 60:40 blend of 1k g/mol PLLA-LA and 100k g/mol PLLA. (Magnification of all micrographs is 1000x.)
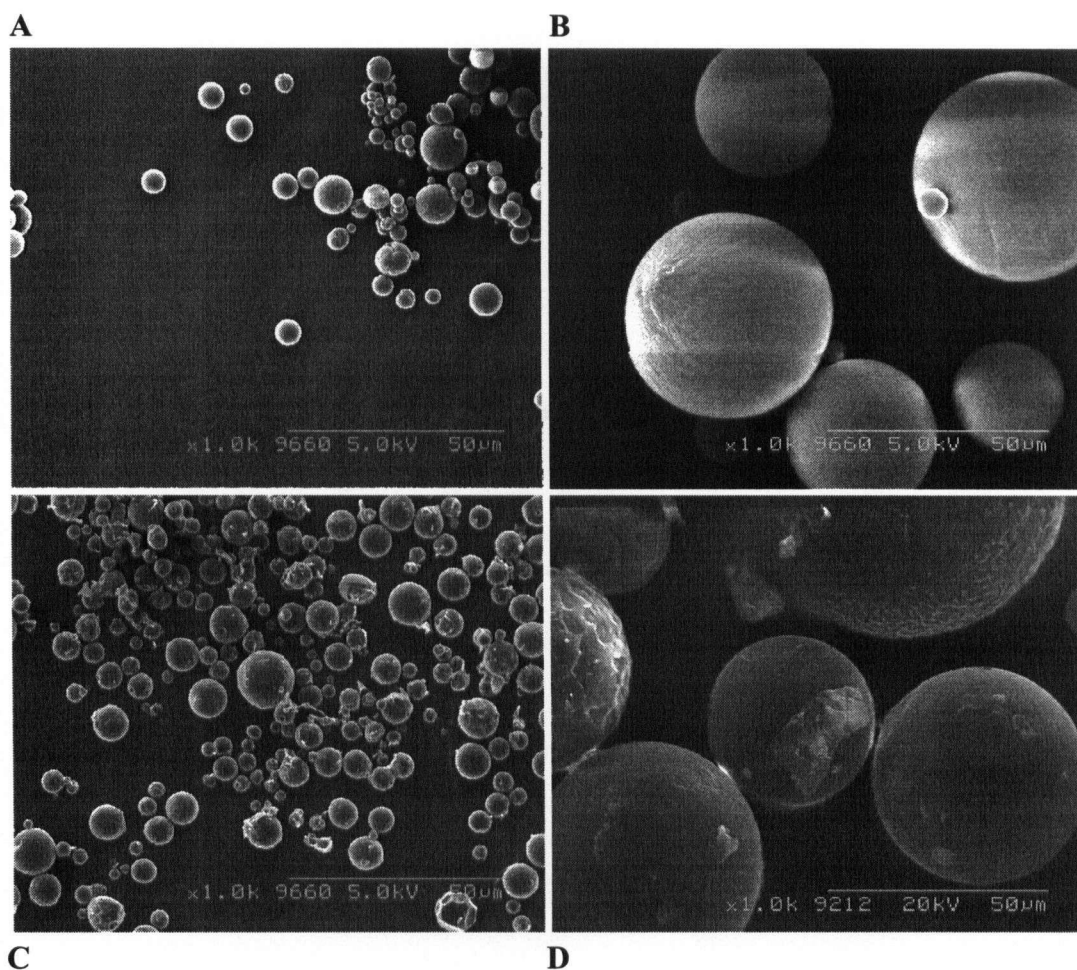
Figure 40. DSC thermograms of A) control and B) 20% paclitaxel loaded 35-105 µm
microspheres made with a 60:40 blend of 1k g/mol PLLA-LA and 100k
g/mol PLLA obtained with a heating rate of 10°C/min.
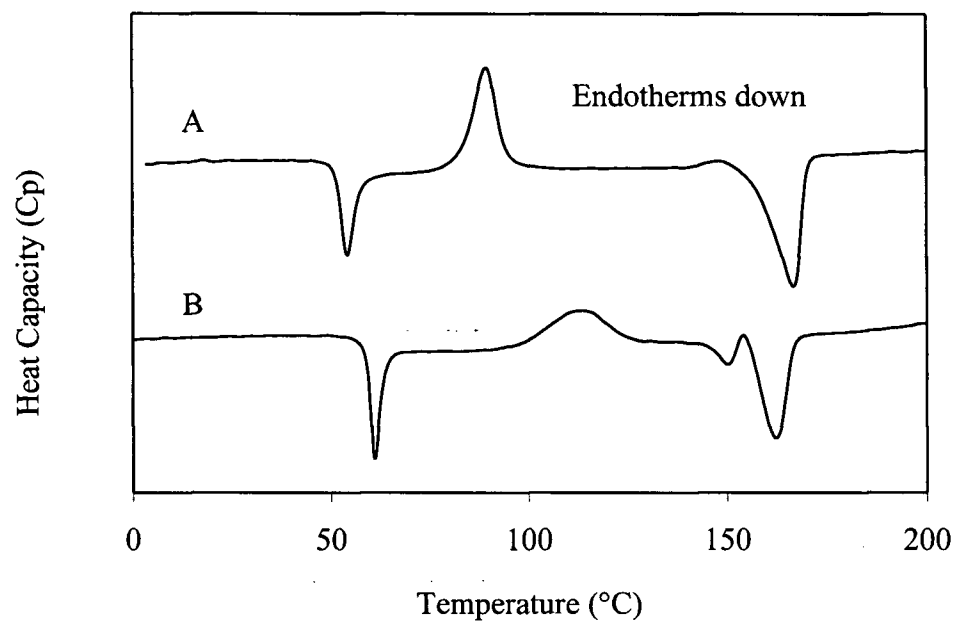
Figure 41. *In vitro* release profiles of paclitaxel from A) 10%, B) 20% and C) 30% paclitaxel loaded microspheres made with a 60:40 blend of 1k g/mol PLLA-LA and 100k g/mol PLLA. Below is a schematic representation of the results of Tukey tests of significant differences in parameters describing the initial rate (V_0) over 24 hours and total extent (M_{63}) of release. Dark lines identify microspheres between which no significant difference (p>0.05) was observed.

Initial rates (V_0) (μg/hr):

| 30%, 1-10μm | 20%, 1-10μm | 30%, 10-35μm | 20%, 10-35μm | 10%, 1-10μm | 20%, 35-100μm | 10%, 10-35μm | 30%, 35-100μm | 10%, 35-100μm |

Total extent of release (M_{63}) (μg):

| 30%, 1-10μm | 20%, 1-10μm | 30%, 10-35μm | 20%, 10-35μm | 30%, 35-100μm | 20%, 35-100μm | 10%, 1-10μm | 10%, 10-35μm | 10%, 35-100μm |

155

Figure 42. The surface morphology of 20% paclitaxel loaded microspheres in the size range of 35-105 μm made from a 60:40 blend of 1k and 100k g/mol PLLA after A) day 0, B) day 15 and C) day 70 of an *in vitro* release study. (Magnification of micrographs is 1000x.)
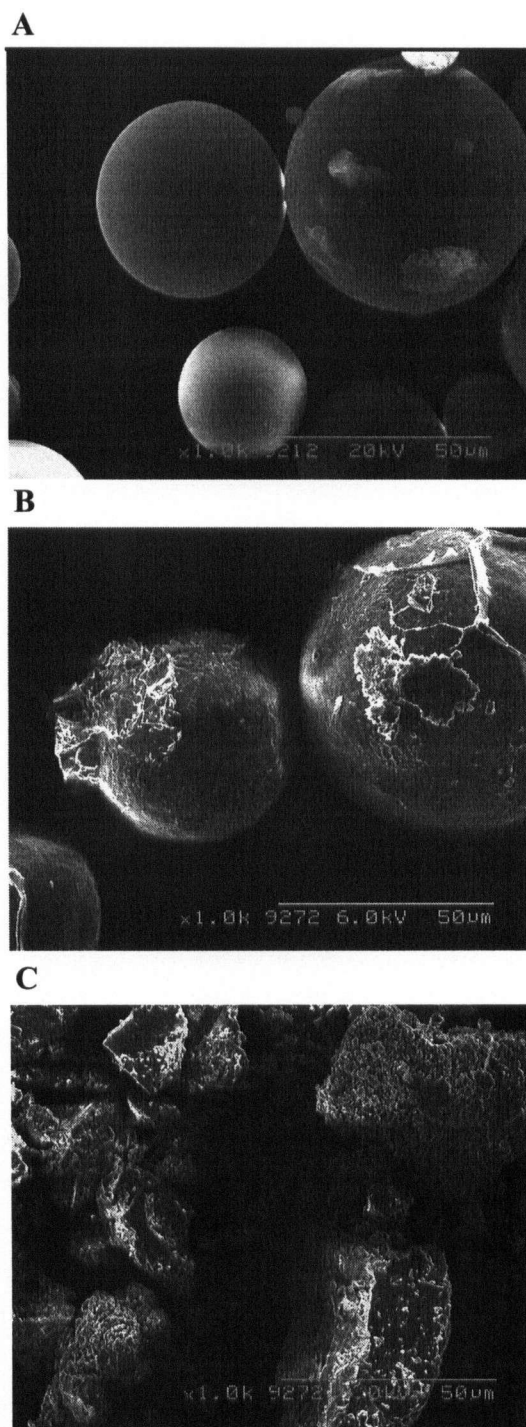
4.6. *In vivo* characterisation of paclitaxel loaded microspheres

For all *in vivo* studies, microspheres were prepared using 100k g/mol PLLA. The microspheres were in the size range of 1-40 μm for studies on microsphere clearance from the peritoneal cavity and 35-105 μm for all efficacy studies.

4.6.1. Clearance of microspheres from the peritoneum

Following intraperitoneal injection of control 1-40 μm microspheres, microspheres were observed in the mediastinal lymph nodes of rats and particle size data for these are shown in Table 19. Table 19 also summarises the particle size analysis data for the microspheres prior to injection. The maximum diameter of microspheres that were observed in the lymphatic tissue was close to 30 μm. However, only one or two microspheres with diameters greater than 10 μm were observed among 200-400 microspheres observed in the lymph tissue of each rat. There was no statistically significant difference in the average or maximum diameters or in the ninety-eighth percentile of diameters of microspheres observed in the lymph nodes when comparing animals which received insufflation and those in the control group (Table 20). A representative photograph of lymph node tissue containing microspheres is shown in Figure 43 compared to a photograph of microspheres prior to intraperitoneal injection. To avoid clearance of microspheres from the peritoneum all further studies in rats were carried out using microspheres with diameters in the range of 35-105 μm.

4.6.2. Efficacy of paclitaxel loaded microspheres in a model of intraperitoneal carcinomatosis

4.6.2.1. Dose escalation study

To establish that 9L glioblastoma tumour cells would produce intraperitoneal carcinomatosis in rats, three animals were given two million cells each through a midline laparotomy incision. After two weeks, all three animals showed evidence of tumour growth. One rat had hundreds of tumour nodules throughout the peritoneum involving all organs and implanted on the abdominal wall as shown in Figure 44A. Two rats had a single tumour 2 to 3 cm in diameter growing on the laparotomy incision site, with small tumour nodules (less than 0.5 cm in diameter) in the omental tissue.

To determine the effective dose of paclitaxel loaded microspheres required to prevent intraperitoneal carcinomatosis from becoming established with the introduction of 9L glioblastoma cells, escalating doses between 50 and 350 mg of 30% paclitaxel loaded 100k g/mol PLLA microspheres were tested in the model and compared to control microspheres. These doses corresponded to total paclitaxel doses to each animal of 15 to 105 mg.

Two weeks after the co-administration of the tumour cells and microspheres, the gastrointestinal tract, omental tissue, liver and abdominal wall were examined for the presence of tumour nodules. No rats receiving doses of 100 mg of paclitaxel loaded microspheres or greater showed any evidence of tumour growth compared to rats in control groups (rats receiving microspheres with no paclitaxel or no treatment) which showed visible tumours (Figure 20). A typical response in the control groups was the presence of a tumour growing on the laparotomy incision site (Figure 44B) and the

presence of small tumour nodules in the omental tissue and on the small bowel.
Responses ranged in severity from that shown in Figure 44B to complete involvement of
the peritoneal cavity, similar to that shown in Figure 44A. Microspheres were found to
be aggregated into white plaques ranging in diameter from approximately 2 to 13 mm
(see Figures 44B and C). The microsphere plaques were observed throughout the
peritoneal cavity, most commonly attached to omental tissue, on the gastrointestinal tract
and on the dome of the liver adjacent to the diaphragm.

For comparison in histological analysis, cells were taken from a tumour in a rat
that had received no treatment (Figure 45A). Tumour cells had irregularly shaped nuclei
and a characteristic swirling pattern. Samples taken from rats that received microspheres
showed that a dose of 100 mg of 30% paclitaxel loaded microspheres was sufficient to
prevent intraperitoneal carcinomatosis in the rat over the two week study period.
Histology samples from two of five rats which received 50 mg of paclitaxel loaded
microspheres showed the presence of tumour cells in the liver and omental tissue. Cells
taken from rats which received control microspheres had a similar appearance to those
from tumours in untreated rats (Figure 45B) Microspheres were observed embedded in
the tumour tissue and no cellular response to the foreign particles was evident. All
omental tissue samples taken in which paclitaxel loaded microspheres were present
showed tissue necrosis and no tumour cells immediately adjacent to or within several
hundred mirometers of the microspheres (Figure 45C). Further evidence of an adverse
response to paclitaxel was the presence of ascitic fluid in the peritoneal cavity of rats
which received 150 and 350 mg of paclitaxel loaded microspheres (refer to Figure 44C).

4.6.2.2. Efficacy of paclitaxel microspheres in the cecotomy repair model

In the second phase of the *in vivo* study each rat underwent cecotomy repair after intraperitoneal injection of the tumour cells but prior to administration of the microspheres and were allowed to live up to six weeks prior to sacrificing. Animals that were not treated with paclitaxel loaded microspheres did not survive past four weeks. Evaluation of the peritoneum of these animals showed the presence of established tumours and tumour nodules throughout the peritoneum. Tumours and nodules were observed with the greatest frequency at the cecotomy repair, and to a lesser extent on the small and large bowel, with involvement of the omentum. Large tumours (greater than 4 cm in diameter) were observed on the cecotomy repair as shown for a rat that received 100 mg of control microspheres, sacrificed after two weeks in Figure 46A. However several animals had very extensive tumour growth similar to that shown in Figure 44A. One animal in the control microsphere two week group died four days post-operatively. A preliminary autopsy did not reveal any cause of death. No evidence of abscess was seen, however small nodules of tumour were already apparent in the peritoneal cavity.

Figure 46B shows a representative photograph of the peritoneal cavity of a rat after six weeks, given 100 mg of 30% loaded microspheres. No tumours or tumour nodules were visible in the peritoneal cavities of any rats which received paclitaxel loaded microspheres, after both two or six weeks. No ascites were observed in the peritoneal cavity of paclitaxel treated animals. Samples of the cecotomy repair, omentum and of the laparotomy incision site harvested from paclitaxel treated rats showed no histological evidence of tumour cells after either two or six weeks. The appearance of the histology slides was similar to those shown in Figure 45C.

4.6.2.3. Analysis of microspheres removed from rats after six weeks *in vivo*

Three paclitaxel loaded microsphere plaques were removed from rats after six weeks. Values of total remaining paclitaxel in each of the plaques were 18, 47 and 60% of the original loaded value, an average of $58 \pm 27\%$ released over six weeks *in vivo*. The microscopic appearance of the microsphere plaques is shown by scanning electron micrographs in Figure 47. Two microsphere plaques that contained 47 and 60% of the original paclitaxel were covered with a smooth capsule (Figure 47A). Inside the capsule, microspheres were observed embedded in a matrix of the capsule material (Figure 47B). The microspheres appeared spherical with a dimpled surface, similar to their appearance prior to administration. A single microsphere plaque that contained 18% of the original amount of paclitaxel was not surrounded with a capsule *in vivo*. Scanning electron micrographs of these microspheres showed spherical, dimpled microspheres along with irregularly shaped particles of a smaller size (Figure 47C). Prior to quantifying the remaining paclitaxel in microspheres as much of the capsule material as possible was removed. However the microspheres could not be completely separated from the capsule, therefore, the reported values for residual paclitaxel, which are dependent on sample weight, underestimate the actual remaining paclitaxel contents.

Table 19. Particle size data for control microspheres made from 100k g/mol PLLA as manufactured, and for microspheres observed in mediastinal lymph nodes of rats.

Sample	Average diameter (μm)	Diameter at 98th percentile (μm)	Maximum diameter (μm)
As manufactured	8.6	29	40
Control rats (n=5)	4.2 ± 0.5	7.6 ± 1.4	24 ± 9
Insufflated rats (n=5)	4.3 ± 0.3	8.3 ± 0.9	20 ± 13

Table 20. Growth of 9L glioblastoma tumours in the peritoneum of rats receiving various doses of 30% paclitaxel loaded 35-105 μm 100k g/mol PLLA microspheres.

Treatment group	Animals with visible tumour growth (%) (n=5)	Animals with histologically confirmed tumour cells (%) (n=5)
No treatment	100	100
100 mg control microspheres	100	100
50 mg paclitaxel microspheres	0	40
100 mg paclitaxel microspheres	0	0
150 mg paclitaxel microspheres	0	0
350 mg paclitaxel microspheres	0	0

Figure 43. Representative optical micrographs of A) 1-40 μm 100k g/mol PLLA microspheres as manufactured and B) the mediastinal lymph nodes of a rat (without insufflation) after intraperitoneal administration of 1-40 μm microspheres.
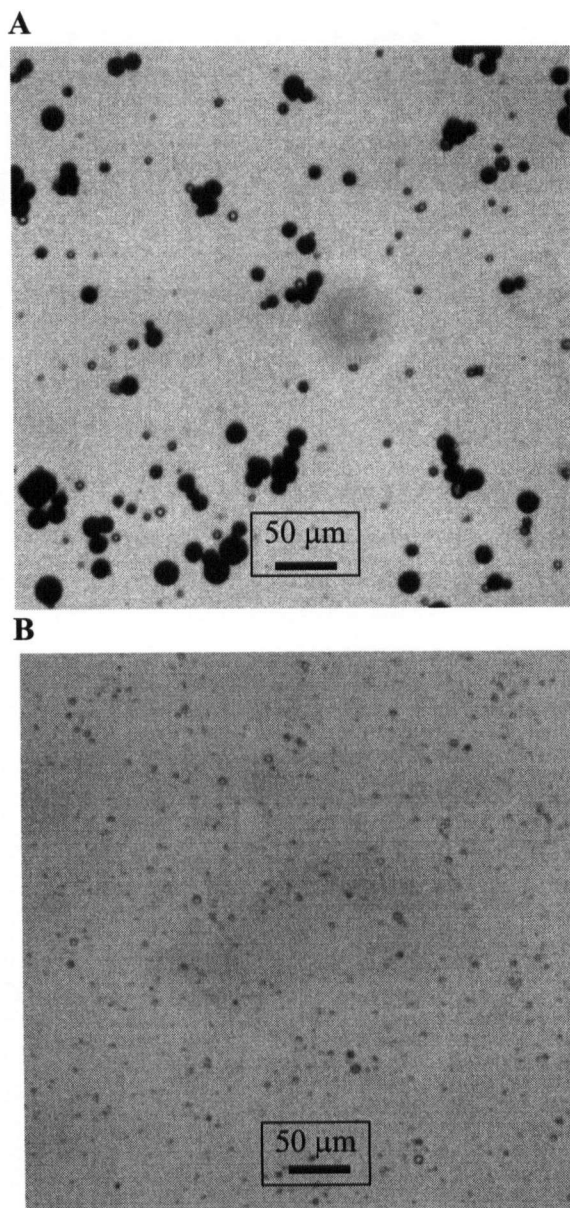
Figure 44. Representative photographs of the peritoneal cavity of rats two weeks after intraperitoneal administration of two million 9L glioblastoma cells with A) no further treatment, B) 100 mg of control 35-105 μm 100k g/mol PLLA microspheres and C) 350 mg of 30% paclitaxel loaded microspheres.
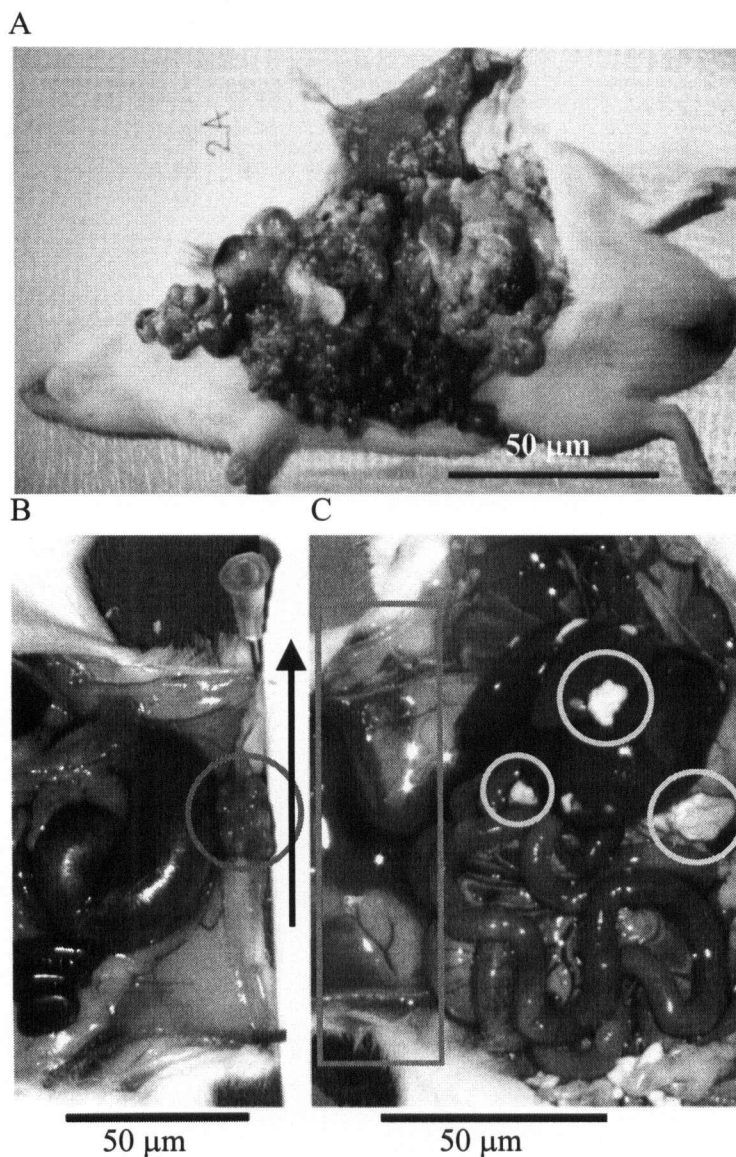
↑ The arrow points toward the head of the rats pictured in Figures B and C.

◯ The circle in Figure B shows a tumour with dimensions of approximately 2.5 x 1.3 cm attached to the laparotomy incision site

◯ The circles in Figure C show microsphere plaques with diameters ranging from 0.7 to 1.25 cm.

▢ The rectangle in Figure C shows a pool of ascitic fluid which was observed in rats receiving 150 and 350 mg of paclitaxel loaded microspheres.

Figure 45. Representative photographs of histological samples harvested two weeks after treatment of A) cells removed from a tumour in the peritoneum of a rat which received two million 9L gliosarcoma cells and no further treatment, B) cells removed from a tumour in the peritoneum of a rat which received tumour cells and 100 mg of control 35-105 μm 100k g/mol PLLA microspheres and, C) omental tissue removed from a rat which received tumour cells with 100 mg of 30% paclitaxel loaded microspheres. The ellipses in Figures B and C identify control microspheres and paclitaxel loaded microspheres, respectively.

165
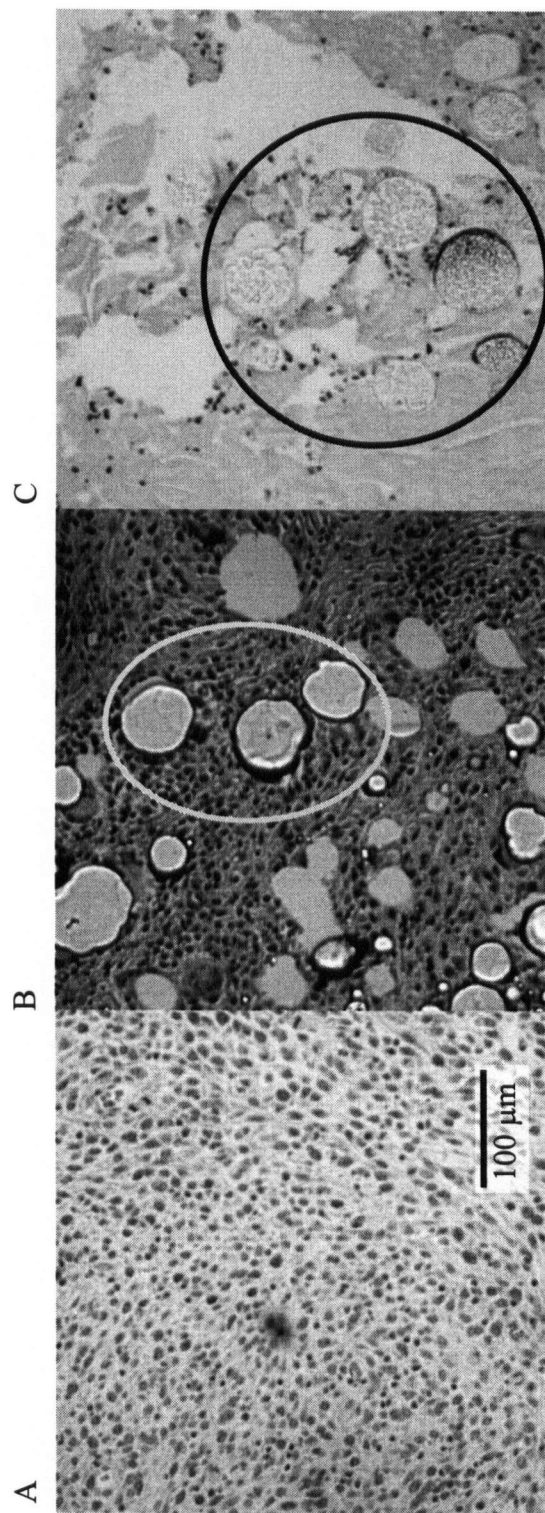
Figure 46. Representative photographs of the peritoneal cavity of rats A) two weeks after intraperitoneal administration of two million 9L glioblastoma cells with no further treatment and B) six weeks after intraperitoneal administration of tumour cells and 100 mg of 30% paclitaxel loaded 35-105 μm microspheres in a model of intraperitoneal carcinomatosis after a cecotomy repair. The white circle identifies a tumour on the cecotomy repair site and numerous tumour nodules attached to the cecum.

A
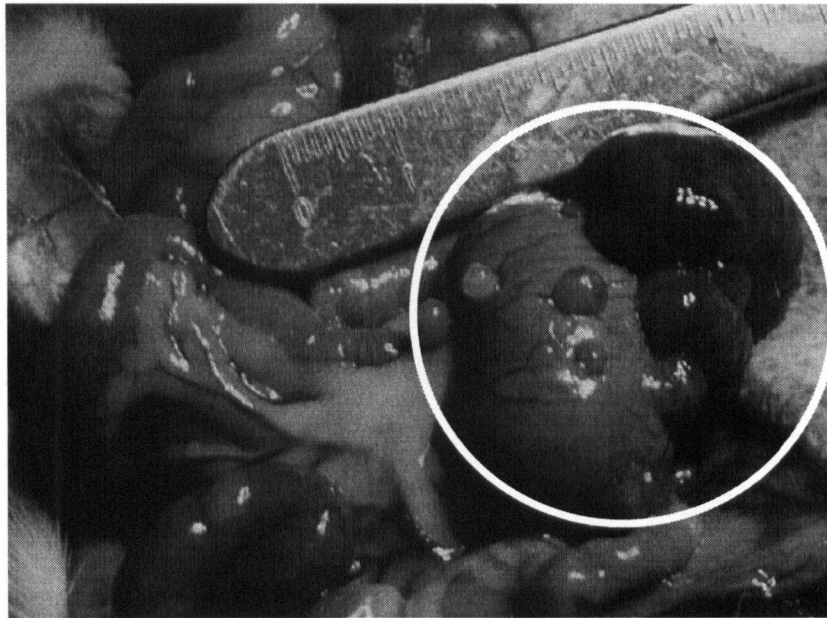
B
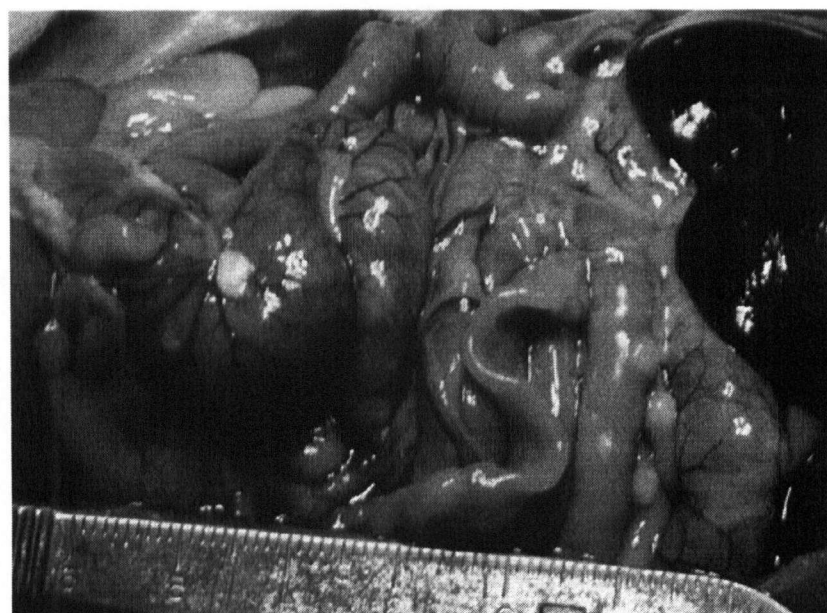
Figure 47. Scanning electron micrographs of samples of 35-105 μm 30% paclitaxel loaded 100k g/mol PLLA microspheres removed from the peritoneum of rats after six weeks *in vivo*. Figure A shows the surface of a capsule surrounding a plaque containing paclitaxel loaded microspheres. Figure B shows a cross sectional view of the capsule containing microspheres and Figure C shows microspheres which were not contained in a capsule *in vivo*. (Magnification of all micrographs is 1000x.)

167
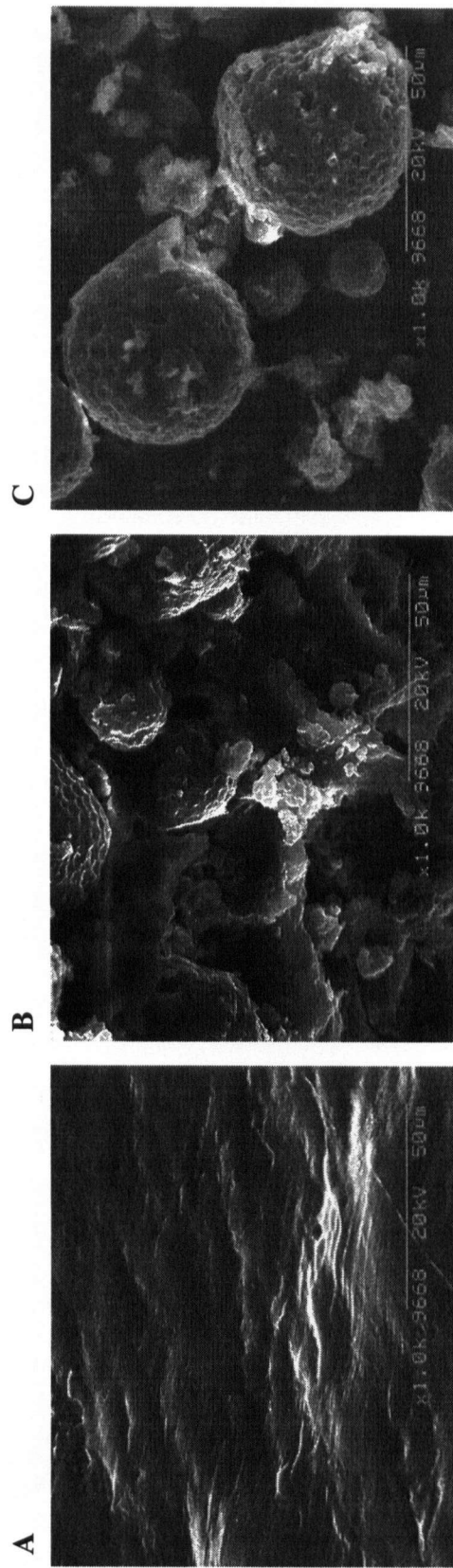
5.   DISCUSSION

5.1.   Solid state characterisation of paclitaxel

Karl Fischer, DSC, TGA and XRPD analysis were used to identify several

different solid forms of paclitaxel. Interconversion between the various forms is

summarised by the flow chart in Figure 48.

Figure 48. A flowchart summarising the conversion of paclitaxel to its various solid forms.
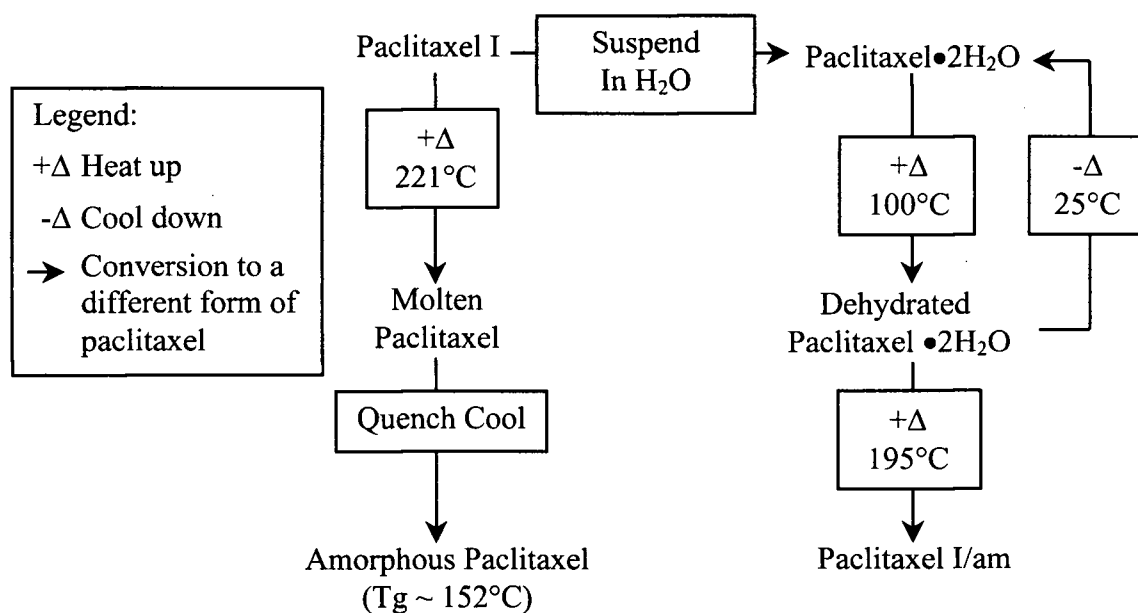
Dordunoo and Burt (1996) provided preliminary evidence that suggested

paclitaxel could exist as a dihydrate. Karl Fischer, DSC and TGA analysis confirmed

that commercial paclitaxel I is an anhydrate form which may be converted to paclitaxel

dihydrate (paclitaxel•2H$_2$O) after 24 hours of incubation in water. The Karl Fischer

method quantifies total water in the material including chemically bound water of crystallisation and physically bound adsorbed water (Suryanarayanan, 1989). The Karl Fischer analysis and the TGA data (Figure 7) both indicate that small amounts of non-structural, physically bound sorbed water were present in both paclitaxel I and paclitaxel•$2H_2O$. Powder X-ray diffraction analysis confirmed the existence of two distinct crystalline phases, an anhydrous form (paclitaxel I) and the dihydrate, produced by suspension of paclitaxel I in water (paclitaxel•$2H_2O$). The powder X-ray diffraction patterns for paclitaxel are not currently listed in the International Powder Diffraction Files.

Paclitaxel I was stable for 96 days in relative humidities up to 94% at 25°C and paclitaxel•$2H_2O$ stored in a vacuum oven at 25°C and 200 mmHg for several weeks showed no evidence of weight loss or dehydration. Hence, a relative humidity phase diagram could not be constructed for the anhydrate and dihydrate forms due to the absence of detectable phase changes at 25°C under these relative humidity conditions.

Dehydration of paclitaxel•$2H_2O$ occurred over a higher temperature range when measured by DSC (35 - 140°C) compared to TGA (25 - 85°C) determined at the same heating rate of 10°C/min. The difference can be explained by a change in dehydration kinetics due to differences in external water vapour pressure in the open TGA system compared to DSC pans (sealed and unsealed) which have a lid. It has been observed for other compounds that a higher external water vapour pressure will slow the dehydration process resulting in dehydration at a higher temperature (Kitaoka *et al*, 1995). At slower scan rates the dehydration events occurred at progressively lower temperatures. This was likely a result of less thermal lag in the DSC measurement and changes in the vapour

pressure inside the DSC sample pan at the slower scan rates. The dehydration

endothermic peak was sharper and occurred over a narrower temperature range in the

pinhole pan compared to the open pan. It is possible that a more controlled water vapour

pressure was obtained upon heating in the DSC when pinhole pans were used. TGA data

obtained isothermally (Figure 9) also resulted in slower dehydration of paclitaxel•$2H_2O$

compared to TGA data obtained at a heating rate of 10°C/min (Figure 7B). Slower

dehydration in the profile obtained at 45°C (Figure 9) provided increased resolution of

the loss of each mole of water.

Dehydration of hydrates has been classified into three types on the basis of the

resulting dehydrated lattice: a) the crystal lattice of the residue is nearly identical to

that of the original hydrate (Dash and Suryanaryanan, 1991) b) the residue is poorly

crystalline and c) the residue recrystallises with a different crystal lattice

(Suryanarayanan, 1989). The X-ray diffraction studies indicate that dehydrated

paclitaxel•$2H_2O$ falls into the third type with dehydrated paclitaxel•$2H_2O$ possessing a

different crystal lattice compared to paclitaxel•$2H_2O$. Since dehydrated

paclitaxel•$2H_2O$ had a different XRPD pattern from paclitaxel I, and both forms are

anhydrous, this suggests that the two forms are polymorphs.

The results of DSC, TGA and gravimetric analysis showed that dehydrated

paclitaxel•$2H_2O$ could be rehydrated to paclitaxel•$2H_2O$ at ambient temperature and

43% relative humidity. Heating dehydrated paclitaxel•$2H_2O$, resulted in a solid-solid

transition (Figure 8C) and conversion to semicrystalline paclitaxel I (paclitaxel I/am).

In contrast to dehydrated paclitaxel•$2H_2O$, neither paclitaxel I/am nor paclitaxel I

previously heated to 195°C were hydrated at ambient conditions (43% RH). Based on similar XRPD patterns, paclitaxel I/am (Figure 10D) has the same crystal lattice structure as paclitaxel I at either 25°C or 195°C (Figure 10A). However the diffraction peak intensities for paclitaxel I/am were much lower than in the pattern for paclitaxel I at 195°C, indicative of a lower degree of crystallinity (see Table 5). This is substantiated by the lower ΔH_f observed by DSC for paclitaxel I/am of 31 J/g compared to the ΔH_f for paclitaxel I of 63 J/g. As paclitaxel I was heated from 25°C to 195°C, the crystallinity apparently increased as evidenced by more intense X-ray diffraction peaks. The increase in crystallinity was probably also responsible for the appearance of several new but very weak peaks between 15 and 25 °2θ. Annealing of a solid by heating can relieve internal strain and result in an increase in crystallinity. Yoshioka *et al* (1994) demonstrated this effect for amorphous indomethacin. The increase in crystallinity was dependent on time and storage temperature.

Paclitaxel I, when quench cooled at 180°C/min from the melt does not recrystallise immediately. Instead it forms an amorphous solid which is a glass at 25°C. Amorphous paclitaxel conforms to the criteria for a fragile glass, having a relatively large ΔCp and a ratio of Tm/Tg (degrees K) < 1.5 (Table 4). Trends in values of ΔCp and Tm/Tg with changes in glass fragility are illustrated by the thermal properties of other pharmaceutical materials such as indomethacin and sucrose (Hancock *et al.*, 1995). Amorphous materials may be ranked according to their observed glass transition properties. Table 4 summarises these results and shows the tendency to observe a higher ΔCp when a lower ratio of Tm/Tg is observed. Paclitaxel

forms the most fragile glass (highest ΔCp and lowest Tm/Tg), followed by sucrose, followed by indomethacin.

The presence of a Tg in the DSC thermogram for paclitaxel I/am similar to amorphous paclitaxel indicates that paclitaxel I/am is semicrystalline. The one state model of crystallinity describes a semicrystalline solid as being an intermediate state between a crystalline solid (perfectly ordered lattice) and an amorphous solid (disordered lattice). The transition from a crystalline to a semicrystalline solid therefore represents an increase in lattice disorder, which is believed to be a result of increasing lattice defect content (Suryanarayanan and Mitchell, 1985). Pharmaceutical processes such as milling, compression and drying (dehydration) have been shown to result in increased lattice defect content and disorder and decreased crystallinity (Hutterauch et al., 1979; York, 1983; Suryanarayanan and Mitchell, 1985). Hence, the decreased crystallinity of paclitaxel I/am compared to paclitaxel I is probably due to greater defect content and greater lattice disorder caused by the dehydration event and the solid-solid transition.

Paclitaxel I has an apparent solubility of around 3.5 μg/ml at 37°C in water giving rise to a supersaturated solution which recrystallised as a stable dihydrate with lower solubility (1 μg/ml) (see Figure 12). The higher apparent solubility of the anhydrous material relative to the dihydrate has been observed for many drugs including caffeine and theophylline (Angell et al, 1994). The solubility data shown here are consistent with reported literature values of 6 μg/ml (Swindell et al., 1991) and 0.7 μg/ml (Mathew et al., 1992) which may represent the higher apparent solubility of

172

the anhydrate and the equilibrium solubility of the dihydrate, respectively. The value

of 30 μg/ml reported by Tarr and Yalkowsky (1987) may reflect a less crystalline form

of paclitaxel. Other studies have demonstrated the higher apparent solubility of

amorphous compared to crystalline forms (Chiou and Riegelman, 1971).

This is the first report in which two polymorphic anhydrous forms, an

amorphous form and a dihydrate of paclitaxel have been characterised. The existence

of numerous solid forms of paclitaxel and the data in Figure 12 may help to explain the

variability in values reported for paclitaxel's water solubility.

5.2.   Polymer synthesis

PLLA polymers were synthesised in the molecular weight range of 500 to

10k g/mol by ring opening polymerisation using a tin catalyst and either stearyl alcohol

(PLLA-SA) or L-lactic acid oligomer (PLLA-LA) as initiators. The oligomer was

synthesised by polycondensation.

The catalytic mechanism of stannous 2-ethyl hexanoate has not been completely

elucidated because the instability of intermediate complexes makes their identification

difficult (Leenslag and Pennings, 1987). However the conversion of stannous 2-ethyl

hexanoate into two more catalytically active species (Figure 49) has been proposed.

Leenslag and Pennings (1987) have suggested a non-ionic mechanism for PLLA

synthesis in which reactive hydroxyl groups supplied by an initiator, attack the lactone

group, open the lactide ring and produce an ester bond and a new hydroxyl group on the

end of the growing chain.

173

Figure 49. Reactive catalytic tin species produced by conversion of stannous 2-ethylhexanoate.

[R = CH(CH$_2$CH$_3$)-(CH$_2$)$_4$-CH$_3$]
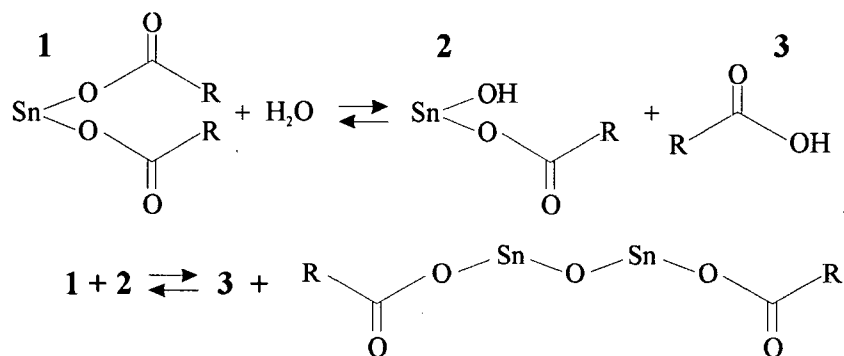
A reaction time for the synthesis of PLLA-SA and PLLA-LA was selected based on reaction times for similar syntheses reported in the literature. When using stannous 2-ethyl hexanoate and dodecanol as an initiator at 150-170°C, the maximum polymer molecular weight was achieved for PCL after less than 5 hours of synthesis (Schindler *et al.*, 1982). Gilding and Reed (1979) have also reported rapid synthesis of PLGA polymers by a similar ring-opening polymerisation mechanism with catalysis by stannous 2-ethyl hexanoate and 96% conversion of monomers after 4 hours at reaction temperatures above 200°C.

Schindler *et al* (1982) stated three conclusions regarding PLLA synthesis: 1) initiation of the reaction occurs rapidly in the presence of tin catalysts, 2) the number of growing chains, determined by the number of hydroxyl groups present, does not change throughout the reaction and 3) reactions between growing chains may occur although the number of growing chains will remain constant. The final conclusion means that M$_w$ may be altered by reactions between chains but M$_n$ will not, thus broadening the molecular weight distribution. Interchain reactions are most commonly "ester

174

interchange" reactions in which a reactive chain end attacks an ester group in another polymer chain rather than the lactone of a L(-)lactide molecule (Saotome and Kodaira, 1968, Schindler et al., 1982). The result is cleavage of the polymer chain and transfer of the ester group to the reactive chain end. In thermal stability studies of PLLA, Jamshidi et al (1988) described several ester interchange reactions that occur at 180°C. In all cases, the number of hydroxyl end groups was conserved. In ring-opening polymer synthesis this means that the reactive hydroxyl groups are preserved and ester interchange does not affect the number of polymer chains or M_n. Ester interchange occurs most readily in the presence of tin catalysts at temperatures above 140°C during polymer synthesis, after greater than 95% conversion has been achieved (Schindler et al., 1982). Selection of a four hour reaction time was made based on the reaction times reported for PLLA (Schindler et al., 1982) and PLGA (Gilding and Reed, 1979) synthesis which gave high degrees of conversion while minimising the potential for ester interchange reactions.

Stearyl alcohol has several characteristics that make it a good initiator. It possesses only a single functional group, is non-volatile and stable at the reaction temperature, and has a monodisperse molecular weight. The L-lactic acid oligomer initiator possesses a carboxylic acid group in addition to its hydroxyl group and thus chain termination reactions may occur via condensation reactions. The oligomer may undergo depolymerisation reactions at the reaction temperature. As well, Karl Fischer analysis of the oligomer showed that greater than 0.5 mole of water was present per mole of oligomer molecules. Schindler et al (1982) noted that hydroxyl groups from water may lower the polymer molecular weight. However this process may not be predictable since some water would be vaporised and less likely to interfere with polymerisation.

5.3. Molecular weight determination

Regression analysis of the data in Figure 19 demonstrates the good correlation between M_n^* values predicted by Equation 15 and M_{GPC} values for PLLA-SA polymers in the molecular weight range of 500-10k g/mol. Thus the molecular weight of PLLA-SA initiated using stearyl alcohol can be controlled by controlling the ratio of monomer to stearyl alcohol used in synthesis (Equation 15). However, the intercept of the regression equation shows that Mn^* values were 1.2k g/mol less than M_{GPC}. Differences in M_{GPC} and M_n^* most likely reflect a broadened molecular weight distribution in which M_{GPC} lies between M_w and M_n. At the lower molecular weights of PLLA-SA, M_{GPC} may differ from Mn^* due to changes in composition of the polymer chains. PLLA-SA polymers may be considered to be "AB" block copolymers with a block of $-CH_2-$ repeating units contributed by stearyl alcohol attached to a block of $-OC(CH_3)CO-$ repeating units contributed by lactic acid. With a total molecular weight of 500 g/mol, each chain would contain approximately 55%w/w $-CH_2-$ repeat units. However, as the molecular weight increases, the contribution of hydrocarbon by weight decreases rapidly so that a 2k g/mol polymer chain would contain only 14%w/w $-CH_2-$ groups. The values of K and a used to calculate $M_{GPC,}$ are derived for homopolymers of PLLA and will not accurately reflect the molecular weight-viscosity relationship for very low molecular weight PLLA with a structure approaching that of a block copolymer. Thus these polymers were referred to by their M_n^* values rather than M_{GPC}.

Values of Mn^* and M_{GPC} were identical for PLLA-LA polymers in the range of 500 to 2k g/mol (Figure 19). The deviation of M_{GPC} from Mn^* above 2k g/mol may have occurred because the properties of the oligomer (water content, presence of an acid group

and polydispersity of molecular weight) make it a poor initiator with respect to molecular weight control for Mn^* greater than 2k g/mol.

Calculation of intrinsic viscosity was accomplished using the approximation method of Solomon and Ciuta (Equation 20). Calculation of M_v from intrinsic viscosity data (Equation 9) required K and a constants from the literature (Schindler and Harper, 1979) which reflect polymer-solvent interactions and are therefore accurate only for a single polymer -solvent combination at a specific temperature. Values of K and a reported by Schindler and Harper are for PLLA in chloroform at 30°C. However, the GPC system used in this work, which also required K and a constants for calibration curves, was operated under ambient conditions. Viscometry experiments demonstrated that within the range of 22 - 30°C, intrinsic viscosities were not changed by more than 2%. Thus the K and a constants were assumed to be valid in this temperature range. M_{GPC} values for commercially obtained polymers were consistently higher but closer to the manufacturer's claimed molecular weight values than the corresponding values of M_v (Table 7). The difference between values of M_{GPC} and M_v may be due to the use of constants from the literature for calculation of M_v (using Equation 23) while values of M_{GPC} were calculated (using Equation 24) from values of intrinsic viscosity.

5.4. Characteristics of microspheres made from 100k g/mol PLLA

Microspheres were manufactured from 100k g/mol PLLA in two size ranges with initial paclitaxel loadings between 0 and 30% to establish the effects of microsphere size and paclitaxel loading on the formation, morphology and thermal properties of PLLA microspheres.

5.4.1. Microsphere size

It is well established that microsphere size can be controlled by altering the stirring speed and polymeric stabilizer (PVA) concentration used in the solvent evaporation manufacturing process (Lin *et al.*, 1985; Mumper and Jay, 1992). Generally, as the stirring rate and aqueous PVA concentration increase, microsphere size is decreased. A faster stirring rate and a higher concentration of PVA both result in an increased shear stress on the organic phase droplets, resulting in the formation of a dispersion with smaller organic phase droplet size. The stirring rate, PVA concentration, the geometry of the vessel which contained the dispersion, and the size and shape and location of the impeller were held constant in the manufacturing of microspheres since all of these parameters can affect microsphere size. Particle size data obtained for 100k g/mol PLLA microspheres, shown in Table 8 and Figure 24, showed that particle size distributions were reproducible between batches made with a given stirring rate and PVA concentration.

The appearance of small shoulder peaks on the upper end of the particle size distribution of paclitaxel loaded microspheres (Figure 24B) was due to aggregation during particle size analysis. It is likely that paclitaxel located on the surface of microsphere resulted in increased interaction between the microspheres, causing aggregation. Another explanation for the aggregation could be the presence of small amounts of PVA on the surface of the microspheres. PVA may have been adosrbed onto the microsphere surface during the manufacturing process and not completely removed by washing with water immediately after the manufacturing process. Aggregation of microspheres as a result of adsorption onto the microsphere surface of poly(vinyl alcohol-

co-vinyl acetate) used as a polymeric stabiliser in the manufacturing process has been observed (Harley *et al.*, 1992).

5.4.2. Solvent evaporation during microsphere manufacture

In the solvent evaporation method of microsphere manufacture, the microspheres form as the polymer matrix precipitates in the organic phase due to the removal of the organic solvent. The rate at which this process occurs depends on the solubility of the polymer in the organic phase and on the rate of solvent removal. Similar solvent removal profiles and values of t_{50} (time for weight loss equal to half the weight of the organic solvent) are expected for microspheres made in a controlled system with a single set of manufacturing parameters. These microspheres would be expected to have reproducible thermal and surface properties since these properties are dependent on solidification during the microsphere formation process (Li *et al.*, 1995b).

The solidification process occurs first on the surface of the organic droplets, forming a "skin" of precipitated material which later forms the surface of the solid microsphere (Li *et al.*, 1995b). Crotts and Park (1995) and Li *et al* (1995a) both reported that in microsphere manufacture, the concentration of dichloromethane in the aqueous phase rises within minutes of beginning manufacture, until it reaches a value close to the saturation solubility of dichloromethane in the aqueous phase. The rapid partitioning of dichloromethane out of the organic droplets in these first minutes results in the onset of precipitation of polymer as the solvent is removed from the surface of the organic phase droplet. This type of behaviour is similar to that observed during the initial evaporation of solvent from cast polymer films (Schwartz and Hicke, 1989). In film casting, the subsequent rate of evaporation is controlled by transport of solvent through the partially

179

solidified skin layer (Young and Chen, 1991). In microsphere formation, the rate controlling process in organic solvent removal is also believed to be transport through the skin layer (Li et al., 1995a).

After the formation of the skin layer on the surface of the organic phase droplet, the solidification process proceeds with continued partitioning of dichloromethane into the aqueous phase. Two mechanisms by which the solidification process occurs in microspheres have been proposed (Li et al., 1995b). The precipitation of the polymer may occur either from the outside of the microsphere towards its centre, beginning with the skin layer and proceeding deeper into the organic phase droplet, or the entire organic phase droplet (except the already solidified skin layer) may solidify at the same rate as the organic solvent is removed. The solidification process is completed when all but trace amounts of the organic solvent have been removed from the microspheres.

The effect of paclitaxel on the solidification of large microspheres was observed as a paclitaxel concentration dependent increase in t_{50} (Table 9). It is hypothesised that the incorporation of paclitaxel into the polymer solution resulted in earlier solidification of the microsphere surface and the formation of a skin less permeable to dichloromethane. Small microspheres had the smallest values of t_{50}. This was due to several factors including shorter diffusion path length for solvent to escape the organic droplets, a higher specific surface area, and the introduction of more air into the dispersion due to more vigorous stirring, compared to large microspheres (Table 9). The introduction of more air into the dispersion by rapid stirring resulted in an increase in the surface area of the aqueous phase/air interface, increasing the rate of evaporation of dichloromethane which had partitioned into the aqueous phase. Despite the effect of

paclitaxel on the permeability of the skin layer, no effect of paclitaxel on the t_{50} of small microspheres was observed. It is likely that the high surface area of microspheres resulted in rapid transport of the dichloromethane from the organic phase and transport across the skin layer was no longer the rate limiting step for solvent removal from the stirring dispersion.

The surface morphology of paclitaxel loaded microspheres of all sizes and loadings showed evidence of dimpling, while control microspheres had a smooth surface. Paclitaxel loaded microspheres manufactured from a blend of isopropyl myristate and PLLA also had a dimpled surface (Wang *et al.*, 1997). However, incorporation of paclitaxel into PLGA (Wang *et al.*, 1996) and PCL (Dordunoo *et al.*, 1995) produced smooth microspheres in both cases.

The surface morphology of microspheres can be influenced by the presence of PVA in the aqueous phase (Kwong *et al.*, 1986) and the solvent evaporation process (Kofler *et al.*, 1996). The transport of solvent molecules through the partially solidified skin layer is believed to result in disruption of this layer, resulting in a surface that exhibits cracks, or irregularly shaped distortions (Kofler *et al.*, 1996). Solvent removal is not expected to result in a dimpled pattern as was observed for the paclitaxel loaded microspheres.

The incorporation of precipitated paclitaxel into the skin layer may result in a different surface morphology than was observed for control microspheres. The deposition of paclitaxel in the superficial layers may be affected by the presence of a polymeric stabiliser. Adsorption of PVA and the incorporation of water in the superficial layers of the forming microsphere may reduce the solubility of paclitaxel in this layer

181

resulting in precipitation of the drug. PVA in solution in the aqueous environment has resulted in the precipitation of other drugs on the surface of PDLLA microspheres (Kwong *et al.*, 1986). The authors studied the transport of insulin from the organic phase into the aqueous phase and its subsequent deposition, mediated by PVA, onto the surface of the forming PDLLA microspheres with the result that the surface layers contained a higher drug concentration than the bulk matrix. Therefore, the regular pattern on the surface is believed to be caused by processes which occur during solidification on the surface as a result of the presence of paclitaxel, and not of disruption of the surface by solvent removal.

Encapsulation efficiency of hydrophobic drugs into microspheres made by the solvent evaporation method is generally very high. Hydrophobic drugs, such as paclitaxel, having a high o/w partition coefficient are generally retained in the organic phase as the microspheres solidify. The total content data in Table 11 are consistent with literature reports of encapsulation efficiencies greater than 90% of initially loaded paclitaxel into PCL (Dordunoo *et al.*, 1995) and PLGA (Wang *et al.*, 1996) microspheres.

5.4.3. Thermal properties of microspheres

The solidification of 100k g/mol PLLA in the microspheres resulted in a semicrystalline polymer matrix with a degree of crystallinity around 40% for all sizes and paclitaxel loadings. The amorphous component of the PLLA matrix showed a Tg that was depressed by the addition of paclitaxel (Table 12). Above Tg, a crystallisation exotherm was observed as the polymer chains gained more mobility and were able to align into a more stable configuration. The crystallisation exotherm was most pronounced for small microspheres. Further heating resulted in melting of the crystalline

182

regions of the polymer matrices. Depression of the Tm indicated that paclitaxel was dissolved in the polymer matrix.

The rate of solvent removal from microspheres can affect the degree of perfection of polymer crystallites and thermal transition temperatures (Izumikawa *et al.*, 1991) and this was observed for PLLA microspheres. Higher values of Tg and Tm were observed for large compared to small control microspheres (Table 12). This is expected when comparing polymer matrices that have solidified at different rates. The larger microspheres had longer t_{50} times for solvent removal meaning they solidified more slowly than the smaller microspheres. Other effects of particle size on polymer thermal properties, such as surface properties of the microspheres, have been ruled out by Izumikawa *et al* (1991). They prepared microspheres using different pressures to achieve slow and rapid solvent removal, and therefore alter solidification rates, while maintaining a particle size range of 44-88 μm.

The effect on Tg of the addition of a drug to a polymer matrix depends on the type of drug-polymer dispersion that results. Mumper and Jay (1992) have summarised the possible states in which a drug may exist within the amorphous matrix: 1) crystalline drug particles are dispersed in the polymer, 2) drug is dissolved (miscible) in the polymer and acts either to stiffen or plasticize polymer chains, or 3) non-crystalline drug is dispersed in the polymer matrix in a separate phase. Cases 1 and 3 represent drug-polymer phase separation in the amorphous regions of the matrix and no effect of drug loading on Tg would be expected. Case 2 represents miscible dispersions in which the polymer chains are stiffened by interactions with the drug molecules or plasticized by interruption of polymer-polymer interactions by the presence of drug molecules. The

183

decrease in Tg observed indicates that amorphous PLLA and paclitaxel form a matrix which may be described as a plasticized miscible system.

Paclitaxel appears to be a more effective plasticizer of the amorphous regions of large 100k g/mol PLLA microspheres that solidify more slowly than smaller microspheres. The absence of an effect of paclitaxel on the Tg in small microspheres could reflect the lower total content of paclitaxel in the matrix (Table 11) or could indicate that the paclitaxel is not completely dissolved in the matrix.

Generally, diluents such as solvent molecules, affect Tg in a manner similar to that of a second polymer blended into the matrix (Kelley and Bueche, 1961). That is, the Tg of the two miscible components is intermediate between the Tgs of the two pure compounds. If this relationship were true for PLLA and paclitaxel, the Tg for the two miscible components would be greater than the Tg of the polymer alone, given the Tg of amorphous paclitaxel of 155°C.

The addition of drugs to polymer matrices may cause an increase or decrease in the polymer Tg depending on the nature of the dispersion which is formed. The addition of many drugs to PDLLA results in a decrease in the Tg of the matrix (Benoit *et al.*, 1986). However, an increase in the Tg of PDLLA by the addition of neurotensin analogue has also been reported (Yamakawa *et al.*, 1992). Both authors describe their observations in a manner similar to the classification of Mumper and Jay (1992). The increase or decrease of Tg is discussed in terms of the drug's ability to enhance or impede segmental motion of polymer chains, representing miscible plasticized or stiffened systems, respectively. It was suggested that the cationic neurotensin analogue resulted in chain stiffening by interactions with the negative partial charges of chain ends on PDLLA

chains while other drugs are believed to disrupt inter-chain interactions, acting as plasticizers.

The effect of paclitaxel on the melting of PLLA matrices was elucidated by thermal analysis of paclitaxel-PLLA dispersions containing between 0 and 60% paclitaxel. This allowed the examination of paclitaxel loadings in PLLA exceeding those which could be achieved by manufacturing microspheres. The melting point depression data for paclitaxel-PLLA dispersions were linear when plotted using Equation 14, which relates the paclitaxel concentration to the degree of melting point depression (Figure 23). The linear relationship indicates that all of the paclitaxel was dissolved in the polymer matrix at all compositions. The limit of miscibility was not determined although it must exceed 60%. At the limit of solubility, the melting point depression would reach a maximum, with no more drug going into solution.

For microspheres, the effect of paclitaxel on Tm was consistent with the effect observed for the paclitaxel-polymer dispersions. The Tm of PLLA was depressed when paclitaxel was incorporated into microspheres. The magnitude of melting point depression increased with increasing total content of paclitaxel. Furthermore, a greater effect was observed for large microspheres which had greater encapsulation efficiency (Table 11) compared with small microspheres.

The phenomenon of melting point depression in polymers by the addition of a second component has been discussed by Nishi and Wang (1975) and Mandelkern (1964a) for the addition of a second polymer and small molecules, respectively. In polymer chemistry, the second component is referred to as a diluent. Melting point depression may arise from altered crystallite morphology i.e. size and perfection, by

185

insertion of diluent molecules into the crystallites (Feughelman *et al.*, 1955). However

this mechanism has been demonstrated for only a few polymer-diluent systems

(Mandelkern, 1993).

More commonly, diluent molecules are dispersed in the amorphous regions of

the matrix. This increases the entropy of the amorphous phase while not affecting the

enthalpy of fusion of crystallites, represented by the enthalpy of fusion of the repeat unit,

Δh. Thus the driving force for melting is increased by the increase in the entropy of

fusion, ΔS_f, and Tm is decreased. This decrease in Tm is illustrated by the relationship

between melting point and diluent concentration proposed by Nishi and Wang (1979),

shown in Equation 14.

$$\frac{1}{Tm_2} - \frac{1}{Tm_2^o} = \frac{R}{\Delta h} \frac{1}{m_1} (1 - \phi_2)$$

Equation 14

In Equation 14, the decrease in Tm of the polymer (Tm_2) is dependent on the diluent

concentration $(1-\phi_2)$ and the enthalpy of fusion of the repeat unit of the polymer (Δh) with

R and the molar volume of the diluent (m_1) being proportionality constants. For diluents

dispersed in the amorphous phase, where the diluent concentration does not affect Δh, the

only variable affecting melting point depression is the diluent concentration. Therefore

plotting the melting point depression data against the diluent concentration using

Equation 14 can be used to describe the nature of the interaction of the diluent and the

polymer. If the relationship is linear then Δh is independent of the diluent concentration

and the drug molecules are dispersed in the amorphous phase of the matrix. If the

relationship is non-linear then Δh varies with the diluent concentration and the drug

molecules are incorporated into the crystalline regions of the polymer matrix affecting the

enthalpy of fusion of the crystallites. The linear relationship in Figure 14 therefore demonstrates that paclitaxel is dispersed in the amorphous phase of PLLA.

5.5.   The effect of PLLA molecular weight on microsphere properties

Although it is generally accepted that the molecular weight of PLLA influences thermal properties (Jamshidi *et al.*, 1988; Engelberg and Kohn, 1991; Celli and Scandola, 1992), the effect of a wide range of molecular weight of PLLA on drug loaded microsphere morphology, resuspendability and drug release profile has not been studied in detail.

5.5.1.   Properties of PLLA-LA and PLLA-SA polymer microspheres

Despite the differences observed in thermal properties when comparing PLLA-SA and PLLA-LA polymers, the XRPD patterns of microspheres made from the two polymers were identical with respect to peak positions (Figures 29A and C, respectively), indicating similar crystal structure in both polymers. The XRPD pattern of stearyl alcohol had peaks that were distinct from all those observed for PLLA microspheres (Figure 29B). These peaks were not observed even in the lowest molecular weight PLLA-SA (compare Figures 29B and A, respectively), indicating that crystallinity in the microspheres due to stearyl alcohol while observed by DSC (Figure 25A and B), was not great enough to be detected by the X-ray diffraction method.

Polymer molecular weight had a profound effect on thermal properties of PLLA-SA microspheres over the range of 1 to 10k g/mol (Figures 25 and 27, respectively). The effect of polymer molecular weight on Tg, described by the Flory-Fox relationship (Equation 10) for PLLA-SA was linear only at molecular weights above 3k g/mol. Thus 3k g/mol represents a critical molecular weight threshold below which the thermal

187

properties change not only as a function of molecular weight but also of the polymer chain composition. The discontinuity in the Tg-molecular weight relationship and the broad range observed for the Tg of PLLA-SA over the 1 to 10k g/mol molecular weight range reflect the rapidly changing composition of the polymer. The presence of a C_{18} hydrocarbon group on the end of each chain due to stearyl alcohol results in a change in the proportion of stearyl alcohol to L-lactic acid as molecular weight increases. This would cause the thermal properties to vary in the same manner as those of copolymers with varying monomer ratios (Grijpma et al., 1990). The Tg of copolymers varies with the copolymer ratio in a manner similar to polymer blends whose Tg varies with blend composition. The dependence of Tg of a copolymer on the copolymer ratio follow the relationships given for polymer blends in Equations 13 with values of copolymer ratios replacing those of blend ratios.

The melting behaviour of PLLA-SA was also affected by changes in molecular weight. The relationship of $1/Tm$ to $1/M_{GPC}$ is expected to be linear when plotted using Equation 12, with the slope of the line being dependent on the enthalpy of fusion for the polymer repeat unit, Δh. Figure 26B shows that for PLLA-SA, the relationship between Tm and molecular weight deviated from linearity as the molecular weight decreased. A change in the slope indicates that Δh was dependent on molecular weight. This could be due to changes in the polymer composition due to changes in the stearyl alcohol:L-lactic acid ratio or due to the increase in the concentration of polymer chain ends, which can affect the structure of crystallites (Wünderlich, 1973).

The surface morphology of PLLA-SA microspheres shown in Figure 28 shows that at a molecular weight around 2k g/mol, spherical microspheres that were not

deformed during the manufacturing process or on storage were obtained. However, the resuspension index data for microspheres indicated that a molecular weight of 4k g/mol was required to form microspheres that did not aggregate (Figure 25). The method of determining the resuspension index for microspheres is a semi-quantitative method of evaluating to what degree microspheres could be dispersed in water after the drying step in the manufacturing process. The method of resuspension was chosen to reflect the manner in which the microspheres would be dispersed in water for further characterisation such as in determining *in vitro* release profiles of paclitaxel. The molecular weight range of 2k to 4k g/mol above which PLLA-SA can form spherical, resuspendable microspheres coincides with a Tg greater than ambient temperature. At temperatures above Tg polymers may become deformed by plastic flow, the rate of deformation being dependent on both temperature and polymer molecular weight (Rosen 1993d). Storage at ambient temperature of PLLA-SA microspheres, which have a Tg below the storage temperature, will therefore allow the polymer microspheres to deform and become aggregated.

In contrast to PLLA-SA, the effect of polymer molecular weight on Tg, described by the Flory-Fox relationship, was linear for PLLA-LA at molecular weights down to 1k g/mol (Figure 26A). These data were consistent with the values of Tg for PLLA polymers with different molecular weights taken from literature sources (Jamshidi *et al.*, 1988; Celli and Scandola, 1992). For PLLA-LA polymers, the effect of molecular weight on Tg described by the Fox-Flory relationship was linear (Figure 26A) since there was no change in the polymer composition with a change in the molecular weight, in contrast to the PLLA-SA polymers. As well, the range of Tg values was not observed to

189

vary over a broad range at low molecular weights as observed for PLLA-SA polymers that had a stearyl alcohol component. The melting temperature of PLLA-LA decreased as the molecular weight decreased. The Tm-molecular weight relationship plotted using Equation 10 shows a deviation from linearity at the lowest molecular weight, similar to the Tm-molecular weight plot for PLLA-SA (Figure 26B). Deviation of Tm from the linear relationship with molecular weight is expected even for polymers with homogeneous composition because of the increase in the concentration of chain-ends. A higher concentration of chain-ends affects crystallite stability and free volume in the matrix, resulting in a lowered Tm (Wünderlich, 1973).

Based on the properties of microsphere morphology and resuspendability, 2k g/mol PLLA-LA was identified as the lowest molecular weight polymer that could be used to manufacture paclitaxel loaded microspheres. PLLA-LA was selected over PLLA-SA because of its simpler structure, having no stearyl alcohol component, and because the minimum molecular weight required to achieve resuspension of microspheres was higher for PLLA-SA.

5.5.2. Properties of paclitaxel loaded microspheres

Paclitaxel loaded microspheres made from PLLA polymers with molecular weights of 2k to 10k g/mol (Figure 32A) had smooth surfaces as did control microspheres. This is in contrast to the dimpled morphology of 100k g/mol PLLA paclitaxel loaded microspheres (Figure 32D). The difference may be explained by the differences in hydrophilicity of the polymers. Jalil and Nixon (1990) have suggested that polymers with different molecular weights precipitate from a given solvent at different rates based on differences in their hydrophobicity. The deposition of the polymer and

190

drug in the surface layers of the forming microsphere could also be affected by differences in their solubilities in the organic solvent. Chang *et al* (1986) formed microspheres from a blend of PCL and the more hydrophilic cellulose propionate and observed changes in morphology due to differences in hydrophilicity of the two polymers in the blend. Microspheres manufactured from PCL alone had a "orange peel texture" while the addition of the cellulose polymer, having a different solubility in dichloromethane compared to PCL, resulted in smoother microspheres. It is possible that the more hydrophilic low molecular weight polymers solidify prior to paclitaxel due to their relatively lower dichloromethane solubility. The increased hydrophilicity in the surface layer could also allow more PVA to become incorporated into the outer skin of forming microspheres thus altering their morphology.

The total content of paclitaxel in microspheres was influenced by the molecular weight of PLLA-LA. At lower molecular weights, greater than 100% of the expected amount of paclitaxel was incorporated into the polymer. This occurred due to less efficient incorporation of the polymer than of the paclitaxel into the matrix. Less efficient incorporation of polymer than paclitaxel may be expected given the relative hydrophilicity of each component.

Weight loss data indicated that approximately one third of the 1k g/mol PLLA-LA was water soluble. The 1k g/mol PLLA is more hydrophilic than paclitaxel and therefore there is less complete retention of PLLA in the organic phase during microsphere formation compared to paclitaxel. Mumper and Jay (1992) encountered a similar loss of low molecular weight PLLA in the manufacture of microspheres. As expected, the effect of incomplete polymer incorporation decreased with increasing

polymer molecular weight (see Table 13) and a corresponding decrease in hydrophilicity. The effect of incomplete incorporation of a low molecular weight polymer into microspheres has been characterised semi-quantitatively by Grandfils *et al* (1996) by measuring relative GPC peak areas for a polymer blend of low and high molecular weight PDLLA incorporated into microspheres. Based on GPC analysis of the water soluble fraction of low molecular weight PDLLA, the highest molecular weight that dissolved in water was found to be approximately 650 g/mol. In order to eliminate this phenomenon, isopropyl alcohol has been incorporated into the organic phase to more rapidly precipitate the low molecular weight components present (Wichert and Rohdewald, 1990).

5.5.3. *In vitro* paclitaxel release from microspheres

Throughout the *in vitro* release studies, sampling intervals were selected to maintain sink conditions, meaning the concentration of paclitaxel in the release media did not exceed 15% of its aqueous solubility (Carstensen, 1977). However, because of the initial rapid phase of release observed in all release studies performed on paclitaxel loaded microspheres, sink conditions could not be maintained in the first three days of the study despite sampling four times in the first day. If sink conditions could have been maintained, a greater amount of paclitaxel would be expected to be released over this time period. However, this would not be expected to alter the cumulative amount released in the course of the entire study.

The test tubes used for the release studies were tumbled end over end in order to maintain the microspheres in suspension in the release media. Tumbling of the tubes also allows more rapid diffusion of paclitaxel away from the microspheres as it is released, by

decreasing the thickness of the stagnant layer of paclitaxel in solution that surrounds each microsphere.

In vitro paclitaxel release profiles from microspheres made from PLLA polymers with molecular weights ranging from 2 to 50k g/mol (Figure 30) show that the rate and extent of release are dependent on polymer molecular weight. This finding is consistent with the work of Heya et al. (1991) and Omelczuk and McGinity (1992) who showed that a decrease in polymer molecular weight increased the rate and extent of drug release from PDLLA matrices.

There was an initial rapid phase of paclitaxel release for the 2k and 4k g/mol PLLA microspheres due to dissolution of drug near or on the surface of the microspheres. Surface associated paclitaxel could include the paclitaxel that was incorporated into the skin layer during the microsphere formation process. The rapid initial phase was followed by a slower phase of release likely controlled by a combination of drug diffusion and polymer degradation. This was substantiated by the scanning electron micrograph evidence of erosion of the 2k g/mol PLLA microspheres by day five of incubation in PBS-A (Figure 32A-C). In contrast, the 10k and 50k g/mol PLLA microspheres released paclitaxel much more slowly. The initial release of surface associated paclitaxel from the 10k and 50k g/mol PLLA microspheres was slower than was observed from the lower molecular weight formulations. The second phase of release was also much slower than for the lower molecular weight formulations. It was not accompanied by erosion of the matrix, indicating that the major factor contributing to release was diffusion of paclitaxel through the matrix rather than erosion. Therefore the degree to which polymer degradation accounts for paclitaxel release from the

microspheres depends on the molecular weight of PLLA used, with erosion of the matrix occurring only at lower molecular weights of 2k and 4k g/mol for PLLA.

Lowering the molecular weight can have several effects on the microspheres that result in greater erosion of the matrix. As the molecular weight is decreased, the matrix becomes more hydrophilic due to the increased concentration of hydroxyl and carboxyl end groups. This allows water to penetrate the polymer matrix more easily, giving more rapid polymer degradation and loss of mechanical strength. Tg can also be decreased by water uptake as the polymer matrix becomes plasticized by the water. As the Tg of the polymer is decreased below the incubation temperature of 37°C the polymer becomes softer and may undergo deformation which will increase the rate of erosion of the matrix. Decreasing the molecular weight will also result in a decrease in polymer crystallinity and mechanical strength, resulting in greater erosion of the matrix.

The *in vitro* release of paclitaxel from 100k g/mol PLLA microspheres was characterised by an initial rapid phase of release, a phase of apparently zero order release between days 3 and 14, followed by a gradual decrease in the rate of release from day 14 to 30. The linear phase was observed for all formulations except for the 35-105 μm 20% loaded microspheres which showed a discontinuity in the slope on day 12 of the study.

The initial rapid phase is likely due to surface associated paclitaxel that is readily dissolved at the beginning of the release study. The apparently-zero order phase of release is not consistent with the diffusion controlled kinetics described by Equations 5 and 6 (Baker, 1987), which relate the cumulative amount of drug released by diffusion from a one phase spherical matrix to time. For a drug-polymer matrix, where the drug concentration is not saturated the release rate should decrease with time, having a profile

of the shape shown by Curve A in Figure 2. The existence of different phases of release such as the burst phase, a linear phase and a slower phase after day 14 indicated that the release mechanism was not simple diffusion.

Scanning electron micrographs of 100k g/mol PLLA microspheres showed no signs of erosion that would indicate an erosion controlled mechanism of release. In a linear release profile, one or more of the parameters governing release are changing in a manner that tends to increase release rates, off-setting the expected gradual decrease in the rate over time for diffusion controlled systems (Curve A, Figure 2). These parameters are the diffusion path length and the diffusion coefficient. For matrices that do not erode during the release of the drug, such as 100k g/mol PLLA microspheres, the diffusion path length would be expected to remain constant. However the matrix may not have had a homogeneous distribution of paclitaxel, and this would contribute to the deviation of the release kinetics from the predicted form. Polymer crystallinity, which was demonstrated by DSC and XRPD (Table 12 and Figure 29D, respectively) may have contributed to the heterogeneity of the matrix and resulted in a slowing in the rate of release after day 14 (Figure 31). Polymer crystallites themselves may not be distributed in a homogeneous manner in light of the fact that the superficial "skin" layer is believed to solidify at a much greater rate than the microsphere core. The transport of paclitaxel molecules may have been restricted by surrounding polymer crystallites and therefore the diffusion path length for paclitaxel molecules would differ depending on the distribution of crystallites throughout the microspheres.

However, the diffusion coefficient may increase over the course of the release studies due to uptake of water into the matrix and cleavage of polymer chains prior to the

onset of erosion. The degradation process was not characterised for the PLLA microspheres. However, it has been demonstrated that polyesters undergo chain cleavage prior to the onset of weight loss of the polymer matrix due to erosion (Makino *et al.*, 1985; Lam *et al.*, 1994). The deviation of the release profiles from those predicted for monolithic solutions of drugs in a microsphere (Curve A, Figure 2) is due to a combination of several factors including crystallinity and degradation of the polymer chains.

Microsphere size had an effect on the extent of paclitaxel release from the microspheres. The initial phase of release of surface associated drug would be expected to be dependent on the specific surface area of the microspheres (Cowsar *et al.*, 1985) and diffusion controlled release would be expected to be inversely proportional to the diffusional path length of the drug in the matrix, described by the square of the radius of the microspheres (Equations 5 and 6). Thus for both the initial phase and phases that are at least partly diffusion controlled, greater release is expected from smaller microspheres.

Paclitaxel loading levels also affect the rate and extent of paclitaxel release. The value of V_0 was increased with higher loading levels likely due to a higher concentration of drug that can readily dissolve in the release medium. Increased drug concentrations in microsphere surfaces have been observed for cisplatin incorporated into PDLLA microspheres (Spenlehauer *et al.*, 1986). Paclitaxel was also released to a greater extent at higher loading levels. According to the kinetics described for diffusion controlled release from a sphere by Baker (1987) (Equations 5 and 6), the amount of drug released at any given time (M_t) increases directly proportionaly to the total drug loading (M_0).

Profiles of drug release from PLLA and PDLLA microspheres have been obtained for etoposide (Kishida *et al.*, 1990), and 5-fluorouracil (Ciftci *et al.*, 1994). These delivery systems demonstrated the same mechanisms of release observed for the paclitaxel loaded microspheres. The initial phase of rapid release was explained as a "burst effect" in which some drug is present on the surface of the microspheres and is released by dissolution (Langer, 1980). The subsequent slower phase of release was ascribed to diffusion of the drug through the matrix. For etoposide loaded PLLA microspheres there was a linear phase of release (Kishida et al., 1990), indicating that diffusion is not the only mechanism by which etoposide is released from PLLA. However, for 5-fluorouracil loaded microspheres, release followed more closely the profile of diffusion controlled release for spherical matrices (Ciftci *et al.*, 1994). For all of these studies, which measured release in a range of over several hours to several weeks, no evidence of microsphere erosion was reported over the course of the release studies.

The total amount of paclitaxel released from 100 g/mol PLLA microsphere represented between 23 and 92% of the total paclitaxel content of microspheres (Table 14). Therefore a substantial amount of paclitaxel remained within the matrix after the burst and linear phases of release. It is expected that the remaining paclitaxel would slowly be released until the polymer matrix was completely eroded. An identical study was carried out for sixty days and showed a similar pattern up to day thirty and continued slow release over the next thirty days, indicating that erosion controlled release will not occur in these formulations for at least two months. This was consistent with SEM data showing that 100k g/mol PLLA microspheres remained intact after seventy days in PBS-

A (Figure 32D-F). An onset of erosion greater than seventy days for 100k g/mol PLLA is consistent with degradation patterns for PLLA reported in the literature (Reed and Gilding, 1981; Migliaresi *et al.*, 1994) due to the hydrophobic and semicrystalline nature of the polymer and its high molecular weight.

5.6. The effect of polymer blending

The main purpose of polymer blending in drug delivery systems research has been to alter the biodegradation or drug release profiles of drug delivery systems (Grandfils *et al.*, 1996; Yeh *et al.*, 1995). PLLA polymers with molecular weights of 8k and 82k g/mol have been blended to manufacture films with increased biodegradation and erosion rates (von Recum *et al.*, 1995). However, the use of blends of high and very low molecular weights of PLLA (e.g. 1k and 2k g/mol) to modify the drug release profiles from microspheres have not been reported.

Two blend systems have been compared, one containing 1k and 100k g/mol PLLA and the other 2k and 50k g/mol PLLA. The properties of the two high molecular weight polymers (50k and 100k g/mol) used in this work were similar with respect to thermal properties and their ability to form microspheres. However, the 1k and 2k g/mol polymers were different from each other, having different values of Tg, Tc and Tm (Figures 27C and 33C, respectively).

5.6.1. 2k and 50k g/mol PLLA-PS polyblends

The first blend system studied contained varying proportions of 2k and 50k g/mol PLLA-PS. The yield of microspheres increased as the proportion of 50k g/mol PLLA-PS increased in a blend of the two polymers because the incorporation of PLLA into microspheres varied at different blend compositions. The more hydrophilic 2k g/mol

198

PLLA would be expected to be less efficiently retained than the 50k g/mol polymer due to partitioning of the polymer into the aqueous phase. Microspheres with a high proportion of the more hydrophilic polymer in the blend would therefore have less efficient polymer retention and a lower yield.

Values of Tg obtained by DSC for both 2k and 50k g/mol PLLA varied with the heating rate. The linear relationship of the inverse of Tg to the logarithm of heating rate described by Barton (1968) (Equation 27) gives a slope equal to the apparent activation energy (Ea) of the glass transition. This is the amount of energy a polymer chain must gain in order to undergo the glass transition (Clarke and Braden, 1989). Values of Ea of the glass transition for 2k and 50k g/mol PLLA-PS of about 200 kJ/mol were obtained. Celli and Scandola (1991) determined the Ea of PLLA to be 420 kJ/mol using a mechanical testing method and the polymer molecular weight was not specified. Values of Ea for the Tg of PLLA-PS polymers were close to one another despite the difference in molecular weight of the two polymers. The onset of segmental mobility which occurs at Tg involves only 20-30 backbone atoms (Grulke, 1994). This represents only one fifth of the length of the polymer chain for 2k g/mol PLLA and most segmental motion would not involve the chain ends. Therefore the molecular weight would not be expected to greatly affect the Ea.

A single glass transition observed between 52 and 62°C (Figures 33 and 34A) for all 2k/50k g/mol polymer blends indicated that the polymers were miscible. The Tg values were close to those calculated for theoretically miscible polymers using the Fox equation (Equation 13) although they were consistently higher by 1-2°C. Grandfils et al (1996) observed a deviation of Tg values from the Fox equation for microspheres made

from blends of 65k and 3.5k g/mol PDLLA. The authors noted that the observed Tg approached those calculated by the Fox equation for miscible polymers after repeated heating to 50°C above Tg and quench cooling. They suggested that the two polymers experienced a small amount of phase separation during the microsphere manufacturing process and that thermal treatment resulted in a more homogeneous blend. Phase separation of two polymers during the microsphere formation process has also been demonstrated for cellulose and PCL (Chang $et\ al.$, 1986). The authors speculated that phase separation occurred because differences in the solubility of two polymers in the organic solvent resulted in different rates of precipitation for each polymer. The 2k g/mol PLLA would be expected to be more hydrophilic due to a higher number of polar chain ends compared to 50k g/mol PLLA and therefore should have a lower solubility in the dichloromethane than 50k g/mol PLLA. The different solubilities of the two PLLA polymers could therefore result in a small amount of phase separation during the formation of microspheres. This would be consistent with the observed deviation of Tg from the values calculated using the Fox equation.

The composition of the 2k/50k g/mol blends affected the area of the endothermic peak that coincided with the Tg in the microspheres (Figure 33 and 34A). This peak was attributed to enthalpy relaxation at Tg, which has been reported for other PLLA polymers (Celli and Scanodla, 1992). The magnitude of ΔH_r was greater for 2k g/mol than for 50k g/mol PLLA-PS and was intermediate for the blends. Grandfils $et\ al$ (1996) also observed that enthalpy relaxation was a molecular weight dependent phenomenon. The authors observed enthalpy relaxation in 3.5k g/mol PDLLA microspheres that was not observed in 65k g/mol PDLLA microspheres.

Enthalpy relaxation may occur upon heating a polymer through its Tg. Below Tg the polymer chains may relax by undergoing short range motion and becoming ordered over the range of a few monomer units of polymer chains. The region of order is not large enough to be considered crystalline and has been termed "microstructure" in the amorphous phase (Bodmeier et al., 1989). Upon heating through Tg, an enthalpy of relaxation is observed because energy is required to overcome the short-range order established through relaxation. Microstructure in amorphous materials can arise in polymers as they are precipitated from solution (Bodmeier et al., 1989) or upon ageing of materials solidified by cooling from a molten state (Hancock et al., 1995). The microstructure that arises during precipitation is formed rapidly as the material solidifies. In contrast, microstructure in materials solidified from a melt is formed slowly after storage at temperatures below the Tg.

For PLLA microspheres, enthalpy relaxation could be observed by DSC (Figure 33) shortly after manufacture. The microstructure present in the amorphous regions of the polymer matrix is likely, at least in part, to have been formed during the manufacturing process. Furthermore, measurements of ΔH_r for PLLA-PS were similar when obtained one week or two years after the manufacture of microsphere for both 2k and 50k g/mol molecular weights. Paclitaxel loaded PLLA microspheres were stored 35 to 40°C below Tg. Hancock et al. (1995) demonstrated that the storage temperature relative to Tg greatly affected the extent to which enthalpy relaxation peaks were observed by DSC for amorphous sucrose and indomethacin. Hancock et al. (1995) suggested that the process could take several months to go to completion if amorphous materials are held 16-47°C below Tg .

Recrystallisation was observed by DSC when 2k and 50k g/mol PLLA-PS blend microspheres were heated above Tg. The Tc decreased as the proportion of 2k g/mol polymer increased in the blend. Both the Tc and Tg decreased approximately 7°C as the proportion of 2k g/mol polymer increased from 0 to 100%. The value of Tc was approximately 35°C above the Tg for all blend compositions. Nijenhuis *et al.* (1996) also noted that for polymer blends of PLLA with PEG, the Tc of PLLA decreased with a decrease in the Tg so that Tc was always approximately 45°C above the Tg. As the Tg is lowered, the mobility of the polymer chains is increased at any given temperature above Tg and recrystallisation becomes possible at lower temperatures.

The melting of 2k and 50k g/mol PLLA-PS blends occurred at temperatures that were dependent on the blend composition. Values of Tm were highest for 50k g/mol PLLA-PS microspheres and were lowered as the proportion of 2k g/mol PLLA-PS in the blend increased. Double melting endotherms were observed in the DSC thermograms of 80/20 2k/50k g/mol PLLA-PS microspheres (Figure 33D). Melting point depression data also confirmed that 2k and 50k g/mol PLLA-PS were miscible (Figure 34B and 38). However, the relationship between blend composition and melting point depression was non-linear when the data were plotted using Equation 14 (Figure 38). A non-linear relationship between melting point depression and blend composition plotted using Equation 14 means that Δh, the enthalpy of fusion per repeating unit, varies with blend composition. A change in Δh with an increase in the proportion of 2k g/mol PLLA-PS is likely due to an increasing number of chain ends in the blend (Wünderlich, 1973). The presence of an increased number of chain ends with the addition of 2k g/mol PLLA-PS could result in more chain ends being included in crystallites, altering their surface free

energy and thereby affecting their melting temperature. A non-linear relationship between melting point depression and blend composition for data plotted using Equation 14 has also been noted for 8k and 82k g/mol PLLA blends (von Recum *et al.*, 1995). Optical microscopy of these blends showed that two different types of crystallites were present. The crystallites were termed "small" and "large" and were attributed to crystallites that were rich in 8k and 82k g/mol PLLA chains, respectively. It is therefore possible that the chains in the 2k/50k g/mol PLLA-PS blends do not completely mix in the crystallites formed in microspheres. The formation of crystallites rich in 2k and 50k g/mol PLLA-PS could be responsible for the double melting endotherm observed for blends in Figure 33. Crystallites with more 2k than 50k g/mol PLLA-PS would have a lower Tm than those containing proportionately more 50k g/mol PLLA-PS.

5.6.2. 100k and 1k g/mol PLLA polyblends

The second polymer blend system studied was various compositions of 1k g/mol PLLA-LA and commercially obtained 100k g/mol PLLA. Blends of 1k g/mol PLLA-LA and 100k g/mol PLLA had thermal properties that were similar in many respects to those of the 2k/50k g/mol PLLA-PS blends. As with the 2k/50k g/mol polymer blends, a single Tg was observed for the 1k/100k g/mol PLLA blends, indicating polymer miscibility.

An increase in ΔH_r and a decrease in polymer crystallinity were observed with an increase in the proportion of the low molecular weight component (Figure 36A and B, respectively), that were similar to those observed for the 2k/50k g/mol polymer blends. However, in contrast to the 2k/50k g/mol polymer blends, the relationship between the melting point depression data and blend composition was linear when plotted using Equation 14 (Figure 38). Thus Δh, which is proportional to the slope of the linear

melting point depression-molecular weight relationship, was not affected by the addition of 1k g/mol PLLA-LA to the higher molecular weight 100k g/mol polymer. Martinez-Salazar *et al* (1996) observed that addition of paraffin to polyethylene gave a melting point depression that varied with blend composition in the same manner observed for the 1k/100k g/mol PLLA blends. The short chains of the paraffin were too small to be incorporated into the polymer crystallites and did not affect Δh. It is suggested that in the molecular weight range of 1k to 2k g/mol, the polymer crystallisation behaviour of PLLA changes and PLLA with a molecular weight of 2k g/mol is incorporated into crystallites that contain higher molecular weight PLLA whereas 1k g/mol PLLA is not.

Blends containing either 1k or 2k g/mol PLLA as the low molecular weight component also had different resuspension properties. Whereas the 2k/50k g/mol polymer blend microspheres were all freely resuspendable in water after drying, the proportion of 1k g/mol PLLA-LA in the blend affected the resuspension index of the 1k/100k g/mol blend microspheres. The differences in resuspension properties coincided with changes in the surface morphology (Figure 35) of the microspheres.

The 1k/100k g/mol polymer blend with 60% low molecular weight component (PB60) was chosen for further characterisation in order to maximise the amount of low molecular weight material that could be used to formulate spherical, resuspendable microspheres (Figure 35B). A similar ratio was reported for a blend of 2k and 120k g/mol PDLLA used to make microspheres. A blend containing up to 75% of the 2k g/mol PDDLA could be used to manufacture intact microspheres (Bodmeier *et al.*, 1989). The same limit was observed when blending 3.5k and 65k g/mol PDLLA (Grandfils *et al.*, 1996). By maximising the amount of low molecular weight component it was

expected that paclitaxel microspheres could be manufactured which would have significantly different properties compared to 100k g/mol PLLA microspheres.

5.6.3. Properties of paclitaxel loaded PB60 microspheres

Paclitaxel loading did not affect the surface properties of PB60 microspheres, and all PB60 microspheres had smooth surfaces. The smooth surfaces were similar to those observed for microspheres made from PLLA with molecular weights of less than 10k g/mol.

The encapsulation efficiencies of paclitaxel in PB60 microspheres were in the range of 79 to 128% of the expected value compared to a range of 51 to 97% for 100k g/mol PLLA microspheres. The total content was therefore higher for PB60 microspheres. The higher than expected total content can be explained by incomplete incorporation of the 1k g/mol PLLA-LA, as observed previously for other low molecular weight PLLA microspheres (Table 13).

The addition of paclitaxel to PB60 blend microspheres had different effects on the thermal properties of the polymer matrix than were observed for microspheres made from 100k g/mol PLLA. The addition of paclitaxel to PB60 microspheres resulted in an increase in Tg. Thus according to the classification system of Mumper and Jay (1992) for drug-polymer dispersions, this system is described by a Case 2 miscible dispersion, where the paclitaxel acts to restrict the motion of amorphous polymer chains through interactions such as hydrogen bonding. Paclitaxel may have more interaction with the polymer chains through hydrogen bonding due to the fifty to sixty-fold increase in the number of hydroxyl and carboxyl groups contributed by the chain ends of the 1k g/mol PLLA-LA. The addition of a neurotensin analogue to PDLLA resulted in a 12 °C

increase in the polymer Tg due to an interaction between the drug and polymer (Yamakawa *et al.*, 1992). In the PDLLA-neurotensin analogue dispersion, an increase in the activation energy of the glass transition was observed compared to in the PDLLA matrix alone and it was hypothesised that ionic interactions existed between the cationic drug and the polymer chains.

An increase in the Tc of PLLA was observed after the addition of paclitaxel to the microspheres (Figure 40). This is consistent with paclitaxel being dispersed in the amorphous phase and acting as a diluent molecule in the polymer matrix. The presence of a diluent is known to slow the recrystallisation process (Mandelkern, 1964b). For recrystallisation observed at a constant heating rate, a slower recrystallisation process will be observed at a higher temperature than would a faster recrystallisation process. Interactions between paclitaxel and the 1k and 100k g/mol PLLA, such as hydrogen bonding with polymer chain ends, could have contributed to the greater than 20°C increase in Tc of the blend (Figure 40) compared to the 2-6°C increase in Tc for 100k g/mol PLLA microspheres. Hydrogen bonding between paclitaxel molecules and polymer chains would be expected to reduce the rate of polymer chain diffusion through the amorphous regions of the polymer matrix as they migrate towards growing crystallites in the matrix. Furthermore, with respect to crystallites, the 1k g/mol PLLA-LA component acts as a diluent molecule and may not be incorporated into crystallites of the 100k g/mol PLLA. Therefore, the 1k g/mol PLLA chains will dilute the amorphous regions of the polymer matrix and decrease the diffusion rate of higher molecular weight chains towards the growing surface of crystallites.

As observed for 100k g/mol PLLA microspheres, addition of paclitaxel to PB60 microspheres resulted in a depression of Tm. Melting point depression of the polymer provides further evidence for miscibility of paclitaxel in the PB60 matrix. A double melting endotherm was observed when paclitaxel was incorporated into the PB60 matrix that was not observed for control microspheres. It is possible that paclitaxel in the amorphous phase, which resulted in a delay in Tc and a broadening of the recrystallisation exotherm, may also have altered the mechanism of crystallisation so as to produce less perfect polymer crystallites with a lowered Tm (Mandelkern, 1964b). If less perfect crystallites are present in the polymer matrix, they will melt at a lower Tm, and subsequently recrystallise as more perfect crystallites with a higher Tm. These more perfect crystallites melt again at the higher Tm giving rise to the double endotherm. This hypothesis was supported by observing only a single melting endotherm by DSC at a fast heating rate of 40 °C/min. At faster heating rates, the imperfect crystallites melt but do not have time to recrystallise to form more perfect crystallites before the temperature rises above the equilibrium melting temperature of the polymer. This explanation is more likely than the explanation of two different types of crystalline regions containing 1k and 100k g/mol PLLA, respectively. According to Figure 36B, the degree of crystallinity for the 1k g/mol PLLA-LA alone was almost zero. Thus the 1k g/mol PLLA-LA chains excluded from the crystallising polymer in the PB60 blends are not believed to recrystallise on their own to form a second type of crystallite, one rich in 1k g/mol PLLA-LA chains.

In vitro paclitaxel release from microspheres was modulated by the addition of 1k g/mol PLLA to the polymer matrix. The initial rate of release of paclitaxel (V_0) was

greater from microspheres manufactured from 100k g/mol PLLA alone than from PB60 microspheres, when comparing microspheres of similar sizes and loadings. Differences in the surface properties of the microspheres, which may reflect differences in the deposition of paclitaxel in the surface of microspheres during their manufacture likely contributed to the differences in V_0. The amount of paclitaxel released from both 100k g/mol PLLA and PB60 microspheres were similar after fourteen to twenty one days, when comparing similar sizes and loading levels. The greatest difference in the release profiles was observed after day twenty one of the study where an increase in the rate of release from PB60 microspheres (Figure 41) coincided with the onset of erosion of the matrix (Figure 42).

Thomas *et al* (1997) blended low and high molecular weight anhydrides and prepared microspheres loaded with one of two model compounds, *p*-nitrophenol and lysozyme. Blending did not alter release of the low molecular weight compound, *p*-nitrophenol, compared to release from the high molecular weight polyanhydride alone. *p*-Nitrophenol was released predominately by a diffusion controlled mechanism. However, the rate of lysozyme release, which depended on the erosion of the matrix, was increased by the addition of a lower molecular weight polymer. Blend composition has been observed to affect the onset of weight loss for matrices containing 65k and 3.5k g/mol PDLLA (Grandfils *et al.*, 1996) which were exposed to *in vitro* buffered systems. Addition of the lower molecular weight polymer increased water uptake into the matrix resulting in hydrolysis of the polymer. Diffusion of the degraded low molecular weight polymer components out of the polymer matrix resulted in weight loss (Grandfils *et al.*, 1996). A blend composition of 25% 3.5k g/mol polymer resulted in a 100% weight gain

due to water uptake compared to less than 5% for the high molecular weight PDLLA alone. More rapid degradation and erosion of the polymer matrix corresponded to an increased release of a leutinizing hormone releasing hormone agonist from an implant made of a blend of 1.4 and 11k g/mol molecular weight PDLLA (Asano *et al.*, 1991). As the blend composition of 1.4k g/mol PDLLA was increased from 0 to 100%, the weight loss over five weeks due to erosion of the implant increased from 0 to 100% and the time for release of all of the incorporated drug was decreased from twenty to five weeks.

5.7.   *In vivo* evaluation of microspheres

In vivo studies using control and paclitaxel loaded microspheres had two objectives. The first was to characterise the effects of microsphere size and of peritoneal insufflation on the clearance of microspheres from the peritoneum. The second was to establish the efficacy of 30% paclitaxel loaded 100k g/mol PLLA microspheres in preventing tumour cell growth following a simulated tumour cell spill. Microspheres made from 100k g/mol PLLA were selected for *in vivo* evaluation because they were well characterised with respect to morphology, total paclitaxel content and release properties at the time studies in the rat models were begun. *In vitro* release profiles from PB60 microspheres were undetermined at this time and therefore no basis for dosing the PB60 formulation was available, thus they were not evaluated *in vivo*.

5.7.1.   Clearance of microspheres from the peritoneum

Microspheres used to study clearance from the peritoneal cavity were in the size range of 1 to 40 μm with greater than 98% of the total dose of microspheres being less than 30 μm in diameter (Table 19). From the microsphere size data collected for

microspheres observed in the lymph nodes of rats (Table 19 and Figure 43) two inferences were made.

First, the maximum diameter of microsphere that was observed in the lymph tissue reflects the largest diameter of fenestrations in the diaphragm. The 98th percentile diameter indicates that most of the fenestrations are smaller than the maximum diameter of microsphere observed in the lymph nodes (Table 19). Not all of the fenestrations are the same size and the particle size distribution data reflect a diameter distribution for fenestrations of the diaphragm which lead to the lymph nodes. Allen and Weatherford (1959) also reported that particles recovered from the lymph tissue of rats after intraperitoneal administration had a distribution of sizes reflective of different sized fenestrations. Tissue sections of the basement membrane of the diaphragm of mice showed that the fenestrations might be as large as 17 μm, with the majority being in the range of 2 to 6 μm. The authors speculated that a similar situation exists for rats except the size ranges would be larger by 5-10 μm.

The second inference is that insufflation of the peritoneum does not alter the fenestrations in a manner which affects the clearance of PLLA microspheres from the peritoneum through the fenestrations. This was not expected because earlier reports have suggested that fenestration may become deformed, or stretched by insufflation (Abu-Hijleh et al., 1995) and it has been hypothesised that stretching the fenestrations could affect the transport of microspheres through them. The effects of insufflation on the fenestrations of the diaphragm and on clearance of particles from the peritoneum are of particular interest because insufflation is commonly used in laparoscopic procedures for cancer treatment.

5.7.2. Efficacy of paclitaxel loaded microspheres in a model of intraperitoneal carcinomatosis

5.7.2.1. Dose escalation study

Implantation of tumours in the peritoneum resulting in intraperitoneal carcinomatosis is a recognised complication of laparoscopic surgical intervention for the treatment of gastrointestinal cancers (Jacquet *et al.*, 1995). There have been numerous reports of tumour seeding throughout the peritoneum and especially at the incision site (Johnstone *et al.*, 1996). The small incision may make effective irrigation more difficult and conditions in laparoscopic surgery such as a closed peritoneum and insufflation may increase the potential for tumour implantation (Clair *et al.*, 1993, Thomas *et al.*, 1996). Therefore, post-surgical adjunctive chemotherapy has been employed in these cases (Atiq *et al.*, 1993, Jacquet *et al.*, 1995). This model was chosen to reflect the widespread dissemination of tumour cells that can result in intraperitoneal carcinomatosis.

The model demonstrated the effectiveness of paclitaxel loaded microspheres at preventing tumour implantation of 9L glioblastoma cells. This cell line was selected because it grows very rapidly and it has a demonstrated sensitivity to paclitaxel in cell culture studies (Cahan *et al.*, 1994)). In control animals, the tumour cells implanted in the abdominal wall, omentum and on other organs within the peritoneum (Figure 44A and B). Therefore the characteristics of implantation were similar to those observed clinically (Jacquet *et al.*, 1995). A drawback of using the 9L glioblastoma cells is that neural tumour cells do not represent the type of cancer cells that would commonly be present clinically in gastrointestinal and ovarian cancers. However, neuronal blastomas

have been observed in the peritoneum (Lamki et al., 1989) and a case of peritoneal seeding has been reported (Fernbach, 1993).

The dose escalation study demonstrated that a 100 mg dose of 35-105 μm 30% paclitaxel loaded microspheres, given immediately post-operatively, was sufficient to prevent seeding of the peritoneum by tumour cells after a large tumour cell spill in a model of laparoscopic surgery without insufflation (Table 20). A 100 mg dose of microspheres is equivalent to a total dose of paclitaxel to the animals of approximately 75 mg/kg. Based on the in vitro release studies, a 100 mg dose of 30% paclitaxel loaded 100k g/mol PLLA microspheres (Figure 31C) would release approximately 15 mg/kg into the peritoneal cavity of rats over fourteen days. Of the 15 mg/kg, almost 5 mg/kg would be released in the first 24 hours after administration of the microspheres. These values assume that the in vivo release of paclitaxel in rats correlated with the in vitro paclitaxel release profiles for 100k g/mol PLLA microspheres (Figure 31C). However, no studies were conducted to characterise the correlation of in vitro and in vivo release.

The total dose administered to rats in this study was approximately 60 to 85 mg/kg, based on rat weights of 350 to 500 g. This dose is nearly an order of magnitude greater than the values of the MTD reported in human trials using Taxol[®]. In the human trials, the maximum tolerated dose (MTD) of paclitaxel depended on the time period over which the dose is administered. Generally a longer infusion time resulted in a lower MTD. In Phase I human trials using paclitaxel formulated as Taxol[®], MTDs were 250 and 140 mg/m^2 of paclitaxel given as a three hour or seven day continuous intravenous infusion, respectively (Lilenbaum et al., 1998; Soulie et al., 1997). These MTD values correspond to doses of 10 and 5.6 mg/kg based on a human surface area of

2.2 m^2 and an average human weight of 55 kg. For a controlled release formulation such as paclitaxel loaded PLLA microspheres, where the drug is released over several weeks into the peritoneal cavity, the MTD would be expected to be quite different from the MTD observed after a short intravenous infusion.

Due to the severe toxicity encountered with the Cremophor® EL vehicle in Taxol® (Weiss *et al.*, 1990), the formulation of paclitaxel in PLLA microspheres would be expected to improve the tolerability of the drug compared to the Taxol® formulation. A previous study in which paclitaxel was injected into the peritoneum of mice in a polymeric Cremophor® EL-free vehicle showed improved tolerability (Zhang *et al.*, 1997). The MTD of paclitaxel formulated as Taxol® was 20 mg/kg compared to 100 mg/kg for paclitaxel solubilized in a micelles composed of methoxy PEG-PDLLA diblock copolymers (Zhang *et al.*, 1997).

In vivo paclitaxel release from the microspheres was not directly determined in the rats. In three animals, microspheres were retrieved six weeks after administration and the amount of paclitaxel remaining determined. However, the broad range in the amount of paclitaxel remaining in microspheres retrieved from each animal makes it impossible to correlate *in vitro* and *in vivo* drug release. Scanning electron micrographs of microspheres retrieved from the peritoneal cavity (Figure 47C) showed that they remained spherical and intact, and that no erosion of the matrix occured after six weeks *in vivo*. *In vivo* drug release may be controlled by diffusion as well as degradation of polymer chains prior to the onset of matrix erosion. The biodegradation processes which ultimately result in erosion are known to proceed at similar rates *in vitro* and *in vivo*

because they involve primarily chemical hydrolysis with little contribution from enzymes (Leenslag *et al.*, 1987; Therin *et al.*, 1992).

The dose escalation study revealed significant necrosis by histology, of omental tissue immediately adjacent to paclitaxel loaded microsphere (Figure 47C). The presence of ascitic fluid in the peritoneal cavity observed post-mortum was further evidence of necrosis and inflammation. The dose limiting toxicity of intraperitoneal paclitaxel is reported to be severe abdominal pain (Rowinsky *et al.*, 1995). However, the animals did not show signs of discomfort, weight loss or loss of appetite in daily examinations. Signs of necrosis and inflammation localised in the peritoneum were observed only after sacrificing the rats. Control microspheres did not appear to result in inflammation as no ascitic fluid was observed post-mortum and no necrotic cells were observed in close proximity with the control microspheres by histology (Figure 45B).

The advantages of an intraperitoneal microsphere formulation of paclitaxel are as follows. Reduced systemic exposure of paclitaxel is expected due to intraperitoneal administration and the slow clearance of the drug from the peritoneal cavity (Markman *et al.*, 1992). Prolonged exposure, which improves the efficacy of paclitaxel (Rowinsky *et al.*, 1988)) is obtained due to slow drug clearance and prolonged release of the drug from the microspheres. Less toxicity would be expected since the traditional Cremophor vehicle was not employed. Because microspheres can release paclitaxel over the course of several weeks, the need for repeated intraperitoneal injections which have been employed for intraperitoneal paclitaxel in phase I trials (Rowinsky *et al.*, 1995) can be eliminated.

5.7.2.2. Intraperitoneal carcinomatosis with cecotomy repair model

The cecotomy repair model showed efficacy of the 100 mg dose of 30% loaded microspheres in preventing tumour growth (Figure 46). These data are consistent with those obtained for the 100 mg dose of paclitaxel loaded microspheres in the dose escalation study.

The improvements in the of intraperitoneal carcinomatosis/cecotomy repair model over the intraperitoneal carcinomatosis model alone were 1) introduction of a surgical repair similar to that which would result from a resection of tumour or anastomosis in gastrointestinal cancers, and 2) an increase in the duration of the study from two to six weeks.

Introduction of the surgical repair is an important improvement to the model because the site of a surgical repair following tumour resection will be preferentially seeded with tumour cells (Skipper *et al*, 1989, Murthy *et al*, 1989) with an implantation rate as high as 70% (Hughes *et al.*, 1983) compared to rates of 1-2% for abdominal wall implantation (Ramos *et al.*, 1994). In a rat model of a surgical wounding, 100% of rats that were administered colon cancer cells developed tumours at the wound site (Jacquet *et al.*, 1996). The healing process at surgical repair sites such as anastomoses may also increase the likelihood of tumour growth because of growth factor production (Jaquet and Sugarbaker, 1995).

Jaquet *et al.* (1996) observed that for intraperitoneal doxorubicin therapy to be effective at preventing tumour implantation, treatment must be administered post-operatively within the first three days. However the long-term outcome of intraperitoneal chemotherapy to treat large tumour spills in animal models is unknown. The extension of

the study to six weeks provides evidence that either tumour cells are killed early in the treatment, or are suppressed by prolonged exposure to paclitaxel by the controlled release formulation. The histological evidence suggests that no microscopic tumours were present. However, it cannot be assumed that all of the tumour cells were killed by the paclitaxel. The death of all the tumour cells could be only confirmed by harvesting the entire contents of the peritoneal cavity.

The dose required to prevent the growth of gross tumours may not be the same as the dose required to kill all of the tumour cells (Itoi et al., 1996). In a study of mice that received cisplatin loaded PLGA microspheres and five million P815 mastocytoma cells by intraperitoneal injection, a dose dependent effect of tumour cell kill was observed. In a group of mice receiving 30 mg/kg cisplatin, one million tumour cells were recovered from the peritoneal cavity 198 days after treatment. At a dose of 70 mg/kg of cisplatin, no viable tumour cells were observed in the peritoneal cavity.

5.7.2.3. Analysis of microspheres removed from the peritoneum after six weeks

Microspheres removed after six weeks *in vivo* had aggregated together and microspheres in two of the three samples were surrounded by a capsule. (Figure 47A and B). The formation of a capsule around PLLA implants occurs *in vivo* as a response to foreign material (Leenslag et al., 1987, Pistner et al., 1993). Although polyesters are considered biocompatible, implants made of this type of polymer may cause a localised inflammatory reaction (Vert et al., 1992). Initially, the implant is surrounded by polymorphonuclear leukocytes, macrophages, giant cells and fibroblasts. Fibroblast activity results in the deposition of a capsule around the foreign material over several weeks and the number of macrophages and giant cells decreases as the capsule forms

(Pistner *et al.*, 1993). The capsule would be expected to decrease paclitaxel release from microspheres. Measurement of the paclitaxel remaining after six weeks confirmed this. Nevertheless, between 40 and 50% of the initial amount of paclitaxel was released over six weeks from microspheres that were covered with a capsule. Most of this release would be expected to occur early in the study, during the burst phase of release and prior to the formation of the capsule.

6.   SUMMARY AND CONCLUSIONS

6.1.   Solid-state characterisation of paclitaxel

1.   The existence of several solid forms of paclitaxel were identified for the first time. Paclitaxel was shown to exist in the solid state as anhydrous paclitaxel I, paclitaxel•2H$_2$O or amorphous paclitaxel. A polymorphic form of anhydrous paclitaxel, called dehydrated paclitaxel•2H$_2$O was obtained by dehydrating paclitaxel•2H$_2$O by heating above 45°C.

2.   These findings were suggested to explain the wide range in the reported values of water solubility for paclitaxel.

6.2.   The effect of polymer blending on microsphere properties

1.   In microspheres made from 1k/100k g/mol PLLA blends, the 1k g/mol PLLA polymer was not completely incorporated due to its hydrophilicity.

2.   Blends of 2k/50k g/mol PLLA and 1k/100k g/mol PLLA were completely miscible. Therefore, the effect of adding the low molecular weight component in the 2k/50k and 1k/100k g/mol blends was to decrease the values of Tg, Tm and degree of crystallinity of the polymer blend.

3.   Unexpectedly, the crystallisation behaviour of the 2k/50k g/mol PLLA blends was different from that of the 1k/100k g/mol blends. Blends of 100k g/mol PLLA with 1k g/mol PLLA-LA crystallised with the low molecular weight fraction acting as a diluent, being excluded from the crystallites, as predicted by Martinez-Salazer *et al.* (1996). However, blends of a 50k g/mol PLLA with

218

2k g/mol PLLA-PS crystallised with both small and large polymer chains being incorporated into crystallites.

4.   Paclitaxel was miscible in all single component and polyblend PLLA microspheres at all loading levels. However, the effect of paclitaxel on the Tg of PLLA was different for 100k g/mol PLLA and PB60 blends. In 100k g/mol PLLA microspheres, paclitaxel acted as a plasticizer of the amorphous phase, reducing Tg, whereas in PB60 microspheres, paclitaxel acted to stiffen the amorphous phase through interactions with chain ends, increasing Tg and reducing polymer crystallinity.

5.   Paclitaxel release from microspheres was modulated by blending high and low molecular weight PLLA in microspheres. The mechanism of *in vitro* paclitaxel release from 100k g/mol PLLA microspheres was different than from PB60 microspheres. Release profiles for 100k g/mol PLLA indicated that paclitaxel was released by a diffusion controlled mechanism. In contrast, paclitaxel was released from PB60 microspheres by a diffusion controlled mechanism followed by an erosion controlled mechanism.

6.   Polymer blending is a convenient and effective method for modulating drug release profiles from polymeric matrices.

6.3.   *In vivo* characterisation of paclitaxel loaded microspheres.

1.   There was a maximum size of microspheres (around 20 μm) that could be cleared from the peritoneum into lymphatic tissues, through fenestrations in the diaphragm of rats. However, the majority of fenestrations in the diaphragm

appeared to allow the clearance of microspheres with diameters only up to around 8 μm.

2.   Despite the effect of insufflation on diaphragmatic tension and patency of fenestrations (Abu-Hijelh *et al.*, 1995), insufflation of the peritoneal cavity did not affect the clearance of microspheres through the lacunae in the diaphragm.

3.   A 100 mg dose of 30% paclitaxel loaded 35-105 μm PLLA microspheres administered intraperitoneally was sufficient to prevent tumour growth for six weeks in a rat model of intraperitoneal carcinomatosis caused by a tumour cell spill with or without cecotomy repair.

7.   FUTURE WORK

There is some preliminary evidence that paclitaxel forms solvates. Therefore the solid state characterisation of paclitaxel should be continued to examine the formation and properties of other solvated forms of the drug. Solvents of interest would include dichloromethane, which is used in the microsphere manufacturing process as well as other commonly used solvents such as methanol, ethanol, acetonitrile, and chloroform.

Differences in the melting behaviour of the 1k/100k and 2k/50k g/mol PLLA blend systems were an interesting observation since the Tm of 1k/100k g/mol PLLA varied with the blend composition as predicted by Nishi and Wang (1975) whereas the Tm of the 2k/50k g/mol PLLA blends did not. Characterisation of the dependence of the kinetics of crystallisation and the composition of individual crystallites on blend composition for both 2k/50k and 1k/100k g/mol PLLA blend systems could help to explain differences in mechanisms of crystallisation of these blends which result in the observed melting behaviours.

The *in vivo* studies showed that the 100k g/mol PLLA microspheres tended to aggregate in the peritoneal cavity, forming plaques. The microspheres remained intact and did not release the entire amount of paclitaxel incorporated into the matrix. A microsphere formulation that would not aggregate *in vivo* and would erode over the course of the study, releasing all of the paclitaxel would represent an improvement in the formulation. Complete drug release over the course of the study could result in a lower dose of paclitaxel being required for efficacy in the model. Possible approaches to improving the formulation include the use of PLLA with molecular weights less than 10k g/mol that release paclitaxel and erode more quickly than the 100k g/mol PLLA

microspheres. Aggregation could be prevented by altering the surface properties of the microspheres.

8. REFERENCES

Abernethy NJ, Chiun W, Hay JB, Rodela H, Oreopoulos D, Johnston MG, Lymphatic drainage of the peritoneal cavity in sheep. *Am. J. Physiol.* 1991(260) 353-8

Abu-Hijleh MF, Habbal OA, Moqattash ST, The role of the diaphragm in lymphatic absorption from the peritoneal cavity. *J. Anat.* 1995(186) 453-67

Abu-Hijleh MF, Scothorne RJ, Regional lymph drainage routes from the diaphragm in the rat. *Clin. Anat.* 1994(7) 181-8

Adams JD, Flora KP, Goldspiel BR, Wilson JW, Arbuck SG, Finley R, *J. Natl. Cancer Inst. Monogr.* 1993(15) 141-7

Agrawal CM, Haas KF, Leopold DA, Clark HG, Evaluation of poly(L-lactic acid) as a material for intravascular polymeric stents. *Biomaterials* 1992(13) 176-82

Alberts DS, Liu PY, Hannigan EV, O'Toole R, Williams SD, Young JA, Franklin EW,Clarke-Pearson DL, Malviya VK, DuBeshter B, Intraperitoneal cisplatin plus intravenous cyclophosphamide versus intravenous cisplatin plus intravenous cyclophosphamide for stage III ovarian cancer. *New Engl. J. Med.* 1996(335)1950-5

Allen L, On the penetrability of the lymphtics of the diaphragm. *Anat. Rec.* 1956(124) 639-57

Allen L, The peritoneal stomata. *Anat. Rec.* 1936(67) 89-102

Allen L, Weatherford T, Role of fenestrated basement membrane in lymphatic absorpeiton from peritoneal cavity. *Am. J. Physiol.* 1959(197) 551-4

Angell CA, Bressel RD, Green JL, Kanno H, Oguni M, Sare EJ, Liquid fragility and the glass transition in water and aqueous solutions. *J. Food Eng.* 1994(22) 115-42

Angell CA, Monnerie L, Torell LM, Strong and fragile behaviour in liquid polymers. *Symp. Mat. Res. Soc.* 1991(215) 3

Anselme K, Flautre B, Hardouin P, Chanavaz M, Ustariz C, Vert M, Fate of bioresorbable poly(lactic acid) microbeads implanted in artificial bone defects for cortical bone augmentation in dog mandible. *Biomaterials* 1993(14) 44-50

Arbuck SG, Canetta R, Onetto N, Christian MC, Current dosage and schedule issues in the development of paclitaxel (Taxol®). *Semin. Oncol.* 1993(20) 31-9

Asano M, Fukuzaki H, Yoshida M, Kumakura M, Mashimo T, Yuasa H, Imai K, Yamanaka H, Kawaharada U, Suzuki K, *In vivo* controlled release of a luteinizing

hormone-releasing hormone agonist from poly(DL-lactic acid) formulations of varying degradation pattern. *Int. J. Pharm.* 1991(67) 67-77

Atiq OT, Kelsen DP, Shiu MH, Saltz L, Tong W, Niedzwieki D, Trochanowski B, Lin S, Toomasi F, Brennan M, Phase II trial of postoperative adjuvant intraperitoneal cisplatin and fluorouracil and systemic fluorouracil chemotherapy in patients with resected gastric cancer. *J. Clin. Oncol.* 1993(11) 425-33

Aubin M, Prud'homme RE, Miscibility in blends of poly(vinylchloride) and polylactones. *Macromolecules* 1980(13) 365-9

Baker R, *Controlled release of biologically active agents*; Academic Press: New York, 1987

Balasubramanaian SV, Alderfer JL, Straubinger RM, Solvent- and concentration-dependent molecular interactions of Taxol (paclitaxel). *J. Pharm. Sci.* 1994(83) 1470-6

Bartoli MH, Boitard M, Fessi H, Beriel H, Devissaguet JP, Picot F, Puisieux F, *In vitro* and *in vivo* antitumoral activity of free, and encapsulated taxol. *J. Microencap.* 1990(7) 191-7

Barton JM, Dependence of polymer glass transition temperatures on heating rate. *Polymer* 1969(10) 151-5

Behme RJ, Brooke D, Farney RF, Kensler TT, Characterization of polymorphism of gepirone hydrochloride. *J. Pharm. Sci.* 1985(74) 1041-6

Benoit JP, Courteille F, Thies C, A physicochemical study of the morphology of progesterone-loaded poly(D,L-lactide) microspheres. *Int. J. Pharm.* 1986(29) 95-102

Berek JS, Hacker NF, Lichtenstein A, Jung T, Spina C, Knox RM, Brady J, Greene T, Ettinger LM, Lagasse LD, Bonnem EM, Spiegel RJ, Zighelboim J, Intraperitoneal recombinant alpha-interferon for "salvage" immunotherapy in stage III epithelial ovarian cancer: a Gynecologic Oncology Group study. *Cancer Res.* 1985(44) 4447-53

Berger HL, Shultz AR, Gel permeation chromatograms: approximate relation of line shape to polymer polydispersity. *J. Poly. Sci. Pt. A* 1965(2) 3643-8

Bergsma EJ, Rozema FR, Bos RRM, DeBruijn WC, Foreign body reactions to resorbable poly(L-lactide) bone plates and screws used for the fixation of unstable zygomatic fractures. *J. Oral. Maxillofac. Surg.* 1993(51) 666-70

Billmeyer FW, *Textbook of polymer science* 3rd ed.; Wiley: New York, 1984

Black DB, Lovering EG, Estimation of the degree of crystallinity in digoxin by X-ray and infrared methods. *J. Pharm. Pharmacol.* 1977(29) 684-7

Bleday R, Babineau T, Forse RA, Laparoscopic surgery for colon and rectal cancer. *Sem. Surg. Onocol.* 1993(9) 59-64

Blümm E, Owen AJ, Miscibility, crystallization and melting of poly(3-hydroxybutyrate)/poly(L-lactide) blends. *Polymer* 1995(36) 4077-81

Bodmeier R, Oh KH, Chen H, The effect of the addition of low molecular weight poly(DL-lactide) on drug release from biodegradable poly(DL-lactide) drug delivery systems. *Int. J. Pharm.* 1989(51) 1-8

Bogdansky S, Natural polymers as drug delivery systems. In *Biodegradable polymers as drug delivery systems*; M Chasin, R Langer, Eds.; Marcel Dekker Inc.: New York, 1990; pp 231-60

Bos RRM, Rozema FR, Boering G, Nijenhuis AJ, Pennings AJ, AB Verwey, Nieuwenhuis P, Jansen HWB, Degradation of and tissue reaction to biodegradable poly(L-lactide) for use as internal fixation of fractures: a study in rats. *Biomaterials* 1991(12) 32-6

Boury F, Olivier E, Proust JE, Benoit JP, Interactions of poly(α-hydroxy acid)s with poly(vinyl alcohol) at the air/water and at the dichloromethane/water interfaces. *J. Colloid Interface Sci.* 1994(163) 37-48

Brandrup J, Immergut EH, *Polymer Handbook* 3rd ed.; John Wiley and Sons: New York, 1989; p V81

Brunacci A, Cowie JMG, Ferguson R, McEwen IJ, Enthalpy relaxation iin glassy polystyrenes: 2. *Polymer* 1997(38) 3263-8

Burt HM, Jackson JK, Bains SK, Liggins RT, Oktaba AMC, Arsenault AL, Hunter WL, Controlled delivery of taxol from microspheres composed of a blend of ethylene-vinyl acetate copolymer and poly(d,l-lactic acid). *Cancer Lett.*, 1995(88) 73-9

Cahan MA, Walter KA, Calvin AM, Brem H, Cytotoxicity of taxol *in vitro* against human and rat malignant brain tumours. *Cancer Chemother. Pharmacol.* 1994(33) 441-4

Caplow M, Shanks J, Ruhlen R, How taxol modulates microtubule assembly. *J. Biol. Chem.* 1994(269) 23399-23402

Carstensen JT, *Pharmaceutics of solids and solid dosage forms*; Wiley Interscience: New York, 1977; p 64

Cavaletti G, Tredici G, Braga M, Tazzari S, Experimental peripheral neuropathy induced in adult rats by repeated intraperitoneal administration of Taxol. *Exp. Neurol.* 1995(133) 64-72

Celli A, Scandola M, Thermal properties and physical ageing of poly(L-lactic acid). *Polymer* 1992(33) 2699-704

Cha Y, Pitt CG, A one-week subdermal delivery system for L-methadone based on biodegradable microcapsules. *J. Cont. Rel.* 1988(7) 69-78

Cha Y, Pitt CG, The biodegradability of polyester blends. *Biomaterials* 1990(11) 108-12

Chang RK, Price JC, Whitworth CW, Control of drug release rates through the use of mixtures of polycaprolactone and cellulose propionate polymers. *Pharm. Tech.* 1986 24-33

Charnley RM, Banerjee AK, Whitaker SC, Spiller RC, Doran J, Peritoneal seeding of pancreatic cancer following transperitoneal biliary procedures. *Br. J. Surg.* 1995(82) 392-3

Chasin M, Domb A, Ron E, Mathiowitz E, Langer R, Leung K, Laurencia C, Brem H, Grossman S, Polyanhydrides as drug delivery systems. In *Biodegradable polymers as drug delivery systems*; M Chasin, R Langer, Eds.; Marcel Dekker Inc.: New York, 1990; pp 43-70

Chiou WL, Riegelman S, Pharmaceutical applications of solid dispersion systems. *J. Pharm. Sci.* 1971(60) 1281-302

Chmurny GN, Hilton BD, Brobst S, Look SA, Witherup KM, Beutler JA, ^{1}H- and ^{13}C-NMR assignments for taxol, 7-*epi*-taxol , and cephalomannine. *J. Nat. Prod.* 1992(55) 414-23

Chu C, Berner B, Thermal analysis of poly(acrylic acid)/poly(oxyethylene) blends. *J. Appl. Polym. Sci.* 1993(47) 1083-7

Çiftçi K, Hincal AA, Kas HS, Ercan MT, Ruacan S, Microspheres of 5-fluorouracil using poly(dl-lactic acid): *in vitro* release properties and distribution in mice after i.v. administration. *Eur. J. Pharm. Sci.* 1994(1) 249-58

Clair DG, Lautz DB, Brooks DC, Rapid development of umbilical metastases after laparoscopic cholecystectomy for unsuspended gallbladder carcinoma. *Surgery* 1993(113) 355-8

Coll H, Gilding DK, Universal calibration in GPC: a study of polystyrene, poly(α-methylstyrene) and polypropylene. *J. Poly. Sci. Pt A-2* 1970(8) 89-103

Collins CA, Vallee RB, Temperature dependent reversible assembly of taxol-treated microtubules. *J. Cell Biol.* 1987(105) 2847-54

Cowsar DR, Tice TR, Gilley RM, English JP, Poly(lactide-co-glycolide) microcapsules for controlled release of steroids. *Meth. Enzymol.* 1985(112) 101-16

Crank J, *The mathematics of diffusion*; Oxford University Press: London, 1956

Cresteil T, Monsarrat B, Alvinerie P, Treluyer JM, Vieira I, Wright M, Taxol metabolism by human liver microsomes: identification of cytochrome P450 isozymes involved in tis biotransformation. *Cancer Res*. 1994(54) 386-92

Crotts G, Park TG, Preparation of porous and nonporous biodegradable polymer hollow microspheres. *J. Cont. Rel*. 1995(35) 91-105

Cruz CA, Barlow JW, Paul DR, The basis of miscibility in polyester-polycarbonate blends. *Macromolecules* 1979(12) 726-31

Dash AK, Determination of the physical state of drug in microcapsule and microsphere formulations. *J. Microencap*. 1997(14) 101-12

Dash AK, Suryanarayanan R, Solid-state properties of tobramycin. *Pharm. Res*. 1991(8) 1159-65

Decorti G, Bartoli-Klugmann F, Candussio L, Baldini L, Effect of paclitaxel and Cremophor EL on mast cell histamine secretion and their interaction with adriamycin. *Anticancer Res*. 1996(16) 317-20

Denis JN, Correa A, Greene AE, Direct, highly efficient synthesis from (S)-(+)-phenylglycine of the taxol and taxotere side chains. *J. Org. Chem*. 1991(56) 6939-42

Domb A, Maniar M, Bogdansky S, Chasin M, Drug delivery to the brain using polymers. *Crit. Rev. Ther. Drug Carrier Sys*. 1991(8) 1-17

Dordunoo SK, Burt HM, Solubility and stability of taxol: effects of buffers and cyclodextrins. *Int. J. Pharm*. 1996(133) 191-201

Dordunoo SK, Jackson JK, Arsenault LA, Oktaba AMC, Hunter WL, Burt HM, Taxol encapsulation in poly(ε-caprolactone) microspheres. *Cancer Chemother. Pharmacol*. 1995(36) 279-82

Duncan-Hewitt WC, Grant DJW, True density and thermal expansivity of pharmaceutical solids: comparison of methods and assessment of crystallinity. *Int. J. Pharm*. 1986(28) 75-84

Edman P, Sjöholm I, Acrylic microspheres in vivo. II. The effect in rat of L-asparaginase given in microparticles of poly-acrylamide. *J. Pharmacol. Exp. Ther*. 1979(211) 663-7

Eiseman JL, Eddington ND, Leslie J, MacAuley C, Sentz DL, Zuhowski M, Kujawa JM, Young D, Egorin MJ, Plasma pharmacokinetics and tissue distribution of paclitaxel in CD_2F_1 mice. *Cancer Chemother. Pharmacol*. 1994(34) 465-71

227

Eisenberg A, The glassy state and the glass transition. In *Physical Properties of Polymers* 2nd ed.; JE Mark, A Eisenberg, WW Graessley, L Mandelkern, ET Samulski, JL Koenig, GD Wignall, Eds.; American Chemical Society: Washington DC, 1993; pp 61-95

El-Arini SK, Leuenberger H, Modelling of drug release from polymer matrices: effect of drug loading. *Int. J. Pharm.* 1995(121) 141-8

Embleton JK, Tighe BJ, Polymers for biodegradable medical devices. X. Microencapsulation studies: control of poly-hydroxybutyrate-hydroxyvalerate microcapsule porosity via polycaprolactone blending. *J. Microencap.* 1993(10) 341-52

Engelberg I, Kohn J, Physico-mechanical properties of degradable polymers used in medical applications: a comparative study. *Biomaterials* 1991(12) 292-304

Enzig AI, Wiernik PH, Susioff J, Rumowicz CD, Goldberg GL, Phase II study and long term follow up of patients treated with taxol for advanced ovarian adenocarcinoma. *J. Clin. Oncol.* 1992(10) 1748-53

Fernbach SK, Ascites produced by peritoneal seeding of neuroblastoma. *Pediatr. Radiol.* 1993(23) 569

Feughelman M, Langridge R, Seeds WE, Stokes AR, Wilson HR, Hopper CW, Wilkins MHF, Barclay RK, Hamilton LD, Molecular structure of deoxyribose nucleic acid and nuceloprotein. *Nature* 1955(175) 834-??

Flessner MF, Parker RJ, Sieber SM, Peritoneal lymphatic uptake of fibrinogen and erythrocytes in the rat. *Am. J. Physiol.* 1983(244) H89-96

Florence AT, Salole EG, Changes in crystallinity and solubility on comminution of digoxin and observations on spirinolactone and oestradiol. *J. Pharm. Pharmacol.* 1975(28) 637-42

Florey H, Witts LJ, Absroption of blood from the peritoneal cavity. *Lancet* 1928(1) 1323-5

Fox TG, Influence of diluent and of copolymer composition on the glass temperature of a polymer system. *Bull. Am. Phys. Soc.* 1956(1) 123

Fukuzaki H, Yoshida M, Asano M, Kumakura M, Synthesis of copoly(D,L-lactic acid) with relatively low molecular weight and *in vitro* degradation. *Eur. Polym. J.* 1989(25)0 1019-26.

Garner WE, *Chemistry of the Solid State*; Academic Press: New York, 1955; pp 213-31

Gee G, The glassy state in polymers. *Contemp. Phys.* 1970(11) 313-34

Gelmon K, Nabholtz JM, Bontenbal M, Spielman M, Conte P, Klassen U, Catimel G, Namer M, Fumoleau J, Bonnneterre P, Sulkes A, Sauter C, Roche H, Calvert H, Kaufmann J, Chazard M, Diergarten K, Gallant G, Thompson M, Winograd B, Hellmann S, Randomized trial of two doses of paclitaxel in metastatic breast cancer after failure of standard therapy. *Ann. Oncol.* 1994(5) Supp 5, 198

Gesner BD, Polyblends. In: *Encyclopedia of Polymer Science and Technology*; HF Mark, NG Gaylord, NM Bikole, Eds.; Interscience: New York, 1969; vol 10

Ghaderi R, Sturesson C, Carlfors J, Effect of preparative parameters on the characteristics of poly(D,L-lactide-co-glycolide) microspheres made by the double emulsion method. *Int. J. Pharm.* 1996(141) 205-16

Gilding DK, Biodegradable polymers. *Biocompat. Clin. Implant. Mater.* 1981(2) 209-32

Gilding DK, Reed AM, Biodegradable polymers for use in surgery – polyglycolic/poly(lactic acid) homo- and copolymers: 1. *Polymer* 1979(20) 1459-64

Göpferic A, Alonso MJ, Langer R, Development and charaterization of microencapsulated microspheres. *Pharm. Res.* 1994(11) 1568-74

Gordon M, Taylor JS, Ideal copolymers and the second-order transition of synthetic rubbers. I. Non-crystalline copolymers. *J. Appl. Chem.* 1952(2) 495-500

Gourlay SJ, Rice RM, Hegyeli AF, Wade CW, Deillon JG, Jaffe H, Kulkarni RK, Biocompatibility testing of polymers: *in vivo* implantation studies. *J. Biomed. Mater. Res.* 1978(12) 219-32

Grandfils C, Flandroy P, Jérôme R, Control of the biodegradation rate of poly(DL-lactide) microparticles intended as chemoembolization materials. *J. Cont. Rel.* 1996(38) 109-22

Griesser UJ, Burger A, Mereiter K, The polymorphic drug substances of the European Pharmacopoeia Part 9. Physicochemical properties and crystal structure of acetazolamide crystal forms. *J. Pharm. Sci.* 1997(86) 352-8

Griffin GJL, Synthetic polymers and the living environment. *Pure Appl. Chem.* 1980(52) 399-407

Grijpma DW, Nijenhuis AJ, Pennings AJ, Synthesis and hydrolytic degradation behaviour of high-molecular-weight L-lactide and glycolide copolymers. *Polymer* 1990(31) 2201-6

Grulke EA, *Polymer Process Engineering*; Prentice Hall: Engelwood Cliffs, 1994, p 345

Guan D, Unpublished results: preparation of paclitaxel loaded microspheres with different molecular weights and copolymer ratios of PLGA, 1996

Guéritte-Voegelein F, Guénard D, Lavelle F, LeGoff MT, Mangatal L, Potier P, Relationships between the structure of taxol analogues and their antimitotic activity. *J. Med. Chem.* 1991(34) 992-8

Häfeli US, Sweeney SM, Beresford BA, Sim EH, Macklis RM, Magnetically directed poly(lactic acid) 90Y-microspheres: novel agents for targeted intracavitary radiotherapy. *J. Biomed. Mater. Res.* 1994(28) 901-8

Hagiwara A, Takahashi T, Sawai K, Sakakura C, Hoshima M, Ohyama T, Ohgaki M, Imanishi T, Yamamoto A, Muranishi S, Methotrexate bound to carbon particles used for treating cancers with lymph node metastases in animal experiments and a clinical pilot study. *Cancer* 1996(78) 2199-209

Haleblian J, Characterization of habits and crystalline modification of solids and their pharmaceutical applications. *J. Pharm. Sci.* 1975(64) 1269-88

Haleblian J, McCrone W, Pharmaceutical applications of polymorphism. *J. Pharm. Sci.* 1969(58) 911-29

Hamielec AE, Ouano AC, Generalized universal molecular weight calibration parameter in GPC. *J. Liquid Chromtogr.* 1978(1) 111-20

Hancock BC, Shamblin SL, Zografi G, Molecular mobility of amorphous pharmaceutical solids below their glass transition temperatures. *Pharm. Res.* 1995(12) 799-806

Hancock BC, Zografi G, Characterisitcs and significance of the amorphous state in pharmaceutical systems. *J. Pharm. Sci.* 1997(86) 1-12

Harley S, Thompson DW, Vincent B, The adsorption of small particles onto larger particles of opposite charge. Direct electron microscope studies. Colloids Surfaces 1992(62) 163-76

Hartshorne NH, Stuart A, *Crystals and the polarizing microscope* 3rd ed.; Edward Arnold Publishers: London, 1960

Hearle JWS, *Polymers and their properties, fundamentals of structure and mechanics*; Ellis Horwood Ltd.: Chichester, 1982

Hester RD, Mitchell PH, A new universal GPC calibration method. *J. Poly. Sci. Poly. Chem. Ed.* 1980(18) 1727-38

Heya T, Okada H, Ogawa Y, Toguchi H, Factors influencing the profiles of TRH release from copoly(d,l-lactic/glycolic acid) microspheres. *Int. J. Pharm.* 1991(72) 199-205

Higuchi T, Rate of release of medicaments from ointment bases containing drugs in suspension. *J. Pharm. Sci.* 1961(50) 874-5

Higuchi T, Mechanism of sustained-actionn medications. *J. Pharm. Sci.* 1963(52) 1145-9

Hirano K, Hunt CA, Lymphatic transport of liposomes-encapsulated agents: effects of liposome size following intraperitoneal administration. *J. Pharm. Sci.* 1985(74) 915-21

Holland SJ, Tighe BJ, Gould PL, Polymers for biodegradable medical devices. 1. The potential of polyesters as controlled macromolecular release systems. *J. Cont. Rel.* 1986(4) 155-80

Holmes FA, Water RS, Theriault RL, Furman AD, Newton LK, Raber MN, et al., Phase II trial of taxol, an active drug in the treatment of metastatic breast cancer. *J. Natl. Cancer Inst.* 1991(83) 1797-805

Holton RA, *2nd National Cancer Institute Workshop on Taxol and Taxus*; National Cancer Institute: Bethesda, 1992

Holton RA, Samoza C, Kim HB, Liang F, Beidiger RJ, Boatman PD, Shindo M, Smith CC, Kim S, Nadizadh H, Suzuki Y, Tao C, Vu P, Tang S, Zhang P, Murthi KK, Gentile LN, Liu JH, First total synthesis of taxol. *J. Am. Chem. Soc.* 1994(116) 1597-600

Hoogsteen W, Postema AR, Pennings AJ, ten Brinke G, Zugenmaier P, Scrystal structure, conformation, and morphology of solution-spun poly(L-lactide) fibers. *Macromol.* 1990(23) 634-42

Hopkins MP, von Gruenigen VE, Holda S, Weber B, The effect of intermittent-release intraperitoneal chemotherapy on wound healing. *Am. J. Obstet. Gynecol.* 1997(176) 819-25

Hseih DT, Peiffer DG, Compatibility behavior of thermoplastic polymer blends containing poly(*t*-butylstyrene-co-acrylonitrile). *J. Appl. Polym. Sci.* 1993(47) 1469-76

Hughes ES, McDermot FT, Polglase AL, Johnson WR, Tumour recurrence in the abdominal wall scar tissue after large-bowel cancer surgery. *Dis. Col. Rectum* 1983(26) 571-2

Huggins ML, The viscosity of dilute solutions of long-chain molecules. IV. Dependence on concentration. *J. Am. Chem. Soc.* 1942(64) 2716-8

Huizing MT, Keung ACF, Rosing H, van der Kuij V, ten Bokkel Huinink WW, Mandjes IM, Dubbelman AC, Pinedo HM, Beijnen JH, Pharmacokinetics of paclitaxel and metabolites in randomized comparative study in platinum-pretreated ovarian cancer patints. *J. Clin. Oncol.* 1993(111) 273-9

231

Huttenrauch R, Keiner I, Producing lattice defects by drying processes. *Int. J. Pharm.* 1979(2) 59-60

Ike O, Shimizu Y, Ikada Y, Watanabe W, Natsume T, Wada R, Hyon SH, Hitomi S, Biodegradation and antitumor effect of adriamycin-containing poly(L-lactic acid) microspheres. *Biomaterials* 1990(12) 757-62

Innocenti F, Danesi R, Di Paolo A, Agen C, Nadini D, Bocci G, del Tacca M, Plasma and tissue disposition of paclitaxel (Taxol) after intraperitoneal administration in mice. *Drug Metab. Dispos.* 1995(23) 713-7

Itoi K, Tabata CY, Ike O, Shimizu Y, Kuwabara M, Kyo M, Hyon SH, Ikada Y, In vivo suppressive effects of copoly(glycolic/L-lactic acid) microspheres containing CDDP on murine tumor cells. *J. Cont. Rel.* 1996(42) 175-84

Izumikawa S, Yoshioka S, Aso Y, Takeda Y, Preparation of poly(l-lactide) microspheres of different crystalline morphology and effect of crystalline morphology on drug release rate. *J. Cont. Rel.* 1991(15) 133-40

Jacquet P, Averbach AM, Stephen AD, Sugarbaker PH, Cancer recurrence following laparoscopic colectomy. *Dis. Colon Rectum* 1995(38) 1110-4

Jacquet P, Sugarbaker PH, Influence of wound healing in gastrointestinal cancer recurrence. *Wounds* 1995(7) 40-7

Jalil R, Nixon JR, Microencapsulation using poly(L-lactic acid) I: Microcapsule properties affected by the preparative technique. *J. Microencap.* 1989(6) 473-84

Jalil R, Nixon JR, Microencapsulation using poly(L-lactic acid). IV. Release properties of microcapsules containing phenobarbitone. *J. Microencap.* 1990(7) 53-66

Jamshidi K, Hyon SH, Ikada Y, Thermal characterization of polylactides. *Polymer* 1988(29) 2229-34

Jacquet P, Stuart OA, Dalton R, Chang D, Sugarbaker PH, Effect of intraperitoneal chemotherapy and fibrinolytic therapy on tumour implantation in wound sites. *J. Surg. Oncol.* 1996(62) 128-34

Johnstone PAS, Rhode DC, Swartz SE, Fetter JE, Wexner SD, Port site recurrences after laparoscopic and thoracoscopic procedures in malignancy. *J. Clin. Oncol.* 1996(14) 1950-6

Jolley EI, The microstructure of photographic gelatin binders. *Photograph. Sci. and Eng.* 1970(14) 169-77

Jordan MA, Toso RJ, Thrower D, Wilson L, Mechanism of mitotic block and inhibition of cell proliferation by taxol at low concentrations. *Proc. Natl. Acad. Sci.* 1993(90) 9552-6

Kelley FN, Bueche F, Viscosity and glass temperature relations for polymer-diluent systems. *J. Poly. Sci.* 1961(50) 549-56

Kempainen E, Talja M, Riihelä M, Pohjonen T, Törmälä P, Alfthan O, A bioresorbable urethral stent. *Urol. Res.* 1993(21) 235-8

Ketolainen J, Poso A, Viitasaari, Gynther J, Pirttimäki J, Laine E, Paronen P, Changes in solid-state structure of cyclophosphamide by mechanical treatment and storage. *Pharm. Res.* 1995(12) 299-304

Kingston DGI, Samaranayake G, Ivey CA, The chemistry of taxol, a clinically useful anticancer agent. *J. Nat. Prod.* 1990(53) 1-12

Kingston DGI, Hawkins DR, Ovington L, New taxanes from *Taxus brevifolia*. *J. Nat. Prod.* 1982(45) 466-70

Kingston DGI, The chemistry of taxol. *Pharmac. Ther.* 1991(52) 1-34

Kishida A, Dressman JB, Yoshioka S, Aso Y, Takeda Y, Some determinants of morphology and release rates from poly(L)lactic acid microspheres. *J. Cont. Rel.* 1990(13) 83-9

Kitaoka H, Ohya K, Hakusui H, Thermal dehydration of nafagrel hydrochloride hydrate at controlled water vapor partial pressures. *Chem. Pharm. Bull.* 1995(43) 1744-50

Kofler N, Ruedl, Klima J, Recheis H, Böck G, Wick G, Wolf H, Preparation and characterization of poly-(D,L-lactide-co-glycolide) and poly-(L-lactic acid) microspheres with entrapped pneumotropic bacterial antigens. *J. Immunol. Meth.* 1996(192) 25-35

Kolínský N, Janca J, Some applications of gel-permeation chromatography in investigations of structure and solution properties of radical-initiated poly(vinyl chloride). *J. Poly Sci. Poly. Chem. Ed.* 1974(12) 1181-91

Kraemer EO, Molecular weights of celluloses and cellulose derivatives. *Ind. Eng. Chem.* 1938(30) 1200-3

Kuhn JG, Pharmacology and pharmocokinetics of paclitaxel. *Ann. Pharmacother.* 1994(28) S15-7

Kulkarni RK, Moore EG, Hegyeli AF, Leonard F, Biodegradable poly(lactic acid) polymers. *J. Biomed. Mater. Res.* 1971(5) 169-81

Kulkarni RK, Pani KC, Neuman C, Leonard F, Polylactic acid for surgical implants. *Arch. Surg.* 1966(93) 839-43

Kumagai S, Sugiyama T, Nishida T, Ushijima K, Yakushiji M, Improvement of intraperitoneal chemotherapy for rat ovarian cancer using cisplatin-containing microspheres. *Jap. J. Cancer. Res.* 1996(87) 412-7

Kumar GN, Oatis JEJ, Thornburg KR, Heldrich FJ, Hazard ES, Walle T, 6α-Hydroxytaxol isolation and identification of the major metabolites of taxol in human liver microsomes. *Drug Metab. Dispos.* 1994a(22) 177-9

Kumar GN, Walle UK, Walle T, Cytochrome P450 3A-mediated human liver microsomal taxol 6α-hydroxylation. *J. Pharmacol. Exp. Ther.* 1994b(268) 1160-5

Kwong AK, Chou S, Sun AM, Sefton MV, Goosen MFA, In vitro and in vivo release of insulin from poly(lactic acid) microbeads and pellets. *J. Cont. Rel.* 1986(4) 47-62

Kwei TK, Chapter 4, Macromolecules in Solution. In *Macromolecules: an Introduction to Polymer Science*; FA Bovey, AB Winslow; Academic Press: New York, 1979; pp 145-200

Lam KH, Nieuwenhuis P, Molenaar I, Esselbrugge H, Feijen J, Dijkstra PJ, Schakenraad JM, Biodegradation of porous versus non-porous poly(L-lactic acid) films. *J. Mater. Sci. Mater. Med.* 1994(5) 181-89

Lamki DR, Fan S, Singleton EB, Eftekhari F, Shirkhoda A, Kumar R, Madewell JE, The many faces of neuroblastoma. *Radiographics* 1989(9)859-82

Langer R, New methods of drug delivery. *Science* 1990(249) 1527-33

Langer R, Controlled drug delivery systems. *Chem. Eng. Comm.* 1980(6) 1-48

Lataste H, Senilh V, Wright M, Gunard D, Potier P, Relationship between the structures of taxol and baccatin III derivatives and their *in vitro* action on the disasembly of mammalian brain and physarum amoebal microtubules. *Proc. Natl. Acad. Sci. USA* 1984(81) 4090-4

Ledwidge MT, Draper SM, Wilcock DJ, Corigan OI, Physicochemicalcharacterization of diclofenace N-(2-hydroxyethyl)pyrrolidine: anhydrate and dihydrate crystalline forms. *J. Pharm. Sci.* 1996(85) 16-21

Leelarasamee N, Howard SA, Malanga CJ, Luzzi LA, Hogan TF, Kandzari SJ, Ma JKH, Kinetics of drug release from poly(lactic acid)-hydrocortisone microcapsules. *J. Microcencap.* 1986(3) 171-9

Leenslag JW, Pennings AJ, Bos RRM, Rozema FR, Boering G, Resorbable materials of poly(L-lactide). VII. *In vivo* and *in vitro* degradation. *Biomaterials* 1987(8) 311-4

Leenslag JW, Pennings AJ, Synthesis of high-molecular-weight poly(L-lactide) initiated with tin 2-ethylhexanoate. *Makromol. Chem.* 1987(188) 1809-14

234

Lemstra PJ, Kooistra T, Challa G, Melting behavior of isotactic polystyrene. *J. Poly. Sci. Pt. A-2* 1972(10) 823-33

Li C, Yang DJ, Nikifarow S, Tansey W, Kuang LR, Wright KC, Wallace S, Formation and characterisation of cisplatin-loaded poly(bebzyl l-glutamate) microspheres for chemoembolization. *Pharm. Res.* 1994(11) 1792-9

Li S, Garreau H, Vert M, Structure-property relationships in the case of the degradation of massive poly(α-hydroxy acids) in aqueous media). *J. Mater. Sci. Mater. Med.* 1990(1) 198-206

Li WI, Anderson KW, DeLuca PP, Kinetic and thermodynamic modelling of the formation of polymeric microspheres using solvent extraction/evaporation method. *J. Cont. Rel.* 1995(37) 187-98

Li WI, Anderson KW, Mehta RC, Deluca PP, Prediction of solvent removal profile and effect on properties for peptide-loaded PLGA microspheres prepared by solvent extraction/evaporation method. *J. Cont. Rel.* 1995(37) 199-214

Lilenbaum RC, MacManus D, Engstrom C, Green M, Phase I study of paclitaxel and etoposide for metastatic or recurrent malignancies. *Am. J. Clin. Oncol.* 1998(21) 129-34

Lin SY, Ho LT, Chiou HL, Microencapsulation and controlled release of insulin from polylactic acid microcapsules. *Biomat. Med. Dev. Art. Org.* 1985-6(13) 187-201

Lindenmeyer PH, A molecular theory of polymer chain folding. *J. Poly. Sci.* 1967(C20) 145-58

Litterst CL, Torres IJ, Arnold S, McGunagle D, Furner R, Sikic BI, Guarino AM, Absorption of antineoplastic drugs following large volume IP administration to rats. *Cancer Treat. Rep.* 1980(66) 147-55

Liu Y, Donovan JA, Miscibility and crystallization of semicrystalline nylon 6 and amorphous nylon 6IcoT blends. *Polymer* 1995(36) 4797-803

Longnecker S, Doonehower R, Cates A, Chen TL, Brundrett RB, Grochow LB, Ettinger DS, Colvin M, High-performance liquid chromatographic assay for taxol in human plasma and urine and pharmacokinetics in a phase I trial. *Cancer Treat. Rep.* 1987(71) 53-9

Ludwig J, Trapping of calibrated microspheres in rat lymph nodes. *Lymphology* 1971(1) 18-24

Lundberg B, A submicron lipid emulsion coated with amphipathic polyethylen glycol for parenteral administration of paclitaxel (Taxol). *J. Pharm. Pharmcol.* 1997(49) 16-21

Lythgoe B, Nakanishi K, Uyeo S, Taxane. *Proc. Chem. Soc.* 1964 301

MacEachern-Keith GJ, Butterfield LJW, Mattina MJI, Paclitaxel stability in solution. *Anal. Chem.* 1997(69) 72-77

Magri NF, Modified taxols as anticancer agents. PhD. Thesis, Virginia Polytechnic Institute and State University, 1985

Maincent P, Thouvenot P, Amicabile C, Hoffman M, Kreuter J, Couvreur P, Devissaguet JP, Lymphatic targeting of polymeric nanoparticles after intraperitoneal administration in rats. *Pharm. Res.* 1992(9) 1534-9

Makino K, Arakawa M, Kondo T, Preparation and *in vitro* degradation properties of polylactide microcapsules. *Chem. Pharm. Bull.* 1985(33) 1195-201

Makino K, Ohshima H, Kondo T, Mechansim of hydrolytic degradation of poly(L-lactide) microcapsules: effects of pH, ionic strength and buffer concentration. *J. Microencap.* 1986(3) 203-12

Mandelkern L, *Crystallization of polymers*; McGraw-Hill: New York, 1964a; pp 38-73

Mandelkern L, *Crystallization of polymers*; McGraw-Hill: New York, 1964b; pp 273-88

Mandelkern L, The crystalline state. In *Physical Properties of Polymers* 2nd ed.; JE Mark, A Eisenburg, WW Graessley, L Mandelkern, ET Samulski, JL Koeing, GD Wignall; American Chemical Society: Washington DC, 1993; pp 145-200

Markman M, Intraperitoneal chemotherapy in the treatment of ovarian cancer. *Ann. Med.* 1996(28) 293-6

Markman M, Intraperitoneal paclitaxel in the management of ovarian cancer. *Sem. Oncol.* 1995(22, 5 suppl 12) 86-7

Markman M, Reichman B, Hakes T, Jones W, Lewis JL Jr., Rubin S, Almadrones L, Hoskia W, Responses to second-line cisplatin-based intraperitoneal therapy in ovarian cancer: influence of a prior response to intravenous cisplatin. *J. Clin. Oncol.* 1991(9) 1801-5

Markman M, Rowinsky E, Hakes T, Reichman B, Jones W, Lewis Jr. JL, Rubin S, Curtin J, Barakat R, Phillips M, Hurowitz L, Almadrones L, Hoskins W, Phase I trial of intraperitoneal Taxol: a Gynecologic Oncology Group study. *J. Clin. Oncol.* 1992(10) 1485-91

Martin A, *Physical Pharmacy* 4th ed.; Lea and Febiger: Philadelphia, 1993a; p 35

Martin A, *Physical Pharmacy* 4th ed.; Lea and Febiger: Philadelphia, 1993b; p 561-3

Martin A, *Physical Pharmacy* 4th ed.; Lea and Febiger: Philadelphia, 1993c; p 570

Martinez-Salazar J, Alizadeh A, Jiménez JJ, Plans J, On the melting behavior of polymer single crystals in a mixture with a compatible oligomer: 2. Polyethylene/paraffin. *Polymer* 1996(37) 12

Mastropaolo D, Camerman A, Luo Y, Brayer GD, Camerman N, Crystal and molecular structures of paclitaxel (Taxol). *Proc. Natl. Acad. Sci. USA* 1995(92) 6920-4

Mathew AE, Mejillano MR, Nath JP, Himes RH, Stella VJ, Synthesis and evaluation of some water soluble pro-drugs and derivatives of taxol with antitumor activity. *J. Med. Chem.* 1992(35) 145-51

Matsusue Y, Yamamuro T, Oka M, Shikinami Y, Hyon SH, Ikada Y, *In vitro* and *in vivo* studies on bioabsorbable ultra-high-strength poly(L-lactide) rods. *J. Biomed. Mater. Res.* 1992(26) 1553-67

McCrone WC, In *Microchemcial Techniques*; ND Cheronis Ed.; Interscience Publishers: New York, 1962

McCrone WC, Polymorphism. In *Physics and chemistry of the organic solid state*; D Fox, MM Labes, A Weissberger, Eds.; Interscience Publishers: New York, 1965; vol 2, pp 725-67

McGee JP, Singh M, Li XM, Qui H, O'Hagan DT, The encapsulation of a model protein in poly(D,L-lactide-co-glycolide) microparticles of various sizes: an evaluation of process reproducibility. *J. Microencap.* 1997(14) 197-210

McGuire WP, Rowinsky EK, Rosenshein NB, Grumbine FC, Etinger DS, Armstron DK, Donehower RC, Taxol: a unique antineoplastic agent with significant activity in advanced ovarian epithelial neoplasms. *Ann. Intern. Med.* 1989(111) 273-9

McVie JG, Dikhoff T, van der Heide J, Dubbelman R, ten Bokel WW, Tissue concentration of platinum after intraperitoneal cisplatin administration in patients. *Proc. Am. Assoc. Cancer Res.* 1985(26) 162

Mesley RJ, Johnson CA, Infrared identification of pharmaceutically important steroids with particular reference to the occurrence of polymorphism. *J. Pharm. Pharmacol.* 1965(17) 329-40

Mesley RJ, Clements RL, Flaherty B, Goodhead K, The polymorphism of phenobarbitone. *J. Pharm. Pharmacol.* 1968(20) 329-40

Mesley RJ, Clements RL, Infrared identification of barbiturates with particular refernce to the occurrence of polymorphism. *J. Pharm. Pharmacol.* 1968(20) 341-7

Migliaresi C, Fambri L, Cohn D, A study on the in vitro degradation of poly(lactic acid). *J. Biomater. Sci. Polymer Edn.* 1994(5) 591-606

Miller ML, *The structure of polymers*; Reinhold: New York, 1962

Miller RW, Powell RG, Smith CR Jr., Arnold R, Clardy J, Antileukemic alkaloids and other taxane derivatives. *J. Nat. Prod.* 1981(46) 1469-74

Mole-Bajer J, Bajer AS, Action of taxol on mitosis: modification of microtubule arrangements and function of the mitotic spindle in Haemanthus endosperm. *J. Cell Biol.* 1983(96) 527-40

Monsarrat B, Mariel E, Crois S, Gares M, Guenard D, Gueritte-Voegelein F, Wright M, Taxol metabolism. Isolation and identification of three major metabolites in rat bile. *Drug Metab. Dispos.* 1990(18) 895-901

Moore DH, Valea F, Walton LA, Soper J, Clarke-Pearson D, Fowler Jr. WC, A phase I study of intraperitoneal interferon-α_{2b} and intravenous *cis*-platinum plus cyclophosphamide chemotherapy in patients with untreated stage III epithelial ovarian cancer: a Gynecologic Oncology Group pilot study. *Gynecol. Oncol.* 1995(59) 267-72

Mumper RJ, Jay M, Poly(L-lactic acid) microspheres containing neutron-activatable holium-165: a study of the physical characteristics of microspheres before and after irradiation in a nuclear reactor. *Pharm. Res.* 1992(9) 149-54

Mumper RJ, Mills BJA, Ryo UY, Jay M, Polymer microspheres for radionuclide synovectomy containing neutron-activated holium-166. *J. Nuc. Med.* 1992(33) 398-402

Murthy SM, Goldschmidt RA, Roa LN, Ammirati M, Buchmann T, Scanlon EF, The influence of surgical trauma on experimental metastases. *Cancer* 1989(64) 2035-44

Nakai Y, Fukuoka E, Nakajima SI, Moriat M, Physicochemical properties of crystalline lactose. I. Estimation of the degree of crystallinity and the disorder parameter by an X-ray diffraction method. *Chem. Pharm. Bull.* 1982(30) 1811-8

Nicholaou KC, Yang Z, Liu JJ, Ueno H, Nantermet PG, Guy RK, Claiborne CF, Renaud J, Couladouros EA, Paulvannan, Sorenson EJ, Total synthesis of taxol. *Nature* 1994(367) 630-4

Nicoletti MI, Lucchini V, D'Incalci M, Giavazzi R, Comparison of paclitaxel and docetaxel activity on human ovarian carcinoma xenografts. *Eur. J. Can.* 1994(30A) 691-6

Nicoletti MI, Lucchini V, Massazza G, Abbott BJ, D'Incalci M, Giavazzi R, Antitumor activity of taxol (NSC-125973) in human ovarian carcinomas growing in the peritoneal cavity of nude mice. *Ann. Oncol.* 1993(4) 151-5

Nijenhuis AJ, Colstee E, Grijpma DW, Pennings AJ, High molecular weight poly(L-lactide) and poly(ethylene oxide) blends: thermal characterization and physical properties. *Polymer* 1996(37) 5849-57

238

Nishi T, Wang TT, Melting point depression and kinetic effects of cooling on crystallization in poly(vinylidene fluoride)-poly(methylmethacrylate) mixtures *Macromolecules* 1975(8) 909-15

Nyquist H, Saturated salt solutions for maintaining specific relative humidities. *Int. J. Pharm. Technol. & Product. Technol.* 1983(4) 47-8

O'Reilly JM, Karasz FE, Specific heat studies of transition and relaxation behavior in polymers. *J. Poly. Sci. Pt. C* 1966(14) 49-68

Omelczuk MO, McGinity JW, The influence of polymer glass transition temperature and molecular weight on drug release tablets containing poly(DL-lactic acid). *Pharm. Res.* 1992(9) 26-32

Oswald HT, Turi EA, Harget PJ, Khanna YP, Development of a middle endotherm in DSC thermograms of thermally treated drawn PET yarns and its structural and mechanistic interpretation. *J. Macromol. Sci. Phys.* 1977(B13) 231-54

Otsuka M, Kaneniwa N, A kinetic study of the crystallization process of noncrystalline indomethacin under isothermal conditions. *Chem. Pharm. Bull.* 1988(36) 4026-32

Ozols RF, Locker GY, Doroshow JH, Grotzinger KR, Myers CE, Young RC, Pharmacokinetics of Adriamycin and tissue penetration in murine ovarian carcinoma. *Cancer Res.* 1979(39) 3209-14

Park TG, Cohen S, Langer R, Ploy(L-lactic acid)/pluronic blends: characterisation of phase separation behaviour, degradation, and morphology and use as protein-releaseing matrices. *Macromolecules* 1992(25) 116-22

Parness J, Horwitz SB, Taxol binds to polymerized tubulin *in vitro*. *J. Cell Biol.* 1981(91) 479-87

Pavanetto F, Genta I, Giunchedi P, Conti B, Evaluation of spray drying as a method for polylactide and polylactide-co-glycolide microsphere preparation. *J. Microencap.* 1993(10) 487-97

Pearce R, Brown GR, Marchessault RH, Crystallization kinetics in blends of isotactic and atactic poly(β-hydroxybutyrate). *Polymer* 1994(35) 3984-9

Pekarek KJ, Jaco JW, Mathiowitz E, Double-walled polymer microspheres for controlled drug release. *Nature* 1994(367) 258-60

Pfeiffer RR, Yang KS, Tucker MA, Crystal pseudopolymorphism of cephaloglycin and cephalexin. *J. Pharm. Sci.* 1970(59) 1809-14

Pikal MJ, Lukes AL, Lang JE, Gaines K, Quantitative crystallinity determination for β-lactam antibiotics by solution calorimetry: correlation with stability. *J. Pharm. Sci.* 1978(67) 767-73

Pistner H, Bendix DR, Mühling, Reuther JF, Poly(L-lactide): a long-term degradation study *in vivo*. *Biomaterials* 1993(14) 291-8

Pitt CG, Gu ZW, Modification of the rates of chain cleavage of poly(ε-caprolactone) and related polyesters in the solid state. *J. Cont. Rel.* 1987(4) 283-92

Pitt CG, Poly-ε-caprolactone and its copolymers. In: Chasin M and Langer R, Eds.; *Biodegradable polymers as drug delivery systems*. Marcel Dekker Inc.: New York, 1990; pp 71-120

Pulapura S, Kohn J, Trends in the development of bioresorbable polymers for medical applications. *J. Biomed. App.* 1992(6) 216-50

Ramos JM, Gupta S, Anthone GJ, Ortega AE, Simons AJ, Beart RW, Laparoscopy and colon cancer: is the port site at risk? A preliminary report. *Arch. Surg.* 1994(129) 897-900

Rao KV, Hanuman JB, Alvarez C, Stoy M, Juchum J, Davies RM, Baxley R, A new large-scale process for Taxol and related taxanes from *Taxus brevifolia*. *Pharm Res.* 1995(12) 1003-10

Rao S, Krauss NE, Heerding JM, et al., 3'-(p-azidobenzamido)taxol photolabels the N-terminal 31 amino acids of beta-tubulin. *J. Biol. Chem.* 1994(269) 312-4

Reed AM, Gilding DK, Biodegradable polymers for use in surgery – poly(glycolic)/ poly(lactic acid) homo and copolymers: 2. *In vitro* degradation. *Polymer*, 1981(22) 494-8

Ringel I, Horwitz SB, Taxol is converted to 7-epitaxol, a biologically active isomer, in cell culture medium. *J. Pharmacol. Exp. Ther.* 1987(242) 692-8

Rosen SL, Characterisation of polymer molecular weight. In: *Fundamental principles of polymeric materials* 2nd ed.; John Wiley and Sons Inc.: New York, 1993a; pp 53-61

Rosen SL, Polymer morphology. In *Fundamental principles of polymeric materials* 2nd ed.; John Wiley and Sons Inc.: New York, 1993b; pp 39-52

Rosen SL, Transitions in polymers. In *Fundamental principles of polymeric materials* 2nd ed.; John Wiley and Sons Inc.: New York, 1993c; pp 103-115

Rosen SL, Transitions in polymers. In *Fundamental principles of polymeric materials* 2nd ed.; John Wiley and Sons Inc.: New York, 1993d; pp 244-88

Rosenburg HM, *The solid state* 3rd ed.; Oxford Science Publications: Oxford, 1988; pp 35-77

Rowinsky EK, Donehower RC, Jones RJ, Tucker RW, Microtubule changes and cytotoxicity in leukemic cell lines treated with taxol. *Cancer Res.* 1988 (48) 4093-100

Rowinsky EK, Donehower RC, Paclitaxel (Taxol). *New Engl. J. Med.* 1995(Apr 13) 1004-14

Rowinsky EK, Onetto N, Canetta RM, Arbuck SG, Taxol: the first of the taxanes, an important new class of antitumor agents. *Semin. Oncol.* 1992(19) 646-62

Rowinsky EK, Update on the antitumor activity of paclitaxel. *Ann. Pharmacother.* 1994(28) S18-22

Rozema FR, Bergsma JE, Bos RRM, Boering G, Nijenhuis AJ, Pennings AJ, De Bruijn WC, Late degradation simulation of poly(l-lactide). *J. Mater. Sci. Mater. Med.* 1994(5) 575-81

Sah H, Smith MS, Chern RT, A novel method of preparing PLGA microcapsules utilizing methylethyl ketone. *Pharm. Res.* 1996(13) 360-7

Sailer M, Debus S, Fuchs KH, Thiede A, Peritoneal seeding of gallbladder cancer after laparoscopic cholystectomy. *Surg. Endoscopy* 1995(9) 1300-1

Saleki-Gerhardt A, Ahlneck C, Zografi G, Assessment of disorder in crystalline solids. *Int. J. Pharm.* 1994(101) 237-47

Saleki-Gerhardt A, Stowell JG, Byrn SR, Zografi G, Hydration and dehydration of crystalline and amorphous forms of raffinose. *J. Pharm. Sci.* 1995(84) 318-23

Sanders LM, Kell BA, McRae GI, Whitehead GW, Prolonged controlled-release of nafarelin, a leuteinizing hormone-releasing hormone analogue, from biodegradable polymeric implants: influence of composition and molecular weight of polymer. *J. Pharm. Sci.* 1986(75) 356-60

Saotome K, Kodaira Y, Polymerization of δ-valerolactone and preparation of a thermostable derivative from its polyester. *Makromol. Chem.* 1965(82) 41

Sato T, Kanke M, Schroeder HG, DeLuca PP, Porous biodegradable microspheres for controlled drug delivery. I. Assessment of processing conditions and solvent removal techniques. *Pharm. Res.* 1988(5) 21-30

Sautner T, Hofbauer F, Depisch D, Schissel R, Jakesz R, Adjuvant intraperitoneal cisplatin chemotherapy does not improve long-term survival after surgery for advance gastric cancer. *J. Clin. Oncol.* 1994(12) 970-4

Schiff PB, Horwitz SB, Taxol stabilizes microtubules in mouse fibroblast cells. *Proc. Natl. Acad. Sci. USA* 1980(77) 1561-5

Schindler A, Harper D, Polylactide. II. Viscosity-molecular weight relationships and unpertuerbed chain dimensions. *J. Poly. Sci. Poly. Chem. Edn.* 1979(17) 2593-9

Schindler A, Hibionada YM, Pitt CG, Aliphatic polyesters. III. Molecular weight and molecular weight distribution in alcohol-initiated polymerization of ε-caprolactone. *J. Poly. Sci. Poly. Chem. Edn.* 1982(20) 319-26

Schneebaum S, Arnold MW, Staubus A, Yound DC, Dumond D, Martin Jr. EW, Intraperitoneal hyperthermic perfusion with mitomycin C for colorectal cancer with peritoneal metastases. *Ann. Surg. Oncol.* 1996(3) 44-50

Schwartz HH, Hicke HG, Influence of casting solution concentration on structure and performance of cellulose acetate membranes. *J. Membr. Sci.* 1989(46) 325-34

Seidman A, Reichman B, Crown J, Begg C, Heelan R, Hakes T, Activity of taxol with recombinant granulocyte colony stimulating factor (GCSF) as first chemotherapy © of patients (pts) with metastatic breast cancer. *Proc. Am. Soc. Clin. Oncol.* 1992(11) 59

Shah VP, Midha KK, Dighe S, McGilveray IJ, Skelly JP, Yacobi A, Layloff T, Viswanathan CT, Cook CE, McDowall RD, Pittman KA, Spector S, Analytical methods validation: bioavailability, bioequivalence and pharmacokinetic studies. *Pharm. Res.* 1992(9) 588-92

Sharm D, Chelvi TP, Kaur J, Chakravorty K, De TK, Maitra A, Ralhan R, Novel taxol formulation: polyvinylpyrrolidone nanoparticle-encapsulated taxol for drug delivery in cancer. *Oncol. Res.* 1996(8) 281-6

Sharma US, Balasubramanian SV, Strabinger RM, Pharmaceutical and physical properties of paclitaxel (Taxol) complexes with cyclodextrins. *J. Pharm. Sci.* 1995(84) 1223-30

Shefter E, Higuchi T, Dissolution behaviour of crystalline solvated and nonsolvated forms of some pharmaceuticals. *J. Pharm. Sci.* 1963(52) 781-91

Skipper D, Jeffrey MJ, Cooper AJ, Alexander P, Taylor I, Enhanced growth of tumour cells in healing colonic anastomoses and laparotomy wounds. *Int. J. Colorectal Dis.* 1989(4) 172-7

Solomon OF, Ciuta IZ, Determination de la viscosité intrinsèque de solutions de polymers par une simple determination de la viscosité. *J. Appl. Poly. Sci.* 1962(VI-24) 683-6

Song D, Hsu LF, Au LS, Binding of Taxol to plastic and glass containers and protein under *in vitro* conditions. *J. Pharm. Sci.* 1996(85) 29-31

Soulie P, Tradafir L, Taamma A, Lokie F, Brain E, Delord JP, Mita A, Vannetzel JM, Cuitkovic E, Misset JL, Schedule dependent paclitaxel tolerance/activity: data from a

7 day infusion phase I study with pharmacokinetics in paclitaxel refractory ovarian cancer. *Anticancer Drugs*, 1997(8) 763-6

Spencer CM, Faulds D, Paclitaxel. A review of its pharmacodynamic and pharmacokinetic properties and therapeutic potential in the treatment of cancer. *Drugs* 1994(48) 794-847

Stearns ME, Wang M, Taxol blocks processes essential for prostate tumour cell (PC-3 ML) invasion and metastases. *Cancer Res.* 1992(52) 3776-81

Summers MP, Carless JE, Enever RP, The polymorphism of aspirin. *J. Pharm. Pharmacol.* 1970(22) 615-6

Suryanarayanan R, Determination of the relative amounts of anhydrous carbamazepine ($C_{15}H_{12}N_2O$) and carbamazepine dihydrate ($C_{15}H_{12}N_2O \bullet 2H_2O$) in a mixture by powder X-ray diffractometry. *Pharm. Res.* 1989(6) 1017-24

Suryanarayanan R, Mitchell AG, Evaluation of two concepts of crystallinity using calcium gleceptate as a model compound. *Int. J. Pharm.* 1985(24) 1-17

Sweet GE, Bell JP, Multiple endotherm melting behavior in relation to polymer morphology. *J. Poly. Sci. Pt. A-2* 1972(10) 1273-83

Swindell CS, Krauss NE, Horwitz SB, Ringel I, Biologically active taxol analogues with deleted A-ring side chain substituents and variable C-2' configuration. *J. Med. Chem.* 1991(34) 1176-84

Takahasi T, Hagiwara A, Shimotsuma M, Sawai K, Yamaguchi T, Prophylaxis and treatment of peritoneal carcinomatosis: intraperitoneal chemotherapy with mitomycin C bound to activated carbon particles. *World J. Surg.* 1995(19) 565-9

Tarr BD, Yalkowsky SH, A new parenteral vehicle for the administration of some poorly water soluble anti-cancer drugs. *J. Parenteral Sci. Technol.* 1987(41) 31-3

Therin M, Christel P, Li S, Garreau H, Vert M, *In vivo* degradation of massive poly(α-hydroxy acids): validation of *in vitro* findings. *Biomaterials* 1992(13) 594-600

Thigpen T, Blessing J, Ball H, Hummel S, Barret R, Phase II trial of taxol as second-line terapy for ovarian carcinoma: a Gynecologic Oncology Group study. *Proc. Am. Soc. Clin. Oncol.* 1990(9) 156

Thomas PA, Padmaja T, Kulkarni MG, Polyanhydride blend microspheres: novel carriers for the controlled release of macromolecular drugs. *J. Cont. Rel.* 1997(43) 273-81

Thomas WM, Eaton MC, Hewett PJ, A proposed model for the movement of cells within the abdominal cavity during carbon dioxide insufflation and laparoscopy. *Austral. NZ, J, Surg.* 1996(66) 105-6

Tros de Ilarduya MC, Martín C, Goñi MM, Martínez-Ohárriz MC, Polymorphism of sulindac: isolation and characterisation of a new polymorph and three new solvates. *J. Pharm. Sci.* 1997(86) 248-51

Tsai DC, Howard SA, Hogan TF, Malanga CJ, Kandzari SJ, Ma JKH, Preparation and in vitro evaluation of poly(lactic acid)/mitomycin-c microcapsules. *J. Microencap.* 1986(3) 181-93

Tsakala M. Gillet J. Gillard J. New antimalarial sustained-release formulations based on bioresorbable polymers: therapeutic evaluation using the Plasmodium berghei model. *J. Pharmacie Belgique* 1990(45) 5-11

Tsuji H, Hyon SH, Ikada Y, Stereocomplex formation between enantiomeric poly(lactic acid)s. 3. Calorimetirc studies on blend films cast from dilute solution. *Macromolecules* 1991(24) 5651-6

Tsuji H, Hyon SH, Ikada Y, Stereocomplex formationn between enantiomeric poly(lactic acid)s. 4. Differential scanning calorimetric studies on precipitates from mixed solutions of poly(D-lactic acid) and poly(L-lactic acid). *Macromolecules* 1991(24) 5651-6

Vander Velde DG, Georg GI, Grunewald GL, Gunn CW, Mitscher LA, "Hydrophobic collapse" of Taxol and Taxotere solution conformations in mixtures of water and organic solvent. *J. Am. Chem. Soc.* 1993(115) 11650-1

Vercer F, Srcic S, Smid-Korbar J, Investigation of piroxicam polymorphism. *Int. J. Pharm.* 1991(68) 35-41

Vert M, Li SM, Spenlehauer G, Guerin P, Bioresorbability and biocompatibility of aliphatic polyesters. *J. Mater. Sci. Mater. Med.* 1992(3) 432-46

Vidmar V, Smolcic-Bubalo A, Jalsenjak I, Poly(lactic acid) microencapsulated oxytetracycline: in vitro and in vivo evaluation. *J. Microencap.* 1984(1) 131-6

von Recum H, Cleek RL, Eskin SG, Mikos AG, Degradation of polydisperesed poly(L-lactic acid) to modulate lactic acid release. *Biomaterials* 1995(16) 441-7

Wakiyama N, Juni K, Nakano M, Preparation and evaluation *in vitro* of polylactic acid microspheres containing local anesthetics. *Chem. Pharm. Bull.* 1981(29) 3363-8

Walter KA, Cahan MA, Gur A, Tyler B, Hilton J, Colvin M, Burger PC, Domb A, Brem H, Interstitial Taxol delivered from a biodegradable polymer implant against experimental malignant glioma. *Cancer Res.* 1994(54) 2207-12

Wang YM, Sato H, Adachi I, Horikoshi I, Preparation and characterization of poly(lactic-co-glycolic acid) microspheres for targeted delivery of a novel anticancer agent, Taxol. *Chem. Pharm. Bull.* 1996(44) 1935-40

Wang YM, Sato H, Horikoshi I, *In vitro* and *in vivo* evaluation of taxol release from poly(lactic-co-glycolic acid) microspheres containing isopropyl myristate and degradation of the microspheres. *J. Cont. Rel.* 1997(49) 157-66

Wani MC, Taylor HL, Wall ME, Coggon P, McPhail AT, Plant antitumor agents. VI. The isolation and structure of taxol, a novel antileukemic and antitumor agent from *Taxus brevifolia. J. Am. Chem. Soc.* 1971(93) 2325-7

Weiss RB, Donehower RC, Wiernik PH, Ohnuma T, Gralla RJ, Trump DL, Baker JR, VanEcho DA, VonHoff DD, Leyland-Jones B, Hypersensitivity reactions from taxol. *J. Clin. Oncol.* 1990(8) 1263-8

Wichert B, Rhodewald P, A new method for the preparation of drug containing polylactic acid microparticles without using organic solvents. *J. Cont. Rel.* 1990(4) 269-83

Wiernik PH, Schwartz EL, Einzig A, Strauman JJ, Liptonn RB, Dutcher JP, Phase I trial of taxol given as a 24-hour infusion every 21 days: responses observed in metastatic melanoma. *J. Clin. Oncol.* 1987(5) 1232-9

Wiernik PH, Schwartz EL, Strauman JJ, Dutcher JP, Lipton RB, Paietta E, Phase I clinical and pharmacokinetic study of taxol. *Cancer Res.* 1987(47) 2486-93

Williams DF, Biodegradation of surgical polymers. *J Mater. Sci.* 1982(17) 1233-46

Williams DF, Enzymatic hydrolysis of polylactic acid. *Eng. Med.* 1981(10) 5-7

Winternitz C, Jackson J, Cindric S, Arsenault L, Burt H, Use of paclitaxel loaded surgical paste to delay regrowth of partially resected RIF-1 tumours in mice. *Pharm. Res.* 1996(13) S-211

Winternitz CI, Jackson JK, Oktaba AM, Burt HM, Development of a polymeric surgical paste formulation for Taxol. *Pharm. Res.* 1996(13) 368-75

Winternitz CI, Unpublished results: solubility of paclitaxel in phosphate buffered saline with albumin. 1997

Witherup KM, Look SA, Stasko MW, Ghiorzi TJ, Muschik GM, Cragg GM, *Taxus spp.* Needles contain amounts of taxol comparable to the bark of *Taxus brevifolia. J. Nat. Prod.* 1990(53) 1249-55

Wood AJJ, Paclitaxel (Taxol). *New Engl. J. Med.* 1995(332) 1004-14

Woodward SC, Brewer PS, Moatmed F, Schindler A, Pitt CG, The intracellular degradation of poly(ε-caprolactone). *J. Biomed. Mat. Res.* 1985(19) 437-44

Wu LS, Gerard C, Hussain MA, Thermal analysis and solution calorimetry on losartan polymorphs. *Pharm. Res.* 1993(10) 1793-5

Wünderlich B, *Macromolecular Physics, Crystal Structure, Morphology, Defects*; Academic Press: New York, 1973; vol 1

Wünderlich B, *Macromolecular Physics, Crystal Melting*; Academic Press: New York, 1980; vol 3

Yamakawa I, Ashizawa K, Tsuda T, Watanabe S, Hayashi M, Awazu S, Thermal characteristics of poly(DL-lactic acid) microspheres containing neurotensin analogue. *Chem. Pharm. Bull.* 1992(40) 2870-2

Yeh MK, Jenkins PG, Davis SS, Coombes AGA, Improving the delivery capacity of microparticle systems using blends of poly(DL-lactide-co-glycolide) and poly(ethylene glycol). *J. Cont. Rel.* 1995(37) 1-9

Yonemochi E, Ueno Y, Ohmal T, Oguci T, Nakajima S, Yamamoto K, Evaluation of amorphous ursodeoxycholic acid by thermal methods. *Pharm. Res.* 1997(14) 798-803

Yoshioka M, Hancock BC, Zografi G, Crystallization of indomethacin from the amorphous state below and above its glass transition temperature. *J. Pharm. Sci.* 1994(83) 1700-5

Young TH, Chen LW, A diffusion-controlled model for wet-casting membrane formation. *J. Membr. Sci.* 1991(59) 169-81

Yu L, Inferring thermodynamic stability relationship of polymorphs from melting data. *J. Pharm. Sci.* 1995(84) 966-74

Zhang X, Burt HM, Mangold G, Dexter D, VonHoff D, Mayer L, Hunter WL, Anti-tumor efficacy and biodistribution of intravenous polymer micellar paclitaxel. *Anticancer Drugs* 1997(8) 696-701

Zhang X, Unpublished results: solubility of paclitaxel in phosphate buffered saline with albumin. 1997

Zhou ZL, Eisenberg A, Ionomeric blends. II. Compatibility and dynamic mechanical properties of sulfonated *cis*-1,4-polyisoprenes and styrene/4-vinylpyridine copolymer blends. *J. Polym. Sci. Phys. Edn.* 1983(21) 595-603

APPENDIX I. SAMPLE CALCULATIONS OF M_n, M_w AND POLYDISPERSITY

1. Consider a polymer composed of twelve polymer chains (N=12) having weights between 1 and 10 weight units. The weights of each of the chains are: 1, 2, 2, 2, 4, 5, 5, 8, 8, 8, 9 and 10 weight units.

2. The sum of the weights of each chain gives a total weight (W) of the polymer of 64.

3. M_n is calculated as follows:

$$M_n = \sum_{x=1}^{10} \left(\frac{n_x}{N} \right) M_x$$

$$M_n = \left(\frac{1}{12} \right) \times 1 + \left(\frac{3}{12} \right) \times 2 + \left(\frac{1}{12} \right) \times 4 + \left(\frac{2}{12} \right) \times 5 + \left(\frac{3}{12} \right) \times 8 + \left(\frac{1}{12} \right) \times 9 + \left(\frac{1}{12} \right) \times 10$$

$$M_n = \frac{64}{12} = 5.33$$

where: n_x is the number of polymer chains with molecular weight of M_x, where x is a number from 1 to 10.

4. M_w is calculated as follows:

$$M_w = \sum_{x=1}^{10} \left(\frac{w_x}{W} \right) M_x, \quad \text{where } w_x = n_x \times M_x$$

$$M_w = \left(\frac{1 \times 1}{64} \right) \times 1 + \left(\frac{3 \times 2}{64} \right) \times 2 + \left(\frac{1 \times 4}{64} \right) \times 4 + \left(\frac{2 \times 5}{64} \right) \times 5 + \left(\frac{3 \times 8}{64} \right) \times 8 + \left(\frac{1 \times 9}{64} \right) \times 9 + \left(\frac{1 \times 10}{64} \right) \times 10$$

$$M_w = \frac{452}{64} = 7.06$$

where: w_x is the total weight of polymer chains with molecular weight of M_x, where x is a number from 1 to 10.

5. The polydispersity index (PDI) is calculated as follows:

$$PDI = \frac{M_w}{M_n} = \frac{7.06}{5.33} = 1.32$$

APPENDIX II. VALIDATION OF HPLC METHODS

Data used to determine precision within and between days for paclitaxel in acetonitrile are summarised in Table 21. Values of RSD of less than 10% for all average peak areas within and between days were obtained for standards at concentrations greater than or equal to 0.2 µg/ml, or a total amount of paclitaxel injected of 4 ng. ANOVA of peak area values at each concentration showed no statistical significance between days at concentrations greater than or equal to 0.2 µg/ml (see Table 21). Data used to express accuracy are shown in Table 22. Values of bias of less than 10% were observed for all concentrations of paclitaxel greater than or equal to 0.2 µg/ml. The average R^2 value for all twelve standard curves (four a day for three days) was 0.9998 ± 0.0002.

Precision data within and between days for the paclitaxel standard curve in 60:40 acetonitrile:water are summarised in Table 23. Values of RSD of less than 10% for all average peak areas within and between days were observed at all concentrations of paclitaxel down to 0.2 µg/ml, or a total amount of paclitaxel injected of 4 ng. ANOVA of peak area values at each concentration showed a statistical difference between average peak areas at 1 and 2 µg/ml, which was due to very low inter-day precision. Intra-day precision at 1 and 2 µg/ml was still very good, with a RSD of less than 3%. Table 24 summarises the accuracy of injections of paclitaxel at each concentration on each day. No more than 10% bias was observed for all concentrations of paclitaxel greater than or equal to 0.2 µg/ml. The linearity of all twelve standard curves, expressed as R^2 was 0.9999 ± 0.0001.

Table 21. Inter- and intra-day precision of a standard curve of paclitaxel in acetonitrile.

Paclitaxel Concentration (µg/ml)	Day 1 Peak Area[a]	Day 1 RSD[b] (%)	Day 2 Peak Area	Day 2 RSD (%)	Day 3 Peak Area	Day 3 RSD (%)	All Days Peak Area	All Days RSD (%)	ANOVA p value[c]
0.2	20528	5.08	16155	7.26	15696	5.16	16332	6.51	0.142
0.5	45420	2.78	44228	1.20	42822	8.23	43814	5.67	0.662
1	89155	7.53	84376	3.80	84726	6.00	85890	5.15	0.364
2	180069	2.92	168575	4.56	163992	3.47	168184	3.89	0.237
5	433366	2.89	432422	3.21	431798	4.25	433071	3.24	0.953
10	844850	3.48	849452	3.10	852222	3.55	854833	3.12	0.790
20	1698888	3.64	1704289	1.93	1664377	4.31	1693799	3.51	0.514

[a] Peak area is the average calculated from four standards at each concentration for each day (n = 16 for all days).

[b] RSD (Relative standard deviation) is the ratio of the standard deviation to the average, expressed as a percentage. A value less than 10% indicates sufficient precision at each concentration.

[c] ANOVA p values are level of significance for single factor ANOVA tests between each day's peak areas at each concentration. $P<0.05$ indicates a significant difference between peak areas on different days.

Table 22. Accuracy of standard curves of paclitaxel in acetonitrile.

Paclitaxel Concentration (µg/ml)	Day 1			Day 2			Day 3		
	Predicted Value[a]	RSD[b] (%)	Bias[c] (%)	Predicted Value	RSD (%)	Bias (%)	Predicted Value	RSD (%)	Bias (%)
0.2	0.21	5.39	3.38	0.19	5.90	5.51	0.22	6.73	8.38
0.5	0.51	3.45	1.31	0.53	8.97	5.70	0.54	1.41	8.84
1	1.03	6.28	2.86	1.04	6.12	4.34	1.01	4.17	0.94
2	2.01	3.09	0.47	1.99	4.17	0.35	2.01	5.50	0.65
5	5.06	3.74	1.15	5.29	4.44	5.76	5.20	0.65	3.99
10	10.07	3.76	0.69	10.44	3.35	4.40	10.06	3.73	0.60
20	19.75	4.92	1.23	20.23	5.20	1.15	20.13	2.35	0.63

[a] Predicted value is the average (n = 3 for each day) of values of concentration calculated from one standard curve on each day.
[b] RSD (Relative standard deviation) is the ratio of the standard deviation to the average, expressed as a percentage. A value less than 10% indicates sufficient accuracy at each concentration.
[c] Bias is the ratio of the deviation of predicted value from the actual concentration measured, expressed as a percentage.

Table 23. Inter- and intra-day precision of a standard curve of paclitaxel in 60:40 acetonitrile:water.

Paclitaxel Concentration (µg/ml)	Day 1		Day 2		Day 3		All Days		ANOVA p Value[c]
	Peak Area[a]	RSD[b] (%)	Peak Area	RSD (%)	Peak Area	RSD (%)	Peak Area	RSD (%)	
0.2	20117	1.39	19060	8.22	19442	1.28	19540	4.90	0.31
0.5	49041	1.76	49630	5.98	48868	1.40	49180	3.43	0.82
1	99092	2.03	96123	0.87	99538	2.03	98251	2.26	0.04
2	202576	2.12	195317	1.10	199391	1.13	199095	2.09	0.03
5	489960	1.23	505825	4.48	487896	0.67	494560	3.02	0.18
10	987376	0.74	977835	0.36	988904	0.90	984705	0.82	0.1
20	1966355	0.74	1967193	1.01	1958408	0.68	1963985	0.77	0.71

[a] Peak area is the average calculated from four standards at each concentration for each day (n = 16 for all days).

[b] RSD (Relative standard deviation) is the ratio of the standard deviation to the average, expressed as a percentage. A value less than 10% indicates sufficient precision at each concentration.

[c] ANOVA p values are level of significance for ANOVA tests between each day's peak areas at each concentration. P<0.05 indicates a significant difference between peak areas on different days.

Table 24. Accuracy of standard curves of paclitaxel in 60:40 acetonitrile:water.

Paclitaxel Concentration (μg/ml)	Day 1			Day 2			Day 3		
	Predicted Value[a]	RSD[b] (%)	Bias[c] (%)	Predicted Value	RSD (%)	Bias (%)	Predicted Value	RSD (%)	Bias (%)
0.2	0.20	1.65	2.08	0.18	1.97	9.75	0.20	1.55	1.04
0.5	0.50	1.93	0.29	0.50	7.31	0.01	0.50	1.59	0.20
1	1.02	1.73	1.85	0.97	0.55	3.42	1.03	1.83	2.59
2	2.07	2.58	3.60	1.97	0.88	1.67	2.04	1.13	1.77
5	5.04	0.57	0.72	5.16	5.15	3.19	5.00	0.82	0.01
10	10.12	0.62	1.20	9.90	0.42	0.99	10.14	1.10	1.36
20	20.13	0.82	0.67	19.91	1.19	0.46	20.12	0.55	0.60

a Predicted value is the average (n = 3 for each day) of values of concentration calculated from one standard curve on each day.

b RSD (Relative standard deviation) is the ratio of the standard deviation to the average, expressed as a percentage. A value less than 10% indicates sufficient accuracy at each concentration.

c Bias is the ratio of the deviation of predicted value from the actual concentration measured, expressed as a percentage.

252